FACULTY OF ENGINEERING AND APPLIED SCIENCE

DEPARTMENT OF CIVIL ENGINEERING

SOME ASPECTS OF THE ANALYSIS OF OFFSHORE STRUCTURES

M. EBERT .

A thesis submitted in partial fulfilment of the requirements for the degree of Doctor of Philosophy

University of Southampton 1977

ACKNOWLEDGMENTS

Many thanks are due to Dr. C.A. Brebbia , who supervised this project ; to Prof. P.B. Morice , head of the Department of Civil Engineering ; and to Dr. D.Benedetti and other members of staff of the Politecnico di Milano for their assistance during a year's study of the effects of earthquake vibrations on structures .

UNIVERSITY OF SOUTHAMPTON

ABSTRACT

FACULTY OF ENGINEERING AND APPLIED SCIENCE

DEPARTMENT OF CIVIL ENGINEERING

Doctor of Philosophy

SOME ASPECTS OF THE ANALYSIS OF OFFSHORE STRUCTURES

by Michael Ebert

In this thesis, a study is made of the effect of random wave forces on self-supporting steel and concrete oil drilling platforms. Various methods of estimating the forces on the structure, and various ways of idealising both the forces and the structure itself, are compared, the objective being a realistic and safe design.

The sea is here represented by a wave amplitude spectrum, from which spectra for the forces on the structure are derived using a linear wave theory, in two ways. Firstly, using the well-known Morison equation, which requires experimental drag and inertia coefficients; and secondly by considering wave diffraction from the structural members. A quantitative comparison is made of the two methods. Using the diffraction theory, it is possible to guage the effect of sheltering - i.e. the effect on the forces on one member due to the presence of another.

The principal structures considered here are idealised as plane framed structures (though the theory is applicable for structures with, say, plate elements also) , and in this connection wave forces on inclined frame members are considered. This is particularly useful for steel structures. A comparison is made betweem the results obtained by evaluating the forces 'consistently' and by 'lumping' them at element nodal points.

In addition, a comparison is made of solution methods which ignore certain cross-correlation terms in the equations of motion for the response with one that includes such terms, in an attempt to show that a fuller analysis is no more difficult, and is likely to be safer, than the more approximate methods.

CONTENTS

Everything gathers unto itself some things.

And it is a law, that all things must modify, change and alter to that which is its host or hostess.

Now I say and make known to you that you are, and have been, within the realms of the most high.

And for yourself, try to know that you are being made again new, but in a new way.

Understanding will come to you, and clarity will be your daily companion; purpose, your beacon.

And in the peace and tranquillity that must come, it will be your strength and knowing.

THAT IT CANNOT HAPPEN THAT YOU WILL NOT UNDERSTAND WILL BE MADE PLAIN. BE PATIENT, AND GROW.

EDO 24

SUMMARY

This thesis is concerned with the analysis of any ocean structure that can be idealised as a plane frame . Such structures include steel framed structures , as well as single-leg and multi-leg concrete structures .

Chapter I gives a general appraisal of ocean engineering, in order to emphasise some of the points to be bourne in mind when designing an offshore installation .

Chapter 2 considers various wave theories , and chapter 3 deals with the application of such theories to the determination of wave forces on a structure . Two main methods are considered : an empirical approach as used by Morison et al , and an analytical wave diffraction theory . Certain conclusions are reached about the range of validity of each of the two methods . The sheltering effect of some members on others is also taken into account .

Having derived expressions for the forces acting on a structure, one must then solve the equations of motion of the system , which is the subject matter of chapter 4 . In this thesis , the forces are evaluated statistically in terms of a spectrum of wave amplitudes. It is shown how the equations of motion can be solved for consistent element forces (section 4.4) ; and three methods are indicated for 'lumped' forces (section 4.5) . One method treats the coupling between the forces at

each degree of freedom of the structure ; another treats each degree of freedom independently and superimposes the results ; and the third is called a direct transfer function method , because essentially it consists of finding a 'transfer function' connecting displacements with wave amplitudes directly . This method appears to avoid some of the approximations involved in all the other methods. All the methods are capable of dealing with inclined members as well as vertical ones .

A comparitive study of the various methods of analysis is made in chapter 5 , where the computer results are presented .

To summarise , four main points are considered in this thesis .

Firstly , a comparative study is made of conventional frequency domain analyses and a 'Direct Transfer Function' technique .

Secondly , a comparative study is made of two ways of estimating the forces on a structure - a wave diffraction theory and the standard Morison approach .

Thirdly , the effect of waves on inclined frame members is considered .

Fourthly , the effect of sheltering is considered (i.e. the effect on the forces on a member, of neighbouring members) .

The results are presented in Chapter 5 , and the conclusions follow .

CHAPTER I : INTRODUCTION: OFFSHORE ANALYSIS AND DESIGN

I.I GENERAL

The sea contains wealth in abundance. The chart on the following page shows that each cubic mile of sea water contains up to 25 tons of gold alone and immense quantities of other valuable minerals. The chart does not show that the total weight of a cubic mile of sea water is about 4×10^9 tons, and it does not show the large reserves of wealth under the sea. Both these points highlight one fact, namely that while the wealth is abundant, man is still left with the problem of extracting it.

This thesis is concerned just with the extraction of oil from under the sea, and to narrow the field down further, just with the design and analysis of structures capable of fulfilling this objective.

I.2 AN APPRAISAL OF THE DEVELOPMENT OF OFFSHORE DRILLING PLATFORMS

As early as 1900 drilling for oil was attempted in the Gulf of Mexico using wooden platforms and wooden piles. The depth of water was limited to about 3 metres, and the procedure was that mobile platforms were used for exploration and fixed platforms for development.

In 1947, the first steel template platform was erected in the Gulf of Mexico, this time in about 6 metres of water. By 1967 there were some 2000 platforms in the Gulf of Mexico, and the greatest depth being drilled in was about 110 metres.

Approximate Amounts of Minerals in One Cubic Mile of Sea Water

Sodium Chloride	128,000,000 tons
Magnesium Chloride	17,900,000 tons
Magnesium Sulphate	7,800,000 tons
Calcium Sulphate	5,900,000 tons
Potassium Sulphate	4,000,000 tons
Calcium Carbonate	578,832 tons
Magnesium Bromide	350,000 tons
Bromine	300,000 tons
Strontium	60,000 tons
Boron	21,000 tons
Fluorine	6,400 tons
Barium	900 tons
Iodine	1000 to 1200 tons
Arsenic	50 to 350 tons
Rubidium	200 tons
Silver	up to 45 tons
Copper, Lead, Manganese, Zinc	10 to 30 tons
Gold	up to 25 tons
Uranium	7 tons

From "Treasure from the Sea" by J. W. Chansler. Included in "Science and the Sea", U. S. Naval Oceanographic Office, 1967.

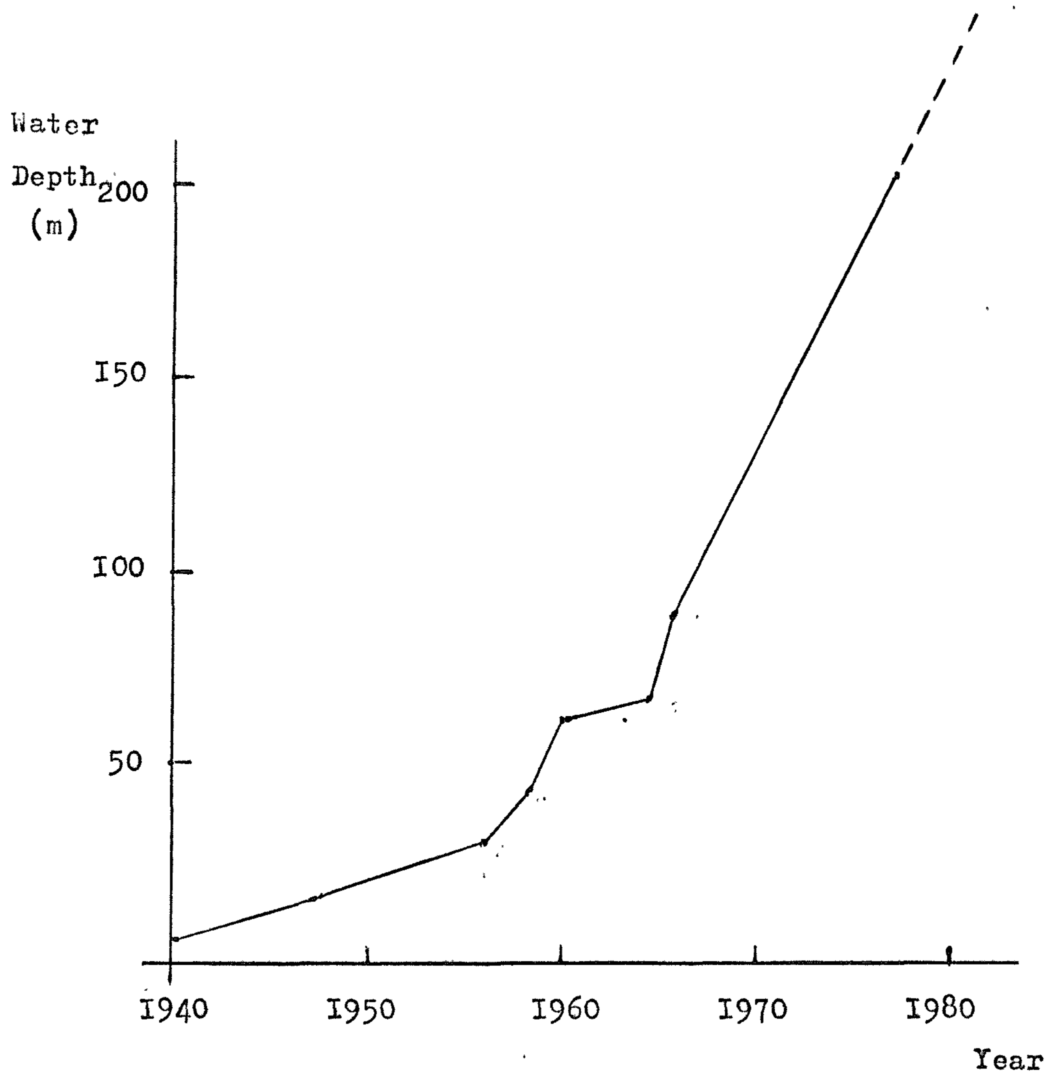

Fig I.I : Water Depth Records By Year

(production drilling)

Failures due to collisions and hurricanes amounted to 22 collapsed platforms and 10 platforms severely damaged. When attempting to assess these collapses, it has been said that some had been designed with a calculated risk for a storm with return period only 25 years. Others were designed before adequate design procedures were known. Only 3 had been designed for today's accepted maximum storm conditions - a storm with a 50 - 100 year return period.

Today drilling is taking place in depths of some 200 metres, and it is likely that the same procedures as are now being used will continue to be used to the limits of the Continental Shelf, where depths do not exceed about 250 metres. Beyond the Continental Shelf, depths increase rapidly, and new design methods may well be needed.

I.3 TYPES OF OFFSHORE PLATFORM

I.3.I. GENERAL

One can classify offshore structures according to a variety of criteria - for example, equipment carried, mobility, method of installation, method of support, and so on. From a structural design point of view, perhaps the most useful division is to distinguish between bottom-supported structures and floating structures

I.3.2. BOTTOM - SUPPORTED PLATFORMS

Examples of bottom-supported structures are given in Figs(I.2) - (I.5) . They consist essentially of a three-dimensional framework which rests on the sea bed and through whose legs piles are driven and made integral. They are usually floated to the site. In this class of structure one should include gravity platforms, which are similar in design to the 'Monopod' platform shown in Fig.(I.4) .

Fig I.2

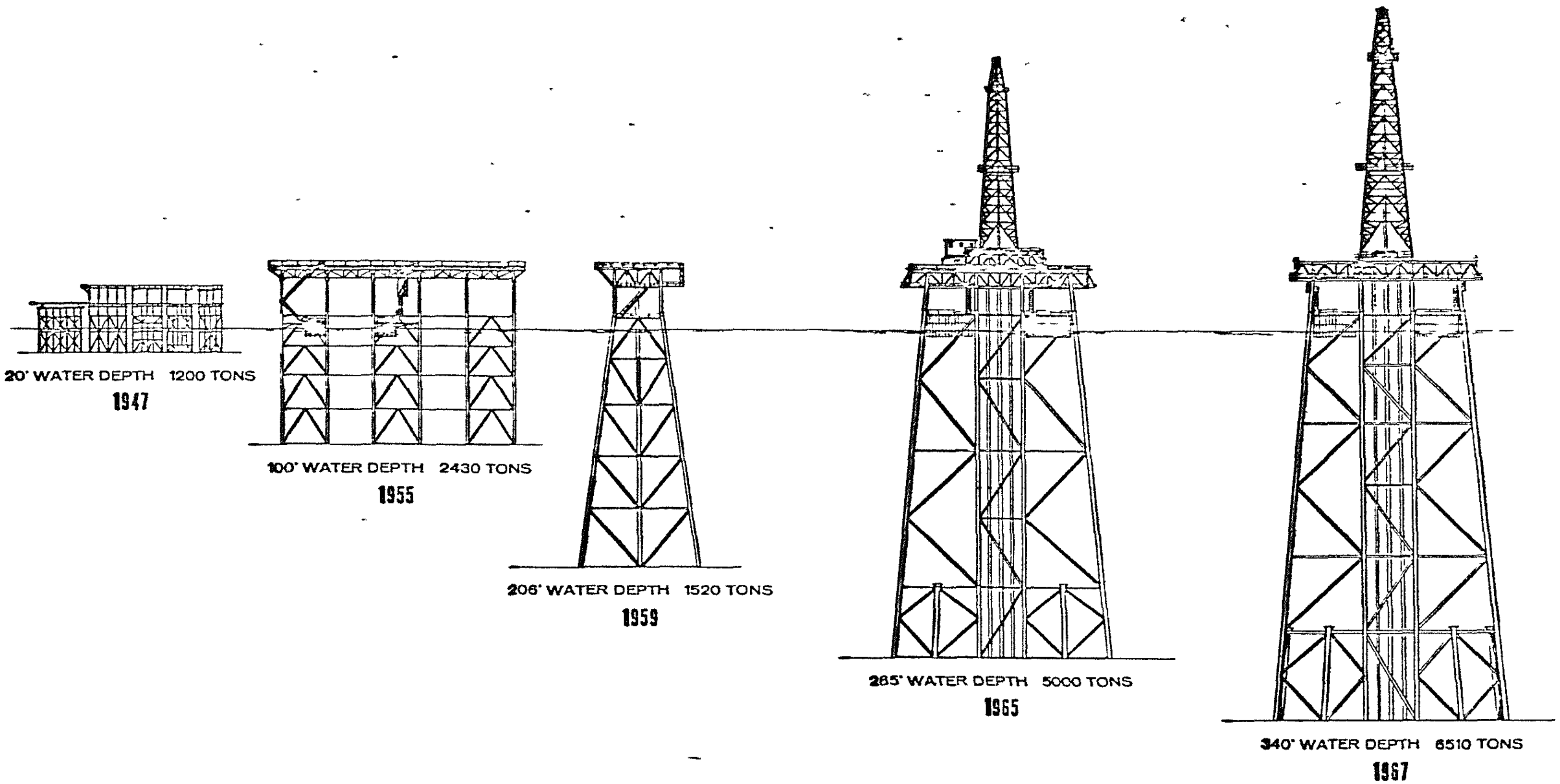

TWENTY YEARS OF PLATFORM DEVELOPMENT

<u>Proceedings of OECON Offshore Exploration Conference - 1968</u>, published by Offshore Exploration Conference, Palos Verdes Estates, California

"Offshore Structures Past, Present and Future Design Considerations" by G. C. Lee

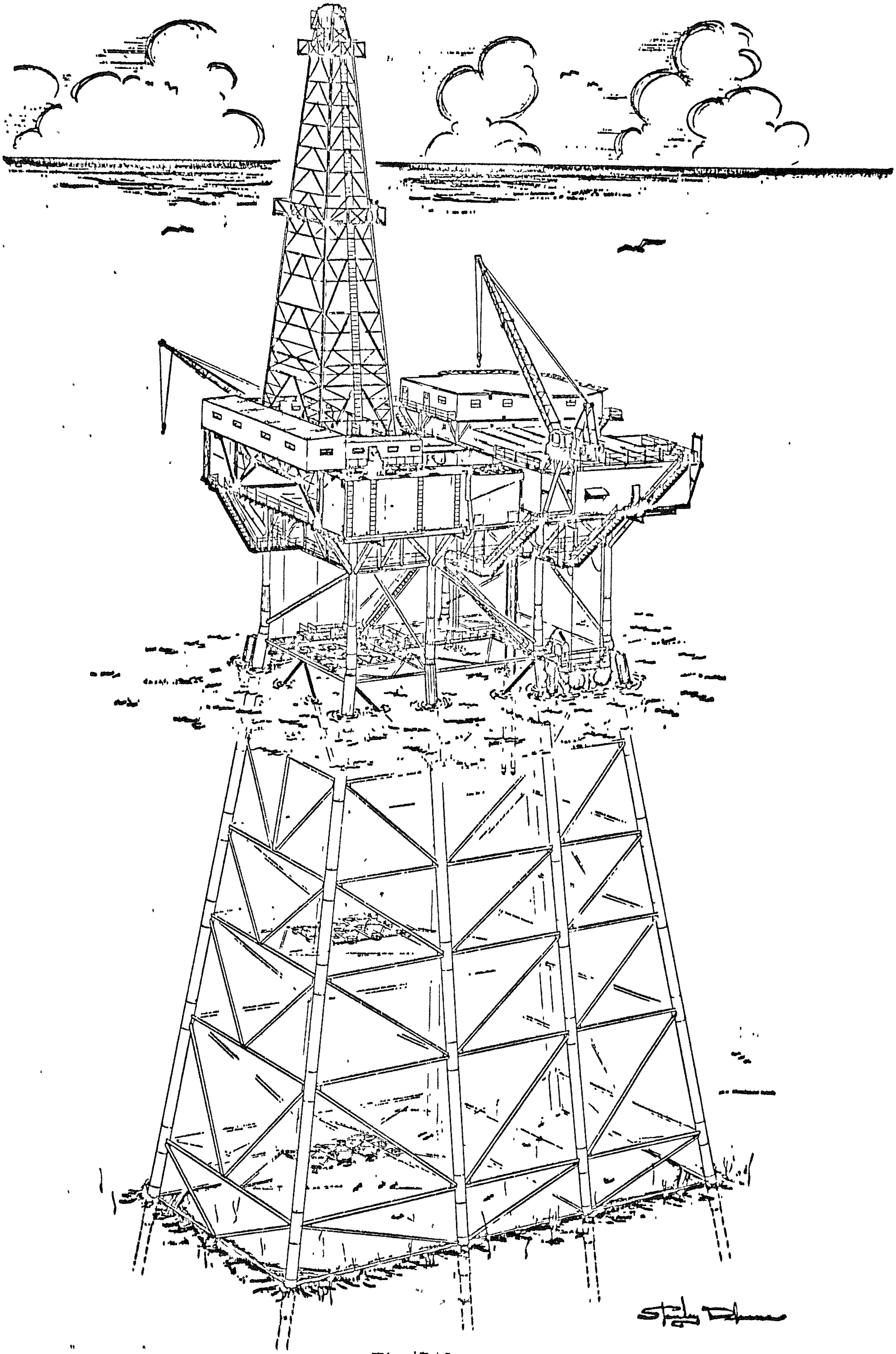

Fig I.3

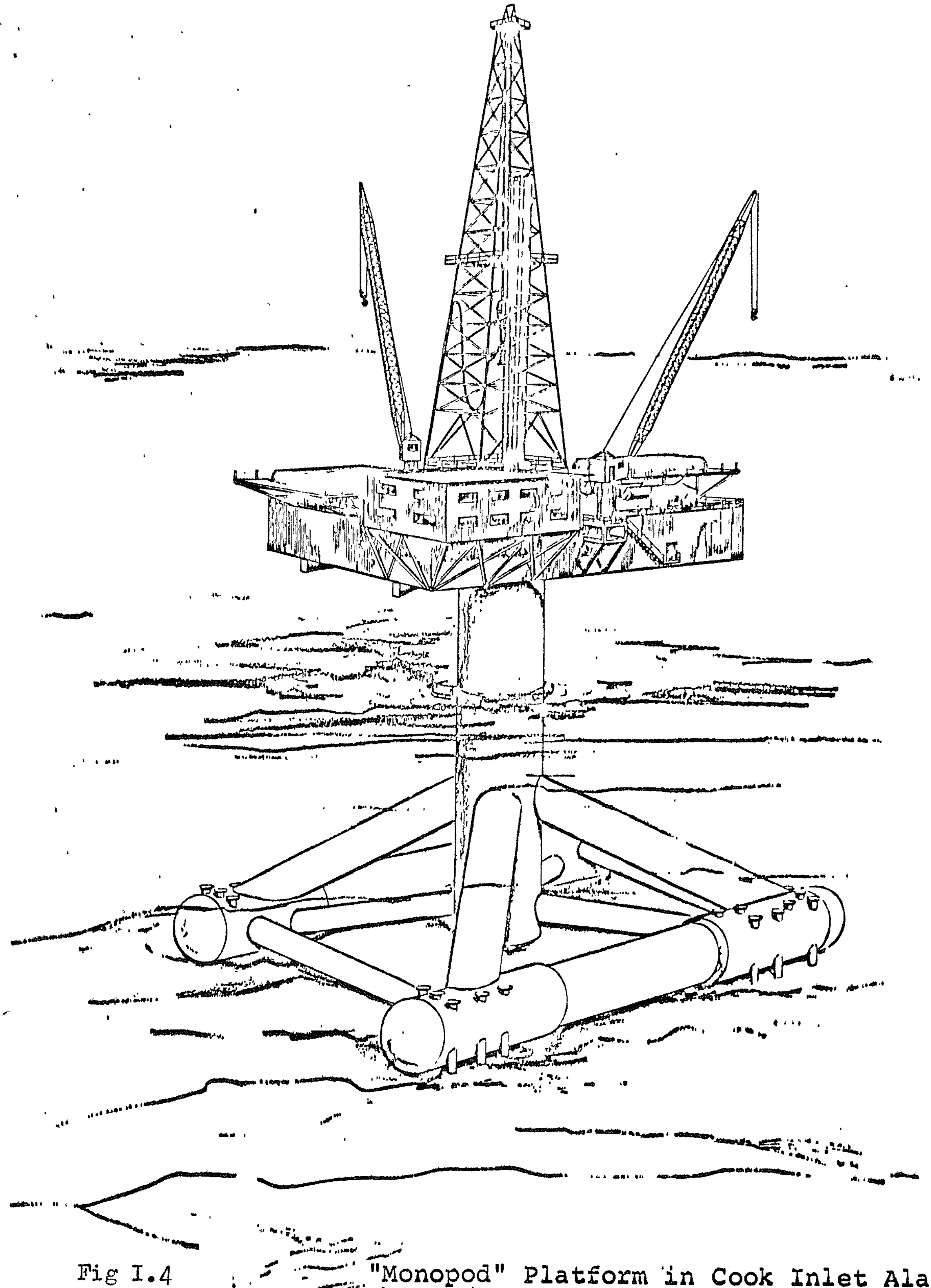

Fig I.4 "Monopod" Platform in Cook Inlet Alaska

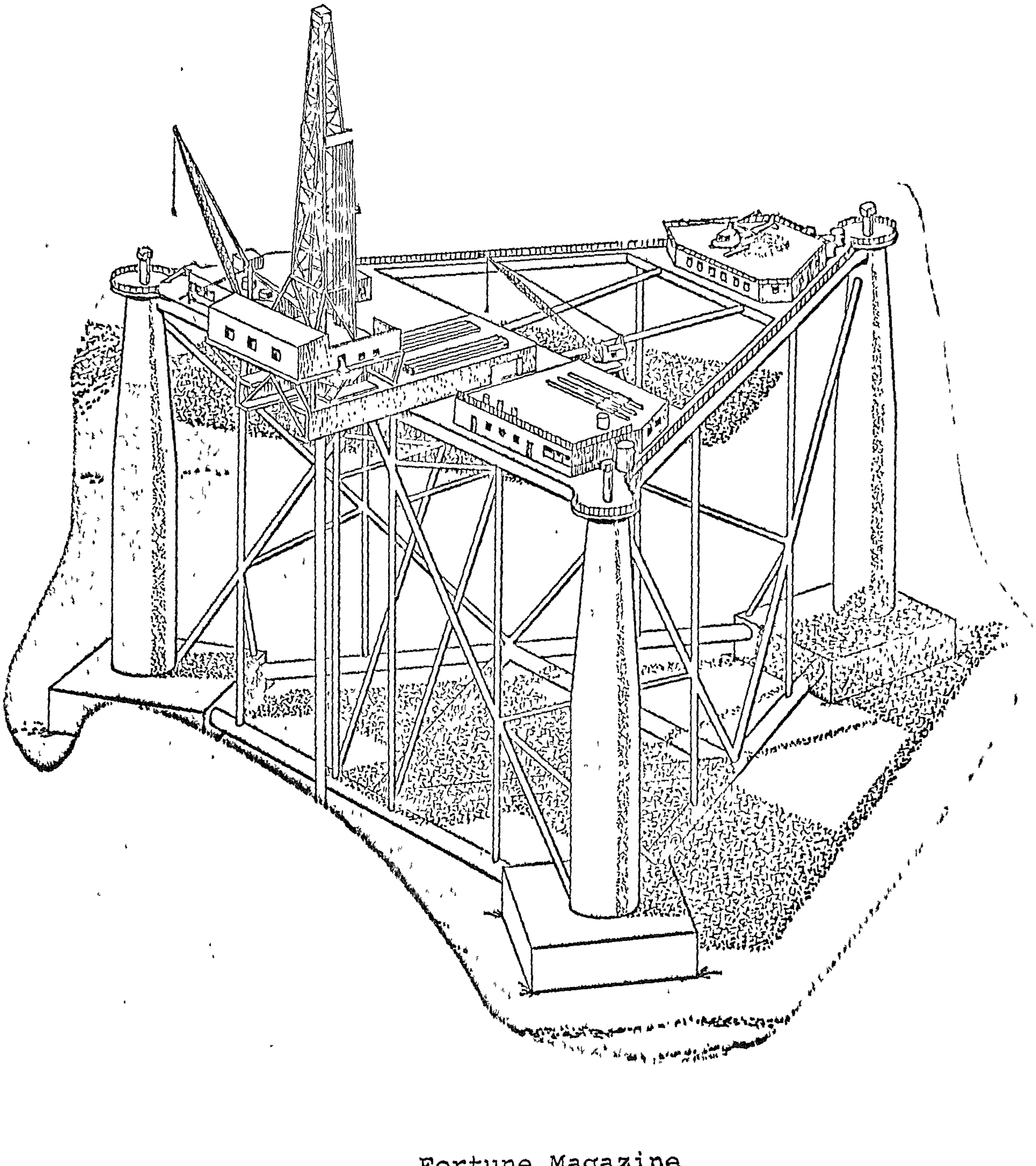

Fig I.5 Fortune Magazine
Feb. 1965

I.3.3. SUBMERSIBLE PLATFORMS

Submersible rigs initially consisted of barges which were sunk in shallow water. Nowadays their distinguishing feature is that they have a buoyant hull which is used to float the rig to the site. On site the hull is sunk to the bottom, leaving a fixed platform above. This type of rig is expensive to tow, is limited to a confined area, and is limited also to shallow depths of water (around 60 metres) . See Fig (I.6) .

I.3.4. SEMI - SUBMERSIBLE PLATFORMS

As their name might imply, semi-submersible rigs were designed for use as submersible units in shallow water or floating units in deep water. When floating, the primary buoyancy is well below the surface to minimise the effects of wave action (see section I.5 on design criteria) . But they are difficult to tow , and expensive to build, transport and insure. Depth capabilities are limited to 500 metres. See Fig (I.7) .

I.3.5. SELF - ELEVATING OR JACK-UP PLATFORMS

The advantage of jack-up rigs is the relative ease of towing them into position, by floating them on their platform-hull structure. On site, hydraulic jacks or similar lower the legs to the sea floor and then lift the platform out of the water. In the absence of piles, a large mattress-like structure may be needed if the sea bed is unstable. These rigs are very stable in operation and can drill to depths of about 100 metres.
See Figs (I.8) and (I.9) .

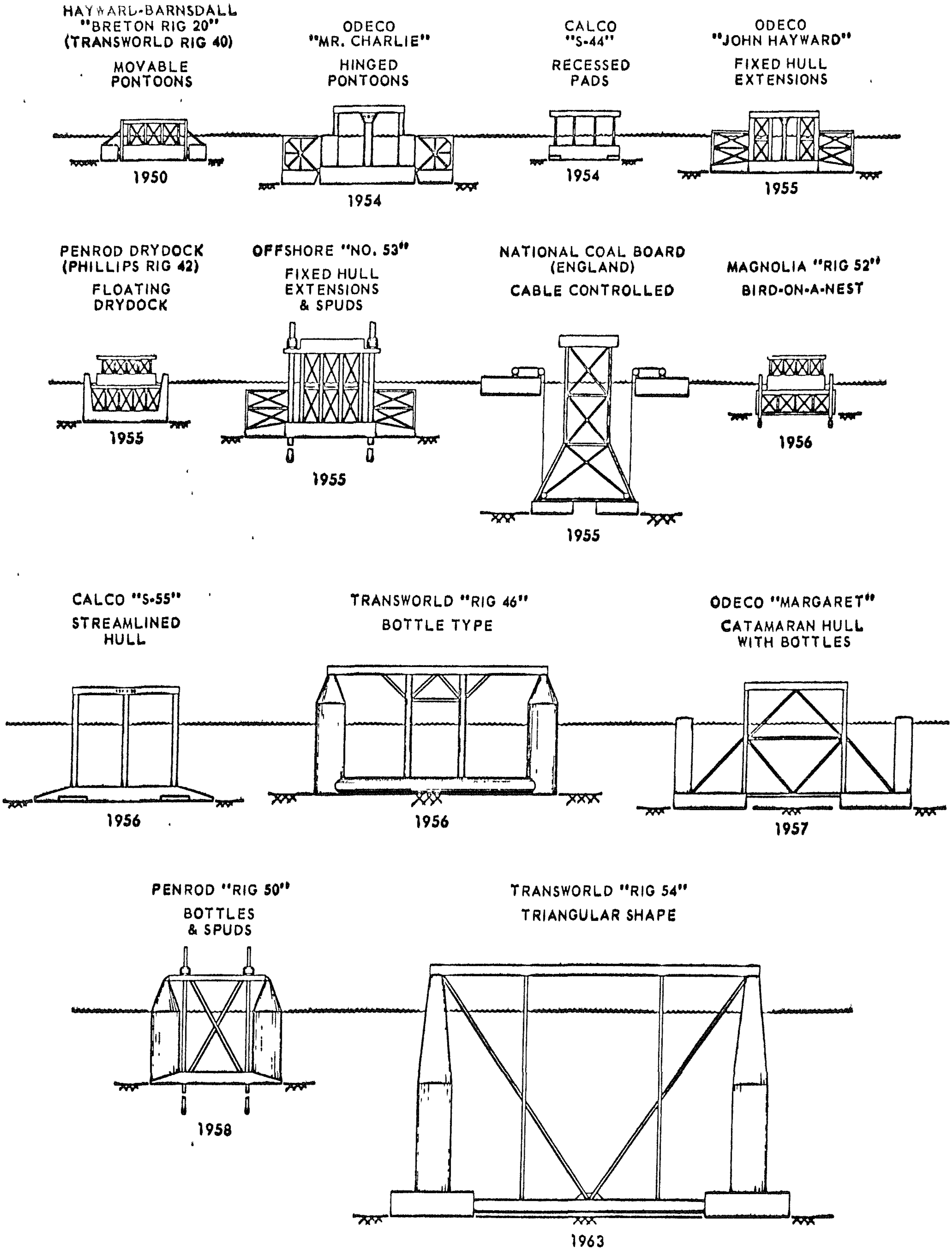

Sketches of Key Submersible Rigs.

"Development of Offshore Drilling and Production Technology" by R. J. Howe
ASME Underwater Technology Division Conference - April 30-May 3, 1967

Fig I.6

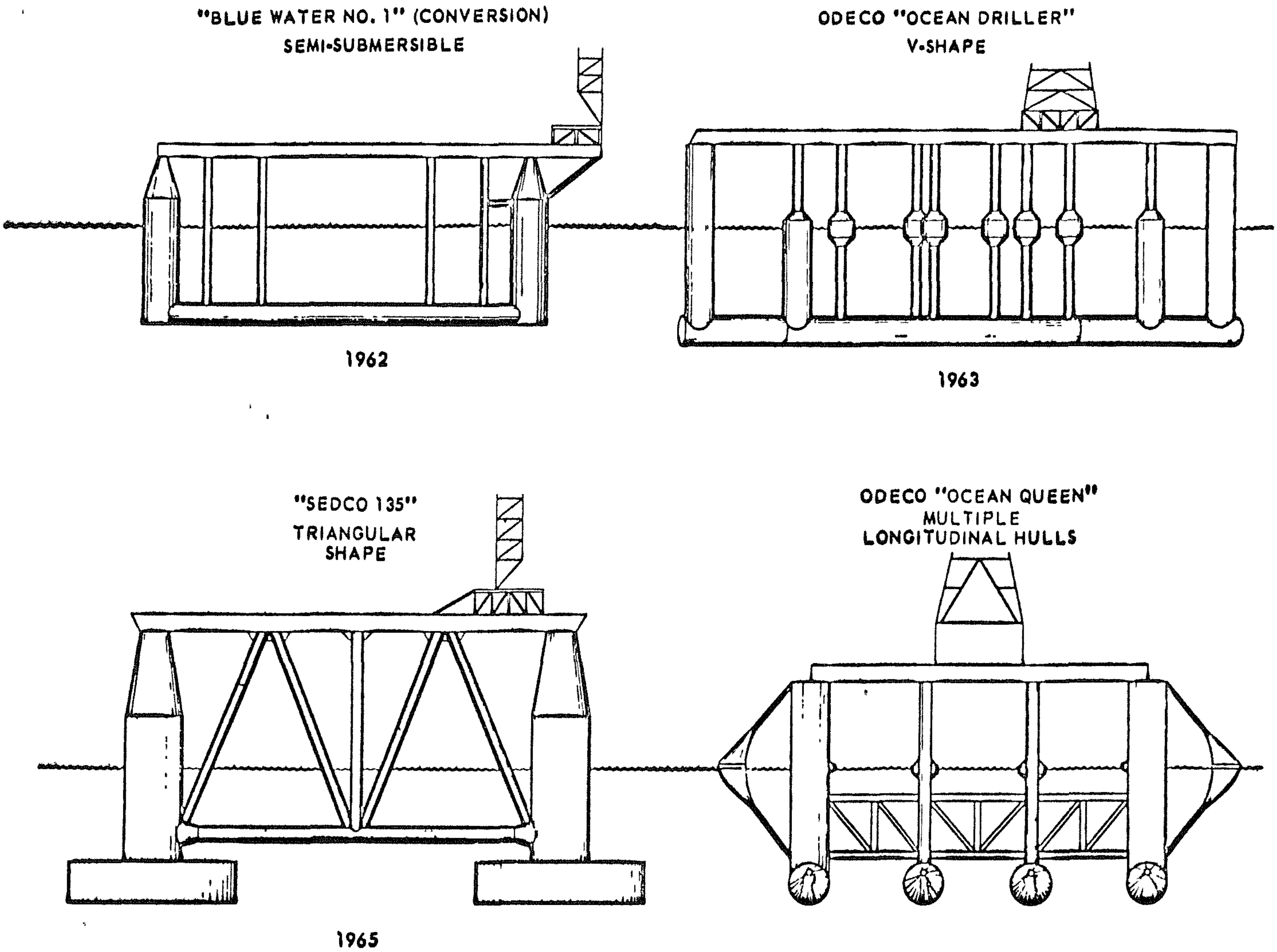

Sketches of Key Semisubmersible Rigs.

"Development of Offshore Drilling and Production Technology" by R. J. Howe
ASME Underwater Technology Division Conference - April 30-May 3, 1967

Fig I .7

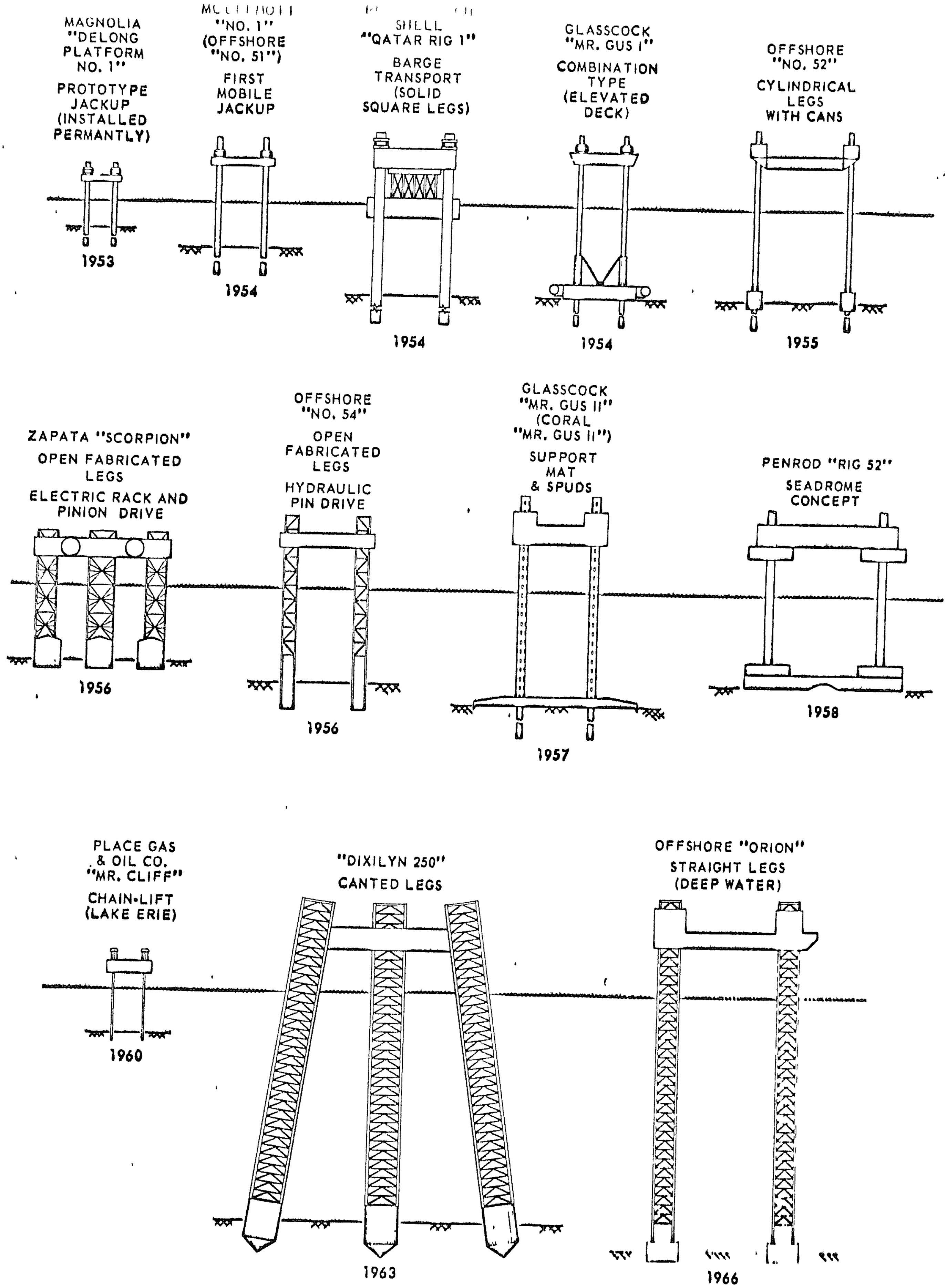

Sketches of Key Self-Elevating Rigs.

"Development of Offshore Drilling and Production Technology" by R. J. Howe
ASME Underwater Technology Division Conference - April 30-May 3, 1967

Fig 1.8

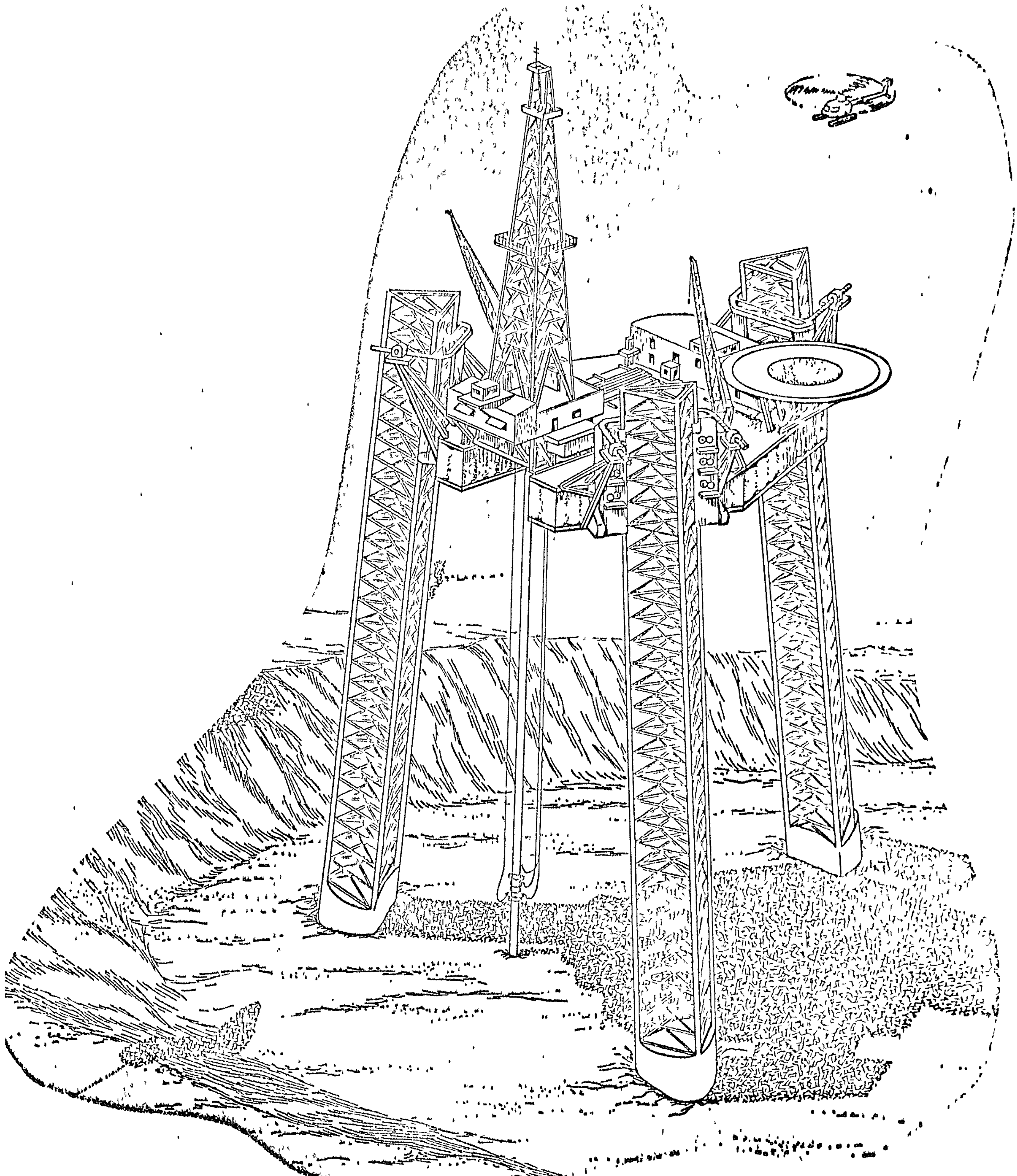

Fig I.9 *Fortune* Magazine Feb. 1965

I.3.6. FLOATING PLATFORMS

Floating platforms are likely to be used extensively for drilling in waters off the Continental Shelf (200 metres). They have been used for some time for production drilling up to 200 metres. The main stability criterion is that the drill does not deviate more than some 3 degrees from the vertical (see section I.5), and this condition is most easily met in deep water rather than shallow water, despite the fact that better mooring is possible in shallower waters. Floating platforms can be towed to position or can be self-propelled. (See Fig (I.IO)) .

I.3.7. THE FUTURE

Without a crystal ball or Churchillian foresight, it is hard to know what developments are likely in the future. One possibility for drilling in deeper waters is the submerged pressure vessel platform, which would be moored to the bottom. However, maintenance and habitability (if applicable) are the two big problems inthis area.

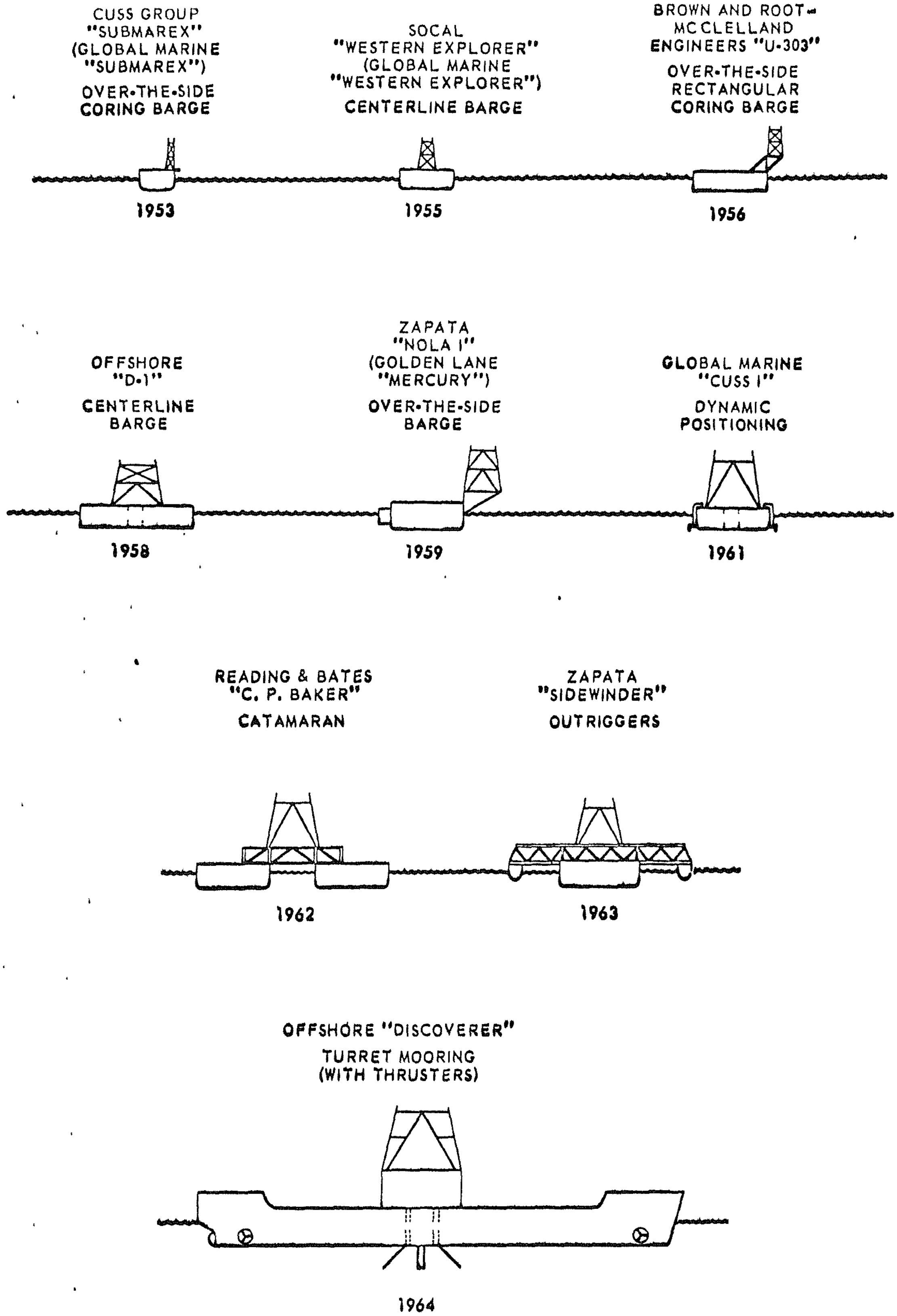

Sketches of Key Ship-Type Rigs.

"Development of Offshore Drilling and Production Technology" by R. J. Howe
ASME Underwater Technology Division Conference - April 30-May 3, 1967

Fig I.10

I.4. THE PRINCIPAL LOADS ON OFFSHORE INSTALLATIONS

I.4.I. GENERAL

Before looking at the main design considerations, we will look at the loads that might be expected on an offshore structure.

I.4.2. WAVE LOADING

Considerable attention is devoted to the subject of wave loading in Chapter 3. Essentially, waves are generated by the frictional drag of the wind on the sea surface, and their properties depend on the time the wind blows for, the strength of the wind, the distance over which the wind blows (the fetch), and the locality.

I.4.3. WIND LOADING

Wind loading usually amounts to about I0% or less of the wave loading, although in the case of hurricanes (winds with speeds of about 200 - 2I6 km/h) it is possible that the wind loading may account for a larger percentage of the total loading, particularly before a steady state is reached. The wind force may be estimated from the formula :

$$F = C_D \frac{A\, v^2 \rho}{2g} \qquad (\text{I.I})$$

where C_D is a drag coefficient

A is the projected area of the obstacle (m^2)

ρ is the density of air (I.295 kg/cu.m at 0 deg C, sea level)

g is the acceleration due to gravity (9.8057 m/sec^2)

v is the wind velocity

I.4.4. CURRENT LOADING

Current loads can be estimated using an expression similar to equation (I.I) with ρ now replaced by the density of sea water (1025 kg/m^3). The shear force due to variations of the current with depth can be considerable (produced, for example, by the Coriolis force due to the Earth's rotation) .

I.4.5. ICE LOADING

In Alaska, ice loading is regarded as more important than earthquake loading. It can take three forms - thermal, dynamic or static. The static loading case simply requires an estimate of the amount of ice on the structure, which can then be treated as a vertical load. The dynamic loading case is due to the movement of large masses of ice through the water, causing collisions with the structure. The thermal loading case is due to temperature gradients set-up by the ice.

I.4.6. IMPACT LOADING

It may be necessary to design against various types of impact loading. The berthing of a servicing vessel is an example. Movement of submarine land masses is another. Tidal waves is yet another.

I.4.7. EARTHQUAKE LOADING

In California, where much of the research on offshore structures has centred, earthquake loading has been a major consideration in design. The procedure seems to have been to analyse the structure for wave loading and earthquake loading independently. This thesis is mainly concerned with the analysis of structures for the North Sea, and earthquake loading will not be considered further.

I.5. BASIC DESIGN CONSIDERATIONS

I.5.I. INTRODUCTION

It has been a natural first step to approach the design of offshore installations by looking at ship design, since ship design has a long history. Ship stability has been extensively studied, but new problems arise if the structure has to remain stationary rather than move efficiently. A platform does not need great mobility, and therefore does not need to be ship-shaped.

The six degrees of freedom for a ship are shown in Fig (I.II), and these will be used to describe the movement of platforms also. Ship designers concentrate on eliminating heave, since they place some emphasis on their product staying afloat. Roll and pitch are also not welcome, because they cause a list or heel or trim. In the case of a platform one is interested in eliminating surge and sway also. The basic criterion encompassing all these points is that the drill should not deviate from the vertical by more than a prescribed amount - often 3 degrees. There are other criteria - the structure must be functional, structurally sound, easy to maintain, habitable (if applicable), and so on.

Firstly, a closer look at the factors determining the minimisation of the six components of motion.

I.5.2. MINIMISATION OF HEAVE, ROLL AND PITCH

There are two ways of minimising heave. Firstly, if the structure is large in horizontal directions, the forces exerted by waves

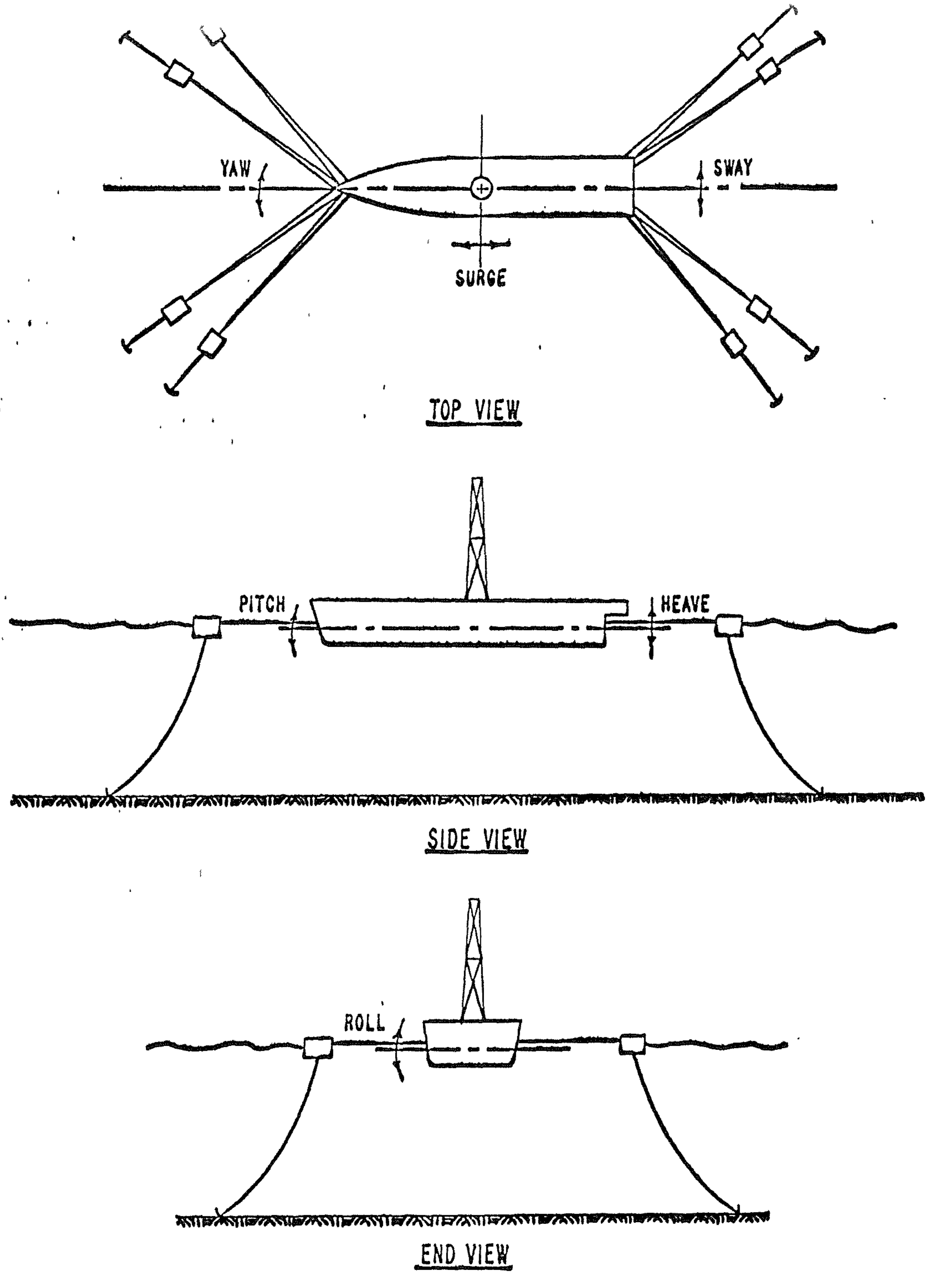

Fig I.II Six Components of Motion of a Typical Moored Vessel tending to lift one portion will be out of phase with those tending to lift another, and the structure will not respond to the waves. Unfortunately, the wave energy is such that the necessary horizontal dimension is 200 - 400 metres, which is too large for most applications. Alternatively, since the wave field varies on a smaller scale in the vertical direction, heave can be minimised by providing a large vertical extent to the structure. Spar buoys are designed on this principle. In addition, the structure should have as small a surface area at the water surface, and as large a surface area at the bottom, as possible. This is to balance vertical pressure forces, and to increase the period of vibration in heave. In this way, the period of vibration can be removed to the low energy area of the wave spectrum. This can be assisted by the use of horizontal fins, which increase the viscous drag, and hence the effective mass of the structure, and lead to a lower natural frequency.

Roll and pitch are also greatly reduced by having a large vertical extent.

I.5.3. MINIMISATION OF SURGE AND SWAY

The methods used in the previous section for reducing heave, pitch and roll are ineffective in sufficiently reducing surge and sway. In this case, a large horizontal extent to the structure is useful. Multi-legged structures can be effective in reducing surge and sway, provided that it is possible to arrange for cancellation of the principle exciting forces. Alternatively, multiple-point moorings may have to be used, but these are difficult to arrange in deep water. Propeller systems have been used, for example in the MOHOLE project (Speiss, Ref I).

I.5.4. EXAMPLES

(a) FLIP (Floating Instrument Platform) (Speiss, Ref I).

FLIP is a spar buoy which was designed with mobility in mind. Accordingly, it is towed with its long axis horizontal, and at the site it is rotated so that its long axis is vertical. It is tuned to reduce heave, and has a natural frequency of 27 seconds, which is well inside the low-energy area of the wave spectrum. It is not moored, and over a 27 day period with winds in excess of 25 km/h, it deviated 64 km from its starting position at an average speed of 0.I km/h .

(b) SEDCO I35 (Speiss, Ref I)

SEDCO I35 is a triangular drilling platform with I00 metre sides and supported by three large cylindrical legs, on the bottom of which are large foot-like tanks. This provides small waterplane area relative to large underwater volume, and hence gives a low natural frequency in heave and pitch. SEDCO can drill up to 200 metres.

I.5.5. TOWING

An additional point to remember when designing a structure that needs to be towed to its site position is that in tow it will be subjected to forces quite unlike those it will receive in use

I.6. MISCELLANEOUS DESIGN CONSIDERATIONS

In addition to the points made in section I.5, the following points may need consideration during the design process :

(a) Pile-Structure Interaction

Are relationships available for predicting the behavior of a structure-pile system under dynamic loading? In connection with this, we need to know some information on dynamic soil properties, with particular reference to the site in question. What percentage effect do different sites have on the results? Are we justified in treating the pile as a beam on an elastic foundation?

(b) Resolution of the Dynamic Results

for easy use by the designer. Is it possible to obtain an equivalent static load, or is it necessary to perform a full dynamic analysis every time?

(c) Fatigue Failure

Fatigue due to an ocean environment is a relatively new field. In the case of framed structures, fatigue failure at the joints is particularly important.

(d) Corrosion

What is the effect of corrosion on structural strength, as a function of time?

CHAPTER 2. SURFACE GRAVITY WATER WAVES

2.I. INTRODUCTION

This chapter is not intended to be an exhaustive treatment of surface gravity waves. There are several good standard texts which provide this. The aim here is to set down the relevant equations concisely, so that the assumptions used for each wave theory can clearly be seen in relation to one-another.

2.2. CONSERVATION OF MASS AND MOMENTUM

In common with other systems, sea water obeys the Principles of conservation of mass (matter cannot be created or destroyed) and conservation of momentum (Newton's second law of motion). Defining a two-dimensional coordinate system as shown, these two laws can be written as:

$$\frac{\partial \rho}{\partial t} + \frac{\partial (\rho u)}{\partial x} + \frac{\partial (\rho w)}{\partial z} = 0 \qquad (2.I)$$

Conservation of Mass

$$\left.\begin{aligned} X - \frac{1}{\rho}\frac{\partial p}{\partial x} + \frac{\partial \tau_{zx}}{\partial z} &= \frac{\partial u}{\partial t} + u\frac{\partial u}{\partial x} + w\frac{\partial u}{\partial z} \\ Z - \frac{1}{\rho}\frac{\partial p}{\partial z} + \frac{\partial \tau_{xz}}{\partial x} &= \frac{\partial w}{\partial t} + w\frac{\partial w}{\partial z} + u\frac{\partial w}{\partial x} \end{aligned}\right| \qquad (2.2)$$

Conservation of Momentum

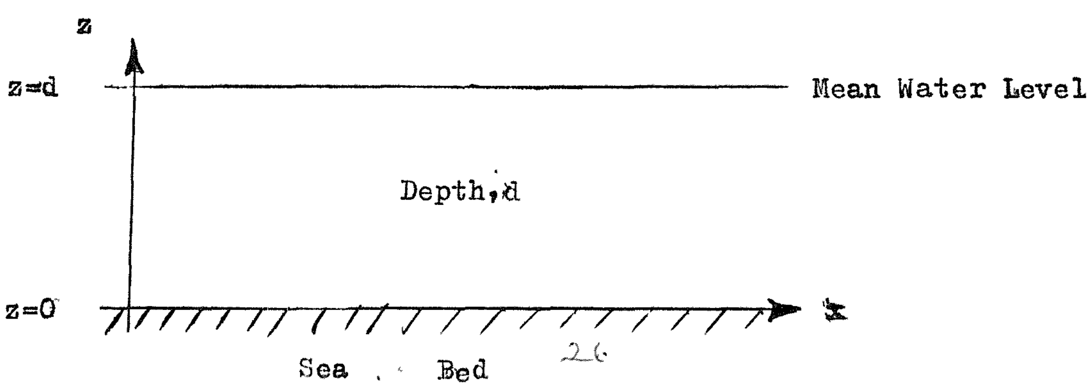

Here u and w are the horizontal and vertical components of velocity, respectively

x and z are the horizontal and vertical coordinates

ρ is the fluid density

X and Z are external body forces in the x and z directions, respectively

P is the fluid pressure

τ_{xz} and τ_{zx} are shear stresses on fluid faces normal to the x and z directions, respectively

---

In the case of sea water, all wave theories assume that the fluid is incompressible (which means that $\frac{\partial \rho}{\partial t} = 0$ in equation (2.I)) ; and the majority of theories assume that the fluid is inviscid (which means the shear stress terms in equation (2.2) are zero), and that the only body force is that due to gravity (which means that $X = 0$, $Z = -g$, in equation (2.2)). Under these assumptions, equations (2.I) and (2.2) now become:

$$\frac{\partial u}{\partial x} + \frac{\partial w}{\partial z} = 0 \tag{2.3}$$

Conservation of Mass, Incompressible Fluid

$$\left.\begin{aligned} \frac{\partial u}{\partial t} + u\frac{\partial u}{\partial x} + w\frac{\partial u}{\partial z} &= -\frac{1}{\rho}\frac{\partial P}{\partial x} \\ \frac{\partial w}{\partial t} + u\frac{\partial w}{\partial x} + w\frac{\partial w}{\partial z} &= -g - \frac{1}{\rho}\frac{\partial P}{\partial z} \end{aligned}\right| \tag{2.4}$$

Conservation of Momentum, Inviscid Fluid (Euler's Equations)

For irrotational flow (i.e. $\frac{\partial u}{\partial z} = \frac{\partial w}{\partial x}$) , equations (2.4) become:

$$\left.\begin{aligned} \frac{\partial u}{\partial t} + \frac{1}{2}\left(\frac{\partial u^2}{\partial x}\right) + \frac{1}{2}\left(\frac{\partial w^2}{\partial x}\right) &= -\frac{1}{\rho}\frac{\partial p}{\partial x} \\ \frac{\partial w}{\partial t} + \frac{1}{2}\left(\frac{\partial u^2}{\partial z}\right) + \frac{1}{2}\left(\frac{\partial w^2}{\partial z}\right) &= -g - \frac{1}{\rho}\frac{\partial p}{\partial z} \end{aligned}\right| \quad (2.5)$$

Euler's Equations, Incompressible, Inviscid Flow

The continuity and irrotational flow conditions, equations (2.3) and (2.4), can be combined using a velocity potential ϕ defined by:

$$u = \frac{\partial \phi}{\partial x} \quad ; \quad w = \frac{\partial \phi}{\partial z}$$

to give Laplace's equation

$$\frac{\partial^2 \phi}{\partial x^2} + \frac{\partial^2 \phi}{\partial z^2} = 0 \quad (2.5a)$$

Using the velocity potential, equations (2.5) can now be integrated to give Bernoulli's equation:

$$\frac{\partial \phi}{\partial t} + \frac{1}{2}\left(u^2 + w^2\right) + \frac{p}{\rho} + g(z-d) = \text{Const} \quad (2.6)$$

Bernoulli's Equation, Steady, Irrotational, Inviscid Flow

2.3. AIRY LINEAR WAVE THEORY

Airy developed a linear theory for waves whose amplitude is small compared with their wavelength and the water depth. Assuming zero vorticity, the equations to be satisfied are equations (2.3) and (2.5), in which, because of the small amplitude assumption, the convective acceleration terms $\frac{1}{2}\left(\frac{\partial u^2}{\partial x}\right)$ and $\frac{1}{2}\left(\frac{\partial w^2}{\partial x}\right)$ are zero. Equations (2.3) and (2.5) then reduce to:

$$\frac{\partial u}{\partial x} + \frac{\partial w}{\partial z} = 0 \tag{2.7}$$

Continuity

$$\left.\begin{aligned} \frac{\partial u}{\partial t} &= -\frac{1}{\rho}\frac{\partial P}{\partial x} \\ \frac{\partial w}{\partial t} &= -\frac{1}{\rho}\frac{\partial P}{\partial z} \end{aligned}\right| \tag{2.8}$$

Momentum

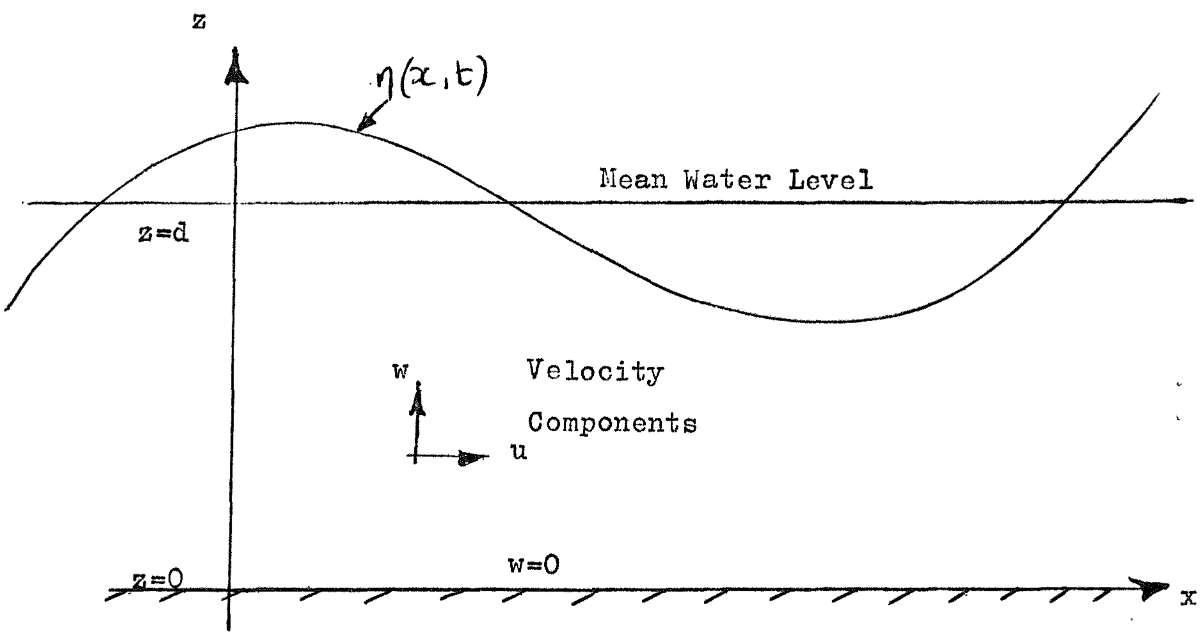

Equations (2.7) and (2.8) have to be solved subject to the following boundary conditions:

At the free surface

($z = 0$, for small amplitude waves)

$$\left.\begin{aligned} p &= p_a + \rho g \eta \\ w &= \frac{\partial \eta}{\partial t} \\ \text{On the sea bed } (z &= 0) \\ w &= 0 \end{aligned}\right| \qquad (2.9)$$

where $\eta(x,t)$ is the wave profile.

Airy assumed that $\eta(x,t)$ was sinusoidal and therefore expressible in the form:

$$\eta(x,t) = a \cos(kx-\omega t) \qquad (2.10)$$

in which $k = \frac{2\pi}{\lambda}$ is the wave number. Equations (2.7) - (2.9) then lead to the following expressions for the fluid particle velocity components u and w and the pressure p at depth z :

$$\left.\begin{aligned} u &= \frac{a\,\omega \cosh(kz) \cos(kx-\omega t)}{\sinh kd} \\ w &= \frac{a\,\omega \sinh kz \sin(kx-\omega t)}{\sinh kd} \end{aligned}\right| \qquad (2.11)$$

$$p = p_a + \rho a \frac{\omega^2 \cosh kz}{k \sinh kd} \cos(kx-\omega t) + \rho g(d-z) \qquad (2.12)$$

Using equation (2.12) and the second boundary condition we can now obtain the dispersion relation connecting w and k:

$$\omega^2 = gk \tanh kd \qquad (2.13)$$

The velocity potential ϕ, used in Laplace's equation, equation (2.5a), can easily be shown to be:

$$\phi = -\frac{a\ c \cosh kz \cos (kx-\omega t)}{\sinh kd} \qquad (2.14)$$

and equations (2.11) immediately lead to the fluid particle acceleration components $\dot{u}$ and $\dot{w}$:

$$\begin{aligned} \dot{u} &= \frac{a\ \omega^2 \cosh kz \sin (kx-\omega t)}{\sinh kd} \\ \dot{w} &= -\frac{a\ \omega^2 \sinh kz \cos (kx-\omega t)}{\sinh kd} \end{aligned} \qquad (2.15)$$

For any fixed value of x, the velocity and acceleration components are in phase for all values of z. By observing equations (2.11) and (2.15), it will be seen that they vary with z according to cosh(kz), which is essentially an exponential decay with increasing depth. Thus longer wavelengths penetrate more deeply than shorter wavelengths. The fluid particle paths are elliptical, the ellipses becoming smaller with increasing depth.

Simplifications arise when $\frac{d}{\lambda}$ is large or small. This is illustrated in Fig (2.1), which shows tanh kd plotted against ω. If ω or d is small ($\frac{d}{\lambda} < \frac{1}{20}$), tanh kd $\approx$ kd (shallow water waves) while if ω or d is large (say $\frac{d}{\lambda} > \frac{1}{2}$) , tanh kd $\approx$ 1 (deep water waves). In the first case , $\omega^2 = gk$ and in the second $\omega^2 = g\ d\ k^2$. From the curves in Fig (2.1), it would appear that one is justified in using the deep water assumption (tanh kd $\approx$ 1) for water depths greater than 25 metres over a large part of the frequency range.

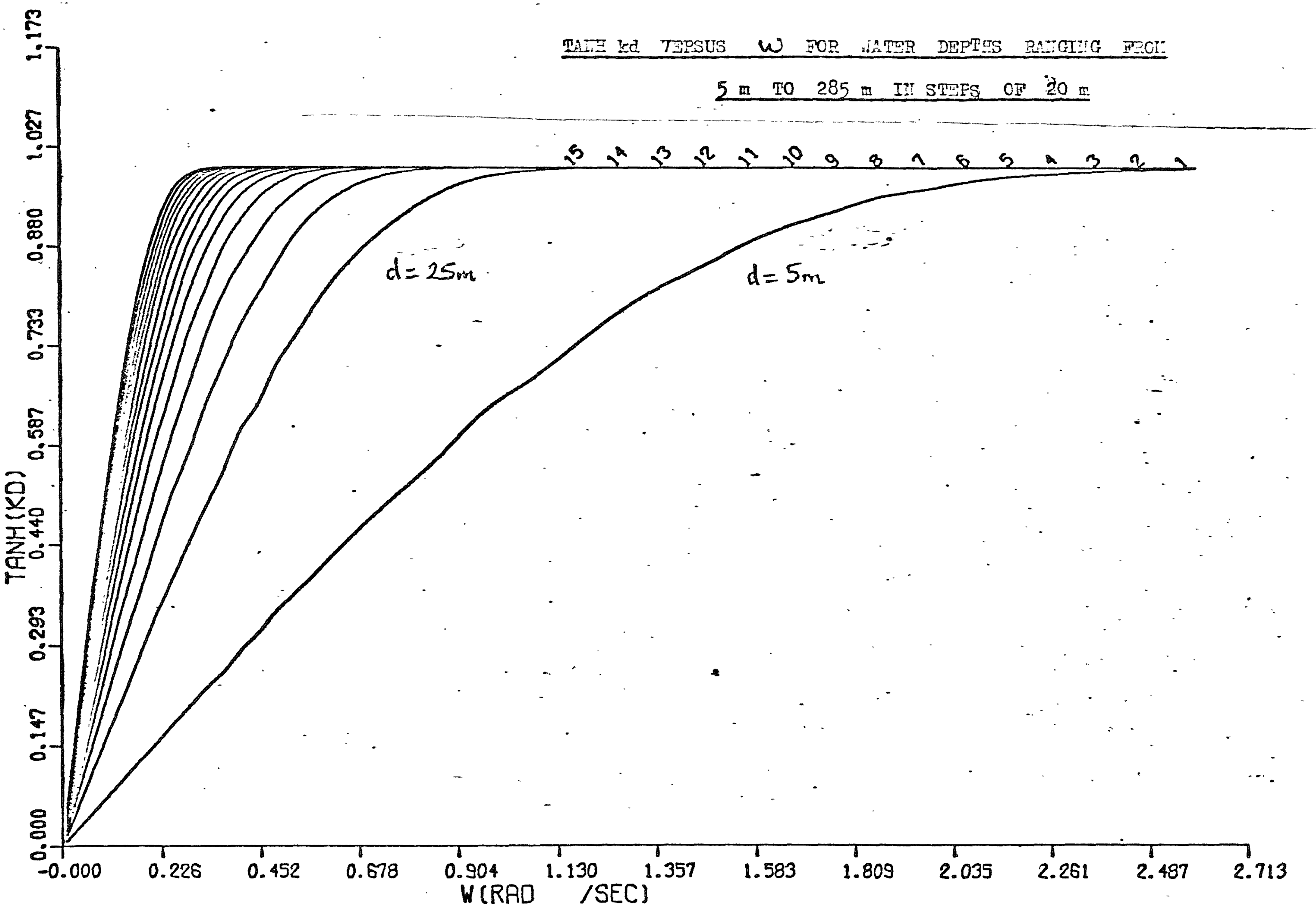
TANH kd VERSUS ω FOR WATER DEPTHS RANGING FROM
5 m TO 285 m IN STEPS OF 20 m
TANH(KD)
W(RAD /SEC)
0.000
0.147
0.293
0.440
0.587
0.733
0.880
1.027
1.173
-0.000
0.226
0.452
0.678
0.904
1.130
1.357
1.583
1.809
2.035
2.261
2.487
2.713
d = 25m
d = 5m
15
14
13
12
11
10
9
8
7
6
5
4
3
2
1

Fig 2.1

2.4. STOKES FINITE AMPLITUDE WAVES

2.4.I. BASIC EQUATIONS

The linear wave theory predicts closed fluid particle paths, and therefore no net transport of the fluid. Observations suggest, however, that there is some overall displacement of the fluid in many cases. The finite-amplitude wave theory can be taken to any desired degree of accuracy to account for this.

If the amplitude of the surface disturbance is not small relative to the depth of the water or the wavelength of the disturbance, the basic equations are:

$$\frac{\partial u}{\partial x} + \frac{\partial w}{\partial z} = 0 \tag{2.I6}$$

Continuity

$$\frac{\partial u}{\partial z} - \frac{\partial w}{\partial x} = 0 \tag{2.I7}$$

Irrotation

$$\begin{aligned} \frac{\partial u}{\partial t} + u\frac{\partial u}{\partial x} + w\frac{\partial u}{\partial z} &= -\frac{1}{\rho}\frac{\partial P}{\partial x} \\ \frac{\partial w}{\partial t} + u\frac{\partial w}{\partial x} + w\frac{\partial w}{\partial z} &= -g-\frac{1}{\rho}\frac{\partial P}{\partial z} \end{aligned} \tag{2.I8}$$

Momentum (Euler)

or alternatively, equations (2.I6) and (2.I7) can be replaced by Laplace's equation, and equation (2.I8) can be replaced by Bernoulli's equation to give :

$$\frac{\partial^2 \phi}{\partial x^2} + \frac{\partial^2 \phi}{\partial z^2} = 0 \tag{2.19}$$

$$\frac{P}{\rho} = g(z+d) + \frac{\partial \phi}{\partial t} - \frac{1}{2}\left[\left(\frac{\partial \phi}{\partial x}\right)^2 + \left(\frac{\partial \phi}{\partial z}\right)^2\right] \tag{2.20}$$

2.4.2. LINEAR THEORY

The Stokes first order approximation to the solution to equations (2.19) and (2.20) duplicates the results of section 2.3 for the Airy linear theory. The results are summarised below for ease of reference :

$$\begin{aligned}
\eta(x,t) &= a \cos (kx-\omega t) \\
\phi &= -\frac{a\, c \cosh kz \sin (kx-\omega t)}{\sinh kd} \\
u &= \frac{a\, \omega \cosh kz \cos (kx-\omega t)}{\sinh kd} \\
w &= \frac{a\, \omega \sinh kz \sin (kx-\omega t)}{\sinh kd}
\end{aligned} \tag{2.21}$$

2.4.3. STOKES SECOND ORDER THEORY

The Stokes second order theory assumes a wave profile containing sine and cosine terms in $2(kx-\omega t)$. The free surface boundary condition now has the form:

$$\frac{\partial P}{\partial t} + u\frac{\partial P}{\partial x} + w\frac{\partial P}{\partial z} = 0 \tag{2.22}$$

where the free surface means that $p(x,\eta,t) = p_a$ = constant.

The resulting expressions for the wave profile, the velocity potential, the fluid particle velocity components, the pressure and the dispersion relation are :

$$\eta(x,t) = a \cos(kx-\omega t) + \frac{k a^2 (2 + \cosh 2kd)\cosh kd}{4(\sinh kd)^3} \cos 2(kx-\omega t) \tag{2.23}$$

$$\phi = -\frac{ac \cosh kz}{\sinh kd} \sin(kx-\omega t) - \frac{3ka^2 c \cosh 2kz}{8(\sinh kd)^4} \sin 2(kx-\omega t) \tag{2.24}$$

$$u = \frac{a\omega \cosh kz}{\sinh kd} \cos(kx-\omega t) + \frac{3(ak)^2 c \cosh 2kz}{4(\sinh kd)^4} \cos 2(kx-\omega t) \tag{2.25}$$

$$w = \frac{a\omega \sinh kz}{\sinh kd} \sin(kx-\omega t) + \frac{3(ak)^2 c \sinh 2kz}{4(\sinh kd)^4} \sin 2(kx-\omega t) \tag{2.26}$$

$$p = p_a - \rho g(z-d) - \frac{\rho (a\omega)^2 \sinh kz}{2 \sinh kd} + \frac{\rho g a \cosh kz}{\cosh kd} \cos(kx-\omega t) + \frac{(a\omega)^2}{4(\sinh kd)}\left[\frac{3 \cosh 2kz}{(\sinh kd)} - 1\right] \cos 2(kx-\omega t) \tag{2.27}$$

$$\omega^2 = gk \tanh kd \tag{2.28}$$

CHAPTER 3 : WAVE FORCES ON STRUCTURES

3.I INTRODUCTION

In the previous chapter , various wave theories were considered , the objective being to predict the behaviour of surface waves through such information as fluid particle velocities and accelerations , pressures , etc..

The next objective is to try to apply this information in order to determine the forces on a structure when it is subjected to such waves . A commonly used deterministic method is to select a 'significant wave' (Sverdrup and Munk , Ref 2) , which has a height H_s defined as the average height of the highest third of all the waves considered , and to evaluate deterministically the forces corresponding to this wave . Statistical expressions can be formulated to connect H_s with H_m , the average height of all the incident waves .

Alternatively , the designer can start with the spectrum of wave energies (Pierson, Neumann and James, Ref 3) , and evaluate the forces probabalistically . This type of approach is used in section 3.5 .

In both methods of analysis , wave information has to be translated into force information before the response of the structure can be determined . This is looked at in section 3.5 . But first, let us consider the main forces on an obstacle in a fluid . Fluid dynamic forces may broadly be divided into two categories - those due to inertial effects , and those due to viscous effects. In the case of water, compressibility effects can be ignored.

These forces will now be derived using two different methods - an empirical approach, as used by Morison et al, and an analytical approach, a wave diffraction theory.

3.2 WAVE FORCES ON VERTICAL CYLINDERS - MORISON'S METHOD

3.2.I MORISON'S BASIC EQUATION

Morison et al (Ref 4) produced an equation for the horizontal force on a stationary vertical in a fluid.

Modifying this for the case of a moving cylinder, the force at depth z takes the form :

$$F(z) = C_H\,(\dot{v}-\dot{u}) + C_D\,(v-u)\left|v-u\right| + C_P\,\dot{v} \qquad (3.I)$$

where C_H is a hydrodynamic mass coefficient

C_D is a drag coefficient

C_P is a pressure gradient coefficient

to be defined later, and

v, $\dot{v}$ are the velocity and acceleration of the fluid

u, $\dot{u}$ are the velocity and acceleration of the cylinder .

By suitably modifying the coefficients C_H, C_D and C_P cylinder shapes other than circular can be analysed.

Equation (3.I) can also be written slightly differently by expressing the coefficients C_H , C_D and C_P in terms of three more fundamental coefficients. These will be defined by consideration of the inertia and drag forces in the subsequent two subsections.

3.2.2 INERTIA FORCES BY MORISON'S METHOD

It is found that of the two types of force under consideration here - inertia and drag forces - the inertia forces are the more significant for large diameter concrete structures, but that the drag forces become as important as the inertia forces for smaller diameter steel structures (see results, sects 5.4,5.5). The inertia forces are represented by the terms containing C_H and C_P in equation (3.I) . The term containing C_H is known as the hydrodynamic or added mass, and is due to the pressure produced by the relative motion between the fluid and the cylinder. In Appendix I it is shown that the added mass force F_{AM} per unit length of the cylinder is given by :

$$F_{AM} = - c_{AM} \rho V (\dot{v} - \dot{u}) \qquad (3.2)$$

where c_{AM} is an added mass coefficient

ρ is the fluid density

V is the volume of the cylinder per unit length .

It is also shown that for a circular cylinder this force becomes :

$$F_{AM} = - \rho V (\dot{v} - \dot{u})$$

In other words, $c_{AM} = I$ in this case. Added mass coefficients for other shapes of cylinder are given in Appendix I .

The term containing C_P is due to variation in the pressure within the accelerating fluid. This effect is analogous to the gravitational buoyancy force and is independent of the acceleration of the structure. In Appendix I this force is shown to be given by :

$$F_P = \rho V \dot{v} \qquad (3.3)$$

Equation (3.I) can now alternatively be written :

$$F(z) = (c_{AM} + I) \rho V \dot{v} - c_{AM} \rho V \dot{u} + \frac{c_D \rho D}{2} (v-u) |v-u| \qquad (3.Ia)$$

for circular cylinder. In Chapter 4, it will be shown that the terms in u and $\dot{u}$ in equation (3.Ia) merge with the terms in u and $\dot{u}$ in the equations of motion for the cylinder, thus leaving only the terms in v and $\dot{v}$ in the force term.

3.2.3 DRAG FORCES BY MORISON'S METHOD

The drag force term in equation (3.I) is the term containing C_D , and is proportional to the square of the relative velocity between the fluid and the structure. As such it is nonlinear. Some authors (Malhotra and Penzien, Ref 5) have replaced the drag term

$$C_D\ (v-u)\,|v-u|$$

by an 'equivalent' linear drag term

$$\bar{c}\ (v-u) \qquad (3.4)$$

where $\bar{c} \doteq C_D \sqrt{\frac{8}{\pi}}\,\sigma_{v-u}$.

The method used to obtain $\bar{c}$, and the rationalisation used in the minimisation of the errors involved , is given in Appendix I .

The drag coefficient C_D is empirical and varies with the Reynolds number ($Re = \frac{vd}{\nu}$) along a curve similar to that given in Fig (3. I) . For low Re , the drag force is almost entirely due to skin friction , which exists because of the viscosity of the fluid . For high Re , form drag dominates, form drag being due to the loss of pressure between the upstream and downstream faces of the body.

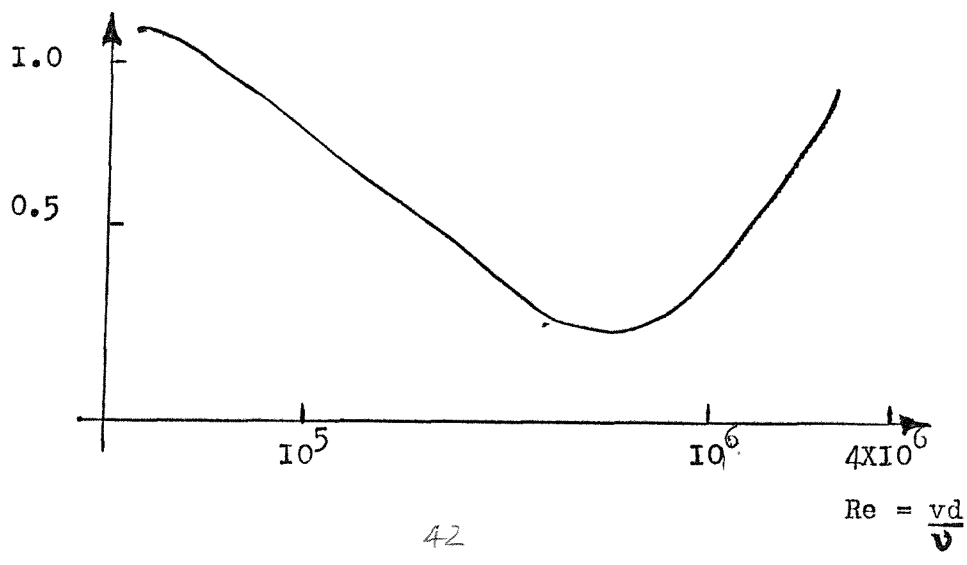

Fig 3.I

In addition to the drag force parallel to the direction of the fluid motion , there will be a force in the direction perpendicular to the flow, which is commonly known as the lift force. Some bodies, such as aerofoils, are designed for maximum lift and minimum drag, but usually the lift force is much less than the drag force for regular bodies. Another case in which there is a force perpendicular to the flow is when vortices are set up in the wake of the body. Vortices are shed alternately from side to side, the shedding frequency f of pairs of vortices being given in terms of the Strouhal Number S by :

$$f = \frac{Sv}{d}$$

where v is the fluid velocity

d is a dimension of the structure (e.g. diameter, for a circular cylinder) .

The lift force F_L due to vortex shedding is then :

$$F_L = C_L A \rho \frac{v^2}{2} \sin 2\pi ft$$

in which C_L is an experimentally determined lift coefficient.

3.3 WAVE FORCES ON VERTICAL CYLINDERS - A DIFFRACTION THEORY

3.3.I INTRODUCTION

The Morison equation, equation (3.I), is based on the assumption that the flow pattern remains unaltered due to the presence of the obstruction. This is generally taken to be the case if the structure dimension d (the diameter, in the case of a cylinder) is less than about $\frac{\lambda}{5}$, where λ is the wavelength of the incident wave. If this is not the case, a more accurate determination of the forces involved can be obtained by considering the wave diffracted from the cylinder. References are few in recent years. Morse (Ref 6) solved the diffraction problem for electromagnetic waves ; and MacCamy and Fuchs (Ref 7) presented a diffraction theory for water waves on piles. This was in 1955.

3.3.2 CALCULATION OF THE VELOCITY POTENTIAL ϕ BY THE DIFFRACTION THEORY

In common with the linear wave theory described in section 2.3, the fluid is assumed to be inviscid and irrotational, and the wave height is assumed to be small, relative to the wavelength, for any wave (this justifies ignoring second order and higher powers of $\frac{a}{\lambda}$) .

Using the same coordinates as before, with the cylinder axis lying along the z-axis, and the z-axis pointing vertically from the sea bed, which is the x-axis, the velocity potential ϕ for a plane two-dimensional wave incident from the negative x direction is given by equation (2.14) :

$$\phi = + \frac{ac \cosh kz \sin (kx-\omega t)}{\sinh kd} \qquad (3.5)$$

(N.B. If measuring z vertically upwards from the mean water level, the corresponding expression is :

$$\phi = + \frac{ga \cosh k(z+d) \sin (kx-\omega t)}{\omega \cosh kd} \qquad)$$

For simplicity it is convenient to change to polar coordinates r and θ at this stage. These are shown below, on a plan view of a cylinder with radius a_o .

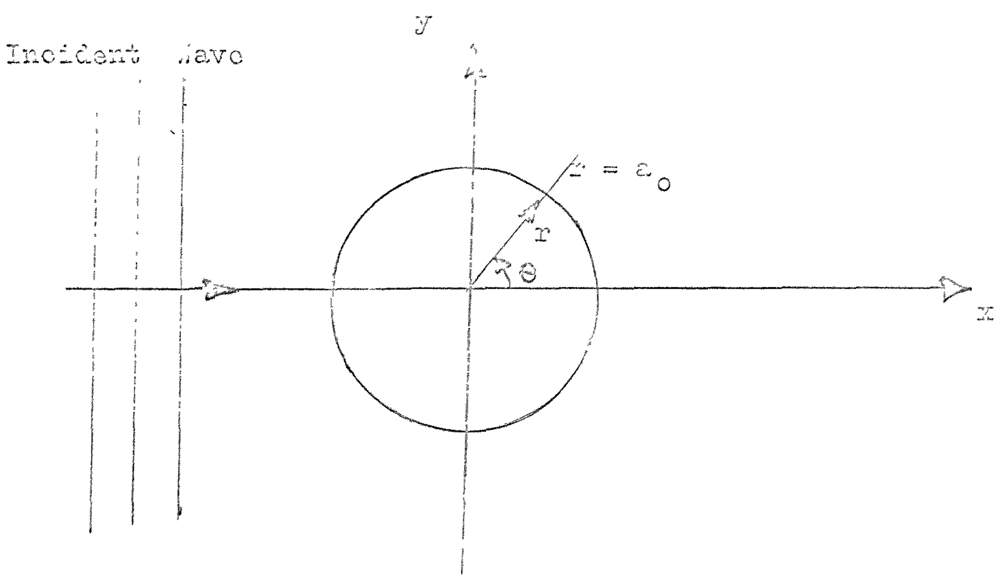

The velocity potential (in polar coordinates) is for the incident wave :

$$\phi_i = - \frac{aci \cosh kz \, e^{i(kr \cos \theta - \omega t)}}{\sinh kd} \qquad (3.6)$$

and this can be expanded as a series :

$$\phi_i = - \frac{ac \cosh kz}{\sinh kd} \sum_{-\infty}^{\infty} (i)^n J_n(kr)\, e^{i(n\theta - \omega t)} \qquad (3.7)$$

where the $J_n(kr)$ are n th order Bessel functions (see Appendix 2) .

A similar expression is assumed for the diffracted wave velocity potential ϕ_d , which must be symmetrical with respect to the incident wave. The following combination of terms is found to be satisfactory :

$$\phi_d = - \frac{ac \cosh kz}{\sinh kd}\, i \sum_{-\infty}^{\infty} \left[H_n^{(1)}(kr)\, e^{i(n\theta - \omega t)}\, \alpha_n \right] \qquad (3.8)$$

The constants α_n must be such that the total velocity potential $\phi = \phi_i + \phi_d$ satisfies the boundary condition $\frac{\partial \phi}{\partial r} = 0$ on $r = a_o$. In other words, the fluid particle velocity normal to the cylinder is zero on the surface of the cylinder. This gives :

$$\alpha_n = - \frac{(i)^n J_n'(ka_o)}{H_n^{(1)\prime}(ka_o)} \qquad (3.9)$$

$$\phi = \frac{ac \cosh kz}{\sinh kd}\, i \sum_{-\infty}^{\infty} \left[(i)^n \frac{J_n'(ka_o)\, H_n^{(1)}(kr)}{H_n^{(1)\prime}(ka_o)} - J_n(kr) \quad e^{i(n\theta - \omega t)} \right] \qquad (3.10)$$

$H_n^{(1)}(kr)$ is known as the n th order Hankel function of the first kind (See Appendix 2) , and the prime refers to differentiation with respect to the argument .

3.3.3 THE INERTIAL FORCE BY THE DIFFRACTION THEORY

Bernoulli's equation, equation (2.20), gives an expression for the pressure on a cylinder in terms of the velocity potential Φ :

$$P = \rho \frac{\partial \phi}{\partial t} - \frac{\rho}{2}\left[\left|\nabla \phi\right|^2 \right] - \rho g(z+d) \qquad (3.11)$$

In the linear diffraction theory, the terms in the square brackets are ignored, and the inertia force per unit length of the cylinder at depth z is :

$$F_z^D(\omega) = \int_0^{2\pi} \rho \frac{\partial \phi}{\partial t} \hat{x}\, a\, d\theta$$

which, on substituting for ϕ, leads to :

$$F_z^{(D)}(\omega) = \frac{4 \rho \omega^2 \cosh kz \quad \eta(\omega)}{k^2 \left| H_1^{(1)\prime}(ka) \right| \sinh kd} \qquad (3.12)$$

(See Appendix 2), where $\eta(\omega)$ is the wave profile at frequency ω, and $H_1^{(1)\prime}(ka)$ is the derivative of the Hankel function of the first kind, first order.

Comparing this with the force predicted by the Morison equation, we consider just the inertia part of equation (3.1), which gives the force per unit length of the cylinder at height z :

$$F_z^{(m)}(\omega) = (C_I + C_D) \dot{v}$$

or

$$F_z^{(m)}(\omega) = \frac{2 \rho \pi r_0^2 \omega^2 \cosh kz}{\sinh kd} \eta(\omega) \qquad (3.13)$$

provided C_M and C_f are both taken to be 1, which is a common assumption. Superfixes m and D denote forces derived by Morison's theory and the diffraction theory, respectively.

As well as the force per unit length of the cylinder, we can derive the expression for the total force on the cylinder by integrating the force per unit length over the length of the cylinder. Equations (3.12) and (3.13) then lead to :

$$F^{(m)}_{Tot}(\omega) = 2\rho\pi g a_o^2 \tanh kd \;\; \eta(\omega) \qquad (3.13a)$$

$$F^{(D)}_{Tot}(\omega) = \frac{4\rho g \tanh kd}{k^2 \left| H_1^{(1)'}(ka_o) \right|} \;\; \eta(\omega) \qquad (3.14)$$

3.3.4 THE DIFFRACTION THEORY INERTIA FORCE FOR SMALL CYLINDER RADII

For cylinders whose radii are small compared with the wavelengths of the incident waves, the expressions for the force on the cylinder can be simplified. For small ka, the Hankel function

$$\left| H_1^{(1)\prime}(ka) \right| = \sqrt{J_1^{\prime}(ka)^2 + Y_1^{\prime}(ka)^2}$$

becomes

$$\left| H_1^{(1)\prime}(ka) \right| = \frac{2}{(ka)^2 \pi}$$

and equations (3.12) and (3.14) for the force per unit length and the total force on the cylinder, respectively, now become :

$$F_z^{(D)}(\omega) = \frac{2 \rho \pi a_o^2 \omega^2 \cosh kz}{\sinh kd} \eta(\omega) \qquad (3.17)$$

and

$$F_{Tot}^{(D)}(\omega) = 2 \rho \pi g a_o^2 \tanh kd \; \eta(\omega) \qquad (3.18)$$

which agree well with the corresponding results from the Morison theory, equations (3.13) and (3.13a) .

3.4 WAVE FORCES ON AN INCLINED CYLINDER

3.4.I NORMAL FORCES ON AN INCLINED CYLINDER

Morison's equation, equation (3.I), gave an expression for the force per unit length on a vertical cylinder at a height z above the sea bed. This was of the form :

$$F(z) = C_H\ (\dot{v}-\dot{u}) + C_D\ (v-u) \left| v-u \right| + C_P\ \dot{v} \qquad (3.19)$$

If the cylinder is inclined at an angle θ to the horizontal, equation (3.I9) may be modified to :

$$F_n(z) = C_H\ (\dot{v}_n-\dot{u}_n) + C_D\ (v_n-u_n) \left| v_n-u_n \right| + C_P\ \dot{v}_n \qquad (3.20)$$

where the suffix n denotes the component normal to the cylinder in each case .

For example, if the cylinder is stationary and has circular cross-section, equation (3.20) becomes :

$$F_n(z) = C_M \rho \frac{\pi D^2}{4} \dot{v}_n + C_D \frac{\rho}{2} D\ v_n \left| v_n \right| \qquad (3.21)$$

where D is the cylinder diameter and C_M is the inertia coefficient, often taken as two .

In terms of θ , the normal component of the fluid particle velocity, v_n , is given by :

$$v_n = u \sin\theta - w \cos\theta \qquad (3.22)$$

where u and w are the horizontal and vertical components of the fluid particle velocity, respectively .

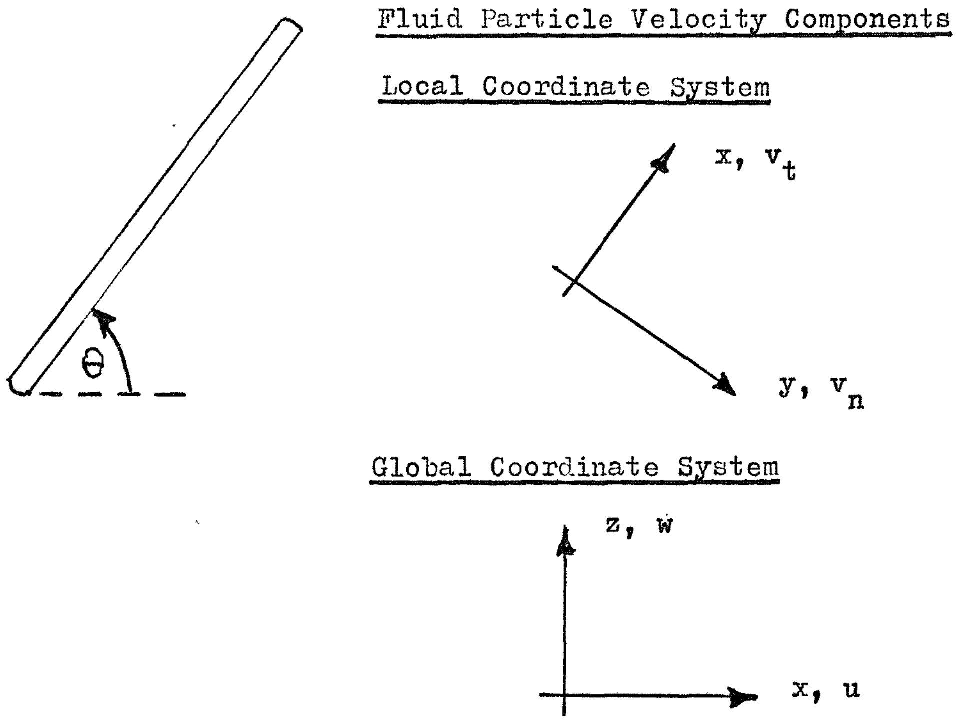

3.4.2 TANGENTIAL FORCES ON AN INCLINED CYLINDER

The fluid particle velocity component tangential to the cylinder is given in terms of u and w by :

$$v_t = u \cos \theta + w \sin \theta \tag{3.23}$$

and in terms of v_t , the tangential force per unit length of the cylinder is given by :

$$F_t(z) = C_{D_t} \frac{\rho \pi}{2} D \, v_t \left| v_t \right| \tag{3.24}$$

where C_{D_t} is a tangential drag coefficient.

This applies to a stationary circular cylinder. An equation analogous to equation (3.20) is applicable to a moving non-circular cylinder.

References are few on the subject of flow past inclined cylinders. Skjelbreia and Hendrickson (Ref 8) use a concept similar to the tangential drag coefficient one, but give no mention of how to find the drag coefficient. Clearly, it is best found experimentally, and, equally clearly, most designers probably ignore the tangential force term on the basis that the normal force is very much larger (expectedly) .

3.5 STATISTICAL REPRESENTATION WAVE FORCES

3.5.I INTRODUCTION

The sea is very difficult to describe analytically, even with very simple models, and modern philosophy accepts that it is probably not too important to be able to do so. Today's designer of offshore installations has concepts that are perhaps more intuitive than the purely deterministic ones.

It is useful to think of the irregular sea surface as the sum of many ideal sine waves of different lengths and heights, from which it is possible to count the number of waves of a certain height and frequency. The sea is then described by a wave height spectrum, compiled from many such observations, from which the designer can see the frequencies at which most of the sea's energy occurs.

This spectral characterisation of the sea is now widely used, since it emphasizes precisely those statistical properties that distinguish one irregular sea state from another. It is also useful in calculating the propagation of waves from the generating area to the object area.

The problem is how to relate a wave height spectrum to a spectrum describing the force on the structure. This will be looked-at in section 3.5.4, et seq , but first we will examine the wave height spectrum.

3.5.2 WAVE HEIGHT SPECTRA

A considerable amount of work has gone into collecting data on the sea, and one of the first things to be done was to try to fit the data collected to an empirical formula, so that for any given set of conditions (wind speed, locality, fetch, etc.) it would not be necessary to keep taking a lot of measurements. Two of the most popular wave height spectra formulae are those due to Bretschneider (Ref 9) and Pierson and Moskowitz (Ref IO). Bretschneider wave spectra are shown in Fig (3.2). For unit significant wave height, the spectra are given by :

$$S_{\eta\eta}(\omega) = \frac{1012}{\omega^5} \exp \left(- 1035 \left[\omega T_s\right]^{-4} \right) \qquad (3.25)$$

where T_s is the significant wave period.

Pierson-Moskowitz spectra are shown in Fig (3. 3) and are given by the expression :

$$S_{\eta\eta}(\omega) = \frac{A}{\omega^5} \exp \left(- B\, \omega^{-4} \right) \qquad (3.26)$$

The Pierson-Moskowitz spectrum is the one which will be used throughout this thesis, and its properties are analysed in Appendix 4, where it is also shown that the Bretschneider spectrum agrees well with the Pierson-Moskowitz spectrum .

BRETSCHNEIDER WAVE HEIGHT SPECTRA (UNIT SIGNIFICANT WAVE HEIGHT)

$$S_{\eta\eta}(\omega) = \frac{1012}{\omega^5}\,\exp\left(-1035\left[\omega T_s\right]^{-4}\right)$$

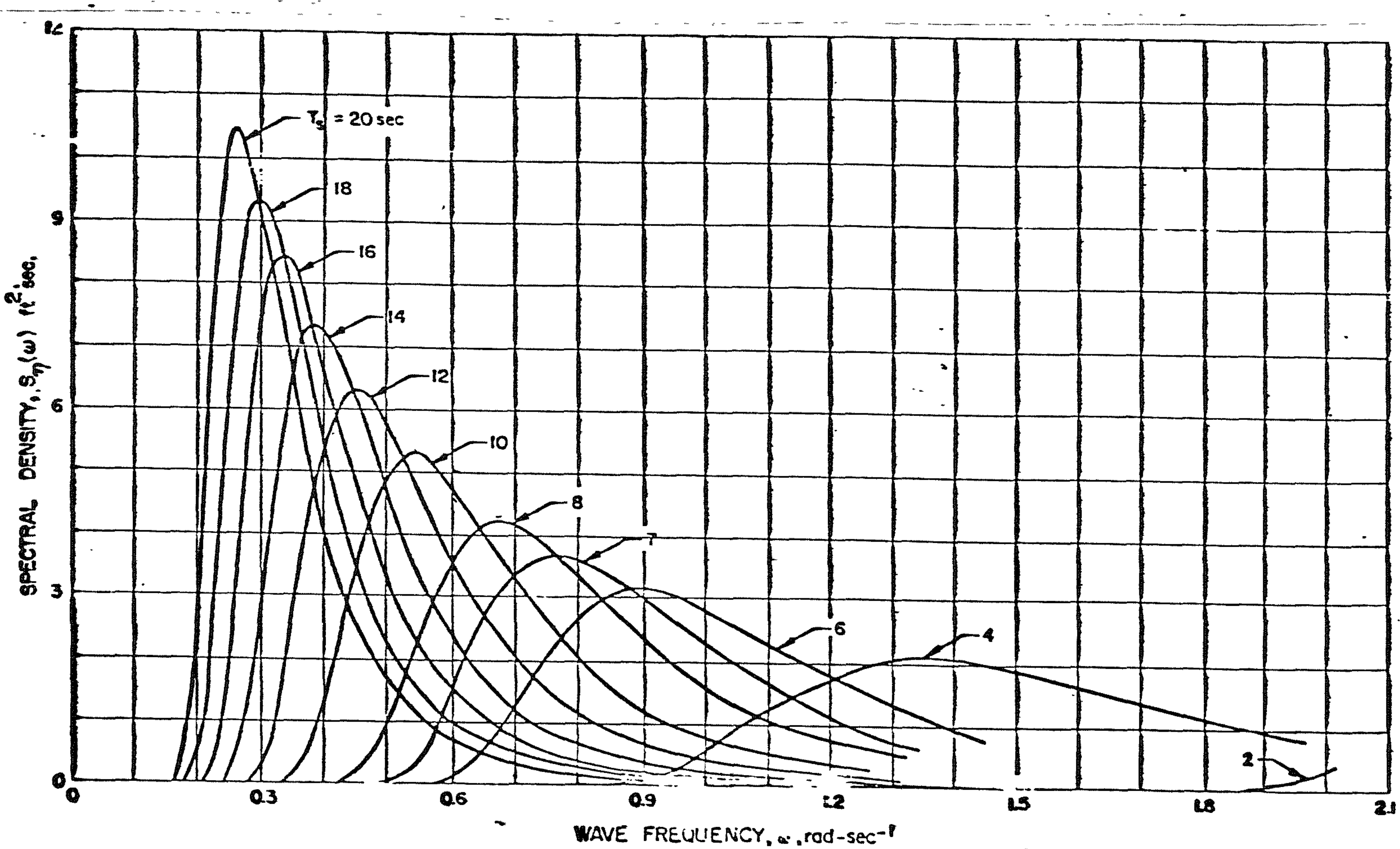

Fig 3.2

PIERSON - MOSKOWITZ WAVE HEIGHT SPECTRA

$$S_{\eta\eta}(\omega) = \frac{A}{\omega^5} \exp\left(\frac{-B}{\omega^4}\right)$$

Curve	A	B	H_s (m)	T_M (sec)
I	2.560	0.0299	I8.5	II.35
2	2.940	0.0754	I2.5	9.0I
3	3.0I5	0.I488	9.0	7.60
4	0.7793	0.0085	I9.I	I5.52
5	0.7793	0.I353	4.8	7.78
6	0.779I	0.6850	2.I	5.I9

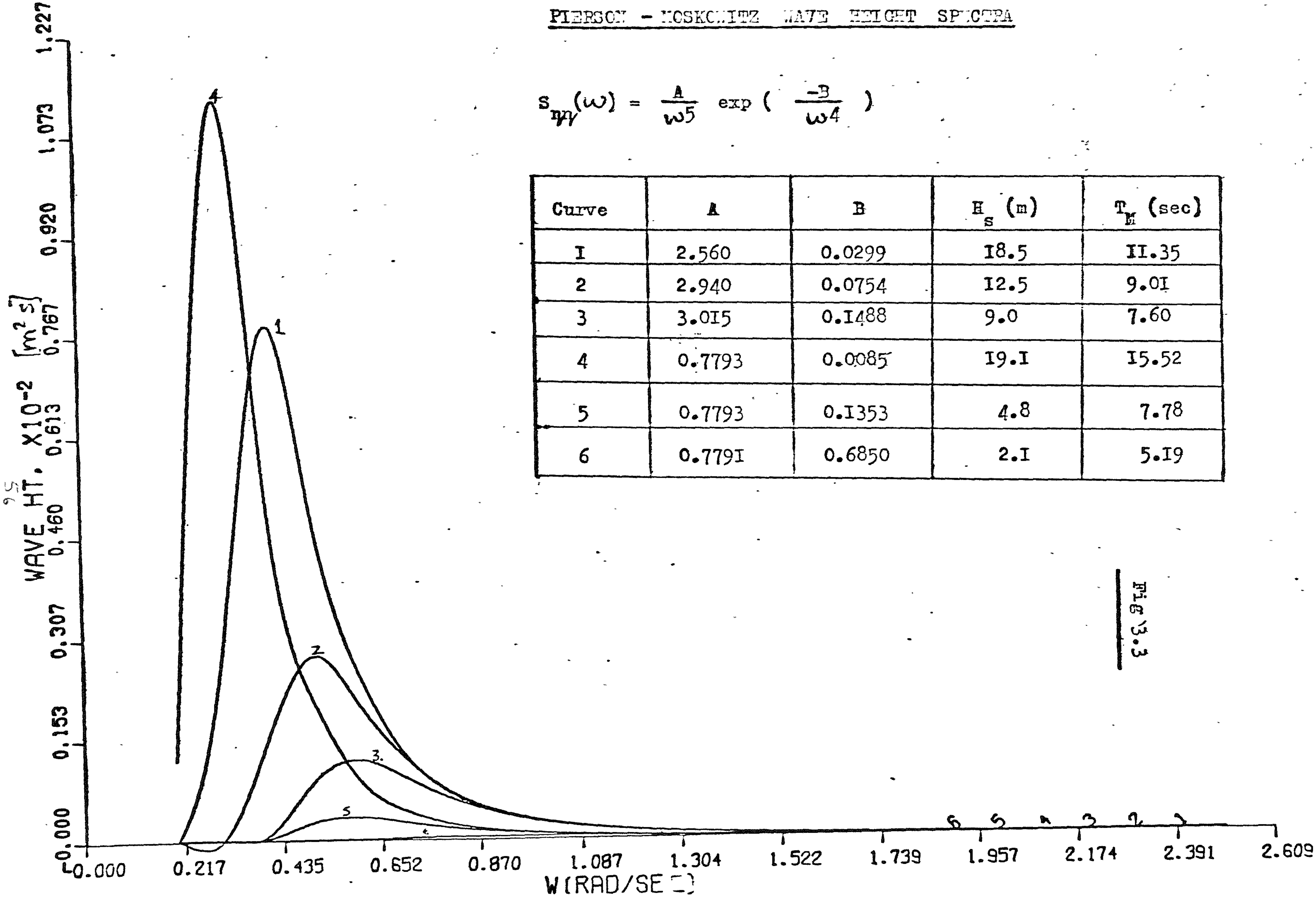

Fig 3.3

The following are some general observations on the form of the spectra shown in Figs (3. 2) and (3. 3) :

(i) Wave periods range from about 5 to 30 seconds . The energy distribution varies smoothly across the spectrum with a principle peak in the period range I.5 - 6 seconds (dependent on wind speed, fetch, wind duration, etc.) .

(ii) The total wave energy (area under the curve) increases rapidly with the wind speed . Some authors replace B by $\left[\frac{\beta g}{W}\right]^4$ in the Pierson-Moskowitz spectrum, equation (3.26), where W is the wind speed . There is therefore a dependence on W^4 inside the exponential of the Pierson-Moskowitz expression .

(iii) There are many waves with frequency greater than the peak frequency, but very few with frequency less than the peak value .

(iv) Waves at peak frequency travel slightly faster than the wind speed, but the majority of the wave energy appears as waves travelling with speeds less than the wind speed.

(v) Energy does not appear to be correlated from one frequency another, which leads to an approximately Gaussian distribution of wave amplitudes .

Having noted some general properties of the wave spectra in Figs (3. 2) and (3. 3) , we will now look more closely at the properties of the Pierson- Moskowitz spectrum .

3.5.3 THE PIERSON - MOSKOWITZ WAVE HEIGHT SPECTRUM

The Pierson - Moskowitz spectrum will later be used with the theory of Chapter 4 in a computer programme for analysing framed structures subjected to random wave loading. The spectrum is described by equation (3.26) and the main problem is how to determine the constants A and B. In Appendix 4 it is shown that A and B are related to the significant wave height H_s, defined as the mean height of the highest third of the waves, and the mean wave period T_M by the expressions :

$$B = \frac{496}{T_M^4} \qquad A = \frac{124\, H_s^2}{T_M^4} \tag{3.27}$$

The significant wave height H_s can be estimated, for a narrow band spectrum, from the most probable maximum wave height in a 10 minute interval, H_{Max}, from the expression:

$$H_{Max} \approx 1.6\, H_s \tag{3.28}$$

The mean wave period T_M is related to the most commonly occuring wave period T_O by the expression :

$$T_O = 1.41\, T_M \tag{3.29}$$

T_0 and H_{Max} are available in contour map form from The National Institute of Oceonography (Ref II), and so via equations (3.28), (3.29) and (3.27) the constants A and B of the Pierson-Moskowitz spectrum can be obtained .

3.5.4 FLUID PARTICLE VELOCITY AND ACCELERATION SPECTRA

In the previous section, the wave height spectrum $S_{nn}(\omega)$ was discussed, and it will now be shown how this can be used to find spectra for wave forces . Some statistical definitions are given in Appendix 3 . Firstly, it is necessary to consider the fluid particle velocity and acceleration and to see how they relate to the wave height.

The horizontal and vertical components of fluid particle velocity are given, according to the linear theory, by equations (2.II) :

$$u = \frac{a\,\omega \cosh kz \;\; \cos(kx-\omega t)}{\sinh kd}$$

$$w = a\,\omega \sinh kz \;\; \sin(kx-\omega t) \qquad (3.30)$$

or

$$u = A \;\; \eta(x,\omega)$$

$$w = B \;\; \eta(x,\omega)$$

where $\eta(x, \omega)$ is the wave profile. It is known that if u and η are related by an equation of the form of equations (3.30), then their spectral densities are related by an equation of the form :

$$S_{uu}(\omega) = A^2 S_{\eta\eta}(\omega) = \frac{\omega^2 \cosh^2 kz}{\sinh^2 kd} \quad S_{\eta\eta}(\omega)$$

Likewise

$$S_{ww}(\omega) = B^2 S_{nn}(\omega) = \frac{\omega^2 \sinh^2 kz}{\sinh^2 kd} \quad S_{\eta\eta}(\omega) \tag{3.31}$$

Similarly, a cross-spectral density $S_{wu}(\omega)$ can be defined :

$$S_{wu}(\omega) = \frac{\omega^2 \cosh kz \ \sinh kz}{\sinh^2 kd} \quad S_{\eta\eta}(\omega)$$

In a like manner, equations (2.15) for the horizontal and vertical fluid particle accelerations yield the following acceleration spectral densities :

$$S_{\dot{u}\dot{u}}(\omega) = \frac{\omega^4 \cosh^2 kz}{\sinh^2 kd} \quad S_{\eta\eta}(\omega)$$

$$S_{\dot{w}\dot{w}}(\omega) = \frac{\omega^4 \sinh^2 kz}{\sinh^2 kd} \quad S_{\eta\eta}(\omega) \tag{3.32}$$

$$S_{\dot{w}\dot{u}}(\omega) = \frac{\omega^4 \sinh kz \ \cosh kz}{\sinh^2 kd} \quad S_{\eta\eta}(\omega)$$

We can now consider the spectral density of the normal fluid particle velocity u_n to a cylinder inclined to the horizontal at an angle θ. Recalling equation (3.22) of section 3.4.I, we know that :

$$u_n = u \sin\theta - w \cos\theta = u' - w', \text{ say} \qquad (3.22a)$$

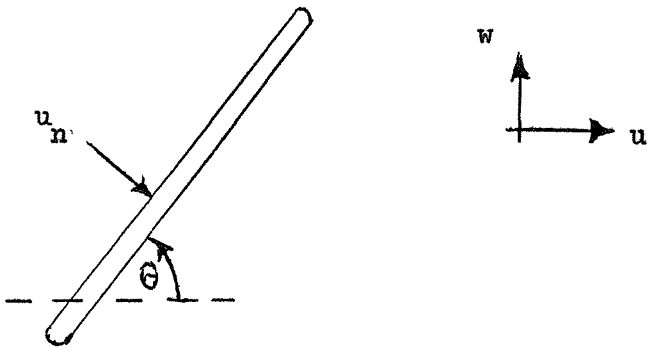

Fluid Particle Velocity Components

The spectral density of u_n can then be written :

$$S_{u_n u_n}(\omega) = S_{u'u'}(\omega) - 2\, S_{u'w'}(\omega) + S_{w'w'}(\omega)$$

$$= \left[\omega^2 \cosh^2 kz \sin^2\theta - 2\,\omega^2 \sinh kz \cosh kz \sin\theta \cos\theta + \omega^2 \sinh^2 kz \cos^2\theta\right] \frac{S_{\eta\eta}(\omega)}{\sinh^2 kd} \qquad (3.33)$$

Similarly, the spectral density of the fluid particle normal acceleration $\dot{u}_n$ is given by :

$$S_{\dot{u}_n \dot{u}_n}(\omega) = S_{\dot{u}'\dot{u}'}(\omega) - 2\, S_{\dot{u}'\dot{w}'}(\omega) + S_{\dot{w}'\dot{w}'}(\omega)$$

$$= \left[\omega^4 \cosh^2 kz \sin^2\theta - 2\,\omega^4 \sinh kz \cosh kz \sin\theta \cos\theta + \omega^4 \sinh^2 kz \cos^2\theta\right] \frac{S_{\eta\eta}(\omega)}{\sinh^2 kd} \qquad (3.34)$$

Graphs of $S_{uu}(\omega)$, $S_{ww}(\omega)$ and $S_{wu}(\omega)$ are given in Appendix 8, along with graphs of $S_{u_n u_n}(\omega)$ for various values of θ, the angle of inclination. The graphs of S_{uu}, S_{ww} and S_{wu} confirm the fact that if z is large compared with d, then $\sinh kz = \cosh kz$ (i.e. $\tanh kz = I$), since all the spectra are the same.

Using this assumption in equation (3.33), we can write :

$$S_{u_n u_n}(\omega) = \frac{\omega^2 \cosh^2 kz}{\sinh^2 kd} \left[\sin^2\theta - 2\sin\theta\cos\theta + \cos^2\theta\right] \times S_{\eta\eta}(\omega)$$

$$= \frac{\omega^2 \cosh^2 kz}{\sinh^2 kd} \left[1 - \sin 2\theta \right] S_{\eta\eta}(\omega) \tag{3.33a}$$

which shows that the spectrum of the normal fluid particle velocity reaches a minimum when $\theta = 45$ deg.

The expression for $S_{\dot{u}_n \dot{u}_n}$ can be obtained by replacing ω^2 by ω^4 in equation (3.33a).

Equations (3.3I) - (3.34) will be used in the next section to find the necessary wave force spectral densities .

3.5.5 WAVE FORCE SPECTRAL DENSITIES

In sections 3.2, 3.3 and 3.4, various expressions were derived for the force per unit length on a cylinder immersed in a fluid (equations (3.I), (3.I2) and (3.2I)) .

(a) Consider first the Morison expression, equation (3.I) . To avoid over-complicating the notation, the cylinder will be assumed to be stationary, and in Chapter 4 it will be seen that if the cylinder is moving it does not affect the theory of this section . Thus the Morison equation can be written :

$$F = K\dot{v} + C\, v|v| \tag{3.35}$$

where $K = C_M \rho V$, $C = \frac{1}{2} C_D \rho V$, and C_M is the inertia coefficient (containing the added mass coefficient) , which is often taken as 2 .

Borgman (Ref I2) derived an expression for the autocorrelation function $R_{FF}(\tau)$ of the force F as given by equation (3.35) . This is of the form :

$$R_{FF}(\tau) = C^2 \sigma_v^4\, G(R_{vv}(\tau) / \sigma_v^2) + K^2 R_{\dot{v}\dot{v}}(\tau) \tag{3.36}$$

(statistical definitions are in Appendix 3) in which $G(r) = \left[(2+4r^2) \arcsin(r) + 6r\sqrt{I-r^2} \right] / \pi$

and $\sigma_v^2 = \int_0^\infty S_{vv}(\omega)\, d\omega$.

This reduces to :

$$R_{FF}(\tau) = \frac{8}{\pi} C^2 \sigma_v^2 R_{vv}(\tau) + K^2 R_{\dot{v}\dot{v}}(\tau) \qquad (3.37)$$

on making the approximation $G(r) = \frac{8}{\pi}$.

Transforming equation (3.36) gives the spectral density of F :

$$S_{FF}^{(m)}(\omega) = \underbrace{\frac{8}{\pi} C^2 \sigma_v^2 S_{vv}(\omega)}_{\text{Drag}} + \underbrace{K^2 S_{\dot{v}\dot{v}}(\omega)}_{\text{Inertia}} \qquad (3.38)$$

$S_{vv}(\omega)$ and $S_{\dot{v}\dot{v}}(\omega)$ were discussed in the previous section . For an inclined cylinder, $S_{vv}(\omega)$ and $S_{\dot{v}\dot{v}}(\omega)$ are given by $S_{u_n u_n}(\omega)$ and $S_{\dot{u}_n \dot{u}_n}(\omega)$, respectively (equations (3.33) and (3.34)) . For a vertical cylinder, these expressions can still be used, although in this case they reduce to the simpler expressions $S_{uu}(\omega)$ and $S_{\dot{u}\dot{u}}(\omega)$, respectively (equations (3.3I) and (3.32)) .

(b) Consider next the diffraction theory expression for the force on the cylinder , equation (3.I2) :

$$F_z(\omega) = \frac{4 \rho \omega^2 \cosh kz \quad \eta(x, \omega)}{k^2 \left| H_I^{(I)\prime}(ka) \right| \sinh kd} \tag{3.39}$$

where for simplicity only the inertia term is being considered here (This is thought to be a reasonable assumption. In most ocean engineering applications, the inertia term dominates quite considerably over the drag term. Equation (3.39) leads to a force spectral density given by :

$$S_{FF}^{(D)}(\omega) = \frac{I6 \rho^2 \omega^4 \cosh^2 kz}{k^4 \left| H_I^{(I)}(ka) \right|^2 \sinh^2 kd} \quad S_{\eta\eta}(\omega) \tag{3.40}$$

Superfixes D and m denote spectra for the diffraction theory and Morison's theory, respectively .

3.5.6 A COMPARISON BETWEEN THE MORISON AND DIFFRACTION THEORY FORCE SPECTRA

(a) It is interesting to compare equations (3.38) and (3.40) for the force spectral density by Morison's equation and the diffraction theory, respectively. Rewriting equation (3.38), taking only the inertia term, and replacing K by $2\rho\pi a^2$, we get, for a vertical circular cylinder :

$$S_{FF}^{(m)}(\omega) = \frac{4\rho^2 a^4 \pi^2 \omega^4 \cosh^2 kz}{\sinh^2 kd} \quad S_{\eta\eta}(\omega) \tag{3.41}$$

while the diffraction theory gives :

$$S_{FF}^{(D)}(\omega) = \frac{16\rho^2 \omega^4 \cosh^2 kz}{k^4 \left| H_1^{(1)'}(ka)\right|^2 \sinh^2 kd} \quad S_{\eta\eta}(\omega) \tag{3.42}$$

These are the spectral densities of the force per unit length of the cylinder. The corresponding expressions for the total force on the cylinder are obtained from equations (3.13a) and (3.14) and are :

$$S_{F_{Tot}F_{Tot}}^{(D)}(\omega) = \frac{16\rho^2 g^2 \tanh^2 kd}{k^4 \left| H_1^{(1)'}(ka)\right|^2} \quad S_{\eta\eta}(\omega)$$

$$S_{F_{Tot}F_{Tot}}^{(m)}(\omega) = 4\rho^2 g^2 \pi^2 a^4 \tanh^2 kd \quad S_{\eta\eta}(\omega) \tag{3.43}$$

(b) The two force spectra given by equations (3.41) and (3.42) have been plotted on a graph plotter for a range of cylinder radii a from 0.I to 20 metres . The force spectra have then been multiplied by a response function $|\alpha(\omega)|^2$ with a peak at I.07 radns/sec to yield a displacement spectrum corresponding to each force spectrum. In this way we can attempt to identify some of the parameters affecting the response. Some of the curves may be seen in Figs (A5.I) - (A5.I4) together with a detailed discussion of the curves in Appendix 5 . The curves for one particular cylinder radius, 5.5 m , are given overleaf in Figs (3.4) and (3.5), and these will serve to illustrate the main points to be made . Refering to the force spectra in Fig (3.4) , it has been found that :

(i) for cylinder radii up to 4 m , the diffraction theory response is larger than the Morison theory response.

(ii) the Morison theory response is larger over most of the frequency range, except near the force spectrum peaks, where in any case resonance would occur if the frequency response curve centred there. In the curves given, only one frequency response curve was used, and that had a peak at I.07 radns/sec., but from the curves it is clear that the displacement response depends mainly on the position of the peak of the frequency response curve, rather than the peak of the force spectrum.

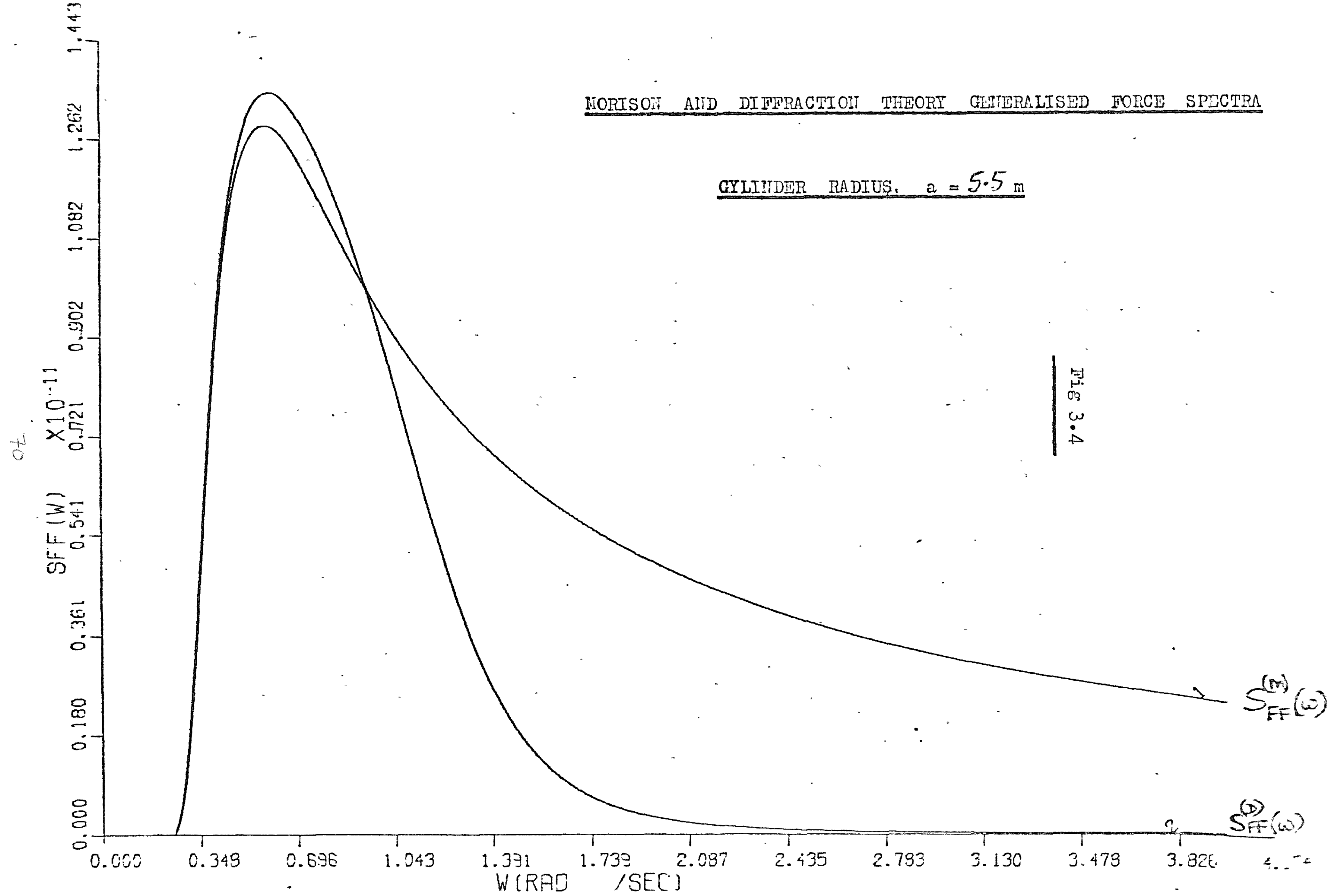
MORISON AND DIFFRACTION THEORY GENERALISED FORCE SPECTRA
CYLINDER RADIUS, a = 5.5 m
Fig 3.4
SFF(W) X10⁻¹¹
1.443
1.262
1.082
0.902
0.721
0.541
0.361
0.180
0.000
0.000
0.348
0.696
1.043
1.391
1.739
2.087
2.435
2.783
3.130
3.478
3.826
W(RAD /SEC)
$S_{FF}^{(M)}(\omega)$
$S_{FF}^{(D)}(\omega)$

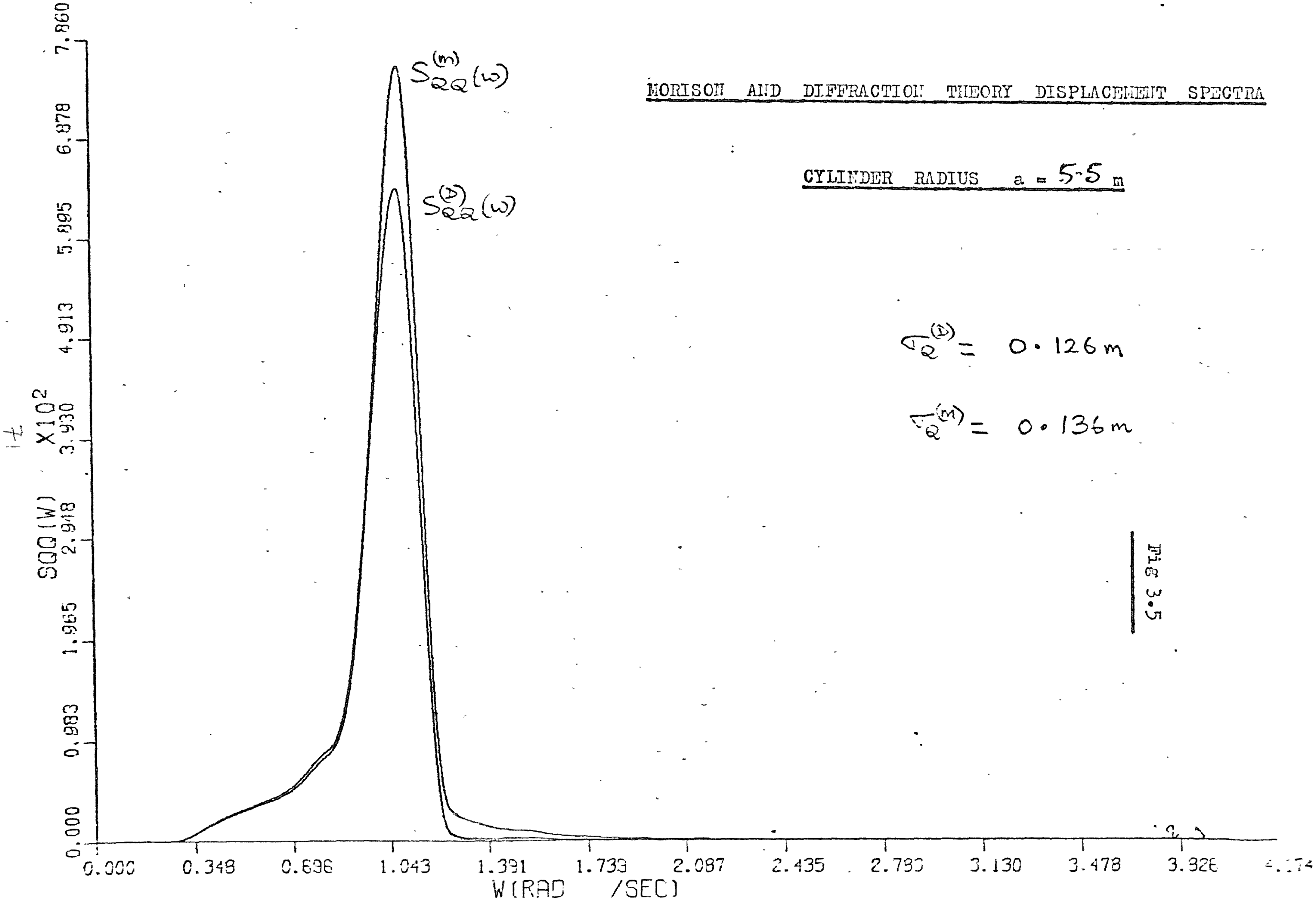

MORISON AND DIFFRACTION THEORY DISPLACEMENT SPECTRA
CYLINDER RADIUS a = 5.5 m
$S^{(m)}_{QQ}(\omega)$
$S^{(D)}_{QQ}(\omega)$
$\sigma_Q^{(D)} = 0.126$ m
$\sigma_Q^{(M)} = 0.136$ m
SQQ(W) X10^2
0.000
0.983
1.965
2.948
3.930
4.913
5.895
6.878
7.860
0.000
0.348
0.696
1.043
1.391
1.739
2.087
2.435
2.783
3.130
3.478
3.826
4.174
W(RAD /SEC)

Fig 3.5

(c) Returning to equations (3.4I) and (3.42), Walker (University of Southampton, private discussion) suggested comparing the two force spectra by dividing one by the other, thus eliminating the dependence on the wave height spectrum $S_{\eta\eta}(\omega)$. This gives :

$$\gamma = \frac{S_{FF}^{(m)}(\omega)}{S_{FF}^{(D)}(\omega)} = \frac{S_{F_{Tot}F_{Tot}}^{(m)}(\omega)}{S_{F_{Tot}F_{Tot}}^{(D)}(\omega)} = \frac{\pi^2}{4}(ka)^4 \left| H_I^{(I)\prime}(ka) \right|^2 \quad (3.44)$$

Clearly, if $\gamma < I$ for some ka , then the diffraction theory force spectrum is greater than the Morison force spectrum . Curves of $\gamma(ka)$ against ω for various cylinder radii are given in Fig (3.6) ; and in Fig (3.7), a curve of ω_c against ω is given, where ω_c is the frequency at which the Morison spectrum and diffraction theory spectrum cross over.

The curve of $\gamma(ka)$ against ω is of little value on its own, since it merely tells the designer which of the two force spectra is the greater. This is of no use without knowing the absolute value of one of the spectra at the frequency under consideration, and how the absolute value compares with the peak value. Accordingly, one needs the force spectra curves as in Fig (3. 4) in addition to the curves given in Figs (3. 6) and (3. 7) before proceeding with the design. In most cases, it is likely that the structure will be overdesigned using the Morison force spectrum.

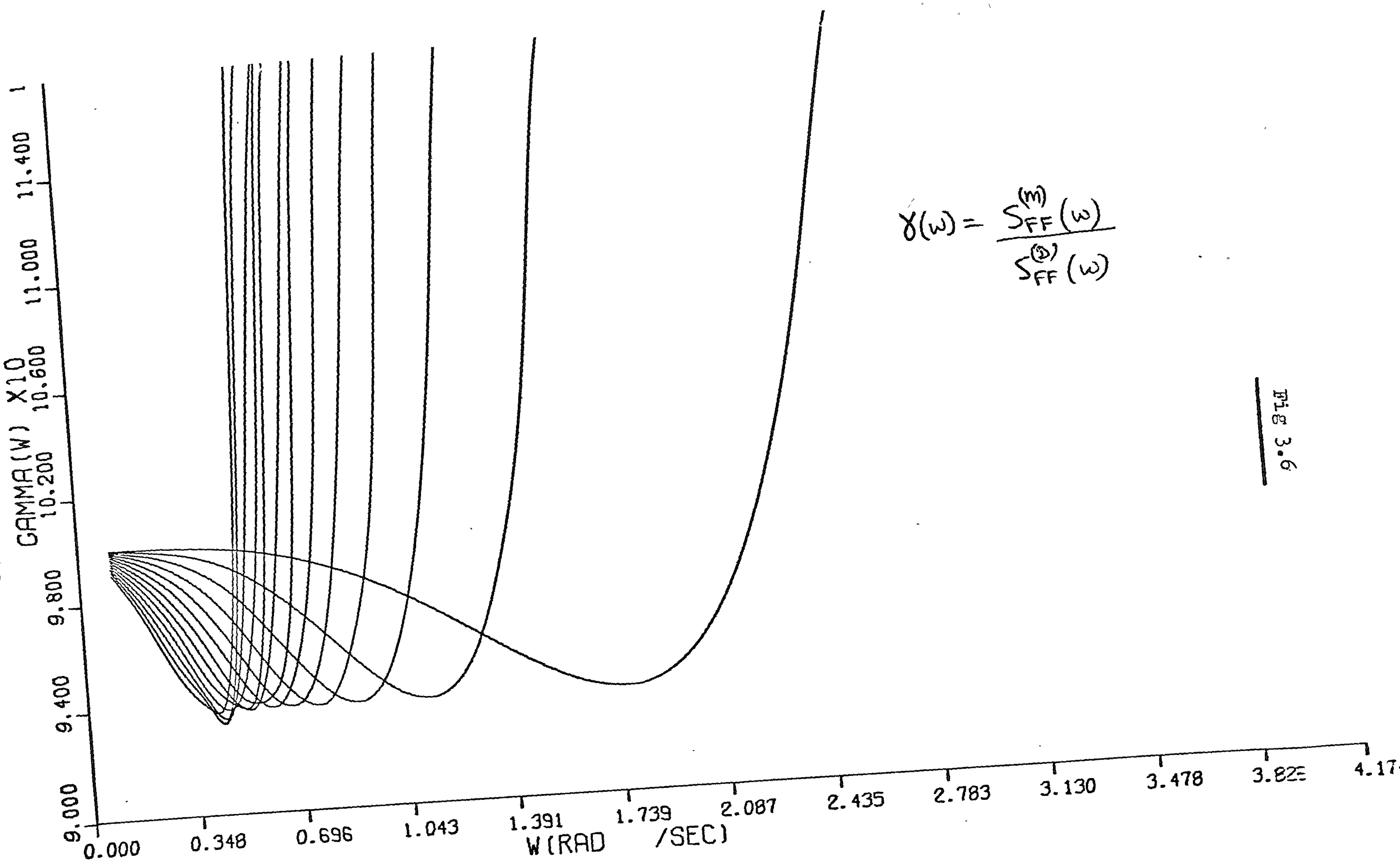

$$\gamma(\omega) = \frac{S_{FF}^{(m)}(\omega)}{S_{FF}^{(D)}(\omega)}$$

Fig 3.6

73

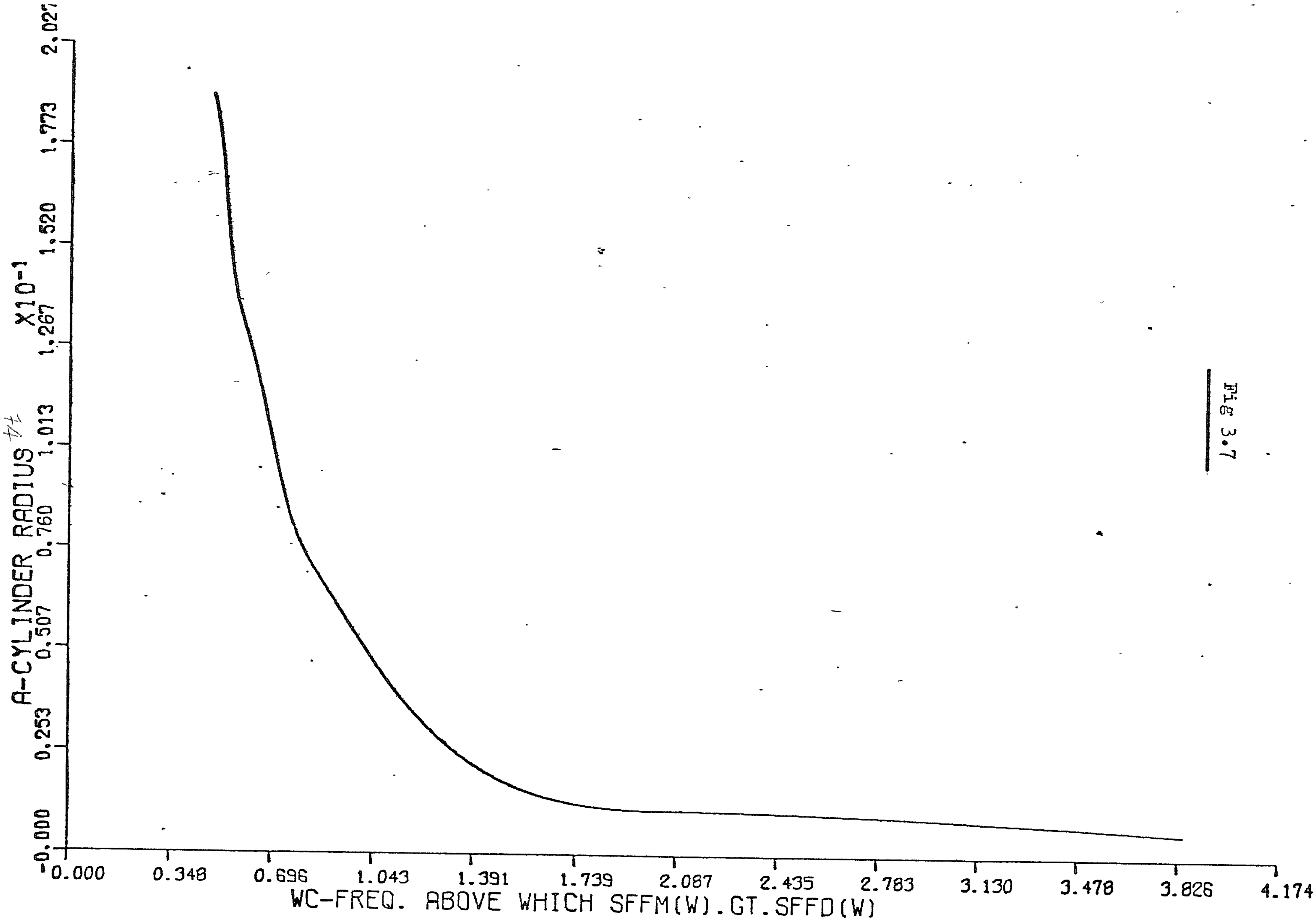
A-CYLINDER RADIUS X10-1
-0.000
0.253
0.507
0.760
1.013
1.267
1.520
1.773
2.027
0.000
0.348
0.696
1.043
1.391
1.739
2.087
2.435
2.783
3.130
3.478
3.826
4.174
WC-FREQ. ABOVE WHICH SFFM(W).GT.SFFD(W)

Fig 3.7

3.6 THE EFFECT OF SHELTERING

3.6.I GENERAL

In section 3.3 , a diffraction theory was presented which was able to predict the inertia force on a single vertical cylinder in a fluid . As an extension of the single cylinder case , Spring and Monkmeyer (Ref 20) considered the interaction of plane waves with two vertical cylinders , for varying angles of incidence of the waves with the line of centres of the two cylinders . These authors presented non-analytical curves giving the force ratio (i.e. the force on one cylinder due to the presence of the other , divided by the force on the same cylinder in the absence of the other) against a spacing parameter (i.e. the cylinder spacing multiplied by the wave number of the incident wave) .

3.6.2 AN ANALYTICAL FORCE RATIO CURVE FOR PLANE FRAMES

This study is limited to plane frames , and it was thought to be of interest to see what effect sheltering has in this case. In order to apply the diffraction theory to practical examples , it is best to fit an analytical curve to the force ratio versus spacing parameter data . Spring and Monkmeyer observe that their graphs appear to be 'not unlike Bessel Functions' , and a very good fit to their graph of the force on the front cylinder due to the back one is found to be given by the curve :

$$F(\ ks\ ) = I.0 + \frac{I}{3} Y_0 (\ I.55\ ks - I.45\ ) \qquad (3.45)$$

where	$F(ks)$	is the force ratio as defined above
	k	is the wave number
	s	is the spacing between the two cylinders
	Y_0	is a Bessel function , the zeroth order weber function

(see Fig 3.8) .

The effect of the front cylinder on the back one is an order of magnitude less and will not be considered further .

The first peak of the curve defined by equation (3.45) occurs at $ks = 2.5$, where $F(ks) = 1.17$. Thus if $s = 40$ m , as in the case of the 4-leg platform of section 5.4.2 , then $k = \frac{2.5}{40} = 0.0625$ and $\omega = 0.78$ rad/s . The second peak occurs at $ks = 6.7$, where $F(ks) = 1.10$. If $s = 40$ m , $k = 0.017$, and $\omega = 1.28$ rad/s .

Let us consider where these two peaks occur in relation to the wave amplitude spectrum and the frequency response function peaks , in the case of the 4-leg platform cited above . Refering to Fig3.9 , it is clear that the first two peaks of the

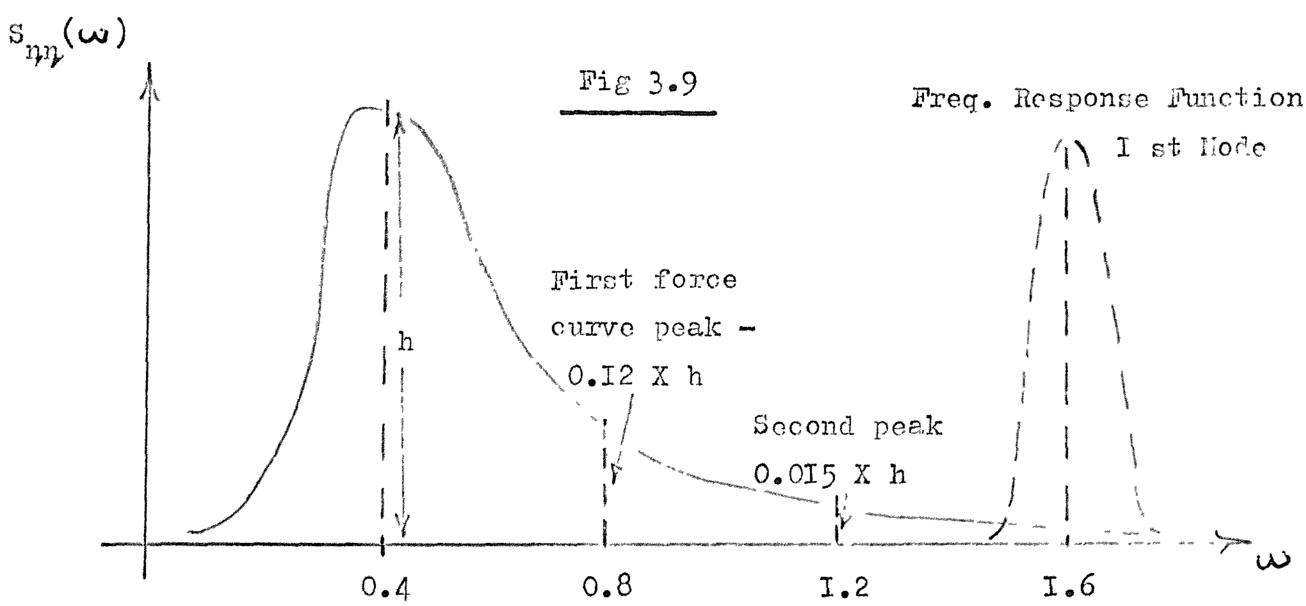

Fig 3.9

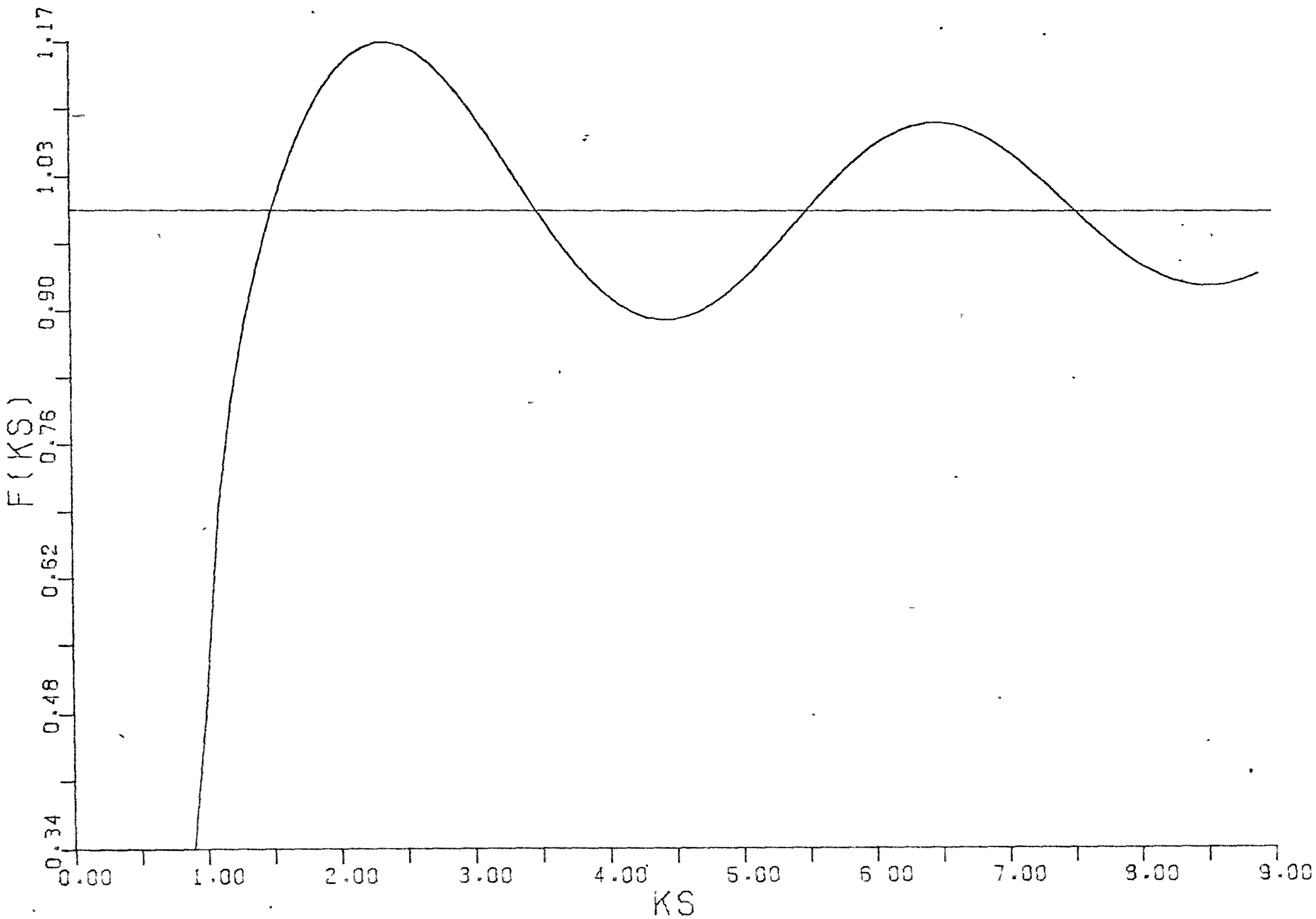

FORCE RATIO VERSUS CYLINDER SPACING PARAMETER

Fig 3.8

force ratio curve will not reinforce either the wave amplitude spectrum or the frequency response function . This is bourne-out in the results (see Table 5.2 , section 5.4.2) , where it is seen that sheltering causes at most a 1% increase in the displacement response .

3.6.3 THE IMPORTANCE OF SHELTERING

From Figs 3.8 and 3.9 , we can predict that the effect of sheltering will be most pronounced when the first peak of Fig 3.9 coincides with the peak of either the wave amplitude spectrum or the first mode frequency response function .

Using the 4-leg platform of section 5.4.2 as an example , we observe that :

(i) if the leg spacing is held fixed at 40 m , a structure with a fundamental frequency of about 0.8 rad/s will be most affected by sheltering

(ii) if the fundamental frequency is held fixed at 1.55 rad/s , a structure with a leg spacing of about 10 m will be most affected by sheltering

In general , a designer can get a feel for the problem by using the two equations :

$$\begin{aligned} \omega^2 &= gk \tanh kd \\ ks &= 2.5 , 6.7 , \text{etc} \end{aligned} \qquad (3.46)$$

from which s can be found knowing ω , or ω can be found knowing s .

Here ω may be either the wave amplitude spectrum peak or the frequency response function peak .

3.6.4 FOUR - LEG PLATFORMS

This thesis is mainly concerned with the analysis of plane frames , and Fig 3.8 shows that sheltering can account for as much as 17% of the force on the front cylinder in the presence of the back one , in a plane frame situation .

Similar curves can be drawn giving the ratio of the force on one cylinder in the presence of another for situations other than plane frame ones , notably 4-leg platforms , such as the one shown below .

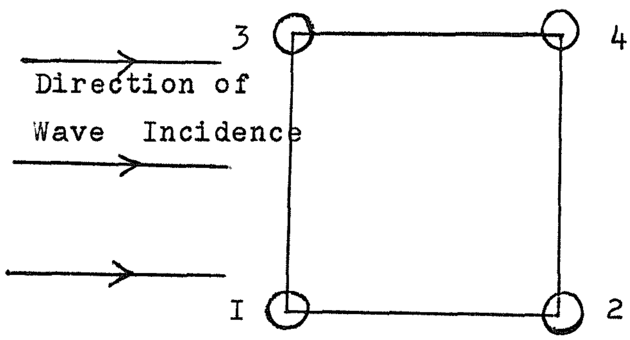

Plan View of 4-leg Platform

The interaction of cylinders I and 2 , and cylinders 3 and 4 , has been mentioned in the preceeding sections . A curve representing the interaction between cylinders I and 3 , and cylinders 2 and 4 , shows that this interaction effect is an order of magnitude less than that existing between I and 2 , over most of the frequency range , which suggests that a plane frame idealisation is a reasonable one , at least as far as the sheltering effect is concerned .

(Thanks are due to S. Walker of the University of Southampton for valuable discussions on the sheltering problem)

CHAPTER 4 : RESPONSE OF MULTI DEGREE OF FREEDOM STRUCTURES TO RANDOM WAVE LOADING

4.I INTRODUCTION

In this chapter, consideration will be given to the response of framed structures to random wave loading. Frames are a particularly important type of ocean structure, and in this thesis they will be idealised as multi degree of freedom plane frames.

In 1963, Harris (Ref I3) approached the problem of random loads on multi degree of freedom systems when he considered wind gust loading on a line-like structure. His method was to decompose the equations of motion using a normal mode approach. Malhotra and Penzien (Ref 5) used a similar approach in considering the response of offshore structures to random wave loading. In this approach, the dynamic deflections of the structure are broken-down into a number of elementary deflections or normal mode shapes, each of which behaves as a single degree of freedom system. It is possible, therefore, to see what contribution to the total response comes from each mode.

This chapter , then , starts by considering the equations of motion of the structure , and outlines the normal mode method for solving them.

Consideration is then given to the representation of the force system on the structure . Section 4.4 looks at consistent nodal forces for beam elements and how they can be related to the force spectral densities that are needed for the solution process of section 4.3. Section 4.5 looks at three different ways of treating the forces by considering them to be 'lumped' at the nodal points of the structure. Two of these are similar to the consistent force representation in that we attempt to form force spectral densities for use in the theory of section 4.3. The third method avoids doing this by solving the decoupled equations of motion explicitly for a particular forcing frequency ω, and using the 'transfer function' thus obtained to provide a direct link between the unknown displacements and the known wave amplitudes . The method appears to avoid most of the assumptions made in section 4.3 for the other two methods.

The chapter closes with a single degree of freedom example , which serves to illustrate the multi degree of freedom theory and also to act as a useful test example for the chapter on the computational results .

4.2 THE EQUATIONS OF MOTION

Using the finite element formulation, a multi degree of freedom system can be represented by its equations of motion in matrix form :

$$\underline{M}\,\ddot{\underline{X}} + \underline{C}\,\dot{\underline{X}} + \underline{K}\,\underline{X} = \underline{P} \tag{4.I}$$

The global mass, stiffness and load matrices, $\underline{M}$, $\underline{K}$ and $\underline{P}$, respectively, are made up from the element mass, stiffness and load matrices, which are of the form :

$$\underline{k}_s = \int \underline{B}^T \,\underline{D}\,\underline{B}\;\; d(Vol)$$

$$\underline{m}_s = \int \underline{\Phi}^T \rho\, \underline{\Phi}\;\; d(Vol) \tag{4.2}$$

$$\underline{f} = \int \underline{\Phi}^T\;\underline{p}\;\; dS$$

giving

$$\underline{m}_s\,\ddot{\underline{x}} + \underline{c}_s\,\dot{\underline{x}} + \underline{k}_s\,\underline{x} = \underline{f} \tag{4.3}$$

where $\underline{c}_s$ is proportional to a linear combination of $\underline{k}_s$ and $\underline{m}_s$.

The load vector $\underline{p}$ is in this case the vector of all the hydrodynamic forces, which according to equation (3.20) is of the form :

$$p = C_H\,(\dot{v}-\dot{u}) + C_D\,(v-u)\left|v-u\right| + C_p\,\dot{v} \tag{3.20}$$

(considering only the component of force normal to the element)

For notational reasons, the cylinder velocity and acceleration u and $\dot{u}$, respectively, have been changed to $\dot{x}$ and $\ddot{x}$. Writing the element velocities and accelerations $\dot{\underline{x}}$ and $\ddot{\underline{x}}$ in terms of the nodal point velocities and accelerations $\dot{\underline{x}}_n$ and $\ddot{\underline{x}}_n$

$$\dot{\underline{x}} = \phi \dot{\underline{x}}_n \qquad , \quad \ddot{\underline{x}} = \phi \ddot{\underline{x}}_n$$

and assuming that fluid velocity and acceleration v and $\dot{v}$ follow the same variation, equation (4.3) gives :

$$\underline{f} = \underline{m}_H \dot{\underline{v}}_n - \underline{m}_H \ddot{\underline{x}}_n + \underline{c}_D \underline{v}_n - \underline{c}_D \dot{\underline{x}}_n + \underline{m}_P \dot{\underline{v}}_n \qquad (4.4)$$

The matrices m_H , $\underline{m}_s$, $\underline{k}_s$, $\underline{m}_P$ and $\underline{c}_D$ are all given in Appendix 6. Substituting equation (4.4) into equation (4.3) and taking terms in $\dot{\underline{x}}_n$ and $\ddot{\underline{x}}_n$ to the left side of the equation, the equations of motion for the element are :

$$(\underline{m}_s + \underline{m}_H) \ddot{\underline{x}}_n + (\underline{c}_s + \underline{c}_D) \dot{\underline{x}}_n + \underline{k}_s \underline{x} = (\underline{m}_H + \underline{m}_P) \dot{\underline{v}}_n + \underline{c}_D \underline{v}_n \qquad (4.5)$$

or

$$\underline{m} \ddot{\underline{x}} + \underline{c} \dot{\underline{x}}_n + \underline{k} \underline{x} = \underline{f} \qquad (4.6)$$

in which the force term $\underline{f}$ now contains only the fluid velocity and acceleration terms and no terms involving the motion of the cylinder .

For the complete structure, equation (4.6) is summed over all the elements to give :

$$\underline{M}\,\ddot{\underline{X}} + \underline{C}\,\dot{\underline{X}} + \underline{K}\,\underline{X} = \underline{F} \tag{4.7}$$

4.3 THE NORMAL MODE METHOD, LEADING TO THE DISPLACEMENT SPECTRAL DENSITY IN TERMS OF THE FORCE SPECTRAL DENSITY

4.3.I GENERAL

The normal mode technique has been used for some time for a variety of problems, and has some big advantages over other methods. Perhaps the biggest is that it enables the designer of a structure to get a 'feel' for its behavior, since the reponse of the structure is considered to be a sum of the responses in the normal modes .

In random vibration analyses, not all methods require the eigenvalues of the system (for example, 'step-by-step' methods) , but in practice the eigenvalues are a useful preliminary guide to a structure's behavior .

4.3.2 THE NORMAL MODE METHOD FOR THE DISPLACEMENT SPECTRAL DENSITY

The normal modes and natural frequencies of a multi degree of freedom structure are found by considering equation (4.7) with no damping term and no force term, i.e.

$$\underline{M}\,\ddot{\underline{X}} + \underline{K}\,\underline{X} = \underline{0} \tag{4.8}$$

The structure will oscillate at its natural frequencies ω if

$$\ddot{\underline{X}} = -\,\omega^2\,\underline{X}$$

in which case equation (4.8) becomes :

$$(\,\underline{K} - \omega^2\,\underline{M}\,)\,\underline{X} = \underline{0} \tag{4.9}$$

The response of the structure $\underline{X}$ is then given by :

$$\underline{X} = \underline{A}\,\underline{q} \cong \sum_{i=1}^{s} q_i\,\underline{A}_i \tag{4.10}$$

where q_i are generalised coordinates and $\underline{A}$ is the matrix whose columns $\underline{A}_i$ are the eigenvectors of the system of equations . For offshore applications, only the first two or three vibration modes are important, so that s = 2 or 3 in equation (4.10) (in fact, the first mode usually contributes over 85 % of the total response). Replacing $\ddot{\underline{X}}$ by $\underline{A}\,\ddot{\underline{q}}$, $\dot{\underline{X}}$ by $\underline{A}\,\dot{\underline{q}}$, and $\underline{X}$ by $\underline{A}\,\underline{q}$, and premultiplying each term by $\underline{A}^T$, equation (4.7) can be written :

$$\left[\underline{A}^T \underline{M}\, \underline{A}\right] \ddot{\underline{q}} + \left[\underline{A}^T \underline{C}\, \underline{A}\right] \dot{\underline{q}} + \left[\underline{A}^T \underline{K}\, \underline{A}\right] \underline{q} = \underline{A}^T \underline{F} \qquad (4.11)$$

or

$$\underline{\bar{M}}\, \ddot{\underline{q}} + \underline{\bar{C}}\, \dot{\underline{q}} + \underline{\bar{K}}\, \underline{q} = \underline{\bar{F}} \qquad (4.12)$$

where $\underline{\bar{M}}$, $\underline{\bar{C}}$, and $\underline{\bar{K}}$ are diagonal matrices.
(Here the assumption is made that the damping matrix $\underline{C}$ is orthogonal with respect to the eigenvector matrix $\underline{A}$)

Equations (4.12) are now uncoupled and can be written down as separate second order differential equations for each mode :

$$\bar{M}_i \ddot{q}_i + \bar{C}_i \dot{q}_i + \bar{K}_i q_i = \bar{F}_i \qquad (4.13)$$

Taking the Fourier transform of equation (4.14) gives :

$$(- \omega^2 \bar{M}_i + i\, \omega \bar{C}_i + \bar{K}_i)\, Q_i = G_i \qquad (4.14)$$

in which Q_i and G_i are the Fourier transforms of q_i and $\bar{F}_i$, respectively . Equation (4.14) holds for the i th generalised coordinate, and similarly for the j th generalised coordinate we find :

$$(- \omega^2 \bar{M}_j + i\, \omega \bar{C}_j + \bar{K}_j)\, Q_j = G_j \qquad (4.15)$$

Taking the complex conjugate of equation (4.I5) yields :

$$(- \omega^2 \bar{M}_j - i\,\omega \bar{C}_j + \bar{K}_j)\ \hat{Q}_j = \hat{G}_j \tag{4.I6}$$

where $\hat{Q}_j$ and $\hat{G}_j$ denote complex conjugates of Q_j and G_j , respectively. Using the usual notation for a single degree of freedom system, we can write :

$$\begin{aligned} \omega_i^{\,2} &= \frac{\bar{K}_i}{\bar{M}_i} \quad ; \quad \omega_j^{\,2} = \frac{\bar{K}_j}{\bar{M}_j} \\ \bar{C}_i &= 2\,\gamma_i \frac{\bar{K}_i}{\omega_i} \quad ; \quad \bar{C}_j = 2\,\gamma_j \frac{\bar{K}_j}{\omega_j} \end{aligned} \tag{4.I7}$$

and express equations (4.I4) and (4.I6) in terms of two transfer functions $\alpha_i(\omega)$ and $\hat{\alpha}_j(\omega)$ thus :

$$\begin{aligned} Q_i &= \alpha_i\ G_i \\ \hat{Q}_j &= \hat{\alpha}_j\ \hat{G}_j \end{aligned} \tag{4.I8}$$

where

$$\begin{aligned} \alpha_i(\omega) &= \left[\left(-\mathrm{I} + 2i\gamma_i \frac{\omega_i}{\omega} + \frac{\omega_i^2}{\omega^2} \right) \bar{K}_i \right]^{-\mathrm{I}} \\ \hat{\alpha}_j(\omega) &= \left[\left(-\mathrm{I} - 2i\gamma_j \frac{\omega_j}{\omega} + \frac{\omega_j^2}{\omega^2} \right) \bar{K}_j \right]^{-\mathrm{I}} \end{aligned} \tag{4.I9}$$

Multiplying equations (4.I8) together gives an expression for the cross spectral density of the generalised coordinates i and j .

$$S_Q(i,j) = \alpha_i \, S_G(i,j) \, \hat{\alpha}_j \tag{4.20}$$

or in matrix form :

$$\begin{bmatrix} S_Q(1,1) & S_Q(1,2) & \cdot & \cdot \\ S_Q(2,1) & S_Q(2,2) & \cdot & \cdot \\ \cdot & & & \\ \cdot & & & \\ \cdot & & & \end{bmatrix} = \begin{bmatrix} \alpha_1 & & \\ & \alpha_2 & \\ & & \ddots \end{bmatrix} \begin{bmatrix} S_G(1,1) & S_G(1,2) & \cdot & \cdot \\ S_G(2,1) & S_G(2,2) & \cdot & \cdot \\ \cdot & & & \\ \cdot & & & \end{bmatrix} \begin{bmatrix} \hat{\alpha}_1 & & \\ & \hat{\alpha}_2 & \\ & & \ddots \end{bmatrix}$$

$$\underline{S}_Q = \underline{\alpha} \; \underline{S}_G \; \underline{\hat{\alpha}} \tag{4.20a}$$

The spectral density matrix $\underline{S}_G$ is related to the spectral density matrix of the untransformed forces by the transformation :

$$\underline{S}_G = \underline{A}^T \; \underline{S}_F \; \underline{A} \tag{4.21}$$

Inserting equation (4.21) into equation (4.20a), the spectral density matrix of the generalised coordinates $\underline{q}$ is found . The spectral density matrix of the displacements $\underline{X}$ in the original coordinate system is now given by the transformation :

$$\underline{S}_X = \underline{A} \; \underline{S}_Q \; \underline{A}^T \tag{4.22}$$

If we choose, we can write equations (4.20) - (4.22) as :

$$\underline{S}_x = \underline{A} \left[\underline{\alpha} \, \underline{A}^T \, \underline{S}_F \, \underline{A} \, \underline{\hat{\alpha}} \right] \underline{A}^T \qquad (4.23)$$

which connects the original forces to the original displacements .

4.3.3 A DIAGONAL FORM FOR THE SPECTRAL DENSITY MATRIX OF THE GENERALISED DISPLACEMENT Q

Returning to equation (4.20a), considerable simplification results if only the diagonal elements

$$\alpha_i \quad S_G(i,i) \quad \hat{\alpha}_i$$

are considered . The off-diagonal terms

$$\alpha_i \quad S_G(i,j) \quad \hat{\alpha}_j \qquad (i \neq j)$$

will in general be small, since for an offshore structure, the peaks of the frequency response curve are very well separated. In this case, therefore, equation (4.20) reduces to :

$$S_Q(i,i) = \left| \alpha_i \right|^2 \; S_G(i,i) \qquad (4.24)$$

in which

$$\left|\alpha_i\right|^2 = \frac{1}{K_i \left[\left[I - \left[\frac{\omega}{\omega_i} \right]^2 \right]^2 + \left[2\gamma \frac{\omega}{\omega_i} \right]^2 \right]}$$

S_Q is now diagonal and the solution of equation (4.23) is much simpler .

However, we still need to compute the force spectral density S_F in equation (4.2I) . Consistent nodal force spectral densities for beam elements are the subject of the next section, and there is no reason in principle why force spectral densities for other elements should not be included in the same way . Three ways of 'lumping' nodal forces are discussed in section 4.5 .

4.4 CONSISTENT NODAL FORCE SPECTRAL DENSITIES FOR BEAM ELEMENTS

In Chapter 3, it was shown that one can express the spectral density of the wave force per unit length on an immersed cylinder in terms of the spectral densities of the fluid particle velocity and acceleration, and ultimately in terms of the wave height spectral density. We will consider the two methods used - the diffraction theory and Morison's theory - side by side, firstly for a vertical cylinder and secondly for an inclined cylinder, and use them to derive expressions for the cross spectral density of two consistent nodal forces. A consistent element nodal force P_i for a prismatic beam element is defined by integrating the force per unit length at depth z_i, $F(z_i)$ (as given by either the diffraction theory or Morison's theory), over the submerged length of the element, with an interpolation function $g_i(z_i)$ as a weighting function.

Hence

$$P_i = \int_{z_I^i}^{z_2^i} F(z_i)\ g(z_i)\ dz_i \qquad (4.25)$$

where z_i is measured in element local coordinates (along the beam).

Equation (4.25) will now be used to derive expressions for the cross spectral density of two consistent nodal forces P_i and P_j.

4.4.1 THE SPECTRAL DENSITY OF CONSISTENT ELEMENT NODAL FORCES FOR A VERTICAL BEAM ELEMENT

The spectral density of the force per unit length on a vertical beam element, $S_{FF}(\omega)$, is given by equations (3.38), (3.40) and (3.41) :

$$S_{FF}^{(m)}(\omega) = K^2 S_{\dot{v}\dot{v}}(\omega) + \frac{8}{\pi} c^2 \sigma_v^2 S_{vv}(\omega)$$

$$= \left[4\rho^2 a^4 \pi^2 \omega^4 + \frac{8 c^2}{\pi}\sigma_v^2 \omega^2\right] \frac{\cosh^2 kz}{\sinh^2 kd} S_{\eta\eta}(\omega) \quad (4.26)$$

$$S_{FF}^{(D)}(\omega) = \left[k_I^2 \omega^4 + \text{DRAG TERM}\right] \frac{\cosh^2 kz}{\sinh^2 kd} S_{\eta\eta}(\omega)$$

From these, the cross spectral density of two consistent nodal forces P_i and P_j (as given by equation (4.25)) is :

$$S_p^{(m)}(i,j,\omega) = \int_{z_1^i}^{z_2^i}\int_{z_1^j}^{z_2^j} \varepsilon_i(z_i)\, \varepsilon_j(z_j) \left[\frac{8 c_i}{\pi} c_j\, \sigma_v(z_i)\, \sigma_v(z_j) \right. \quad (4.27)$$

$$\left. \times\ S_{vv}(i,j,\omega) + K_i K_j S_{\dot{v}\dot{v}}(i,j,\omega)\right] dz_i\, dz_j$$

$$S_p^{(D)}(i,j,\omega) = \int_{z_1^i}^{z_2^i}\int_{z_1^j}^{z_2^j} \varepsilon_i(z_i)\, \varepsilon_j(z_j) \left[\frac{4 K_i K_j}{k^4 a^4 \pi^2} \frac{\cosh kz_i}{H_1^{(1)}(ka)} \frac{\cosh kz_j}{2 \sinh^2 kd}\right]$$

$$\times\ S_{\eta\eta}(\omega) \cos k(x_j - x_i)\ dz_i\, dz_j \quad (4.28)$$

in which

$$S_{vv}(i,j,\omega) = \left[\frac{\omega^2 \cosh kz_i \cosh kz_j}{\sinh^2 kd} \right] S_{\eta\eta}(\omega) \cos k(x_j - x_i)$$

$$S_{\dot{v}\dot{v}}(i,j,\omega) = \left[\frac{\omega^4 \cosh kz_i \cosh kz_j}{\sinh^2 kd} \right] S_{\eta\eta}(\omega) \cos k(x_j - x_i) \tag{4.29}$$

4.4.2 THE SPECTRAL DENSITY OF CONSISTENT ELEMENT NODAL FORCES FOR AN INCLINED BEAM ELEMENT

Only the Morison theory will be considered here. The equation for the spectral density of the normal force per unit length on an inclined cylinder is equation (3.38) :

$$S_{FF}^{(m)}(\omega) = \frac{8}{\pi} C^2 \sigma_v^2 S_{vv}(\omega) + K^2 S_{\dot{v}\dot{v}}(\omega) \tag{4.30}$$

where in this case, S_{vv} and $S_{\dot{v}\dot{v}}$ refer to the normal velocity and acceleration on the cylinder, respectively, and are given by :

$$S_{vv}(\omega) = S_{u_n u_n}(\omega)$$

$$= \Big[\omega^2 \cosh^2 kz \sin^2\theta - 2\omega^2 \sinh kz \cosh kz \sin\theta \cos\theta$$

$$+ \omega^2 \sinh^2 kz \cos^2\theta \Big] \frac{S_{\eta\eta}(\omega)}{\sinh^2 kd} \qquad (4.3I)$$

$$S_{\dot v \dot v}(\omega) = S_{\dot u_n \dot u_n}(\omega)$$

$$= \Big[\cosh^2 kz \sin^2\theta - 2 \quad \sinh kz \cosh kz \sin\theta \cos\theta$$

$$+ \sinh^2 kz \cos^2\theta \Big] \frac{\omega^4 S_{\eta\eta}(\omega)}{\sinh^2 kd} \qquad (4.32)$$

The cross spectral density of two consistent nodal forces P_i and P_j is then given by :

$$S_p(i,j,\omega) = \int_{z_I^i}^{z_2^i} \int_{z_2^j}^{z_2^j} g_i(z_i)\, g_j(z_j) \Big[\frac{8}{\pi} C_i\, C_j\, \sigma_v(z_i)\, \sigma_v(z_j)$$

$$X\, S_{u_n u_n}(i,j,\omega) + K_i\, K_j\, S_{\dot u_n \dot u_n}(i,j,\omega) \Big] dz_i\, dz_j \qquad (4.33)$$

in which

$$S_{u_n u_n}(i,j,\omega) = \Big[\cosh kz_i \cosh kz_j \sin\theta_i \sin\theta_j$$

$$+ \sinh kz_i \sinh kz_j \cos\theta_i \cos\theta_j$$

$$- (\sinh kz_i \cosh kz_j \sin\theta_j \cos\theta_i + \sinh kz_j \cosh kz_i \sin\theta_i \sin\theta_j) \Big]$$

$$X \quad \frac{\omega^2 S_{\eta\eta}(\omega)}{\sinh^2 k\, d} \quad \cos k(x_j - x_i) \qquad (4.34)$$

and

$$S_{\dot{u}_n \dot{u}_n}(i,j,\omega) = \Big[\cosh kz_i \cosh kz_j \sin\theta_i \sin\theta_j + \sinh kz_i \sinh kz_j \cos\theta_i \cos\theta_j$$

$$- (\sinh kz_i \cosh kz_j \sin\theta_j \cos\theta_i + \sinh kz_j \cosh kz_i \sin\theta_i \sin\theta_j) \Big]$$

$$\times \quad \frac{\omega^4 S_{\eta\eta}(\omega)}{\sinh^2 kd} \cos k(x_j - x_i) \qquad (4.35)$$

Clearly, equation (4.33) will reduce to equation (4.27) in the case in which the cylinder is vertical ($\sin\theta = 1$, $\cos\theta = 0$), since in this case the components of $S_{u_n u_n}(\omega)$ and $S_{\dot{u}_n \dot{u}_n}(\omega)$ which are due to the vertical velocity of the wave particles then vanish .

The problem of integrating equation (4.33) is an algebraic headache . This is done in Appendix 7 .

4.4.3 THE OVERALL NODAL FORCE SPECTRAL DENSITY FOR THE COMPLETE STRUCTURE

Equation (4.33) gives the spectral density of two nodal forces i and j taken from two elements (possibly the same element) . For the overall nodal force cross spectral density between two forces i and j , it is necessary to sum terms such as these over all the elements meeting at the nodes corresponding to i and j.

This gives :

$$S_p(i,j,\omega) = \sum_n \sum_m S_p(i^n, j^m, \omega) \qquad (4.36)$$

in which $S_p(i^n, j^m, \omega)$ is given by equation (4.33) , and represents the cross spectral density of nodal force i from element n and nodal force j from element m .

Some results from a programme based on the consistent force theory are given with the rest of the computational results in Chapter 5 .

4.5 'LUMPED' FORCE SPECTRAL DENSITIES FOR BEAM ELEMENTS

4.5.I GENERAL

In the previous section, consistent nodal forces for beam elements were considered, and it was seen that very complicated algebra arises when deriving the spectral densities of these forces. This is principally because of the occurence of the interpolation functions in some of the expressions that have to be integrated.

An alternative approach is to lump the force on each beam element at it's nodes. Three different ways of doing this, of varying degrees of approximation, are now considered. In all cases, the modal decomposition technique, described in sections 4.I - 4.3 , is used. Progressing from section 4.5.3 to 4.5.6 , the three methods are of increasing simplicity, and it is hoped that it will be possible to show that the simplest of the three methods is sufficiently accurate to be useable in subsequent analyses. Computer programmes based on the three methods are given in Chapter 5 .

4.5.2 'LUMPED' ELEMENT FORCES FOR A BEAM ELEMENT

Before cosidering each of the three methods in turn, let us cosider again the force on a typical beam element, say element r , of a structure.

Rewriting equations (3.2I) and (3.22) , we get for the force per unit length $F_n(z)$ normal to the cylinder at height z above the sea bed :

$$F_n(z) = K_r \dot{v}_n + C_r \sqrt{\frac{8}{\pi}}\, \sigma_v(z)\, v_n \qquad (4.25')$$

where

$$v_n = u \sin \theta_r - w \cos \theta_r \qquad (4.26')$$

$$u = \frac{a\,\omega \cosh kz}{\sinh kd} \cos (kx-\omega t)$$

$$w = \frac{a\,\omega \sinh kz}{\sinh kd} \sin (kx-\omega t)$$

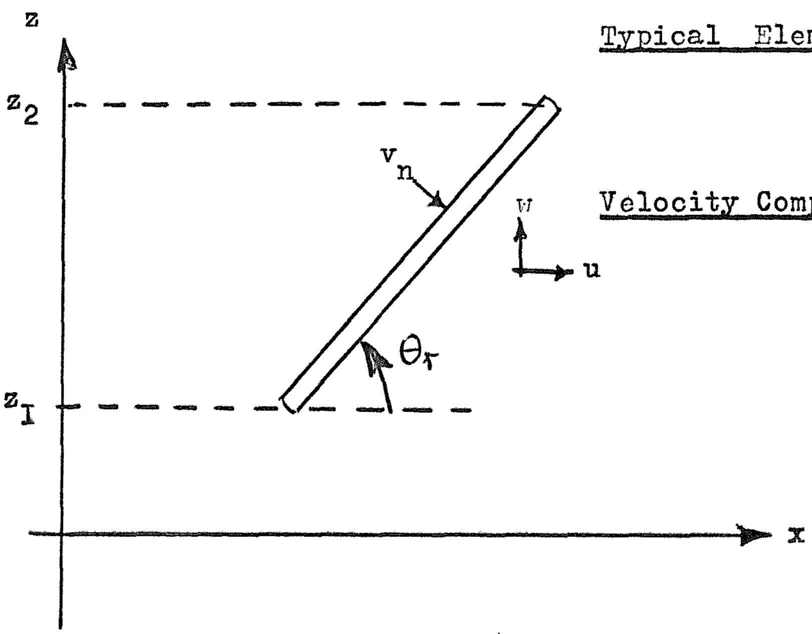

Typical Element r

Velocity Components

Inserting equation (4.26') into equation (4.25') gives :

$$F_n(z) = \frac{K_r a \omega^2}{\sinh kd}\Big[\cosh kz \sin(kx-\omega t)\sin\theta_r + \sinh kz \cos(kx-\omega t)\cos\theta_r\Big]$$

$$+ \frac{C_r\sqrt{\frac{8}{\pi}}\,\sigma_v(z)\, a\,\omega}{\sinh kd}\Big[\cosh kz \cos(kx-\omega t)\sin\theta_r - \sinh kz \sin(kx-\omega t)\cos\theta_r\Big] \qquad (4.27')$$

The total force $F_{N_{Tot}}$ on the r^{th} element is found by integrating $F_n(z)$ over the length of the element, and dividing this by 2 gives the total normal force which may be considered concentrated at each node of the r^{th} element :

$$F_N = \frac{K_r a \omega^2}{2 \sinh kd}\Big[\sin(kx-\omega t)\sin\theta_r \int_{kz_1}^{kz_2} \frac{\cosh u}{k}\,du + \cos(kx-\omega t)\cos\theta_r \int_{kz_1}^{kz_2} \frac{\sinh u}{k}\,du\Big]$$

$$+ \frac{C_r\sqrt{\frac{8}{\pi}}\, a\,\omega}{2 \sinh kd}\Big[\cos(kx-\omega t)\sin\theta_r \int_{kz_1}^{kz_2} \sigma_v(z)\,\frac{\cosh u}{k}\,du - \sin(kx-\omega t)\cos\theta_r \int_{kz_1}^{kz_2} \sigma_v(z)\,\frac{\sinh u}{k}\,du\Big] \qquad (4.28')$$

in which $u = kz$. Performing the integrations yields :

$$F_N = \frac{K_r\, a\, \omega^2}{2 \sinh kd} \left[P_r \sin(kx-\omega t) + Q_r \cos(kx-\omega t) \right]$$

$$+ \frac{C_r \sqrt{\frac{8}{\pi}}\, a\, \omega}{2 \sinh kd} \left[R_r \cos(kx-\omega t) - S_r \sin(kx-\omega t) \right] \quad (4.29')$$

where

$$\left.\begin{aligned}
P_r &= \sin\theta_r\,(\sinh kz_2 - \sinh kz_I)/k = \sin\theta_r\,(I_I) \\
Q_r &= \cos\theta_r\,(\cosh kz_2 - \cosh kz_I)/k = \cos\theta_r\,(I_2) \\
R_r &= \sin\theta_r\,\Big(\sigma_I I_I + \frac{(\sigma_2 - \sigma_I)}{k^2 l}\Big[u \sinh u - \cosh u\Big]\Big|_{kz_I}^{kz_2} \\
S_r &= \cos\theta_r\,\Big(\sigma_I I_I + \frac{(\sigma_2 - \sigma_I)}{k^2 l}\Big[u \cosh u - \sinh u\Big]\Big|_{kz_I}^{kz_2}
\end{aligned}\right| \quad (4.30')$$

From this, the horizontal and vertical components of F_N are given by :

$$F_{N_{H,V}}(\omega) = \frac{K_r\, a\, \omega^2}{2 \sinh kd} \left[P_r A_r \sin(kx-\omega t) + Q_r A_r \cos(kx-\omega t) \right]$$

$$+ \frac{C_r \sqrt{\frac{8}{\pi}}\, a\, \omega}{2 \sinh kd} \left[R_r A_r \cos(kx-\omega t) - S_r A_r \sin(kx-\omega t) \right] \quad (4.3I')$$

where

$$A_r = \begin{cases} \sin \Theta_r \text{ , for the horizontal component, suffix H} \\ \cos \Theta_r \text{ , for the vertical component , suffix V .} \end{cases} \qquad (4.32')$$

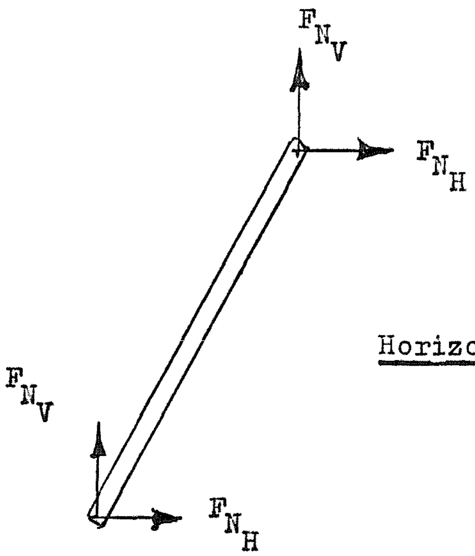

Horizontal and Vertical Nodal Force Components

Having derived an expression for the element nodal forces, the following three sections will be devoted to different ways of combining them in a spectral analysis .

4.5.3 'LUMPED' FORCE APPROACH, IGNORING OFF-DIAGONAL TERMS IN EQUATION (4.2I) (Programme SPECTAI in Chapter 5)

Having idealised the forces on a structure by applying them at the nodes, the best representation of these forces will presumably be given by considering the cross-spectral densities of all these forces. With this in mind, we can start with the force at each node of element r, as given by equation (4.3I'), and we can say that the force at any node i of the complete structure is given by adding together the contributions from all the elements such as r meeting at that node i.

$$F_{i_{H,V}}(\omega) = \frac{a}{2 \sinh kd} \left[\omega^2 \left[T_i \sin(kx-\omega t) + U_i \cos(kx-\omega t) \right] \right. \qquad (4.33')$$

$$\left. \sqrt{\frac{8}{\pi}}\,\omega \left[V_i \cos(kx-\omega t) - W_i \sin(kx-\omega t) \right] \right]$$

in which

$$\left. \begin{aligned} T_i &= \sum_{j=I}^{N_i} (A_{r_j} P_{r_j} K_{r_j}) \\ U_i &= \sum_{j=I}^{N_i} (A_{r_j} Q_{r_j} K_{r_j}) \\ V_i &= \sum_{j=I}^{N_i} (A_{r_j} R_{r_j} C_{r_j}) \end{aligned} \right| \qquad (4.34')$$

$$W_i = \sum_{j=1}^{N_i} (A_{r_j} \, S_{r_j} \, C_{r_j})$$

and N_i is the number of elements meeting at node i .

Collecting sine and cosine terms , equation (4.33') may be written:

$$F_{i_{H,V}}(\omega) = \frac{a}{2 \sinh kd} \Big[(T_i \omega^2 - \sqrt{\tfrac{8}{\pi}} \, W_i \omega) \sin (kx - \omega t)$$

$$+ (U_i \omega^2 + \sqrt{\tfrac{8}{\pi}} \, V_i \omega) \cos (kx - \omega t) \Big] \qquad (4.33a')$$

which may now be written in terms of a single sinusoidal wave as :

$$F_{i_{H,V}}(\omega) = \frac{a}{2 \sinh kd} \; X_i \; \sin (kx - \omega t + Y_i) \qquad (4.33b')$$

where

$$X_i = \omega \sqrt{(T_i - \sqrt{\tfrac{8}{\pi}} \, W_i)^2 + (U_i + \sqrt{\tfrac{8}{\pi}} \, V_i)^2}$$

$$Y_i = \mathrm{Tan}^{-1} \left[\frac{U_i + \sqrt{\tfrac{8}{\pi}} \, V_i}{T_i - \sqrt{\tfrac{8}{\pi}} \, W_i} \right]$$

The cross-spectral density of two nodal forces F_i and F_k is now given by :

$$S_{FF}(i,k,\omega) = \frac{1}{4 \sinh^2 kd} \; X_i \, X_k \; S_{\eta\eta}(\omega) \qquad (4.35')$$

4.5.4 LUMPED FORCE REPRESENTATION , CONSIDERING EACH DEGREE OF FREEDOM INDEPENDENTLY (Programme SPECTA2, Chapter 5)

Equation (4.31') gives an expression for the nodal forces on a typical element of a structure . Proceding as in the previous section , the horizontal and vertical components of the i th nodal force can be written down in the form :

$$F_{i_{H,V}}(\omega) = \frac{a}{2 \sinh kd} \; X_i \; \sin (kx - \omega t + Y_i)$$

where

$$X_i = \omega \sqrt{\left(T_i \omega - \sqrt{\frac{8}{\pi}} \, W_i \right)^2 + \left(U_i \omega + \sqrt{\frac{8}{\pi}} \, V_i \right)^2}$$

$$Y_i = \mathrm{Tan}^{-1} \left[\frac{U_i \omega + \sqrt{\frac{8}{\pi}} \, V_i}{T_i - \sqrt{\frac{8}{\pi}} \, W_i} \right]$$

and , in this case , T_i , U_i , V_i , W_i are due to the contribution from one element only and are given by :

$$T_i = A_r P_r K_r$$

$$U_i = A_r Q_r K_r$$

$$V_i = A_r R_r C_r$$

$$W_i = A_r S_r C_r$$

As before , A_r , P_r , Q_r , R_r , S_r , K_r and C_r are given by equations (4.30') and (4.32') .

Hence the spectral density $S_{FF}(i,i,\omega)$ of F_i is given by :

$$S_{FF}(i,i,\omega) = \frac{I}{4\sinh^2 kd} X_i^{\,2} S_{\eta\eta}(\omega) \qquad (4.36')$$

We can consider the response of the structure to this forcing spectrum alone , and then repeat the process for all the other degrees of freedom of the structure over all the other elements (a total of 4 X (The number of elements) times) . In this way , we can compare the analysis using the fully-coupled force spectra , as described in the previous section , with the analysis using uncoupled spectra , as described in this section .

In order to appreciate the resulting simplifications that arise in the theory by using the uncoupled force spectra , let us return to equation (4.23) , which gives the matrix of displacement spectral densities $\underline{S}_x$ in terms of the matrix of force spectral densities $\underline{S}_F$:

$$\underline{S}_x = \underline{A}\left[\underline{\alpha}\,\underline{A}^T\,\underline{S}_F\,\underline{A}\,\hat{\underline{\alpha}}\right]\underline{A}^T \qquad (4.37')$$

For the uncoupled analysis , we replace $\underline{S}_F(\omega)$ by :

$$\underline{S}_F(\omega) = \begin{bmatrix} 0 & & & & & & \\ & \ddots & & & & \bigcirc & \\ & & 0 & & & & \\ & & & S_F(i,i,\omega) & & & \\ & & & & 0 & & \\ & \bigcirc & & & & 0 & \\ & & & & & & \ddots \\ & & & & & & & 0 \end{bmatrix} \qquad (4.38')$$

This gives for the matrix of spectral densities of the generalised forces $\underline{S}_G$:

$$\underline{S}_G = \underline{A}^T\,\underline{S}_F\,\underline{A}$$

$$= \begin{bmatrix} A_{11} & A_{21} & A_{31} & \cdots \\ A_{12} & A_{22} & A_{32} & \cdots \\ A_{13} & A_{23} & \cdots & \\ \vdots & \vdots & & \end{bmatrix} \begin{bmatrix} 0 & & & \bigcirc \\ & 0 & & \\ & & S_F(i,i) & \\ \bigcirc & & & \ddots \end{bmatrix} \begin{array}{c} \begin{bmatrix} A_{11} & A_{12} & A_{13} & \cdots \\ A_{21} & A_{22} & A_{23} & \cdots \\ A_{31} & A_{32} & & \cdots \\ \vdots & \vdots & & \end{bmatrix} \\ \begin{array}{cc} \uparrow & \uparrow \\ 1^{st} & 2^{nd} \\ \text{Mode} & \text{Mode} \\ \text{Shape} & \text{Shape} \end{array} \end{array}$$

$$= \begin{bmatrix} A_{i1} A_{i1} & A_{i1} A_{i2} & A_{i1} A_{i3} & \cdots \\ A_{i2} A_{i1} & A_{i2} A_{i2} & A_{i2} A_{i3} & \cdots \\ A_{i3} A_{i1} & A_{i3} A_{i2} & A_{i3} A_{i3} & \cdots \\ \vdots & \vdots & \vdots & \end{bmatrix} \times S_F(i,i,\omega) \qquad (4.39')$$

Hence the matrix of spectral densities of the generalised displacements $\underline{S}_Q$ is :

$$\underline{S}_Q = \underline{\alpha}\, \underline{S}_G\, \underline{\hat{\alpha}} = \begin{bmatrix} A_{i1}{}^2 |\alpha_1|^2 & & & \\ & A_{i2}{}^2 |\alpha_2|^2 & & \\ & & A_{i3}{}^2 |\alpha_3|^2 & \\ & & & \ddots \end{bmatrix} \times S_F(i,i) \qquad (4.40')$$

where we have ignored off-diagonal terms in $\underline{\alpha}$ and $\underline{\hat{\alpha}}$.

Finally, the matrix of spectral densities of the original displacements $\underline{S}_x$ is given by :

$$\underline{S}_x = \underline{A}\ \underline{S}_Q\ \underline{A}^T$$

which when expanded leads to :

$$
\underline{S}_x = \begin{bmatrix} A_{11} & A_{12} & A_{13} & \cdots \\ A_{21} & A_{22} & & \cdots \\ \vdots & \vdots & & \end{bmatrix} \begin{bmatrix} A_{i1}^2 |\alpha_1|^2 & & & \\ & A_{i2}^2 |\alpha_2|^2 & & \\ & & \ddots & \\ & & & \cdot \end{bmatrix} \begin{bmatrix} A_{11} & A_{21} & A_{31} & \cdots \\ A_{12} & A_{22} & A_{32} & \cdots \\ \vdots & \vdots & \vdots & \end{bmatrix} \times S_F(i,i) \qquad (4.41')
$$

The diagonal terms of $\underline{S}_x$ are the ones needed for the nodal point displacements . These are given by :

$$
S_x(k,k,\omega) = \Big[A_{k1}^2 A_{i1}^2 |\alpha_1|^2 + A_{k2}^2 A_{i2}^2 |\alpha_2|^2 + \cdots + A_{kn}^2 A_{in}^2 |\alpha_n|^2 \Big] \times S_F(i,i,\omega) \qquad (4.42')
$$

$$
\cong \left[\sum_{j=1}^{n_s} A_{kj}^2 A_{ij}^2 |\alpha_j|^2 \right] S_F(i,i,\omega)
$$

($k = 1,2,3, \ldots ,n$)

where n_s is the number of significant natural frequencies of the structure (dependent on the sea spectrum $S_{\eta\eta}(\omega)$) .

Integrating $S_x(k,k,\omega)$ with respect to ω gives the variance of the displacement at coordinate k due to a forcing spectrum at coordinate i . The process must be repeated for forces F_i at each coordinate i and the results superimposed .

4.5.5 A 'DIRECT TRANSFER FUNCTION' TECHNIQUE (Programme SPECT3 in Chapter 5)

(a) The previous two sections dealt with methods of analysis in which the spectral density matrix of the forces is first computed and this is then used to evaluate the spectral density matrix of the required displacements.

In this section , we solve the equations of motion explicitly at a frequency ω and from this , attempt to find a transfer function $Z_i(\omega)$ connecting the displacement x_i with the wave amplitude $\eta(x_i, \omega)$ for each degree of freedom i , i.e.

$$x_i = Z_i(\omega) \ \eta(x_i, \omega) \qquad (4.53)$$

or in terms of the two spectra

$$S_{x_i x_i}(\omega) = Z_i^2(\omega) \ S_{\eta\eta}(\omega) \qquad (4.54)$$

(b) A modal decomposition technique will be used , where in this case we need to know the form of the forcing function exactly. Starting with the equations of motion for a structure composed of inclined members (equation (4.7)) :

$$\underline{M}\,\ddot{\underline{X}} + \underline{C}\,\dot{\underline{X}} + \underline{K}\,\underline{X} = \underline{F} \tag{4.55}$$

where the force vector $\underline{F}$ is composed of forces F_i at each coordinate i. F_i is made-up of the contributions from all the elements meeting at coordinate i and has already been derived in equations (4.33') and (4.34')

$$F_i(\omega, t) = \frac{a}{2\sinh kd}\left[\left\{T_i \sin(kx-\omega t) + U_i \cos(kx-\omega t)\right\}\omega^2 + \sqrt{\frac{8}{\pi}}\,\omega\left\{V_i \cos(kx-\omega t) - W_i \sin(kx-\omega t)\right\}\right] \tag{4.56}$$

Due to vertical components of vel. and acceleration

Due to horizontal components

Decomposing equations (4.55) using a modal technique, we arrive at equation (4.12):

$$\left[\underline{A}^T\,\underline{M}\,\underline{A}\right]\dot{\underline{q}} + \left[\underline{A}^T\,\underline{C}\,\underline{A}\right]\dot{\underline{q}} + \left[\underline{A}^T\,\underline{K}\,\underline{A}\right]\underline{q} = \underline{A}^T\,\underline{F} = \bar{\underline{F}} \tag{4.57}$$

which leaves n uncoupled second order differential equations of which the i th is:

$$m_i\,\ddot{q}_i + c_i\,\dot{q}_i + k_i\,q_i = \bar{F}_i \tag{4.58}$$

where $\bar{F}_i$ is in this case given by :

$$\bar{F}_i = \sum_{j=1}^{n} A_{ji}\,F_j$$

This may in turn be written :

$$\bar{F}_i = \omega^2 \left[P_i \sin (kx - \omega t) + Q_i \cos (kx - \omega t) \right] + \omega \left[R_i \sin (kx - \omega t) + S_i \cos (kx - \omega t) \right] \quad (4.59)$$

in which

$$\left.\begin{aligned} P_i &= \left[\sum_{j=I}^{n} A_{ji} T_j \right] X \frac{a}{2 \sinh kd} \\ Q_i &= \left[\sum_{j=I}^{n} A_{ji} U_j \right] X \frac{a}{2 \sinh kd} \\ R_i &= \left[-\sum_{j=I}^{n} A_{ji} W_j \right] X \frac{a\sqrt{\frac{8}{\pi}}}{2 \sinh kd} \\ S_i &= \left[\sum_{j=I}^{n} A_{ji} V_j \right] X \frac{a\sqrt{\frac{8}{\pi}}}{2 \sinh kd} \end{aligned}\right| \quad (4.60)$$

(b) Instead of Fourier transforming equation (4.58) , let us solve it for the case of a forcing function given by equation (4.59) . In this way , we can hope to derive a 'transfer function' between displacements and wave amplitudes.

The solution to equation (4.58) will consist of a transient response (the solution to the homogeneous equation) and a steady-state response (due to the forcing function) . Considering just the steady-state response , we look for a solution of the form :

$$q_i = A_i \cos(kx - \omega t) + B_i \sin(kx - \omega t) \qquad (4.61)$$

Inserting equation (4.61) into equation (4.58) and equating coefficients of $\sin(kx - \omega t)$ and $\cos(kx - \omega t)$:

$$\begin{aligned} -m_i \omega^2 A_i - \omega c_i B_i + k_i A_i &= \omega^2 Q_i + \omega S_i \\ -m_i \omega^2 B_i + \omega c_i A_i + k_i B_i &= \omega^2 P_i + \omega R_i \end{aligned} \qquad (4.62)$$

Solving these two equations for A_i and B_i and simplifying the results gives :

$$A_i = \frac{\left[k_i (S_i + \omega Q_i)\left(1 - \frac{\omega^2}{\omega_i^2}\right) + c_i \omega (R_i + \omega P_i)\right]\omega}{c_i^2 \omega^2 + k_i\left(1 - \frac{\omega^2}{\omega_i^2}\right)} \qquad (4.63)$$

$$B_i = \frac{\left[k_i (R_i + \omega P_i)\left(1 - \frac{\omega^2}{\omega_i^2}\right) - c_i \omega (S_i + \omega Q_i)\right]\omega}{c_i^2 \omega^2 + k_i\left(1 - \frac{\omega^2}{\omega_i^2}\right)}$$

Inserting A_i and B_i into equation (4.61) gives the required response q_i which may now be written :

$$q_i = \bar{q}_i \sin(kx - \omega t + \Theta) \tag{4.64}$$

in which

$$\bar{q}_i = \sqrt{A_i^2 + B_i^2} \quad \text{and} \quad \Theta = \mathrm{Tan}^{-1}\left(\frac{A_i}{B_i}\right)$$

In the expressions for A_i and B_i , ω_i is the i th natural frequency of the structure and is related to the generalised stiffness and mass by the equation

$$\omega_i^2 = \frac{k_i}{m_i}$$

Equation (4.64) gives the generalised displacement q_i corresponding to a surface disturbance $\eta = \sin(kx - \omega t)$. In spectral form , we can therefore write :

$$S_{q_i q_j}(\omega) = \bar{q}_i(\omega)\, \bar{q}_j(\omega)\, S_{\eta\eta}(\omega) \tag{4.65}$$

(for $i , j = 1,2,3, \ldots , n_s$)

Finally, the original displacements $\underline{x}$ are given by the diagonal terms of $S_{\underline{x}\,\underline{x}}$:

$$S_{\underline{x}\,\underline{x}} = \underline{A}\, S_{\underline{q}\underline{q}}\, \underline{A}^T \qquad (\text{ since } \underline{x} = \underline{A}\,\underline{q}\,) \tag{4.66}$$

4.6 SINGLE DEGREE OF FREEDOM SYSTEMS

4.6.I INTRODUCTION

Some offshore structures may conveniently be idealised as single degree of freedom systems . This enables the designer to do a hand calculation in order to check his more sophisticated analytical techniques . Typical of such a structure is the single leg platform , one of which is analysed in section 5.4 , example I , using the three computer programmes of chapter 5 . This will now be analysed manually .

4.6.2 EXAMPLE : I2 m DIAMETER SINGLE LEG PLATFORM

The characteristics of the platform are given in Example I of section 4.5 . We first need the mass M and stiffness K of the equivalent single degree of freedom system . Assuming a quadratically varying deflected shape for the structure , i.e.

$$f\left(\frac{z}{l}\right) = \left(\frac{z}{l}\right)^2$$

the mass M is given by :

$$M = (m + m_a)\int_0^d \left(\frac{z}{l}\right)^4 dz + m\int_d^l \left(\frac{z}{l}\right)^4 dz + M_P \left(\frac{z}{l}\right)^4\Bigg|_{z=l}$$

$$= 6.990 \times 10^6 \text{ kg}$$

where m = mass per unit length of concrete (kg)

m_a = mass per unit length of displaced water (kg)

M_P = mass of platform (kg)

The stiffness K is :

$$K = \frac{E\,I}{l^3} \int_0^{\ell} \left(\frac{\partial^2 f}{\partial z^2} \right)^2 dz = 1.10 \times 10^6 \ \mathrm{N/m}$$

Hence the natural frequency ω of the system is :

$$\omega = \frac{K}{M} = 1.25 \ \mathrm{rad/sec}$$

The damping constant γ is then given by :

$$\gamma = \gamma_s + \frac{C_H}{2\,M\,\omega}$$

in which $C_H = C_D \sqrt{\frac{8}{\pi}} \int_0^d \sigma_v(z) \left(\frac{z}{l} \right)^2 dz$

γ_s is the structural damping , in this case 0.05

$$C_D = \frac{c_d\,\rho_w\,D}{2} = 6150 \ \mathrm{kg/m^2}$$

$$\sigma_v^2(z) = \int_0^{\infty} \omega^2 \frac{\cosh^2 kz}{\sinh^2 kd} S_{\eta\eta}(\omega)$$

and $S_{\eta\eta}(\omega)$ is the wave amplitude spectrum , in this case the Pierson-Moskowitz spectrum (Fig 3.3)

Clearly , we need to use numerical integration to find $\sigma_v(z)$, which is then inserted into the expression for C_H , which in turn is inserted into the expression for γ . Curves of $\sigma_v(z)$ against z and $z^4\,\sigma_v(z)$ against z are given subsequently . From these , we obtain :

$$C_H = \frac{6150\sqrt{\frac{8}{\pi}}}{(130)^4} \int_0^{100} z^4\, \sigma_v(z)\, dz = 1.226 \times 10^5$$

$$\gamma = \gamma_s + \frac{C_H}{2\,M\,\omega} = 0.0500 + 0.0081 = 0.0581$$

(c.f. 0.0574 in the computer programme)

Using the above values of K, ω_n and γ, the frequency response function $\left|\alpha(\omega)\right|^2$ is now calculable :

$$\left|\alpha(\omega)\right|^2 = \frac{1}{K^2\left[\left(1 - \left(\frac{\omega}{\omega_n}\right)\right)^2 + \left(2\gamma\frac{\omega}{\omega_n}\right)\right]^2}$$

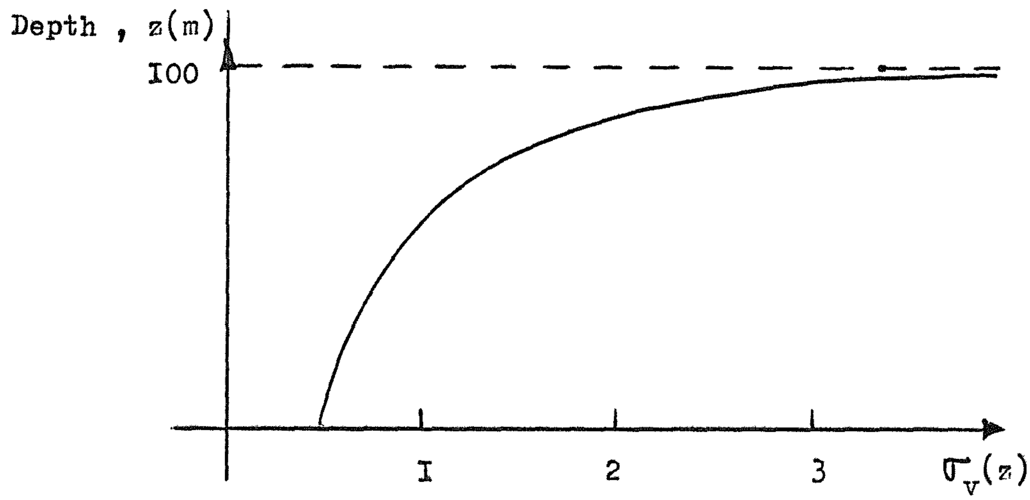

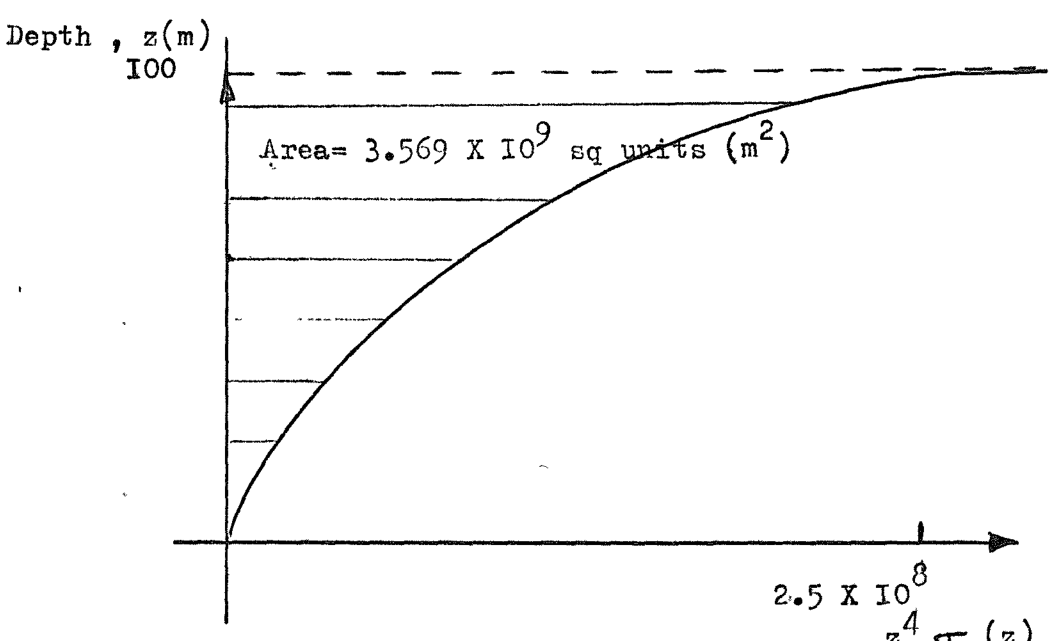

We next calculate the force spectrum $S_{FF}(\omega)$ which is found from the formula :

$$S_{FF}(\omega) = \left\{ \frac{C_I^2 \, \omega^4}{\sinh^2 kd} \left[\int_0^d \cosh kz \;\; f\left(\frac{z}{l}\right) dz \right]^2 \quad \text{Inertia Term} \right.$$

$$\left. + \; C_D^2 \, \frac{8}{\pi} \, \frac{\omega^2}{\sinh^2 kd} \left[\int_0^d \cosh kz \; \sigma_v(z) \;\; f\left(\frac{z}{l}\right) dz \right]^2 \quad \text{Drag Term} \right\}$$

$$X \;\; S_{\eta\eta}(\omega)$$

[N.B. Caution is needed with the inertia and added mass coefficients . In the notation of this thesis , $C_M = 2$ (inertia coefficient) and $C_A = I$ (added mass coeff.). The added mass joins the structural mass on the left hand side of the system of equations . Thus $C_I = C_M$ in the above expression . Other authors take $C_M = I$, $C_A = I$, in which case we need to take $C_I = C_A + C_M$ in the expression above .]

Inserting the appropriate numbers , we get :

$$S_{FF}(\omega) = \frac{(232000)^2 \, \omega^4}{\sinh^2 I00d} \; I^2 \; S_{\eta\eta}(\omega) + \{\text{Drag Term}\}$$

where

$$I = (\sinh I00k) \left(\frac{I0^4}{k} + \frac{2}{k^3} \right) - (\cosh I00k) \, \frac{200}{k^2} \; .$$

A diagram of $S_{FF}(\omega)$ against ω is shown overleaf .

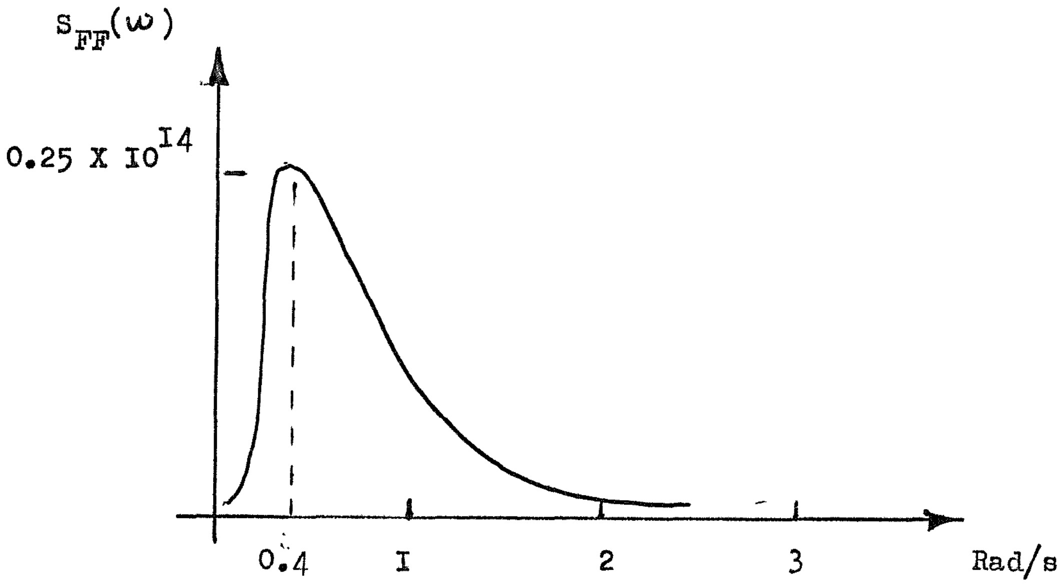

Multiplying the curve above with the frequency response curve for $\gamma = 0.058$, shown on the following page , gives the spectral density of the displacement , i.e.

$$S_{QQ}(\omega) = \left|\alpha(\omega)\right|^2 S_{FF}(\omega)$$

and hence the variance of the displacement is :

$$\sigma_q^{\ 2} = \int_0^{\infty} S_{QQ}(\omega)\, d\omega$$

Clearly , $S_{FF}(\omega)$ and $\left|\alpha(\omega)\right|^2$ have to be evaluated for a series of values of ω , and then the above equation has to be numerically integrated to find $\sigma_q^{\ 2}$.

The final result for σ_q is :

$$\sigma_q = 0.852 \text{ m}$$

FREQUENCY RESPONSE FUNCTION $|\alpha(\omega)|^2$

$$|\alpha(\omega)|^2 = \frac{1}{k^2\left[\left(1-\left(\frac{\omega}{\omega_n}\right)^2\right)^2 + \left(2\gamma\frac{\omega}{\omega_n}\right)^2\right]}$$

Curve	γ
I	0.0I
2	0.02
3	0.03
4	0.04
5	0.05
6	0.06
7	0.07
8	0.08
9	0.09
I0	0.I0

k = 830I800 N/m

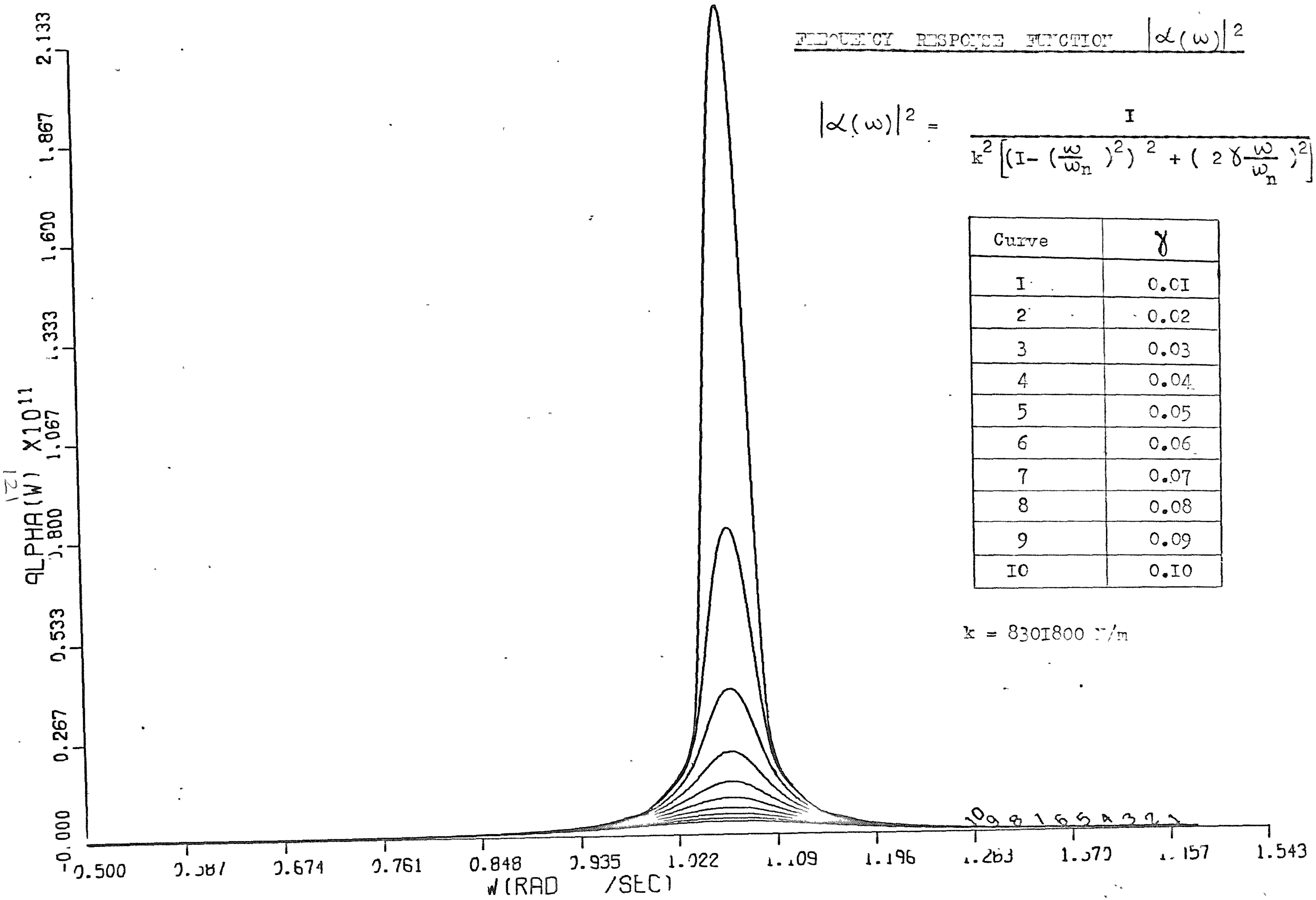

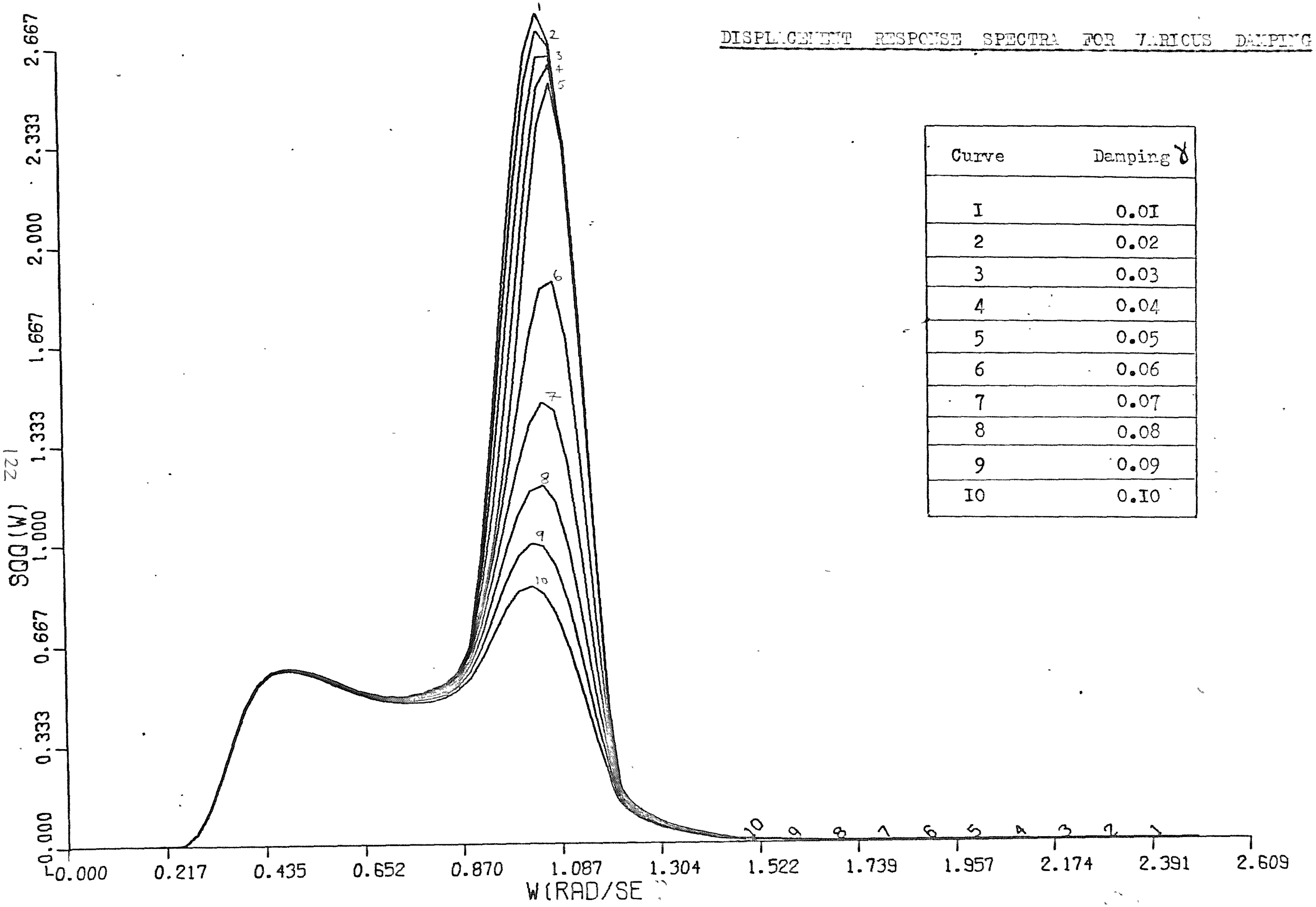
DISPLACEMENT RESPONSE SPECTRA FOR VARIOUS DAMPING
SQQ(W)
W(RAD/SE
0.000
0.333
0.667
1.000
1.333
1.667
2.000
2.333
2.667
0.000
0.217
0.435
0.652
0.870
1.087
1.304
1.522
1.739
1.957
2.174
2.391
2.609
Curve
Damping γ
I 0.0I
2 0.02
3 0.03
4 0.04
5 0.05
6 0.06
7 0.07
8 0.08
9 0.09
I0 0.I0

4.7 MEMBER STRESSES

From a design point of view, one of the most important things to know is the member loads, from which member sizes can be deduced. Sections 4.3-4.5 were concerned with the calculation of the standard deviations of the displacements at each degree of freedom, but clearly this information is insufficient in itself to enable the designer to evaluate the member stresses, since the standard deviations do not take into account the direction of the displacements. Accordingly, the analyst can proceed in several different ways.

One way is to return to the mode shapes of the structure, which do take account of the directions of the displacements, and to use these, together with the standard deviations of the displacements as scaling factors, to calculate the required stresses. In practice, it has been found that all the structures considered in this thesis respond almost entirely in the first mode, so that the displaced shape of the structure is practically a scaled first mode shape. If other modes are important, the modal participation factors, which are found early on in the analysis, can be considered.

Alternatively, one can consider the relationship between member stresses and displacements. For any member of the structure, there exists a relationship connecting the loads in the member with the nodal point displacements. This is of the form :

$$\underline{P}_e = \underline{B}_e \underline{X}_e \tag{4.67}$$

where $\underline{P}_e$ and $\underline{X}_e$ are vectors containing the element loads and displacements, respectively. For a beam element, such as the one used in this thesis, both vectors contain 6 elements. The spectral density containing the covariances of the element loads is therefore given by :

$$\underline{S}_{P_e} = \underline{B}_e \underline{S}_{X_e} \underline{B}_e^T \tag{4.68}$$

The standard deviations $\underline{\sigma}_P$ of the element loads are now given by :

$$\sigma_{P_i} = \sqrt{\int S_{P_{e_i}} \, d\omega} \tag{4.69}$$

$$(i=1,2,. . . ,6)$$

The elements of the matrix $\underline{S}_{X_e}$ have been derived earlier, and equation (4.69) therefore gives the required solution. In practice however, the computer core store required to perform the operation of equation (4.69) is often prohibitive.

CHAPTER 5 : THE COMPUTER ANALYSIS OF PLANE FRAMES SUBJECTED TO RANDOM WAVE LOADING

5.I INTRODUCTION

Chapter 3 was concerned with methods for evaluating the force on a structure due to a sea state described by a wave amplitude spectrum . Chapter 4 then considered the effect of applying such forces to multi degree of freedom systems , which one has when using the Finite Element Method .

Several computer programmes have been written , based on this theory . Results from these programmes is given in condensed form in the Tables in section 5.4 . To avoid confusion only two programmes will be considered in detail , but a complete list of all the programmes used is as follows :

(i) A 'Frequency Domain' method (see Introduction to Chapter 4) , in which the element nodal forces are evaluated '<u>consistently</u>' (section 4.4) .

The other three programmes all assume the element nodal forces to be <u>lumped</u> at the nodes (section 4.5) .

(ii) A 'Frequency Domain' method in which all the element nodal forces are assumed to act simultaneously (section 4.5.3) . This method is similar to that used by Malhotra and Penzien (Refs. 5) . In our case , off-diagonal terms in the frequency response matrix (equation 4.20a and section 4.3.3) are ignored . This is called programme SPLCTAI in section 4.5.3 .

(iii) A 'Frequency Domain' method in which all the element nodal forces are applied independently and then superimposed

(section 4.5.4) . This uses similar theory to the previous programme and is called SPECTA2 .

(iv) A 'Direct Transfer Function' method (see Introduction to Chapter 4 and section 4.5.5) . Element nodal forces are assumed to be lumped at the nodes . This is programme SPECTA3 .

The consistent force programme , programme (i) , has been found to give very similar results to programme SPECTA1 (see Table 5.I) , and SPECTA2 is a simplification of SPECTA1 . Thus , the main comparison is between the 'Frequency Domain' method SPECTA1 and the 'Direct Transfer Function' method SPECTA3 . To avoid proliferation , only these two methods will be discussed in detail . Results from all the programmes are however given in the Tables .

5.2 GENERAL PROGRAMME DESCRIPTIONS AND FLOW CHARTS

The logic of the two programmes considered , SPECTA1 and SPECTA3 , is best described by flow charts . The programmes are written in FORTRAN and have been run on the University of Southampton ICL 1907 and ICL 2970 .

FLOWCHART , PROGRAMMES SPECTAI AND SPECTA3

This page applies to both SPECTI and SPECT3 . For the remainder of SPECTAI , proceed to the next page , and for SPECTA3 proceed two pages .

(START)

↓

Input Data (see user's data sheet)
Initialise Global Mass, Stiffness and Damping Matrices

↓

Calculate Added Mass per Unit Length, and Total Drag and Inertia Coefficients, For Each Member (Equation(3.Ia))

↓

Calculate Standard Deviations of Fluid Particle Velocities at Each Node (Subroutine SIGVEL)

↓

Assemble Global Mass, Stiffness and Hydrodynamic Damping Matrices, M, K, and C, respectively .
Apply Boundary Conditions (Section 4.2)

↓

Evaluate Highest Natural Frequency That It Is Necessary To Consider, F_{Max} (Dependent on Wave Amplitude Spectrum). Find Natural Frequencies (up to F_{Max}) and Mode Shapes (An Iterative Procedure, Subroutine EIGEN) .
Normalise Modes With Respect To Mass Matrix ;
Diagonalise M, K, and C . (Section 4.3.2)

↓

Add Structural Damping To Damping Coefficients and Change To Proportion of Critical Damping

↓

Move on I page for programme SPECTAI
Move on 2 pages for programme SPECTA3

↓

Loop Over The Number of Significant Frequencies

Evaluate Integration Points, According To Natural Frequencies

Loop Over Integration Points

Calculate Spectral Density Matrix $\underline{S}_{FF}$ At Frequency ω
(equation (4.35') ; subroutine SPECT)

Form Triple Product $\underline{S}_G = \underline{A}^T * \underline{S}_{FF} * \underline{A}$
(equation (4.21) ; subroutine SFSTAR)

Form Matrix of Spectral Densities of Generalised Displacements $\underline{S}_X = \underline{A}\ \underline{S}_Q\ \underline{A}^T$
(equation (4.22) ; subroutine SUU)

Numerically Integrate Diagonal Terms of $\underline{S}_X$ To Give Variance of Response in Each Degree of Freedom

End of Integration Points?
No
Yes

End of Significant Frequencies?
No
Yes

Print Standard Deviations of Displacements

Calculate Standard Deviations of Member Stresses

END

Evaluate Integration Points

Loop Over Integration Points

Evaluate Nodal Forces (i.e. coeffs T_i, U_i, V_i, W_i ; equation (4.34')) for Each Nodal Degree of Freedom

Evaluate Generalised Forces (i.e. coeffs P_i, Q_i, R_i, S_i ; equation (4.60))

Evaluate 'Transfer Function' $\left[\bar{q}_i(\omega)\right]^2$
(equations (4.6I),(4.63),(4.64))

Evaluate Matrix of Spectral Densities of Displacement Responses $\underline{S}_x$ (equations (4.65),(4.66))

$$S_{q_i}(\omega) = \left[\bar{q}_i(\omega)\right]^2 S_{\eta\eta}(\omega)$$

$$\underline{S}_x = \underline{A}\ \underline{S}_q\ \underline{A}^T$$

Numerically Integrate Diagonal Terms of $\underline{S}_x$ To Give The Response In Each Degree of Freedom

No

End of Integration Points ?

Yes

Print Standard Deviations of Displacements

Calculate and Print Standard Deviations of Member Stresses

End

5.3 USER INSTRUCTIONS , PROGRAMMES SPECTAI AND SPECTA3

The input data is identical for both programmes .

DATA	FORMAT
I. Single Card Containing :	
Number of elements , NEL	
Number of nodal points , NNP	
Number of reactions , NREAC (see 5 below)	3IIO
2. Single Card Containing The Problem Title	20A4
3. One Card For Each Nodal Point (NNP cards in all) containing :	
Node number	IIO
x-coordinate (parallel to sea bed) in metres	2FIO.3
y-coordinate (vertical from sea bed) in metres	
4. Two Cards For Each Element (NEL times in all) containing :	
(i) member number	
node number of end I	
node number of end 2	
Young's modulus of the material, E (N/m^2)	
second moment of area, I (m^4)	
cross-sectional area of concrete, A (m^2)	
mass per unit length, m (kg)	3IIO
(i.e. cross-sectional area X density)	
displaced volume of water per unit length, V (m^3) (zero for members above the water surface)	5FIO.3
(ii) sheltering factor (i.e. the length between the element under consideration and the one that is assumed to be causing a sheltering effect - see section 3.6	FIO.3

DATA	FORMAT
5. One Card For Each Reaction (NREAC cards in all) containing : number of fixed node direction of fixity (fixity specified by : I - x-direction 2 - y-direction 3 - rotation	2I10
6. Single Card Containing : water depth (m) parameters A and B of the Pierson-Moskowitz spectrum (see Fig 3.3)	3F10.3
7. Single Card Containing : added mass coefficient , C_{am} inertia coefficient, C_M drag coefficient , C_D	3F10.3
8. Single Card Containing : proportion of critical damping due to structural action ,	F10.3
9. Single Card Containing : number of additional sea spectra to be analysed for NSP	I10
10. One Card For Each Additional Sea Spectrum (NSP cards in all) , containing : Pierson - Moskowitz parameters A, B	2F10.3

The maximum allowable number of elements, nodal points, etc., is determined by the dimension statements and data statement at the begining of the master segment. For a structure with 66 nodal points the listing is as given in Appendix 9, and the programme then occupies 58K of core store on an ICL 1907 computer.

5.4 EXAMPLES AND RESULTS

The computer programmes described in this chapter will now be examined by considering three examples - a single-leg concrete platform , a four-leg platform idealised as a plane frame , and a steel framed platform . The first two examples are used to provide a comparative study of the different methods of analysis (described in chapter 4) , and of the diffraction theory against Morison's theory (described in chapter 3) . The third example is more complete (for which thanks are due to Halcrow-Ewbank Ltd., London) , and allows for the utilisation of the theory for inclined cylinders (Chapters 3 and 4) . The descriptions of , and results from , the three examples occupy the remainder of section 5.4 , and the conclusions derived from the results are presented in section 5.5. .

The single-leg platform is described in section 5.4.I and is included for several reasons . Firstly , being very simple , it is cheap and easy to run , and it is very easy to check by hand . It therefore provides a check on the validity of the methods used . Secondly , many offshore structures respond primarily in the first mode , and therefore a single-degree-of-freedom system may well be sufficiently accurate , at least for a preliminary analysis.

Thirdly , some single-leg platforms have been built in their own right.

The four-leg platform described in section 5.4.2 provides a useful test for the importance of the drag force relative to the inertia force , and of sheltering , as well as the effect of cross-correlation terms in the response , which are clearly more important in the four-leg platform than the single-leg platform .

The steel framed jacket described in section 5.4.3 is included primarily to make use of the inclined cylinder theory , but the relative contributions of the drag and inertia terms can also be estimated for this case .

Some results from studies of the three structures of the following three sections are given in Appendix 9, together with a listing of programme SPECTA3 (section 4.5.5)

5.4.1 A SINGLE-LEG PLATFORM

This first example is a single-leg concrete platform, similar to the 'Monopod' platform in Fig 1.4 , some of which have been built in shallow water. In section 4.6, this structure was analysed using a single degree of freedom approximation, which gives a crude check on the validity of the computer programmes. The structure and its finite element idealisation are shown in Fig 5.1, together with other necessary data. The platform consists of a cylindrical concrete column with external diameter 12m and a concrete or steel deck, and has been divided into 6 beam elements.

The objective is to make a comparison between the 4 computer programmes summarised in section 5.1 , for one particular sea state described by the Pierson-Moskowitz wave amplitude spectrum with A=2.56 and B=0.0299 (see Fig3.3) , which corresponds to a significant wave height of 18.5m . The standard deviation of displacement at the top of the platform is used for the comparison, and its value is computed by the Morison theory and the diffraction theory, both including the drag force and neglecting it. The principal results are summarised in Table 5.1 and Figs 5.2- 5.5 , where bending moments, shears, etc. are illustrated.

In all cases, the structure responded almost entirely in the first mode, the contribution from the second mode being about 2½% . A comparison between the Morison theory and the diffraction theory, and an estimate of the effect of the drag force, is dealt with in section 5.5.

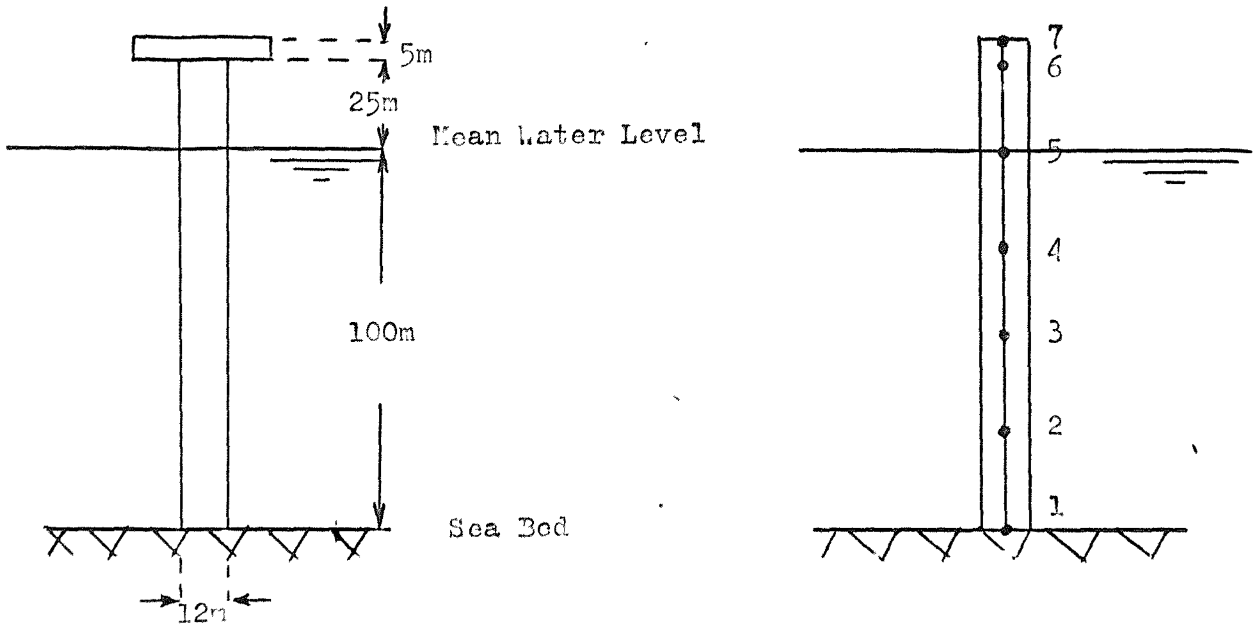

Wave height spectrum : Pierson-Moskowitz , $S_{\eta\eta}(\omega) = \frac{A}{\omega^5} \exp(\frac{-B}{\omega^4})$

with $A = 2.56$, $B = 0.0299$

Concrete :

density , $\rho_c = 2.503 \times IO^3$ kg/m^3

cross-sectional area , $A_c = I8.I$ m^2

mass per unit length , $m = \rho_c A_c = 4.53 \times IO^4$ kg

Second moment of area , $I = 380$ m^4

Displaced volume of water per unit length (submerged section only) = II3.0 m^3

Drag coefficient , $C_D = I$

Inertia coefficient , $C_M = I$ ('Added mass' coefficient also assumed to be I , i.e. overall inertia coefficient = 2)

Structural critical damping ratio $\xi = 0.05$

Young's modulus , $E = 0.I6 \times IO^{II}$ N/m^2

Fig 5.1 : Single-Leg Concrete Platform – Idealisation And General Data

Method	Displacement Standard Deviation at Top, σ_{Top} (r)			Fundamental Natural Frequency ω (Rad/s)
	Including Drag (Morison Theory)	Without Drag		
		Morison	Diffraction	
'Direct Transfer Function' Method, Programme SPECTA3	I.430	I.245	0.643	I.0772
'Frequency Domain Method' Programme SPECTAI (Lumped Element Forces, Considered Together)	0.94I	0.8I9	0.49I	I.0772
'Frequency Domain Method' Programme SPECTA2 (Lumped Element Forces, Considered Independently)	0.809	0.704	0.402	I.0772
'Frequency Domain Method' (Consistent Element Forces)	0.95I	0.827	0.495	I.0772
Single Degree of Freedom Approximation		0.852		I.043

Table 5.I : Results , Single-Leg Platform

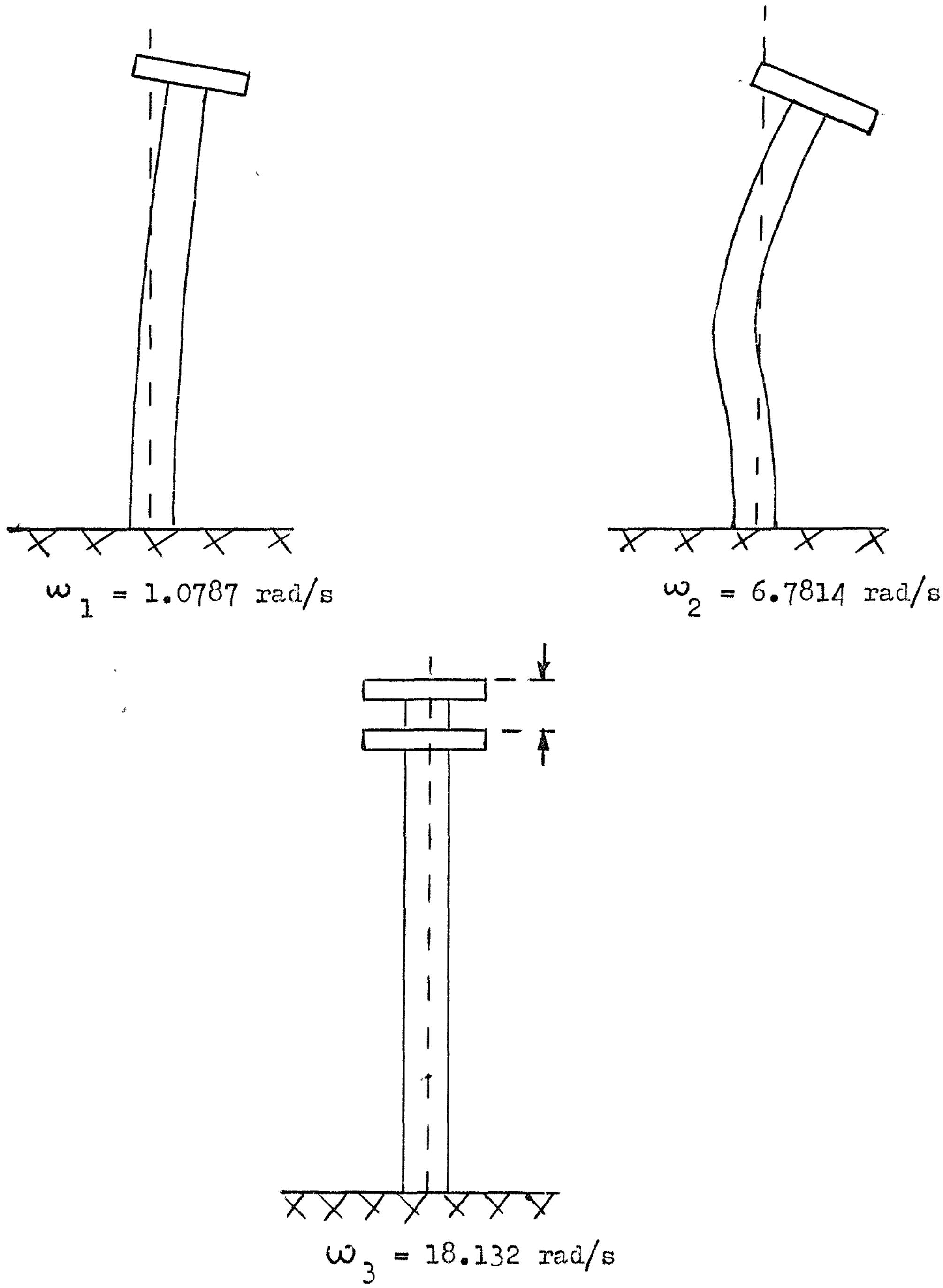

Fig 5.2 : Natural Frequencies and Mode Shapes,

Single-Leg Platform

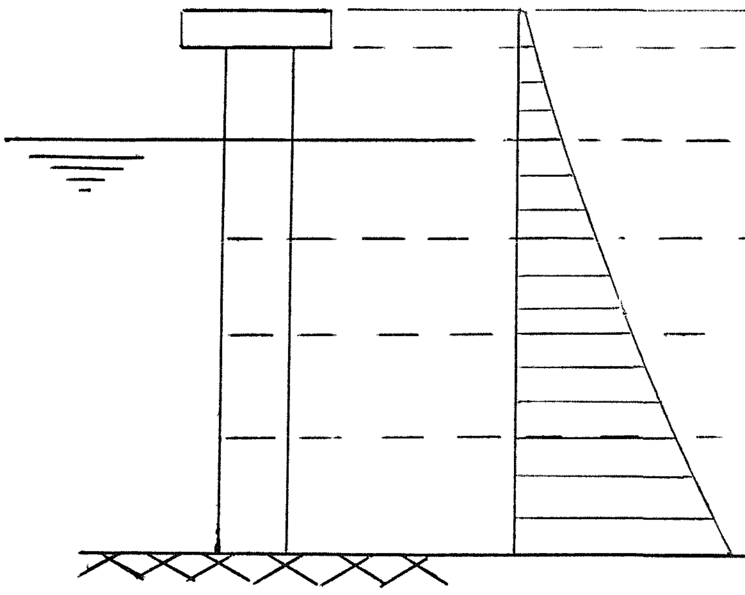

Moments (Nm)	Top Displacement (m) due to moments $\int \frac{Mx}{EI} dx$
	0.00
0.I9E8	
	0.0I
0.24E9	
	0.06
0.53E9	
	0.25
0.90E9	
	0.42
0.I3EI0	
	0.70
0.I7EI0	
	Total Top Displacement = I.43 m

Fig 5.3 : Bending Moment Distribution, Single Leg Platform (Programme SPECTA3, Including drag, see Appendix 9)

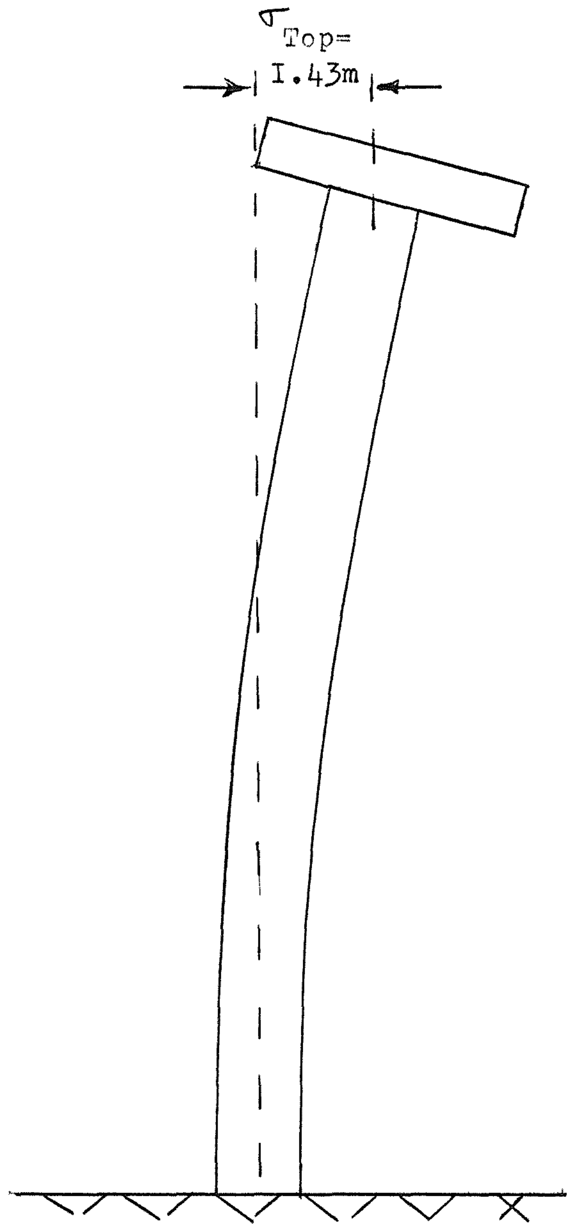

Fig 5.4 : Displacement Shape, Single Leg Platform

(Programme SPECTA3; Including drag; See results Appendix 9)

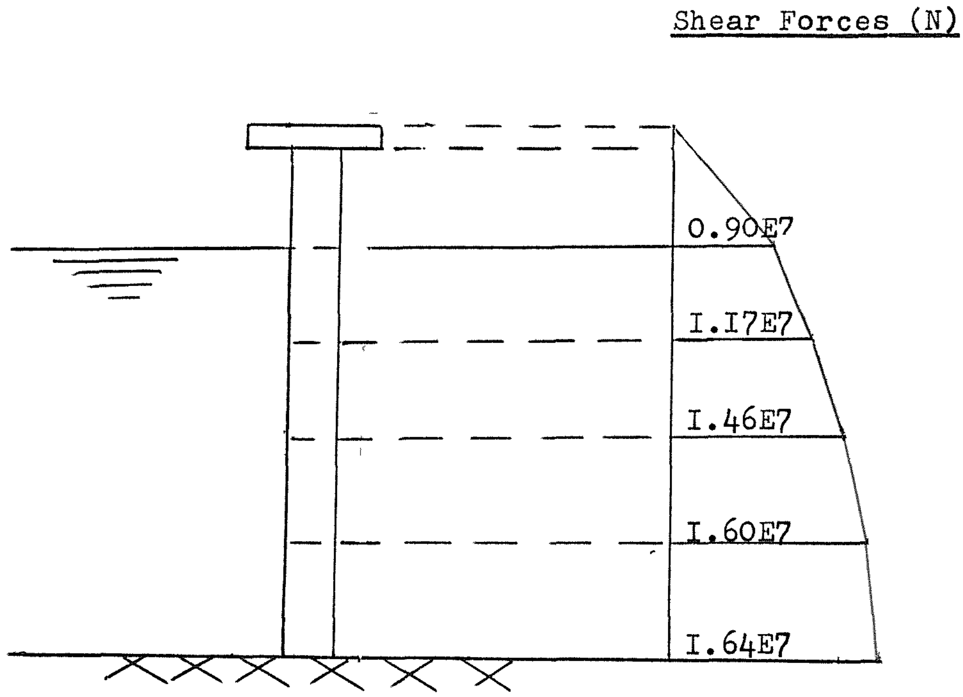

Fig 5.5 : Shear Forces, Single Leg Platform

(Programme SPECTA3; Including drag; see results Appendix 9)

5.4.2 A FOUR-LEG PLATFORM

In this example, a four-leg concrete platform of the AMDOC type is considered. Structures of this form have been built for the North Sea, as well as other parts of the world, and operate typically in waters having a depth of about 150m. The structure and the idealisation used to analyse it are shown in Fig 5.6. The platform columns are fabricated from reinforced concrete and are based on a large concrete 'caisson', which distributes the loads over a large area. The structure is here assumed to be rigidly fixed at the sea bed. The deck is made of reinforced concrete . In order to utilise the theory of Chapter 4, it is necessary to idealise the platform as a plane frame. Fig 5.6 illustrates this. A random sea state represented by the Pierson-Moskowitz spectrum

$$S_{\eta\eta}(\omega) = \frac{A}{\omega^5} \text{ Exp } (-B/\omega^4)$$

with $A = 2.56$ and $B = 0.0299$ (see Fig 3.3) is used.

The objective of this example is to compare Morison's theory with the diffraction theory for the cases in which the drag force is included and neglected. Two programmes SPECTA1 and SPECTA3 (see section 5.1) , are used. In addition, an attempt is made to estimate quantitatively the effect of sheltering using the theory of section 3.6. It is therefore necessary to input with the data a sheltering factor (i.e. the distance between the legs) for each element of one of the legs (see user instructions, section 5.3). The principal results are summarised in Table 5.2 and Figs 5.7-5.10 , and detailed computer results are in Appendix 9 . A discussion of the results is given in section 5.5 and in the conclusions.

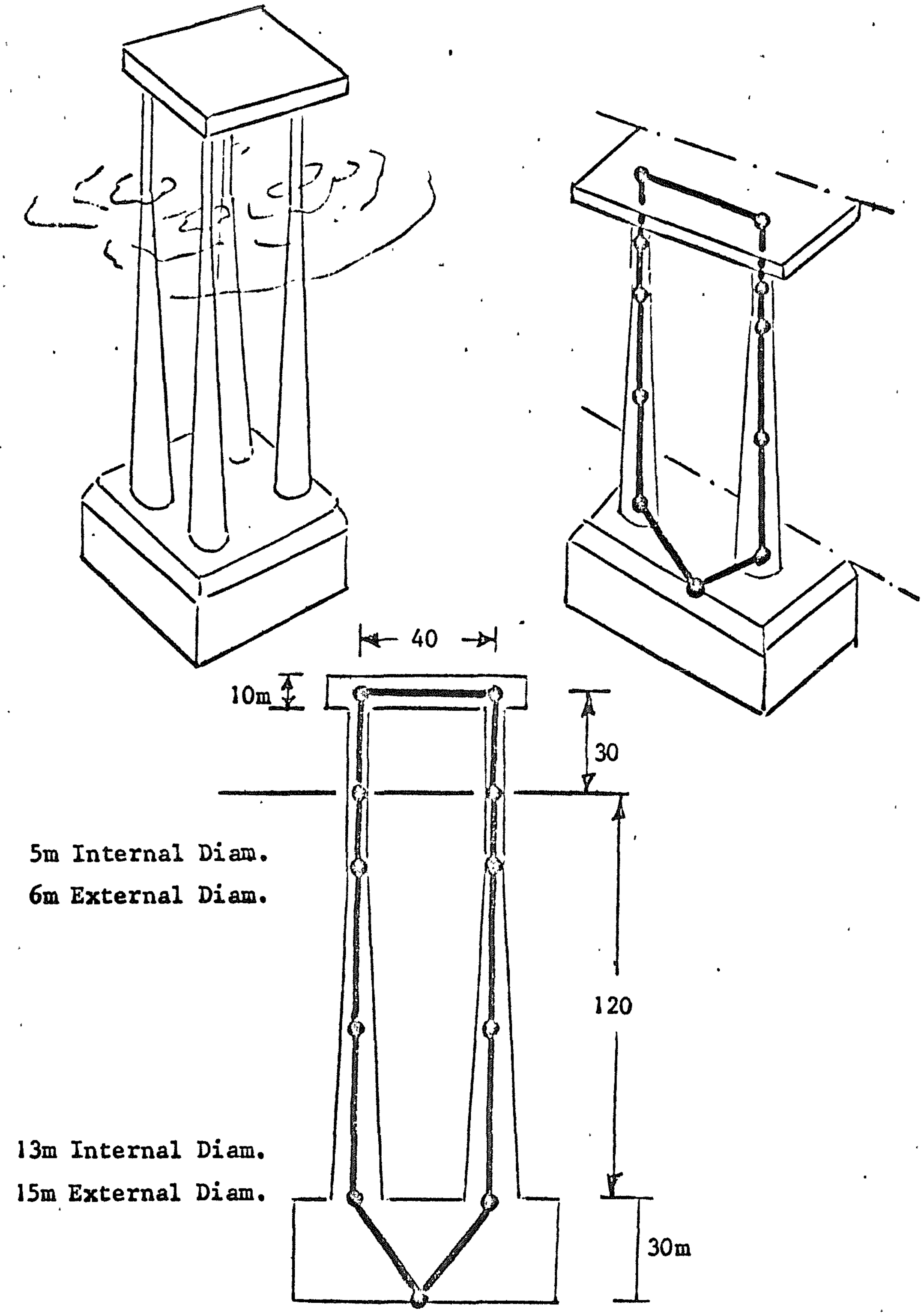

Modulus of Elasticity of concrete $E = 2.00 \times 10^{10}$ N/m^2

Density of concrete ρ_c : 2500 kg/m^3

Coefficient of Added Mass: $C_M = 1.0$ (Overall Inertia Coeff. is 2.0)

Coefficient of drag: 1.0

Structural Critical Damping Ratio $\xi = 0.03$

Platform Mass M_p (divided by 2 for half the complete frame): 9×10^6 kg

Figure 5.6 Four Leg Platform

Method	Displacement Standard Deviation at Top , σ_{Top} (m)					Maximum Expected Displacement Top X 3.5 (m)	Fundamental Natural Frequency ω (Rad/s)
	Morison			Diffraction			
	No Drag or Shelt.	Inc. Drag	Inc.Shelt.	No.Shelt.	Inc.Shelt.		
'Direct Transfer Function' Method , Programme SPECTA3	0.307	0.315 (3%)	0.318 (4%)	0.127	0.128	1.12	1.55
'Frequency Domain Method' Programme SPECTAI (Lumped Element Forces , Considered Together)	0.145	0.165	0.170	0.068	0.069	0.60	1.55
Drobbia, Ferrante, Lima (Ref 21 ; Drag not considered)	0.280					1.03	1.74
'Equivalent' Static Analysis (Maximum Expected Wave)						0.75	

Table 5.2 : Results , MDCC 4-Leg Platform

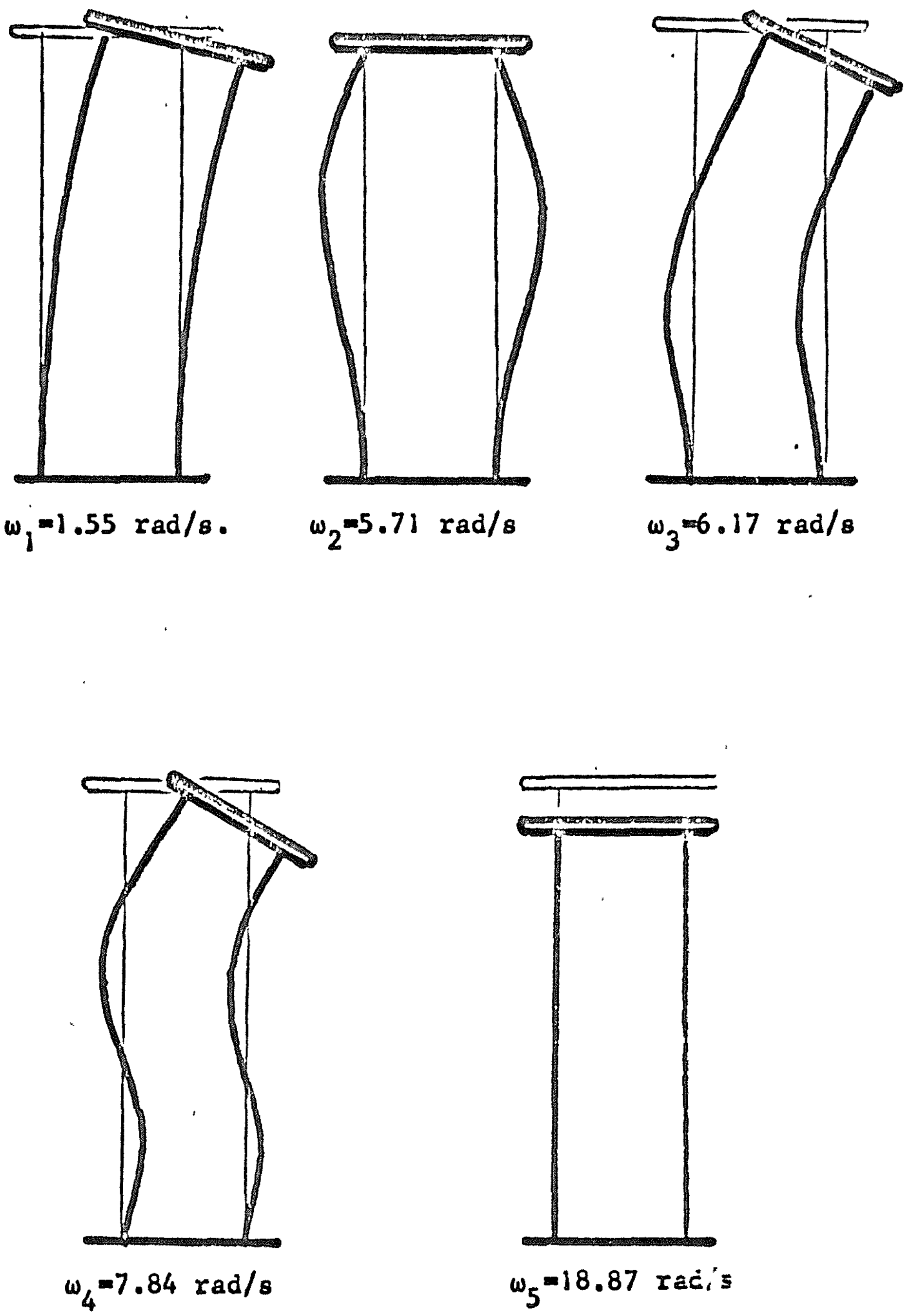

Fig 5.7 : Natural Frequencies and Mode Shapes , ANDOC 4-Leg Platform

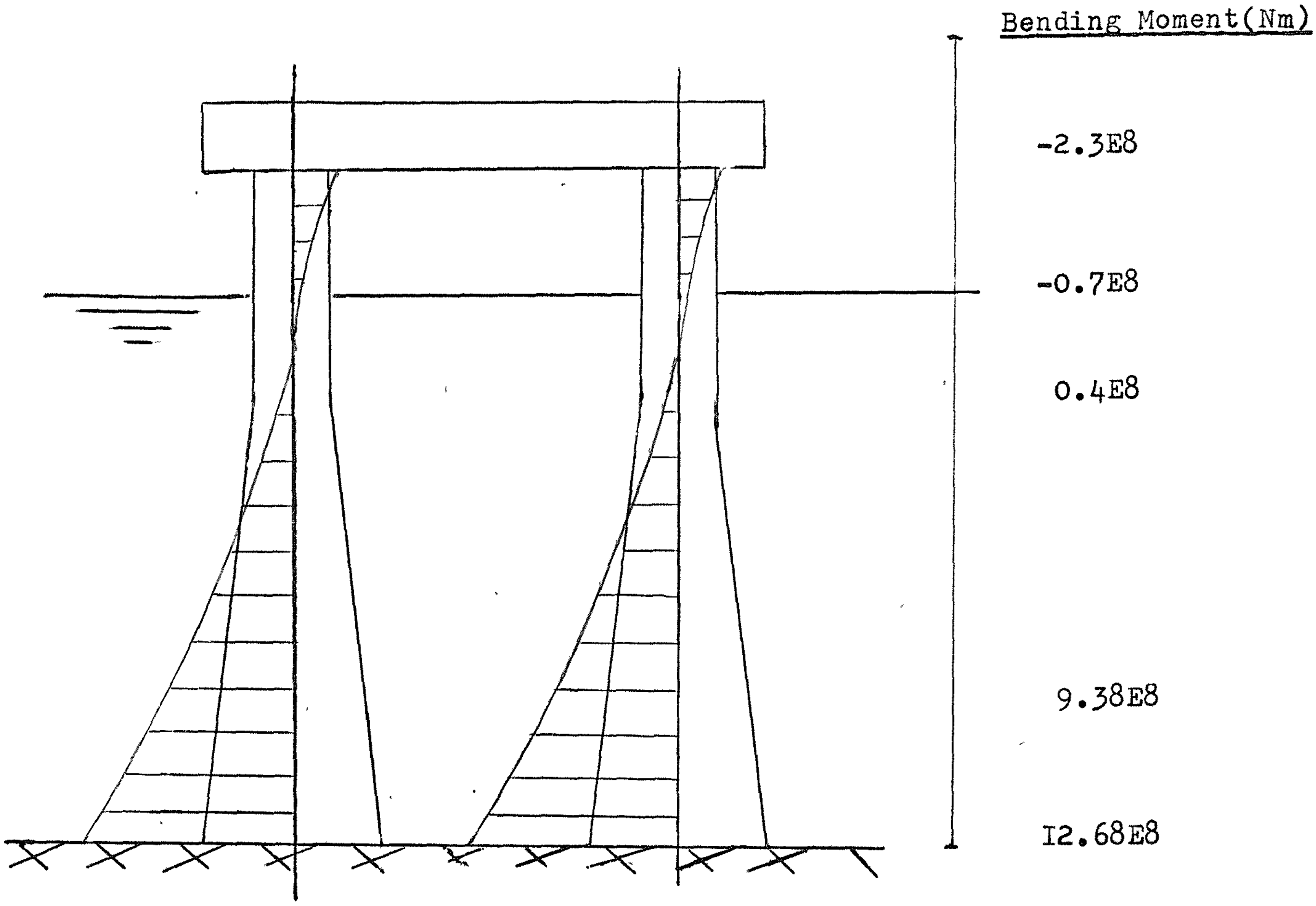

Fig 5.8 : Bending Moment Distribution, ANDOC Platform

(Programme SPECTA3; Including drag; See results in Appendix 9)

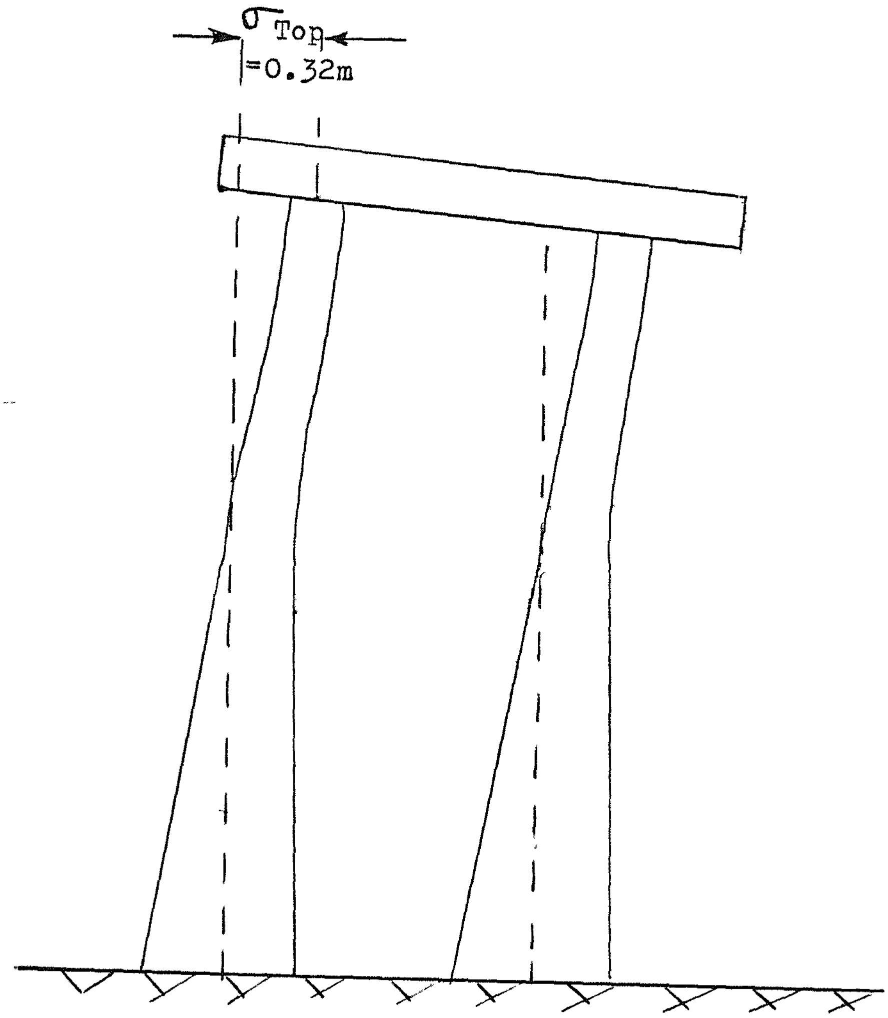

Fig 5.9 : Displacement Shape, ANDOC Platform

(Programme SPECTA3; Including drag; See results, Appendix 9)

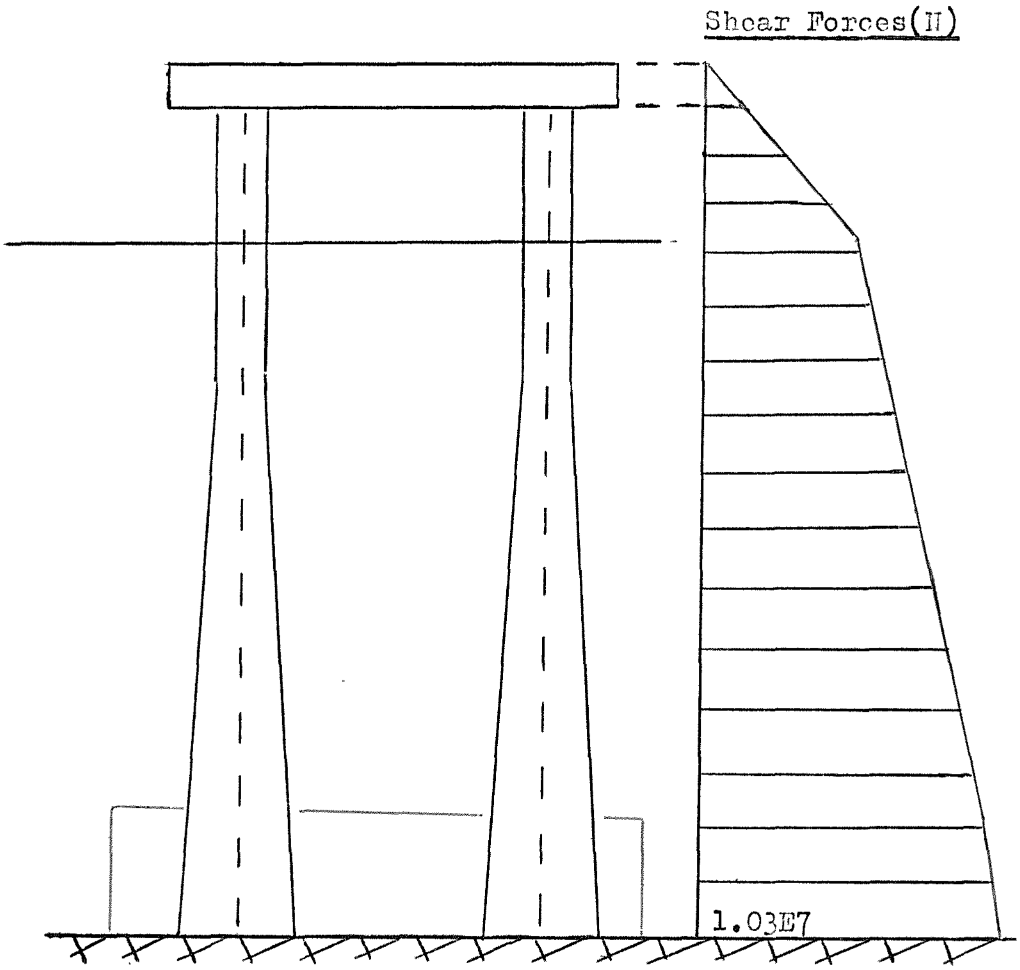

Fig 5.10 : Shear Forces, ANDOC Four-Leg Platform

(Programme SPECTA3; Including drag; see results, Appendix 9)

5.4.3 HALCROW-EWBANK STEEL-FRAMED PLATFORM

The previous two examples were concrete structures, and enabled some conclusions to be drawn about sheltering and drag , and about Morison's theory compared with the diffraction theory . However , both examples included only vertical members . This third example is included in order to utilise the theory for inclined cylinders , given in chapters 3 and 4 .

The general configuration of the structure is shown in Fig 5.11, and detailed elevations and member sizes follow in Figs 5.12 - 5.16. Thanks are due to Halcrow-Ewbank (London) for supplying the drawings , which have since been reduced from A3 size to A4 .

The computer programmes developed in this thesis are written for plane frames , and accordingly the analysis of the Halcrow-Ewbank platform is dealt with by considering two principal elevations , as shown in Figs 5.12 and 5.13. The structure is treated as a plane frame for each of the two elevations . The nodal point numbering scheme and element connectivity for the finite element analysis are shown in Fig 5.17, while the element properties (obtained from Figs 5.12 - 5.16) can be seen in the computer results in Appendix 9 . The mass of the deck is 26800 tonnes (rather high to be typical) and equivalent masses have been associated with the beam elements used to idealise the deck.

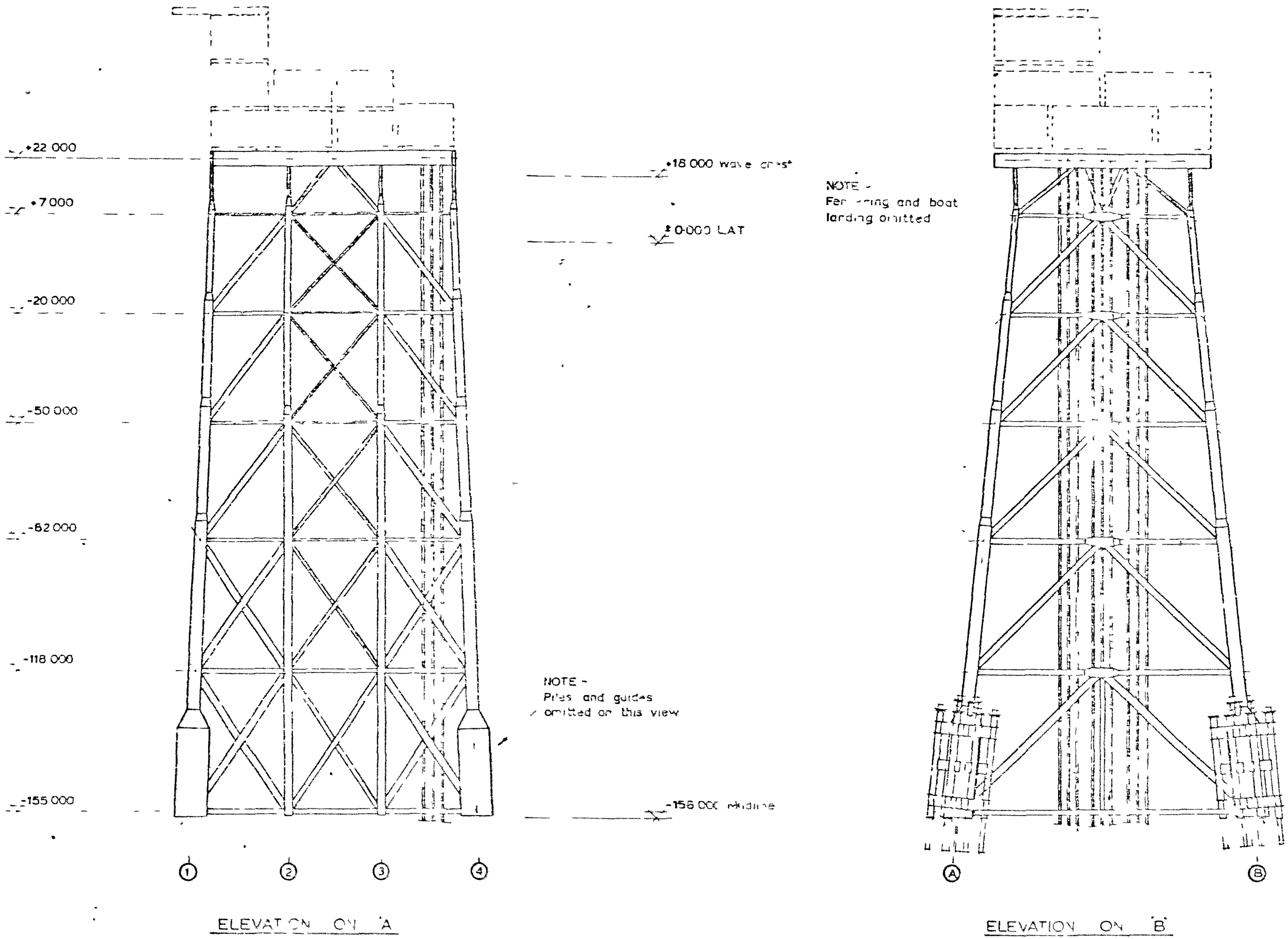

Fig 5.11: General Configuration, Valerow-Embark Platform

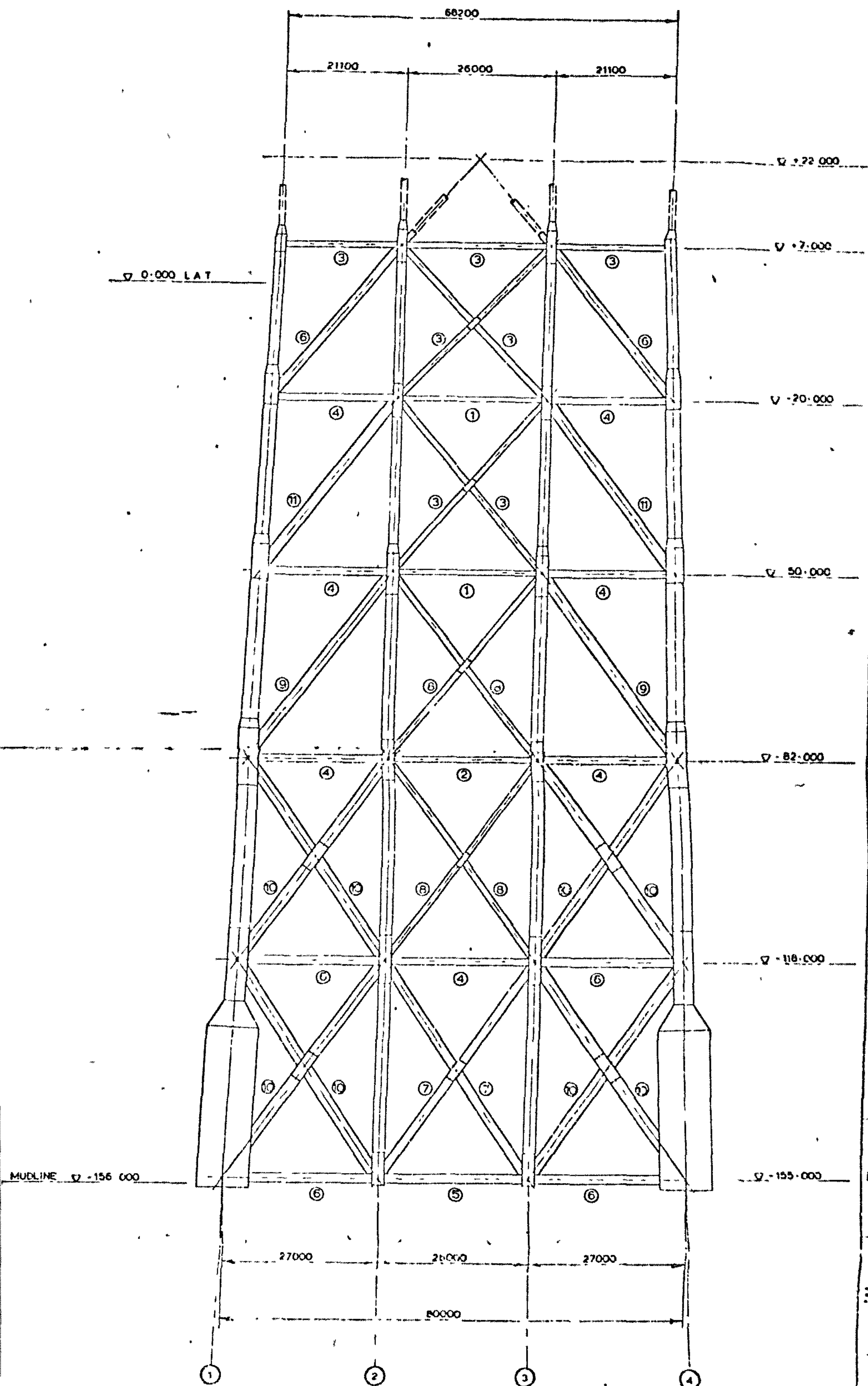

TYPE	DIAMETER	WALL THICKNESS
1	30 in	1 in
2	36 in	1 in
3	36 in	1½ in
4	48 in	1¼ in
5	60 in	1 in
6	60 in	1¼ in
7	60 in	1½ in
8	40 in	1½ in
9	72 in	1½ in
10	80 in	1½ in
11	66 in	1½ in

Fig 5.12

TYPICAL ELEVATION LINES (A) and (3)

DRAWING NO MUB-3 SCALE

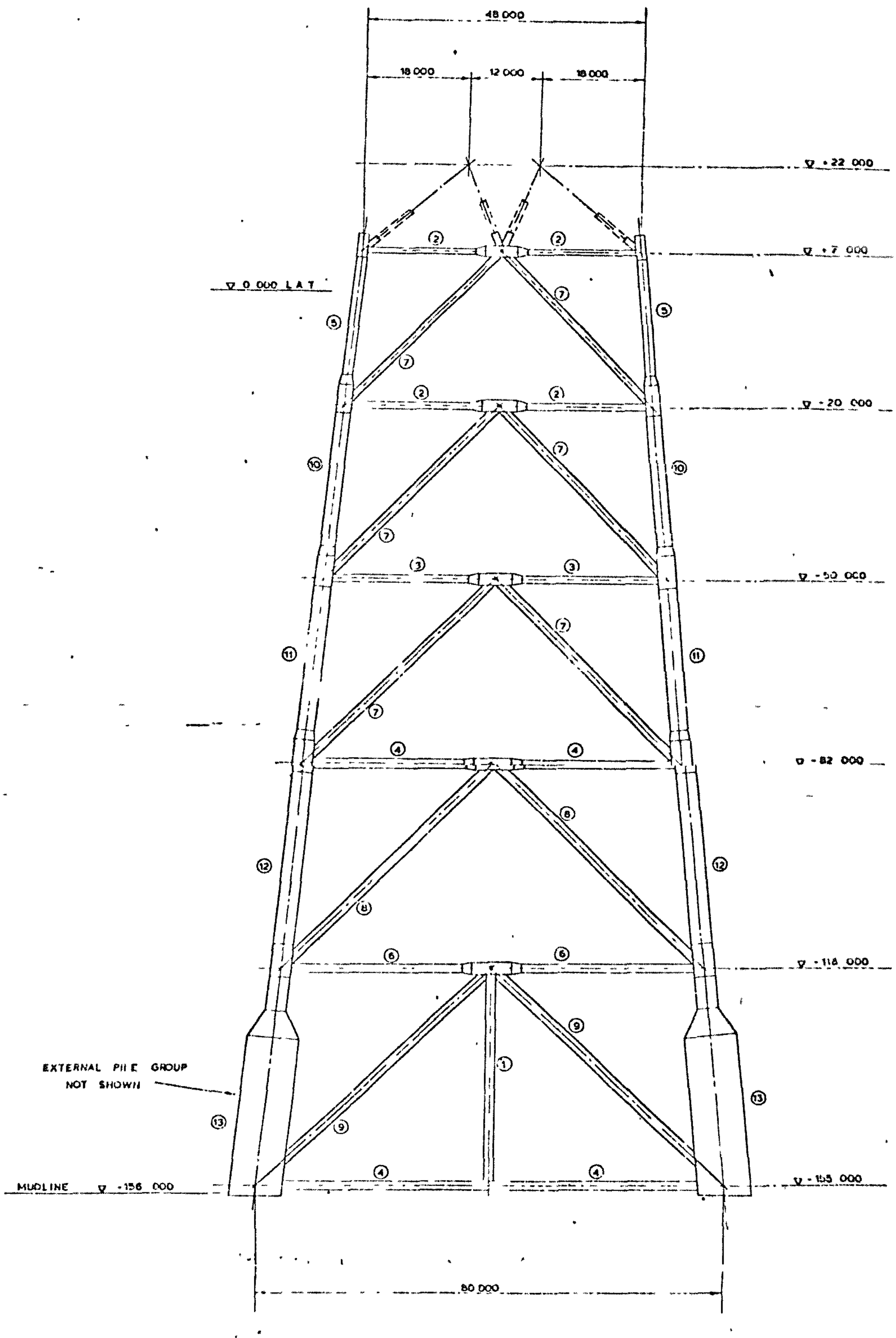

TYPE	DIAMETER (inches)	WALL THICKNESS (inches)
1	40	1
2	48	1
3	54	$1\frac{1}{4}$
4	[illegible]	$1\frac{3}{4}$
[illegible]	70	
5	72	[illegible]
7	[illegible]	[illegible]
8	72	[illegible]
9	84	[illegible]
10	100	[illegible]
11	[illegible]	
12	140	
13	360	

Fig 5.13

TYPICAL ELEVATION LINES (① & ②)

DRAWING NO MUR 4 | SCALE 1:400

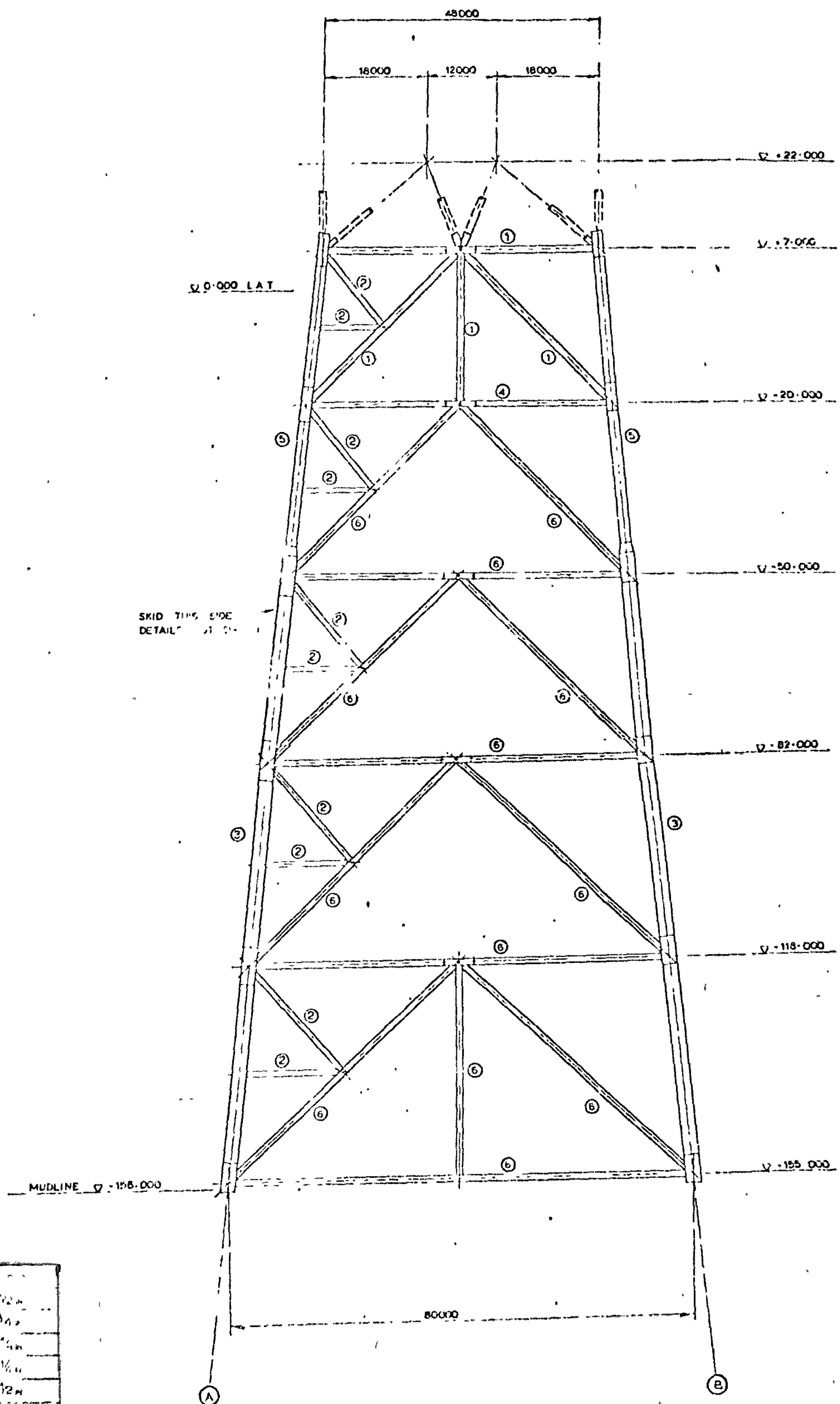

TYPE	DIAMETER	WALL TH.
1	48 in	1 1/2 in
2	24 in	3/4 in
3	80 in	1 3/4 in
4	18 in	1 1/2 in
5	70 in	1 1/2 in
6	46 in	1 in

Fig 5.14

TYPICAL SECTION LINES (A) & (B)

DRAWING NO MUR-5 SCALE 1:400

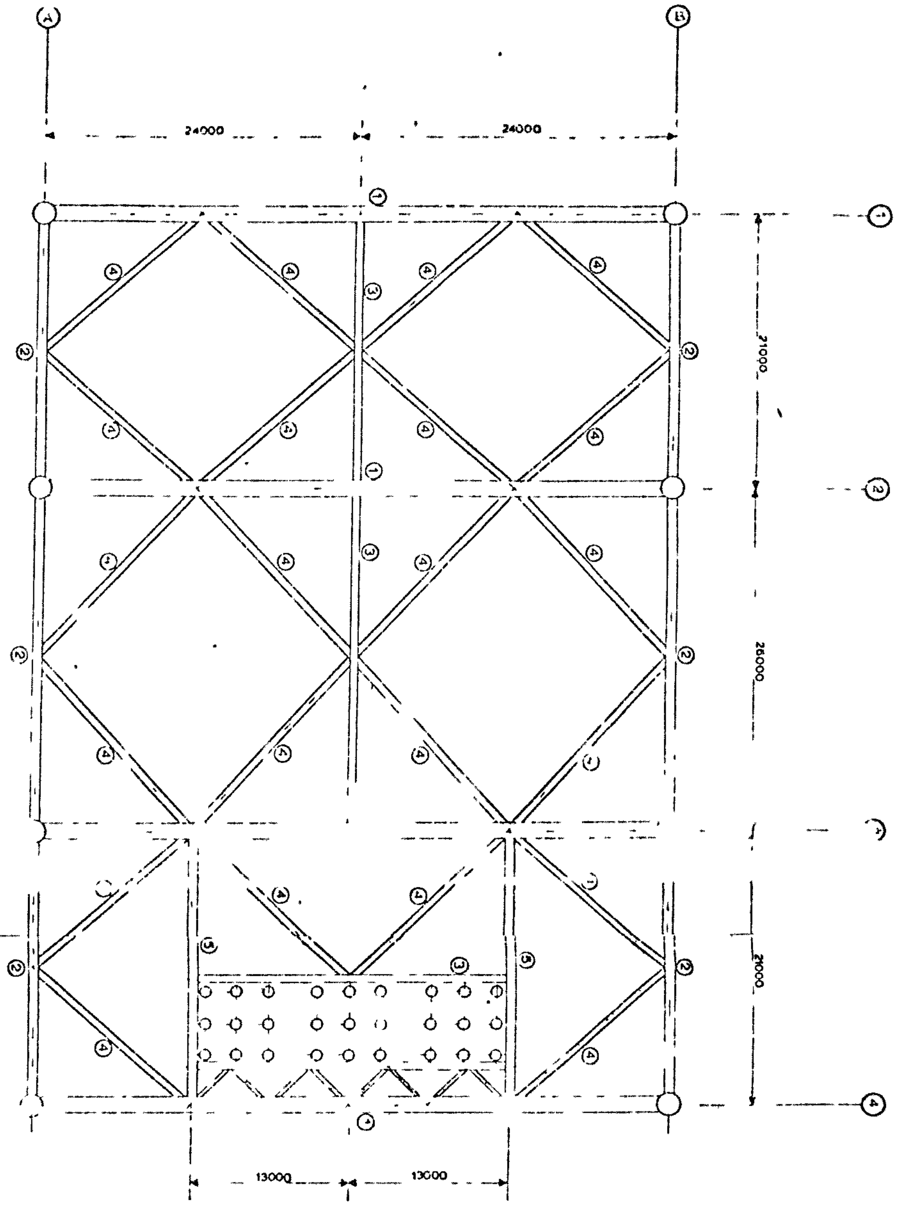

TYPE	DIAMETER	WALL THICKNESS
1	SEE DRG No MUR- 2,3 & 4	
2		
3	24 in	3/4 in
4	18 in	[illegible]4 in
5	3[illegible]	[illegible]

NOTE
FRAMING AROUND CONDUCTORS NOT SHOWN

Fig 5.15

PLAN BRACING SHEET 1

SCALE 1:200

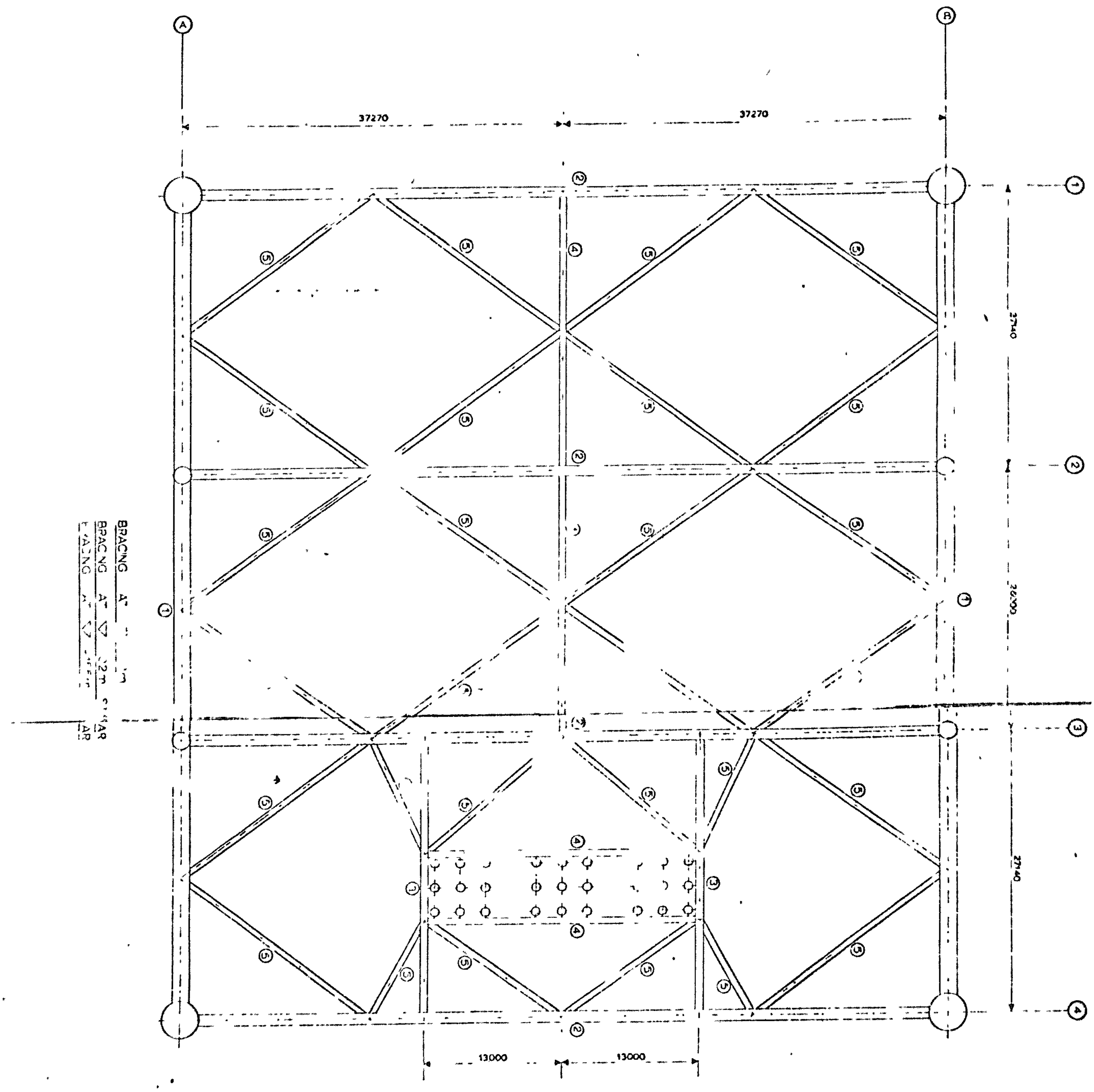

TYPE	DIAMETER	WALL THICKNESS
1	SEE DRG No MUR - 2, 3, & 4	
2		
3	30 IN	3/4 IN
4	24 IN	3/4 IN
5	18 IN	[illegible] IN

NOTE
FRAMING AROUND CONDUCTORS NOT SHOWN

Fig 5.16

PLAN BRACING SHEET 2

DRAWING NO MU[illegible] | SCALE 1:200

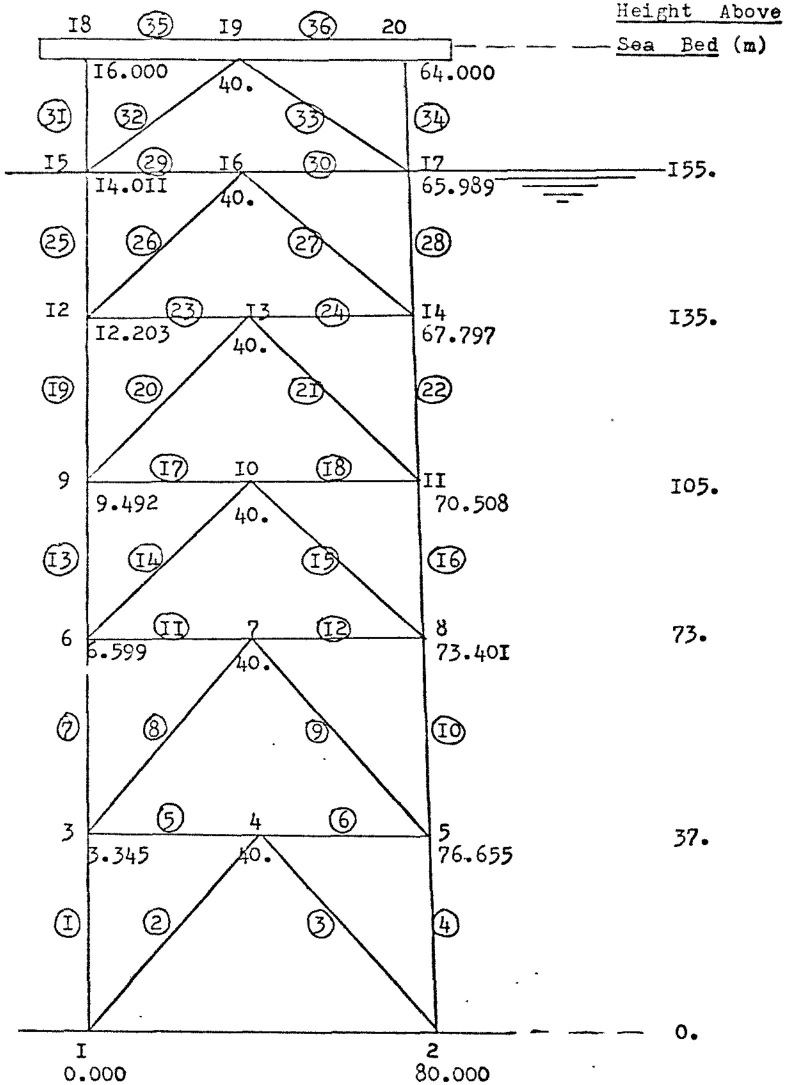

Elevation Through Lines I and 4

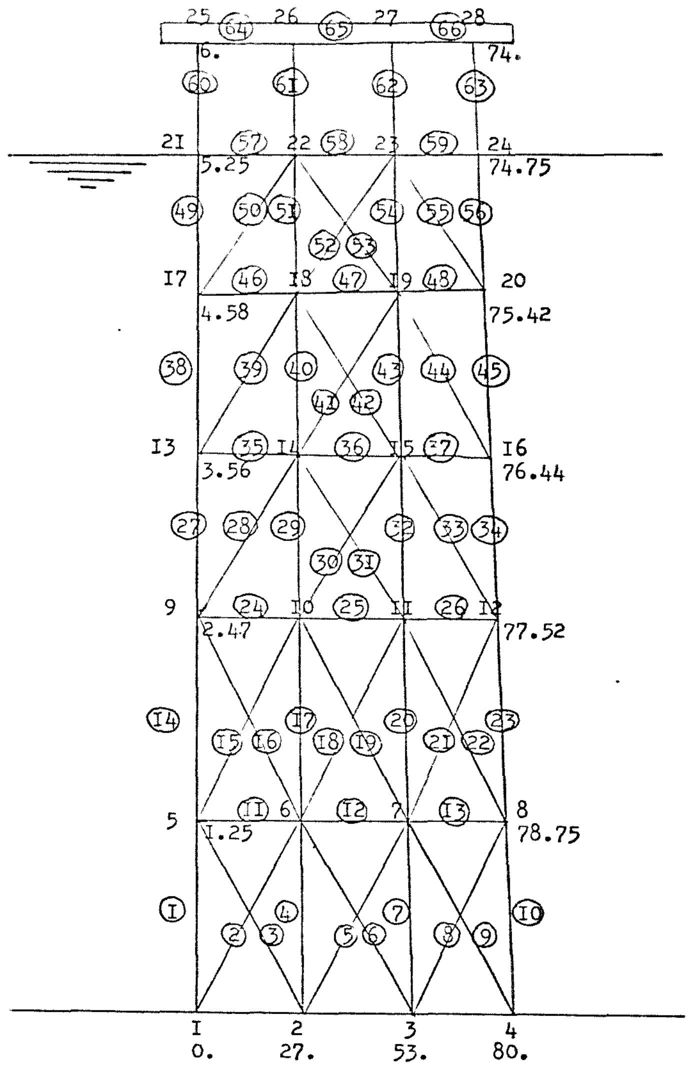

Elevation Through Lines A and B

Element numbers are ringed

Nodal point numbers are unringed integers

Decimal numbers are x-coordinates of nodal points

Fig 5.17: Nodal Point Coordinates and Connectivity

	Displacement Standard Deviation at Top, σ_{Top}(m)		Fundamental Natural Frequency, ω_I (rad/s)	Second Natural Frequency ω_2 (rad/s)	Bending Moment at Base of Leg (Nm) (Inc. drag)
	Inc. Drag	No Drag			
Wave Spectrum I A = 2.56 B = 0.0299	0.1695	0.0626	3.8054	10.714	0.189×10^9
Wave Spectrum 2 A = 0.779 B = 0.0085	0.1214	0.0591	3.8054	10.714	0.0699×10^9
Halcrow-Ewbank Ltd.			3.70		

Results were obtained using programme SPECTA3 (section 4.5.5) .

The wave amplitude spectra I and 2 were Pierson-Moskowitz spectra

$$S_{\eta\eta}(\omega) = \frac{A}{\omega^5} \operatorname{Exp} (- B/\omega^4)$$

with A and B as indicated .

Table 5.3 : Results, Halcrow-Ewbank Steel Platform

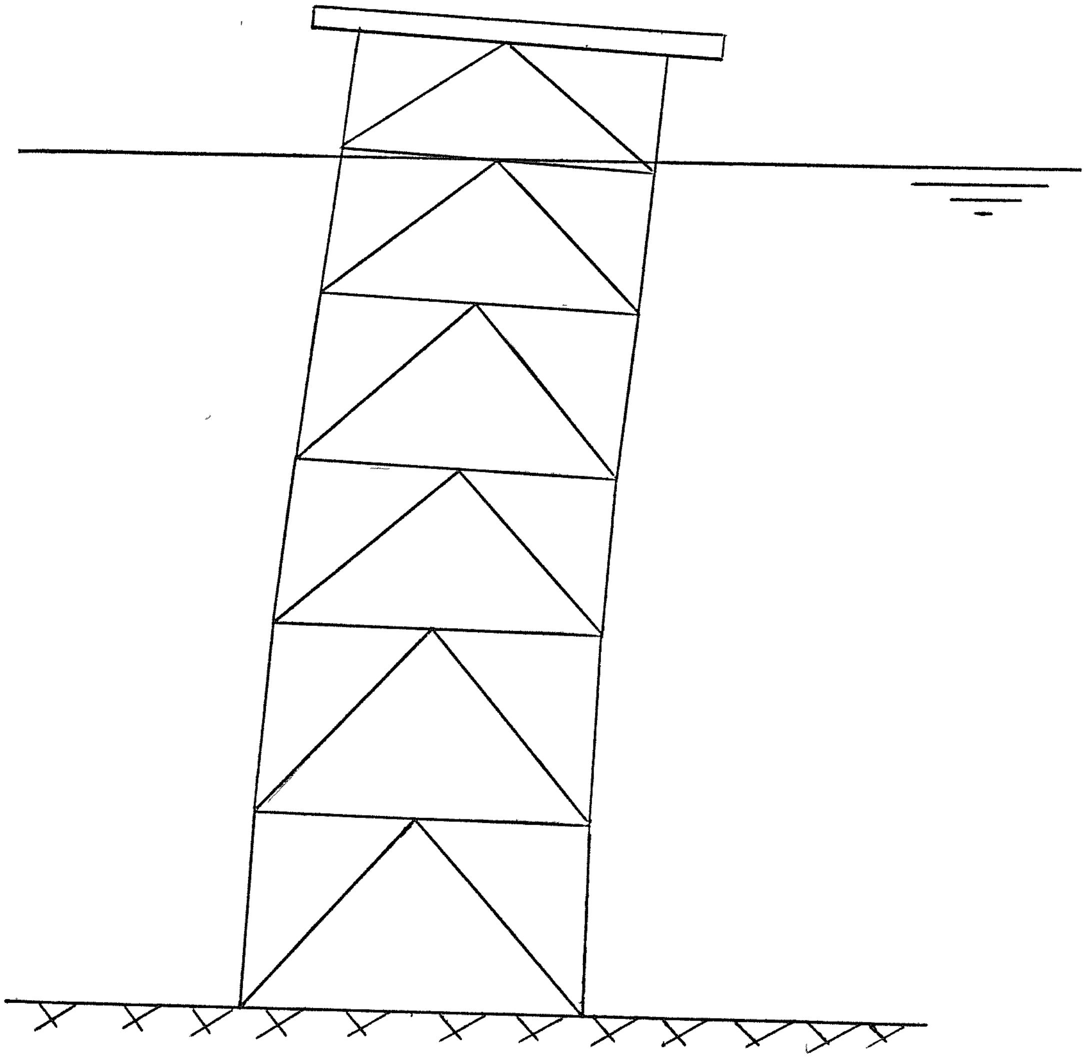

$\omega_I = 3.8I$ rad/s

Fig 5.18 : Fundamental Mode Shape, Halcrow-Ewbank Platform

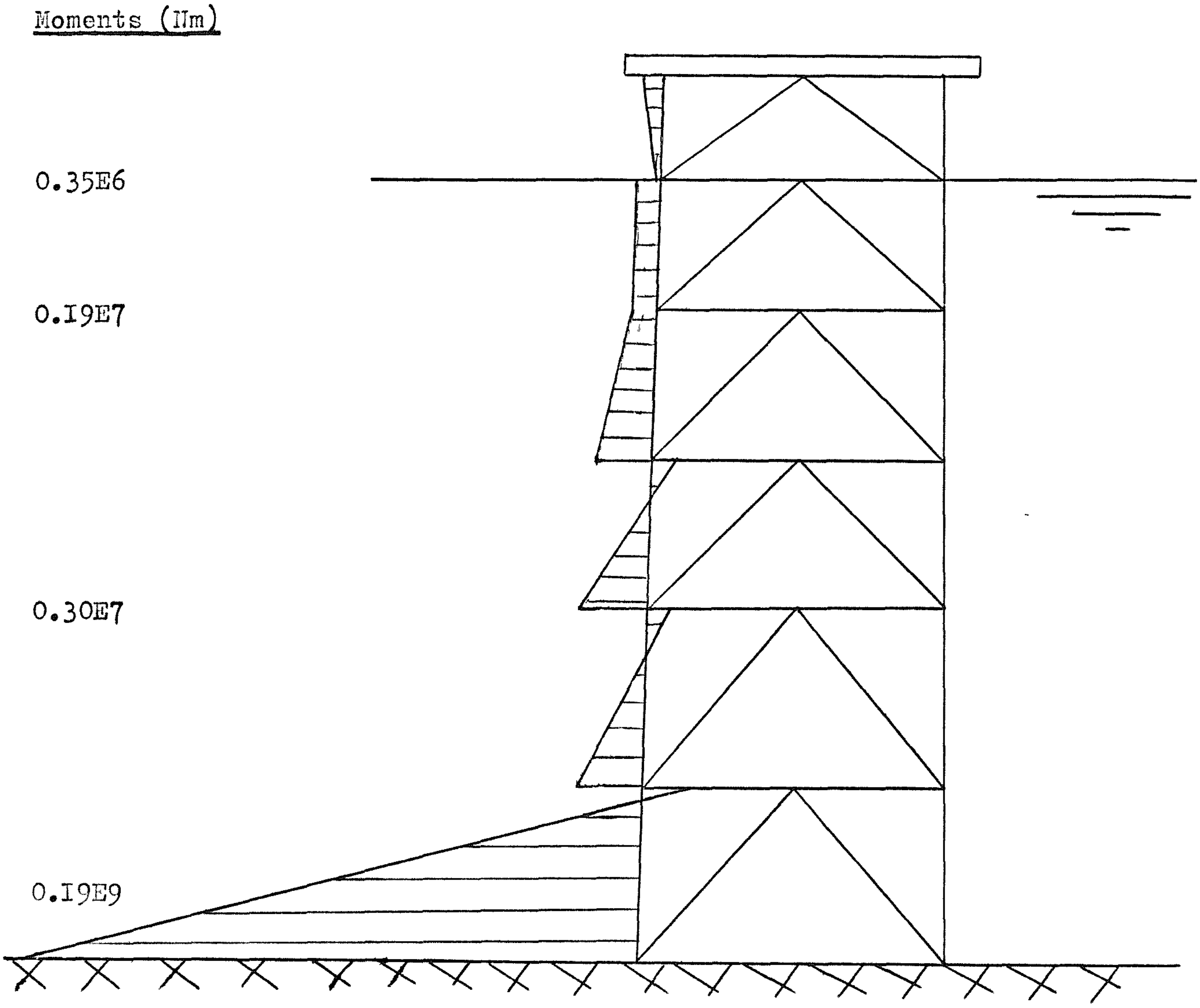

Fig 5.19 : Bending Moments in Legs, Halcrow-Ewbank Platform

(Programme SPECTA3; Including Drag; See results in Appendix 9)

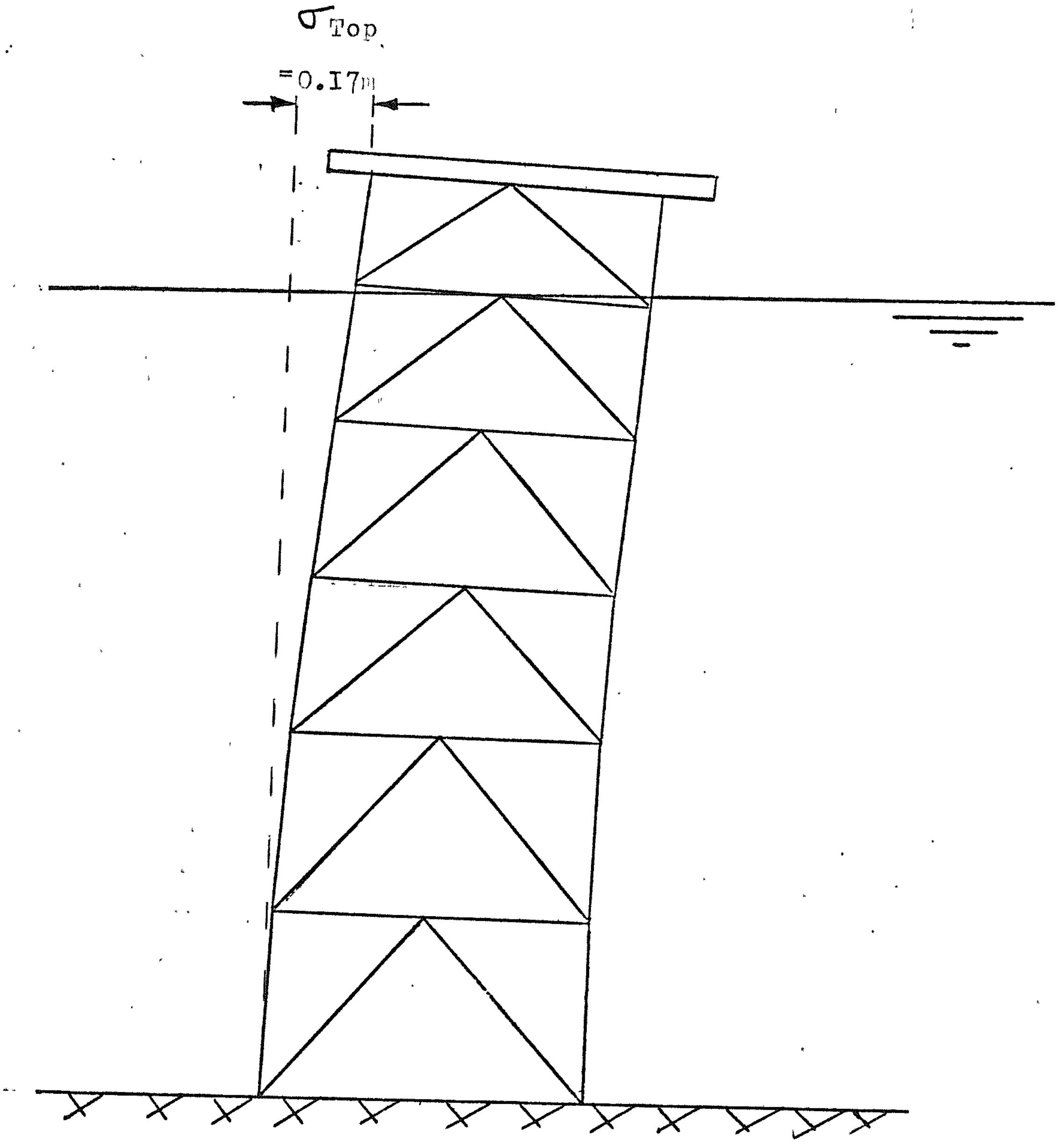

Fig 5.20 : Displacement Shape, Halcrow-Ewbank Platform

(Programme SPECTA3; Including Drag; See results, Appendix 9)

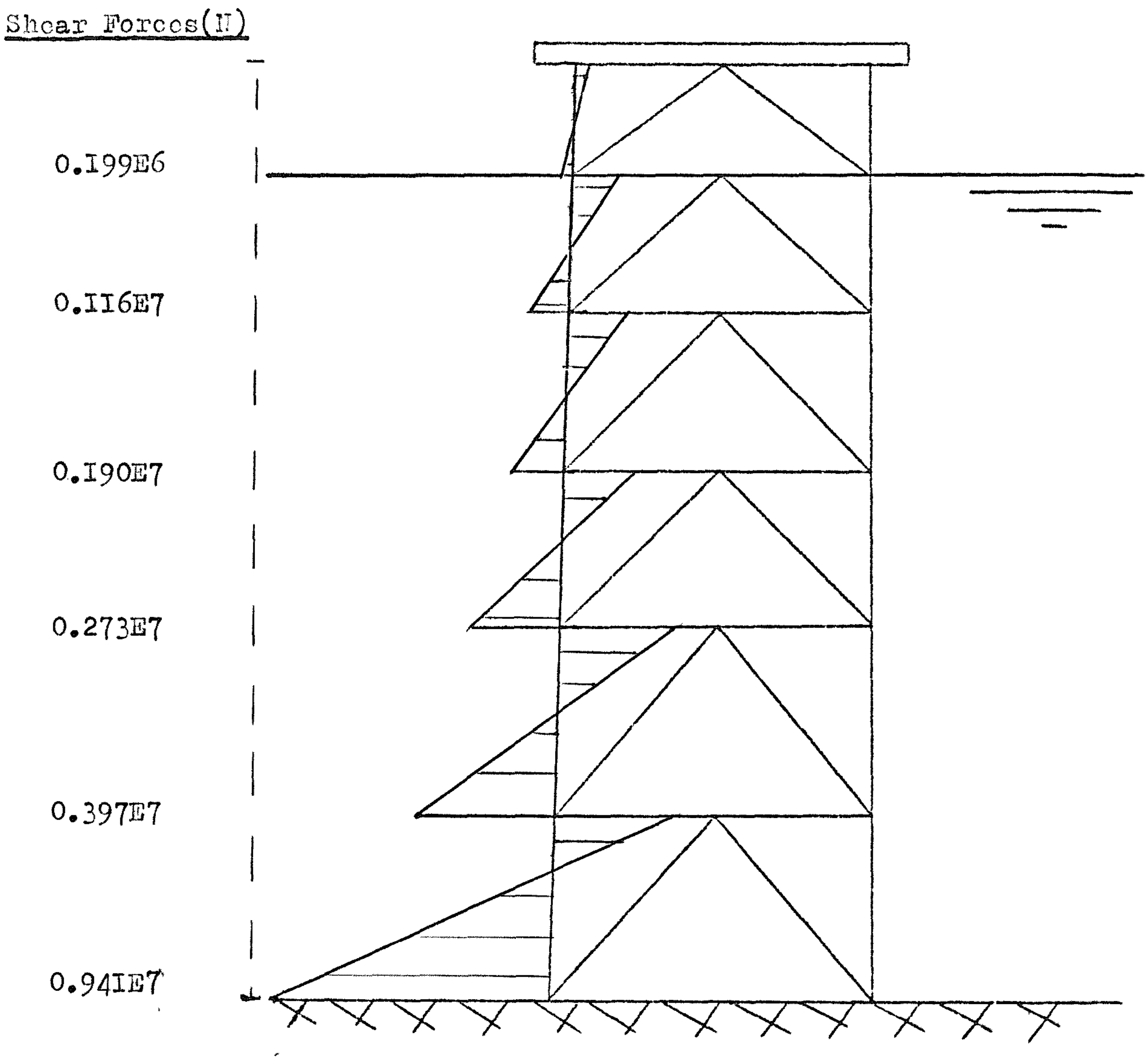

Fig 5.21 : Shear Forces, Halcrow-Ewbank Platform

(Programme SPECTA3; Including Drag; See results in Appendix 9)

5.5 COMMENTS

A summary of the principle results is given in the tables of the previous section . Some observations based on these results follow, and an alternative view is given later in the conclusions .

(i) MORISON THEORY v DIFFRACTION THEORY

The Morison theory and the diffraction theory are compared in the examples of sections 5.4.I and 5.4.2 , and a more general comparison is given in section 3.5.6 and Appendix 5 . The wave amplitude spectrum peaks at 0.4 rad/s, and the two examples considered here have first mode frequency response functions peaking considerably higher than this (I.08 rad/s for the single-leg platform , and I.55 rad/s for the 4-leg platform) . Figs 3.6 and 3.7 indicate that , in this case , a much higher response should be predicted by the Morison theory than by the diffraction theory (the Morison theory probably overdesigns the structure) . The results given in Tables 5.I and 5.2 bear this out , the Morison theory response being over twice as large as the diffraction theory response in both examples .

(ii) 'DIRECT TRANSFER FUNCTION' METHOD v CONVENTIONAL FREQUENCY DOMAIN ANALYSES

Again refering to Tables 5.I and 5.2 , it will be seen that the 'Direct Transfer Function' method , as in programme SPECTA3 , which effectively takes account of force cross - correlations in equation (4.20a) , predicts a larger response than the conventional method of programme SPECTAI , which in this case ignores off-diagonal terms in equation (4.20a) . This amounts to approximately I.4 times as large for the single-leg platform , and I.8 times as large for the 4-leg platform , in which cross-correlations are clearly going to be more important .

Programme SPECTA2 , which treats each nodal force independently and then superimposes the responses , yields a response which is approximately I5% lower than that given by SPECTAI for the single-leg platform , and 5% lower for the 4-leg platform .

(iii) THE EFFECT OF DRAG

The percentage effect of drag can be seen by considering any one of the methods summerised in Tables 5.I - 3 . It can be observed that drag accounts for less than 5% of the total response in the case of the 4-leg platform, and about I2% in the case of the single-leg platform. Both of these two examples are fabricated in concrete and consist of large diameter members. The Halcrow-Ewbank steel platform suggests that drag can account for about 50% of the total response for structures with smaller diameter members.

(iv) THE EFFECT OF SHELTERING

Refering to Table 5.2 , sheltering accounts for about I% of the total response of the 4-leg platform. The reasons for this effect being so small are dealt with in more detail in section 3.6 . Briefly, with a leg spacing of 40m , a structure with a fundamental natural frequency of 0.8 rad/s would be most affected by sheltering (the maximum being about I7%) .

(v) HALCROW-McBANK PLATFORM- NATURAL FREQUENCIES

Refering to the two principle elevations shown in Fig 5.17, it is found that the elevation through the lines A and B is much stiffer than the elevation through the lines 1 and 4. The fundamental natural frequencies are 0.6 and 0.8 cps, respectively. In both cases only one natural frequency is significant (in the sense of being within a certain distance of the wave amplitude spectrum peak), and the response is almost entirely in the first (cantilever) mode (see Figs 5.18 and 5.20) .

CONCLUSIONS AND CLOSING REMARKS

This thesis has been mainly concerned with the response to stochastic wave loading of ocean structures that can be idealised as self-supporting plane frames. The conclusions reached will be looked at under 4 main headings :

1. Overall Structural Response
2. Wave Forces On Vertical Cylinders
3. Wave Forces On Inclined Cylinders
4. Closing Remarks

I. OVERALL STRUCTURAL RESPONSE

(a) General

The three structures considered here - a single-leg concrete platform, a four-leg concrete platform, and a steel platform - all responded almost entirely in the first mode of vibration, which seems to indicate that with a suitable choice of parameters, a single degree of freedom approximation may be a useful guide to the behavior of many ocean structures.

(b) 'Consistent' versus 'Lumped' Element Nodal Forces

Results indicate that the response of the structure is almost identical whether the nodal forces in the finite element analysis are distributed 'consistently' or are 'lumped' at the nodes (sections 4.4 and 4.5). Owing to the relative simplicity of the 'lumped' method over the 'consistent' method, it is recommended that this method is used in this type of analysis.

(c) 'Direct Transfer Function' Method versus Conventional Methods

Two main methods are considered for evaluating the response of multi degree of freedom structures to random wave loading (section 4.5) . Of these, the one termed here the 'Direct Transfer Function' (DTF) method is thought to be better than some conventional methods for the following reasons :

(i) Owing to the approximations which are usually made in the two methods, the DTF method yields a safer design than the conventional methods. This is largely because of the fact that the force cross-correlation terms in the statistical representation are better dealt with by the DTF method. In the case of the single-leg platform of section 5.4 , the DTF method gives a displacement response of about I.4 times that predicted by the conventional method (in which diagonal terms in the complex frequency response matrix are ignored). In the case of the 4-leg platform, the effect of force cross-correlations is clearly more important, and the DTF method gives a response which is 80% or more greater than that given by the conventional method .

(ii) The DTF method is algebraically simpler than the conventional method and is more likely to appeal to a practicing engineer, both for its relative ease of manipulation and the form of its logic.

(d) Two Conventional Methods - A Comparison

Another way of gauging the effect of force cross-correlations is attempted in a computer programme called SPECTA2 (Sect 4.5.4), in which the loads are all applied to the structure individually and the results superimposed. Compared with the method described under (i) above, this method gives a response that is approximately 15% lower for the single-leg platform, and 50% lower for the 4-leg platform, which appears to indicate that this method is sufficiently accurate for structures like the former, but insufficient for more complicated structures.

2. WAVE FORCES ON VERTICAL CYLINDERS

(i) Diffraction Theory v Morison's Theory

(a) Having compared Morison's theory (MT) with the diffraction theory (DT) for vertical cylinders with radii ranging from 0.1 to 19 m (Sect. 3.5.6 ; Appendix 5) it appears that :

A. for cylinder radii less than 4 m the DT predicts a larger response than the MT, whereever the frequency response function curve occurs relative to the forcing function

B. for cylinder radii greater than 4 m, the

MT response is larger than the DT response whereever the frequency response function for the cylinder occurs , except near the force spectrum peak , where in any case resonance would occur . Figs (3.6) and (3.7) summarise these findings.)

The results would therefore appear to show that for cylinder radii less than about 5 m , the diffraction leads to a safer design . For radii greater than 5 m , the MT is likely to be overdesigning the structure , since it ignores the size of the cylinder .

(b) The single-leg platform analysed in sections 4.6 and 5.4 yielded the following results when analysed by the DT and the MT (using the direct transfer function formulation) :

Standard deviation of displacement at the top

$$\sigma_{Top} = 1.43065 \quad m \qquad (MT)$$

$$\sigma_{Top} = 0.64327 \quad m \qquad (DT)$$

(c) The 4 leg platform of section 5.4 yielded the following results when analysed by the DT and the MT (using the Direct Transfer Function formulation) :

$$\sigma_{Top} = 0.32 \quad m \qquad (MT)$$

$$\sigma_{Top} = 0.13 \quad m \qquad (DT)$$

(d) Inspecting the results from the two computer examples , given in (b) and (c) above , with the more general analysis summerised in (a) , it is clear that the two examples fit the general theory well . Refering to Tables 5.I and 5.2 , and Figs (3.6) and (3.7) , it is seen that the first mode frequency response functions for the single-leg platform and the 4-leg platform occur at I.08 rad/s and I.55 rad/s , respectively , which is considerably higher than the peak of the wave height spectrum , which occurs at 0.4 rad/s . One would therefore expect the Morison theory to lead to a much higher response in this case than the diffraction theory .

(ii) <u>Sheltering</u>

The effect on nodal forces of one member on another is considered in section 3.6 , and the 4-leg platform of section 5.4 was re-analysed to estimate quantitatively this effect . An increase in the top displacement of about I% was observed . The reasons for this effect being so small in this case are examined in section 3.6 , the two main variables being the leg spacing and the position of the first mode frequency response function. Section 3.6.3 describes how a designer can decide how to get a feel which leg spacing will be most affected given the fundamental frequency of the structure , or alternatively , which fundamental frequency to avoid given a particular leg spacing .

(iii) Drag

The results obtained with and without consideration of drag for the computer examples are summerised in the Tables in section 5.4 . In the case of the 4-leg platform , drag accounted for about 5% of the total response , and in the case of the single-leg platform , about 12% , while for structures composed of smaller (e.g. steel) members, drag can account for over 50% of the total response.

3. WAVE FORCES ON INCLINED CYLINDERS

(i) Consistent v Lumped Forces

In sections 4.4 and 4.5, it was seen how to treat element forces as 'consistent' and 'lumped'. The examples used to compare these two approaches show that the two methods give almost identical results (section 5.4) . In practice the consistent method is much more difficult to programme, particularly for inclined members, and it is recommended that the lumped approach be used.

(ii) Equation (3.33a) gives an expression for the spectral density of the normal fluid particle velocity $S_{u_n u_n}$ in terms of θ ,the angle of inclination of the member, from which it is possible to deduce the relative magnitudes of $S_{u_n u_n}$ at various angles (see Appendix 8) .

(iii) The Halcrow-Ewbank platform (section 5.4.3) illustrates the use of the inclined member facility in the computer programmes.

4 CLOSING REMARKS

The theory described in this thesis has been modified by the author to give a random response analysis of plane frames under wind loading. This has been used to analyse self-supporting masts, such as radio and television transmission towers, an example of which is shown overleaf (the diagram was obtained from a graph-plotter routine, written by the author, which generates the mesh automatically, given the height, top width and bottom width). The theory might equally well be used to analyse an oil rig gantry, although obviously in this case the tower cannot be considered to be on a fixed foundation. An interesting structural problem arises if one considers the platform jacket subjected to random water waves, and the gantry subjected to random wind. A topic for future research might be to see if the solutions for the two loads acting independently, can be combined to give an overall solution; and if so, what the cross-correlation effects between the two loads are, and in particular, whether the load in one part of the structure can cause resonance in the other part .

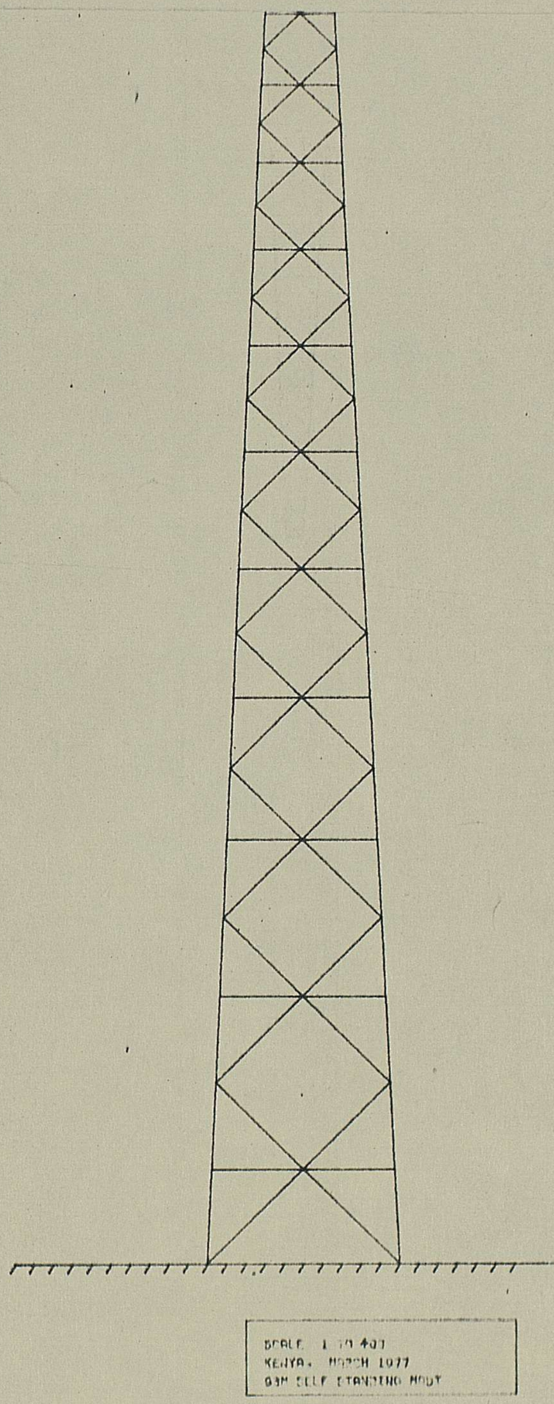

<u>A Typical Self-Supporting Mast</u>

(may be analysed by the methods described in this thesis)

REFERENCES

(in the order in which they first appear in the text)

I. SPIESS, F. N. - Oceanographic and Experimental Platforms (Brahz , Ed. , Oceon Engineering , Wiley 1968)

2. SVERDRUP, H.U. and MUNK, W.H. - Wind, Sea and Swell, Theory of Relations For Forcasting (Hydrographic Office Publication No 60I , U.S. Dept. of Navy 1947)

3. PIERSON, W.J. , NEUMANN, G. and JAMES, R.W. - Observing and Forcasting Ocean Waves By Means of Wave Spectra and Statistics (Hydrographic Office Publication No 603 , U.S. Dept. of Navy , 1955)

4. MORISON, J.R. , O'BRIEN, M.P. , JOHNSON, J.W. , SCHAEF, S.A. - The Force Exerted By Water Waves On Piles (Petroleum Transactions A I M E , Vol I89 , 1950)

5. MALHOTRA, A.K. and PENZIEN, J. - Response of Offshore Structures To Random Wave Forces (A S C E , Jnl. Struct. Div. , October 1970)

MALHOTRA, A.K. and PENZIEN, J. - Nondeterministic Analysis of Offshore Structures (A S C E , Jnl. Eng. Mech. , December 1970)

6. MORSE, P.M. - Vibrations and Sound (First Edition, 1936)

7. MAC CAMY, R.C. and FUCHS, R.A. - Wave Forces On Piles, A Diffraction Theory (Dept. of the Army, Beach Erosion Board, Tech. Memo 69 , 1955)

8. SKJELBREIA, HENDRICKSON AND KILMER - Wave Force Calculation For Three-Dimensional Structures Composed of Tubular Members (Offshore Exploration Conference 1966)

9. BRETSCHNEIDER, C.L - Wave Variability and Wave Spectra For Wind Generated Gravity Waves (TM No II8 , Beach Erosion Board , 1959)

BRETSCHNEIDER, C.L - Significant Waves and Wave Spectrum (Ocèon Industry, Vol 3, No 2 , 1968)

IO. PIERSON, W.J. and MOSKOWITZ - A Proposed Spectral Form For Fully Developed Wind Seas Based On The Similarity Theory of S.A. Kitaigorodskii (Journal of Geophysical Research , Vol 69 , No 24 1964)

II. DRAPER, L. - Extreme Wave Conditions in British and Adjacent Waters (I3 th Coastal Engineering Conference , Vancouver , July 1972)

I2. BORGMAN, L.E. - The Spectral Density For Ocean Wave Forces (Coastal Engineering Speciality Conference , Santa Barbara , October 1965 (A S C E))

I3. HARRIS, H.I. - The Response of Structures To Gusts (International Conference on Wind Effects on Buildings and Structures , Teddington 1963)

14. CARTWRIGHT and LONGUET - HIGGINS - The Statistical Distribution of The Maximum of a Random Function (Proc. Royal Society, A, Vol. 237, pp 212 - 232)

15. PRZEMIENIECKI, J.S. - Theory of Matrix Structural Analysis (Mc Graw - Hill)

Miscellaneous References

16. CLOUGH, R.W. - Effect of Earthquakes On Underwater Structures (Proc. Second World Conference On Earthquake Engineering , Tokyo, 1960)
(Introduces the 'added mass' concept.)

17. LEE, G.C. - Offshore Structures, Past, Present, Future and Design Considerations (OECON 1968)
(Resume of development from 1900 - 1967)

18. HAVELOCK, T.H. - The Pressure of Water Waves On A Fixed Obstacle (Proc. Royal Soc. London, A , Vol 175, 1940)
(A diffraction theory)

19. PUTZ, R.R. - The Motions of Ship-Shaped Vessels in Surface Waves (OECON 1966)
(Good for spectral analysis)

20. SPRING, B.H. and MONKMEYER, P.L. - Interaction of Plane Waves with Vertical Cylinders (Coastal Engineering I974 , Vol 3)

2I. BREBBIA, C.A. , FERRANTE, A.J. and LIMA, E.C.P - Analisis Estructural de Plataformas Marinas Fijas (xviii Jornados Sudamericanos de Ingenieria, Salvador, Bahia, Brasil ; Dec I976)

The following 6 references are concerned with the design of various types of offshore structure .

22. LAMPLOUGH, T.A. - Lloyd's Register's Approach To Ocean Engineering (Tech. Offshore Conf., Gt. Yarmouth I972)

23. ANDERSON, R.H. et al - Fixed Offshore Platform Design Analysis (OECON I967)

24. HROMADIK, J.J. - Deep Ocean Installations and Fixed Structures (Brahz , Ed. , Ocean Engineering , Wiley I968)

25. OAKLEY, O.H. - Vehicles and Mobile Structures (Brahz , Ed. , Ocean Engineering , Wiley I968)

26. DANFORTH, L.J. - The Feasibility of An Offshore Underwater Oil Drilling Platform (OECON I966)

27. HOLMES, J.F. - Vertically Stable Floating Drill Platform (OECON I968)

Three good texts are the following :

28. MUGA, B.J. and WILSON, J.F. - Dynamic Analysis of Ocean Structures (Plenum Press 1970)

29. EVANS, J.H. and ADAMCHAK, J.C. - Ocean Engineering Structures (M.I.T. Lecture Notes 1969)

30. MAXWELL - COOK, P.V. - Concrete Sea Structures (F.I.P. Symposium, Tbilisi , 1972)

APPENDIX I : INERTIA AND DRAG FORCE COEFFICIENTS

AI.I THE HYDRODYNAMIC OR ADDED MASS FORCE, F_{AM}

Considering a body with volume V in an ideal fluid flowing with uniform speed u, one can equate the work done on the fluid due to the resisting force on the body, to the rate of increase of kinetic energy of the fluid.

The resisting force is given by F_{AM} and the rate of work being done on the fluid is therefore $F_{AM}\, u$.

The kinetic energy of the fluid is given by :

$$K.E. = \int_V \frac{\rho v^2}{2}\, dV = \frac{\rho u^2}{2} \int_V \left(f(x,y,z) - I \right) dV$$

where the integration is over the volume of the fluid, and v is the fluid particle velocity, which is proportional to u.

Hence

$$F_{AM}\, u = -\frac{d}{dt}\left(K.E. \right)$$

$$= -\frac{\rho}{2}\, 2u \frac{du}{dt} \int_V \left(f(x,y,z) - I \right) dV$$

or

$$F_{AM} = -\, C_{AM}\, \rho\, V \frac{du}{dt}$$

where

$$C_{AM} = \frac{I}{V} \int_V \left(f(x,y,z) - I \right) dV$$

Here C_{AM} is the hydrodynamic or 'added' mass coefficient . Clearly, it is dependent only on the shape of the body . Since F_{AM} is proportional to the acceleration of the body, the term $C_{AM} \rho V$ can be thought-of as an 'added' mass leading to an increase in the inertia of the body .

AI.2 THE PRESSURE GRADIENT FORCE, F_P

Using Euler's equations, the pressure gradient caused by acceleration in the x-direction only is given by :

$$\frac{\partial P}{\partial x} = - \rho \frac{du}{dt} = - \rho \left(\frac{\partial u}{\partial t} + u \frac{\partial u}{\partial x} + w \frac{\partial u}{\partial z} \right)$$

The force due to the pressure gradient in the x-direction is :

$$F_P = - \int_V \frac{\partial P}{\partial x} \, dV$$

In the case in which the convective acceleration terms $u \frac{\partial u}{\partial x}$ and $w \frac{\partial u}{\partial z}$ are small compared with the acceleration $\frac{\partial u}{\partial t}$, $\frac{\partial P}{\partial x}$ reduces to $\frac{\partial P}{\partial x} = - \rho \frac{\partial u}{\partial t}$ and F_P is now :

$$F_p = \rho V \frac{\partial u}{\partial t}$$

AI.3 A LINEARISED DAMPING COEFFICIENT, $\bar{C}$

Morison's equation was given in equation (3.I) as :

$$F = C_H (\dot{v} - \dot{u}) + C_D (v-u) \left| v-u \right| + C_P \dot{v} \tag{A.I}$$

in which the damping term

$$C_D (v-u) \left| v-u \right|$$

is non-linear . One way to solve the problem is to attempt to linearise the damping term, and to this end one can write equation (A.I) as :

$$F = C_H (\dot{v} - \dot{u}) + \bar{C} (v-u) + C_P \dot{v} + \left[C_D (v-u) \left| v-u \right| - \bar{C} (v-u) \right]$$

in which the term $\bar{C} (v-u)$ has been added and subtracted. The term $\bar{C} (v-u)$ is a linear damping term and it is now necessary to find $\bar{C}$ by minimising the expression in square brackets . This was done by Malhotra and Penzien (Ref 5) using a least squares technique . Letting

$$A = C_D (v-u) \left| v-u \right| - \bar{C} (v-u)$$

gives

$$\left\langle \frac{\partial A^2}{\partial \bar{C}} \right\rangle = -2 \left\langle \left(C_D (v-u) \left| v-u \right| - \bar{C} (v-u) \right) (v-u) \right\rangle = 0$$

in which $\langle \quad \rangle$ refers to a time average .

Hence

$$\bar{C} = \frac{C_D \langle (v-u)^2 \; |v-u| \rangle}{\langle (v-u)^2 \rangle} \tag{A.2}$$

Assuming all the quantities have zero-mean Gaussian distributions, the required quantities in equation (A.2) are given by :

$$\langle (v-u)^2 \rangle = \sigma_{v-u}^2$$

$$\langle |v-u| \rangle = \sqrt{\frac{8}{\pi}}\, \sigma_{v-u}$$

$$\langle (v-u)^2 \; |v-u| \rangle = \sqrt{\frac{8}{\pi}}\, \sigma_{v-u}^3$$

Equation (A.2) then reduces to :

$$\bar{C} = C_D \sqrt{\frac{8}{\pi}}\, \sigma_{v-u}$$

AI.4 INERTIA AND DRAG COEFFICIENTS FOR VARIOUS OBSTACLE SHAPES

Tables AI and A2 show the values of the inertia coefficient C_M and the drag coefficient C_D , respectively, for a variety of obstacle shapes. C_M refers to the sum of the added mass coefficient C_{AM} and the pressure gradient coefficient C_P , i.e. $C_M = C_{AM} + C_P$.

TABLE A1

Values of Inertia Coefficient, C_M

The tabulated values below are for two dimensional flow. Values for three dimensional flow may be approximated by multiplying by the correction factor, K.

With elliptical and rectangular shapes, h is the dimension parallel to the flow, b is the breadth normal to the flow and l is the length normal to the flow. The "lb" plane is the plane normal to the flow.

Cross Sectional Shape	On the Surface	Submerged	On the Bottom
Flat plate (with cross sectional area $= \pi b^2/4$)		1.0	
Circle			
Small Diameter		1.5	
Large Diameter		2.0	
Ellipse		1.0+b/h	
Rectangle			
With l horizontal	1.0+b/2h	1.0+b/h	1.0+2/h
With l vertical	1.0+b/2h	1.0+b/h	

$$\text{Correction factor, } K = \frac{(l/b)^2}{1+(l/b)^2}$$

TABLE A2

Values of Shape Coefficient, C_D

	Length/Width Ratio 1	5	∞
Flat plate (perpendicular to flow)	1.16	1.20	1.90
Prism (axis perpendicular to flow)			
Square			2.00
2:1 (long side parallel to flow)			1.50
Cylinder (axis perpendicular to flow)			
Reynolds No. = 10^5	0.63	0.74	1.20
Reynolds No. = 5×10^5		0.35	0.33

American Bureau of Shipping Design Values

Cylindrical Shapes	0.50
Surface ship hulls, deck house sides, underdeck areas (smooth surfaces)	1.00
Rig derrick (each face)	1.25
Underdeck areas (exposed beams and girders)	1.30
Isolated structural shapes (cranes, angles, channels, beams, etc.)	1.50

APPENDIX 2 : THE DIFFRACTION THEORY - SOME ALGEBRA

A2.I BESSEL AND HANKEL FUNCTIONS

(i) The n th order Bessel function $J_n(x)$, where n is an integer , is given by :

$$J_n(x) = \frac{x^n}{2^n\, n!}\left[I - \frac{x^2}{2^2\; I!\,(n+I)} + \frac{x^4}{2^4\; 2!\;(n+I)\;(n+2)} - \frac{x^6}{2^6\; 3!\;(n+I)\;(n+2)\;(n+3)} + \ldots \right] \qquad (A2.I)$$

(ii) The Weber function $Y_n(x)$ is given, in terms of $J_n(x)$, by :

$$Y_n(x) = \lim_{\nu \to n} \left[\frac{J_\nu(x)\,\cos(\nu\pi) - J_{-\nu}(x)}{\sin(\nu\pi)} \right] \qquad (A2.2)$$

(iii) The n th order Hankel functions of the first and second kind are given by :

$$H_n^{(I)}(x) = J_n(x) + i\,Y_n(x) \qquad (A2.3)$$

$$H_n^{(2)}(x) = J_n(x) - i\,Y_n(x) \qquad (A2.4)$$

(iv) The derivative of the Hankel function $H_n^{(I)}(x)$ is :

$$H_n^{(I)\prime}(x) = J_n'(x) + i\,Y_n'(x) \qquad (A2.5)$$

where the prime denotes differentiation with respect to x .
Equation (A2.5) leads to :

$$\left| H_n^{(I)\prime}(x) \right|^2 = \left[J_n'(x) \right]^2 + \left[Y_n'(x) \right]^2 \qquad (A2.6)$$

Using the recurrence relations

$$J_n'(x) = \frac{n}{x} J_n(x) - J_{n-I}(x)$$

$$Y_n'(x) = \frac{n}{x} Y_n(x) - Y_{n-I}(x) \qquad (A2.7)$$

or

$$J_I'(x) = \frac{J_I(x)}{x} - J_0(x)$$

$$Y_I'(x) = \frac{Y_I(x)}{x} - Y_0(x) \qquad (A2.8)$$

equation (A2.6) gives :

$$\left| H_I^{(I)\prime}(ka) \right|^2 = \left[\frac{J_I(ka)}{ka} - J_0(ka) \right]^2 + \left[\frac{Y_I(ka)}{ka} - Y_0(ka) \right]^2 \qquad (A2.9)$$

Equation (A2.9) expresses $\left| H_I^{(I)\prime}(ka) \right|^2$ in a form suitable for computation .

A2.2 DERIVATION OF THE DIFFRACTION THEORY INERTIA FORCE

The inertia force per unit length of the cylinder at depth z is given by :

$$F_z^{(D)}(\omega) = \mathrm{Re} \int_{-\pi}^{\pi} p(\theta)\, \hat{\underline{r}}\, a_0 \, d\theta \qquad (A2.10)$$

where $\hat{\underline{r}}$ is a unit radial vector given by

$$\hat{\underline{r}} = \hat{\underline{i}} \cos\theta + \hat{\underline{j}} \sin\theta$$

Substituting for $p(\theta)$ the inertia term from Bernoulli's equation, equation (3.11), gives :

$$F_z^{(D)}(\omega) = \mathrm{Re} \int_0^{2\pi} \rho \frac{\partial \phi}{\partial t}\, \hat{\underline{r}}\, a_0 \, d\theta \qquad (A2.11)$$

in which ϕ is given by equation (3.10) as :

$$\phi = ac \frac{\cosh kz}{\sinh kd} \sum_{-\infty}^{\infty} (i)^n \left[\frac{J_n'(ka_0)}{H_n^{(1)'}(ka_0)} H_n^{(1)}(kr) - J_n(kr) \right] e^{i(n\theta - \omega t)} \qquad (A2.12)$$

We require the force on the cylinder, so we therefore need the value of ϕ on $r = a_0$, which is :

$$\phi\Big|_{r=a_0} = ac \frac{\cosh kz}{\sinh kd} \sum_{-\infty}^{\infty} (i)^n \left[\frac{J_n'(ka_0)}{H_n^{(1)'}(ka_0)} H_n^{(1)}(ka_0) - J_n(ka_0) \right] e^{i(n\theta - \omega t)} \qquad (A2.13)$$

and using the identity

$$x\left[H_n^{(1)}(x)\,J_n'(x) - H_n^{(1)\prime}(x)\,J_n(x)\right] = -\frac{2i}{\pi}$$

equation (A2.13) becomes :

$$\phi\Big|_{r=a_0} = -\frac{2ic\,\cosh kz}{ka_0\pi\,\sinh kd}\sum_{-\infty}^{\infty}(i)^{n+1}\frac{e^{i(n\theta-\omega t)}}{H_n^{(1)\prime}(ka_0)}$$

Finally, using the fact that

$$H_{-n}^{(1)}(x) = (-1)^n\,H_n^{(1)}(x)$$

we get

$$\phi\Big|_{r=a_0} = -\frac{4ica\,\cosh kz}{a_0\pi k\,\sinh kd}\sum_{1}^{\infty}(i)^{n+1}\frac{\cos n\theta\;e^{-i\omega t}}{H_n^{(1)\prime}(ka_0)} + \frac{2ca_0}{\pi ka}\frac{e^{-i\omega t}}{H_0^{(1)\prime}(ka)} \qquad (A2.14)$$

Inserting equation (A2.14) into equation (A2.11) gives :

$$F_z^{(D)}(\omega) = (-i\omega)\left(-\frac{2ic}{\pi k^2}\right)\rho a\,\frac{\cosh kz}{\sinh kd}\,2\sum_{0}^{\infty}\left[\frac{(i)^{n+1}}{H_n^{(1)\prime}(ka_0)}\int_0^{2\pi}\cos(n\theta-\omega t)\,\cos\theta\,d\theta\right]$$

Now using the identity

$$\int_0^{2\pi}\cos n\theta\,\cos\theta\,d\theta = \pi\cos n\pi\,\delta_{n1}$$

gives the result :

$$F_z^{(D)}(\omega) = \frac{4\rho\omega^2}{k^2\left[H_1^{(1)\prime}(ka_0)\right]}\cdot\frac{\cosh kz}{\sinh kd} \qquad (A2.15)$$

APPENDIX 3 : SOME STATISTICAL DEFINITIONS

A3.I FOURIER ANALYSIS AND SPECTRAL DENSITY

The random behavior of wind velocity distributions causes the waves produced to be essentially random in nature. One method of quantifying the wave profiles is to consider the wave profile as being built up by a linear combination of components of many different frequencies. Any curve can be described by a Fourier series which adds the contributions of frequencies in multiples of some basic frequency ω , and if ω is made infinitesimally small , the series becomes a Fourier integral of the form :

$$p(t) = \frac{I}{2\pi} \int_{-\infty}^{\infty} A(i\omega) \; e^{i\omega t} \, d\omega \qquad (A3.I)$$

where $$A(i\omega) = \int_{-\infty}^{\infty} p(t) \; e^{i\omega t} \, dt$$

The two functions $p(t)$ and $A(i\omega)$ are a Fourier transform pair, and express the same curve in the 'time' and 'frequency' domains , respectively . However , this representation will only define one specific curve , and with a random process such as wave height, we wish to describe an infinite number of different curves , all of which have the same relative contributions from each element of frequency $\Delta\omega$, but with the phases of the frequency distributions randomly distributed . The elimination of phase is achieved by considering a spectral density function defined by :

$$S_{pp}(\omega) = \lim_{T \to \infty} \left[\frac{1}{\pi T} \left| A_T (i\omega) \right|^2 \right] \qquad (A3.2)$$

where $$A_T (i\omega) = \int_{-T}^{T} p(t) \; e^{-i\omega t} \, dt$$

The spectral density function therefore depends on $\left| A_T (i\omega) \right|$ which is independent of phase, and is the same for many similar functions $p(t)$.

A3.2 MEASURED DATA AND THE WAVE AMPLITUDE SPECTRUM

The relationship between a wave amplitude spectrum and other measured parameters can be deduced from probability theory based on assumed statistical properties of the sea . The usual assumption is that the variation of water surface elevation at any point can be considered as a stationary random process whose statistical properties are defined by the spectral density $S_{\eta\eta}(\omega)$ and a probability distribution function . The probability distribution of the water surface elevation is approximately Gaussian with probability density function :

$$p(\eta) = \sqrt{2\pi \ \sigma_n^{\ 2}} \ \mathrm{Exp} \left(- \frac{\eta^2}{2 \ \sigma_\eta^{\ 2}} \right) \qquad \text{(A3.3)}$$

in which $\sigma_\eta^{\ 2} = \int_0^\infty S_{\eta\eta}(\omega) \ d\omega$ is the variance of η. This ceases to be valid for large values of η when wave breaking occurs .

Equations (A3.2) and (A3.3) completely describe the statistical properties of the random process . It is now simply necessary to fit measured data to these equations . For example, Cartwright and Longuet-Higgins (Ref I4) have shown that the significant wave height H_s (defined as the average height of the highest third of all the waves) and the mean wave period T_M are given by :

$$\begin{aligned} H_s &= 4 \ m_o^{\frac{1}{2}} \\ T_M &= 2 \ \left(\frac{m_o}{m_2} \right)^{\frac{1}{2}} \end{aligned} \qquad \text{(A3.4)}$$

in which $m_n = \int_0^\infty \omega^n \ S_{\eta\eta}(\omega) \ d\omega$.

The application of the above theory to the Pierson - Moskowitz wave amplitude spectrum is dealt with in Appendix 4 .

A.3.3 PROPERTIES OF A SINGLE RANDOM PROCESS

A quantity related to the spectral density function is the <u>autocorrelation function</u> $R_{pp}(t_1, t_2)$ which gives the covariance between the two random variables $P(t_1)$ and $P(t_2)$. It is defined as :

$$R_{pp}(t_1, t_2) = E \left[P(t_1) \times P(t_2) \right] \qquad (A.3.5)$$

where E denotes mathematical expectation .

The usual assumptions are that the random process is stationary (i.e. the probability structure is independent of time) and ergodic (i.e. the probability structure does not vary from one sequence to another) .

If the covariance function depends only on $(t_2 - t_1)$ and not on the individual values of t_1 and t_2 , the process is 'weakly stationary' , and the covariance function is called the <u>autocorrelation function</u> $R_{pp}(\tau)$, i.e.

$$R_{pp}(\tau) = R_{pp}(t_2 - t_1) = R_{pp}(t_1 - t_2) = R_{pp}(t_1, t_2) \quad (A.3.6)$$

The spectral density and autocorrelation functions, equations (A.3.2) and (A.3.6) are related by :

$$\begin{aligned} S_{pp}(\omega) &= \frac{1}{\pi} \int_{-\infty}^{\infty} R_{pp}(\tau) \; e^{-i\omega\tau} \, d\tau \\ R_{pp}(\tau) &= \int_{0}^{\infty} S_{pp}(\omega) \; e^{i\omega\tau} \, d\omega \end{aligned} \qquad (A.3.7)$$

The variance σ_p^2 of the process is independent of time and can be found by putting $\tau = 0$ in equation (13.7) :

$$\sigma_p^2 = E\left[P(t) \times P(t)\right] = R_{pp}(0) = \int_0^{\infty} S_{pp}(\omega)\, d\omega \qquad (13.8)$$

13.4 MULTIPLE RANDOM PROCESSES

The definitions given above can be extended to jointly stationary random processes , in order to cover multi degree of freedom systems . Considering two jointly stationary random processes $P(t)$ and $Q(t)$, the cross - correlation function $R_{PQ}(\tau)$ is defined by :

$$R_{PQ}(\tau) = E\left[P(t) \times Q(t + \tau)\right] \qquad (13.9)$$

Similarly , a cross spectral density can be defined as:

$$S_{PQ}(\tau) = \frac{1}{\pi} \int_{-\infty}^{\infty} R_{PQ}(\tau)\; e^{-i\omega\tau}\, d\tau \qquad (13.10)$$

with inverse transformation :

$$R_{PQ}(\tau) = \int_0^{\infty} S_{PQ}(\omega) \; e^{i\omega\tau} \, d\omega \qquad (4.3.11)$$

S_{PQ} is in general complex valued and will not be defined for negative frequencies . From (4.3.9) , it can be seen that :

$$R_{PQ}(\tau) = R_{PQ}(-\tau) \qquad (4.3.12)$$

from which it may be observed that :

$$S_{PQ}(\omega) = \bar{S}_{QP}(\omega) \qquad (4.3.13)$$

i.e. $S_{PQ}(\omega)$ and $S_{QP}(\omega)$ are complex conjugates.

Putting $\tau = 0$ in equation (4.3.11) gives the covariance of the joint process :

$$R_{PQ}(0) = E\left[P(t) \times Q(t)\right] = K_{PQ} = \int_0^{\infty} S_{PQ}(\omega) \, d\omega \qquad (4.3.14)$$

4.3.5 STATISTICAL PROPERTIES OF VELOCITIES AND ACCELERATIONS

If we are interested in the derivatives with respect to time of the response in question, these statistical properties can be calculated from the statistical properties of the displacements.

One can show that the following relationships exist between the correlation functions :

$$R_{\dot{p}q}(\tau) = -R'_{pq}(\tau)$$

$$R_{p\dot{q}}(\tau) = +R'_{pq}(\tau) \qquad (4.3.15)$$

$$R_{\dot{p}\dot{q}}(\tau) = -R''_{pq}(\tau)$$

where the prime denotes differentiation with respect to τ.

Now since

$$R_{pq}(\tau) = \int_0^{\infty} S_{pq}(\omega)\, e^{i\omega\tau}\, d\omega$$

we get

$$R'_{pq}(\tau) = \int_0^{\infty} S_{pq}(\omega)\, i\,\omega\, e^{i\omega\tau}\, d\omega \qquad (4.3.16)$$

$$R''_{pq}(\tau) = -\int_0^{\infty} S_{pq}(\omega)\, \omega^2\, e^{i\omega\tau}\, d\omega$$

Hence

$$R_{\dot{p}q}(\tau) = -i\omega\, R_{pq}(\tau)$$

$$R_{p\dot{q}}(\tau) = +i\omega\, R_{pq}(\tau) \qquad (4.3.17)$$

$$R_{\dot{p}\dot{q}}(\tau) = \omega^2\, R_{pq}(\tau)$$

and on Fourier transforming :

$$S_{\dot{P}Q}(\omega) = -i\,\omega\, S_{PQ}(\omega)$$

$$S_{P\dot{Q}}(\omega) = i\,\omega\, S_{PQ}(\omega) \qquad (A3.18)$$

$$S_{\dot{P}\dot{Q}}(\omega) = \omega^2\, S_{PQ}(\omega)$$

A3.6 LINEAR TRANSFORMATIONS OF SPECTRAL DENSITY FUNCTIONS OF JOINTLY STATIONARY RANDOM PROCESSES

Consider the linear transformation

$$\underline{Y} = \underline{\underline{A}}\,\underline{X} \qquad (A3.19)$$

where $\underline{Y}$ and $\underline{X}$ are stochastic vectors of order n and m respectively, and $\underline{\underline{A}}$ is an $n \times m$ constant matrix. This may be a coordinate transformation or any linear relationship between two sets of quantities, for example displacements and stresses. The cross-correlation of $Y_i(t)$ and $Y_j(t)$ is :

$$R_Y(i,\ j, \tau) = E\left[Y_i(t)\ Y_j(t + \tau)\right]$$

$$= E\left[\sum_{k=1}^{n} A_{ik}\ X_k(t) \sum_{l=1}^{n} A_{jl}\ X_l(t + \tau)\right]$$

$$= \sum_{k=1}^{n} \sum_{l=1}^{n} A_{ik}\ A_{jl}\ E\left[X_k(t)\ X_l(t + \tau)\right]$$

$$= \sum_{k=1}^{n} \sum_{l=1}^{n} A_{ik}\ A_{jl}\ R_X(k,\ l,\ \tau)$$

Fourier transforming both sides :

$$S_Y(i,\ j, \omega) = \sum_{k=1}^{n} \sum_{l=1}^{n} A_{ik}\ A_{jl}\ S_X(k,\ l,\ \omega)$$

$$= \begin{bmatrix} A_{i1} & A_{i2} & \cdots & A_{im} \end{bmatrix} \underline{S}_X(\omega) \begin{bmatrix} A_{j1} \\ A_{j2} \\ \cdot \\ \cdot \\ \cdot \\ A_{jn} \end{bmatrix} \qquad (4.2.20)$$

or in matrix form :

$$\underline{S}_Y(\omega) = \underline{A}\ \underline{S}_X(\omega)\ \underline{A}^T$$

APPENDIX 4 : WAVE DATA AND WAVE SPECTRA

A4.I PROPERTIES OF THE PIERSON MOSKOWITZ SPECTRUM

A4.I.I SIGNIFICANT WAVE HEIGHT H_S AND MEAN WAVE PERIOD T_M

The Pierson-Moskowitz spectrum is defined by :

$$S_{\eta\eta}(\omega) = \frac{A}{\omega^5} \exp\left(- \frac{B}{\omega^4} \right) \qquad (A4.I)$$

The n th moment m_n is defined by :

$$m_n = \int_0^\infty \omega^n \, S_{\eta\eta}(\omega) \, d\omega \qquad (A4.2)$$

Substituting for $S_{\eta\eta}(\omega)$ and integrating gives for the first few moments :

$$m_0 = \frac{A}{4B}$$

$$m_I = \frac{0.306\ A}{B^{\frac{3}{4}}} \qquad (A4.3)$$

$$m_2 = \frac{A}{4}\sqrt{\frac{\pi}{B}}$$

Then the significant wave height H_S and mean wave period T_M are given by (Ref I4) :

$$H_S = 4\, m_0^{\frac{1}{2}} = 2\sqrt{\frac{A}{B}}$$

$$T_M = 2\left[\frac{m_0}{m_2}\right]^{\frac{1}{2}} = 2\left[\frac{I}{\pi B}\right]^{\frac{1}{4}} \qquad (A4.4)$$

Inverting equations (A4.4) , we get for the constants A and B :

$$B = \frac{16 \pi^3}{T_M^4} = \frac{496}{T_M^4}$$

$$A = \frac{H_S^2 B}{4} = \frac{124 \; H_S^2}{T_M^4} \qquad (A4.5)$$

A4.I.2 MOST COMMONLY OCCURING WAVE PERIOD T_0

T_0 is the wave period which corresponds to the peak frequency ω_0 of the wave spectrum . Differentiating equation (A4.I) with respect to ω gives :

$$\omega_0 = \left[\frac{4\,B}{5}\right]^{\frac{1}{4}}$$

(A4.6)

and

$$S_{\eta\eta}(\omega_0) = A \left[\frac{4\,B}{5}\right]^{-5/4} \exp\left(\frac{-5}{4}\right)$$

It follows that :

$$T_0 = \frac{2\pi}{\omega_0} = 2\pi \left[\frac{4\,B}{5}\right]^{-\frac{1}{4}} \qquad (A4.7)$$

and since, in equation (A4.4) ,

$$T_M = 2\pi\left[\frac{I}{\pi B}\right]^{\frac{1}{4}}$$

we get

$$\frac{T_O}{T_M} = I.4I \qquad (A4.8)$$

A4.2 COMPARISON BETWEEN THE PIERSON-MOSKOWITZ AND BRETSCHNEIDER WAVE SPECTRA

Expressions for the two spectra are given in equations (3.25) and (3.26) , and the spectra may be seen in Figs (3. 2) and (3. 3) . Considering just the highest peak of the Bretschneider spectra, for which T_M = 20 seconds, H_S = I metre , the corresponding Pierson-Moskowitz parameters are :

$$B = \frac{I6\ \pi^3}{T_M{}^4} = 3.I026 \times IO^{-3}$$

$$A = \frac{H_S{}^2\ B}{4} = I.984 \times IO^{-3}$$

The peak frequency occurs at

$$\omega_0 = \left(\frac{4B}{5}\right)^{\frac{1}{4}} = 0.22319 \quad \text{radns/sec}$$

and the corresponding spectrum peak is

$$S_{\eta\eta}(\omega_0) = A \left[\frac{4B}{5}\right]^{-5/4} \exp\left(-\frac{5}{4}\right) = 1.0253 \ m^2 sec$$

The Bretschneider spectrum peak occurs at

$$S_{\eta\eta}(\omega_0) = 10.5 \ ft^2 sec = 0.9941 \ m^2 sec$$

The agreement between the two spectra is good . After some of the early attempts, most authors are now agreed that the best representation of wave height spectra is to have the spectrum inversely proportional to ω^5 , and to have ω^{-4} as an argument within the exponential .

A4.3 WAVE DATA

The two items needed to find the parameters A and B in the Pierson-Moskowitz spectrum are the maximum wave height in a given interval (say 50 years), H_{Max}, and the most commonly occuring wave period T_0. The National Institute of Oceonography (Ref 6) has compiled such data, a little of which is given below.

Latitude North (Degrees)	H_{Max} (m)	T_0 (secs)
52.5	15	11
55.0	20	13
57.5	28	15
60.0	29	15.5
62.5	30	16

Selected Wave Data For The North Sea (50 year period)

APPENDIX 5 : THE DIFFRACTION THEORY VERSUS MORISON'S THEORY

Figures (A5.I) - (A5.I4) show the diffraction theory and Morison theory force spectra and response spectra for cylinders with radii a ranging from 0.I m to 20 m . All the cylinders were assumed to have the same frequency response curve, peaking at I.07 radns/sec..

Using the abbreviations D.T. for diffraction theory, and M.T. for Morison's theory, the following points can be observed from the curves :

(i) At $a = 0.1$ m (this might be a leg of a self-standing mast , for example) , the force spectra are almost identical and the response spectra are inseparable .

(ii) At $a = 0.5$ m , the D.T. force spectrum has crossed over the M.T. force spectrum at a frequency $\omega_c = 2.8$ radns/sec. The D.T. displacement spectrum peak is slightly higher than the M.T. displacement spectrum peak .

(iii) At $a = 1.0$ m , the cross-over frequency ω_c is reduced to 2.2 radns/sec.. The D.T. displacement spectrum peak is still greater than the M.T. displacement spectrum peak .

(iv) At $a = 2.6$ m , $\omega_c = 1.4$ radns/sec., and the D.T. force spectrum is still greater than the M.T. force spectrum over the range of interest (in this case, I.07 radns/sec , the peak of the frequency response curve) .

(v) At $a = 5.5$ m , $\omega_c = 0.8$ radns/sec , which is less than the peak of the frequency response curve . The M.T. M.T. displacement is therefore greater than the D.T. displacement (even though the D.T. force spectrum peak is higher than the M.T. force spectrum peak) .

(vi) Up to $a = 16$ m , ω_c continues to get smaller ; the D.T. force spectrum peak is still greater than the M.T. peak , but elsewhere over the frequency range, the M.T. spectrum is much larger than the D.T. spectrum . This leads to a larger response by the M.T. than by the D.T. for all cylinders with a response function peak outside a narrow band near the force spectrum peaks .

(vii) At $a = 19.0$ m , the M.T. force spectrum is greater than the D.T. force spectrum over the whole frequency range, including the peak values . The force spectrum peaks do not now occur at the same frequency (0.35 for the D.T. and 0.5 radns/sec for the M.T.) .

CONCLUSION

We can conclude that the D.T. leads to a larger response than the M.T. for cylinders with radii between 0.3 and 4.0 m . For larger radii, the M.T. response is larger over most of the frequency range, except near the force spectrum peaks, where in any case resonance would occur if the frequency response curve also peaked there .

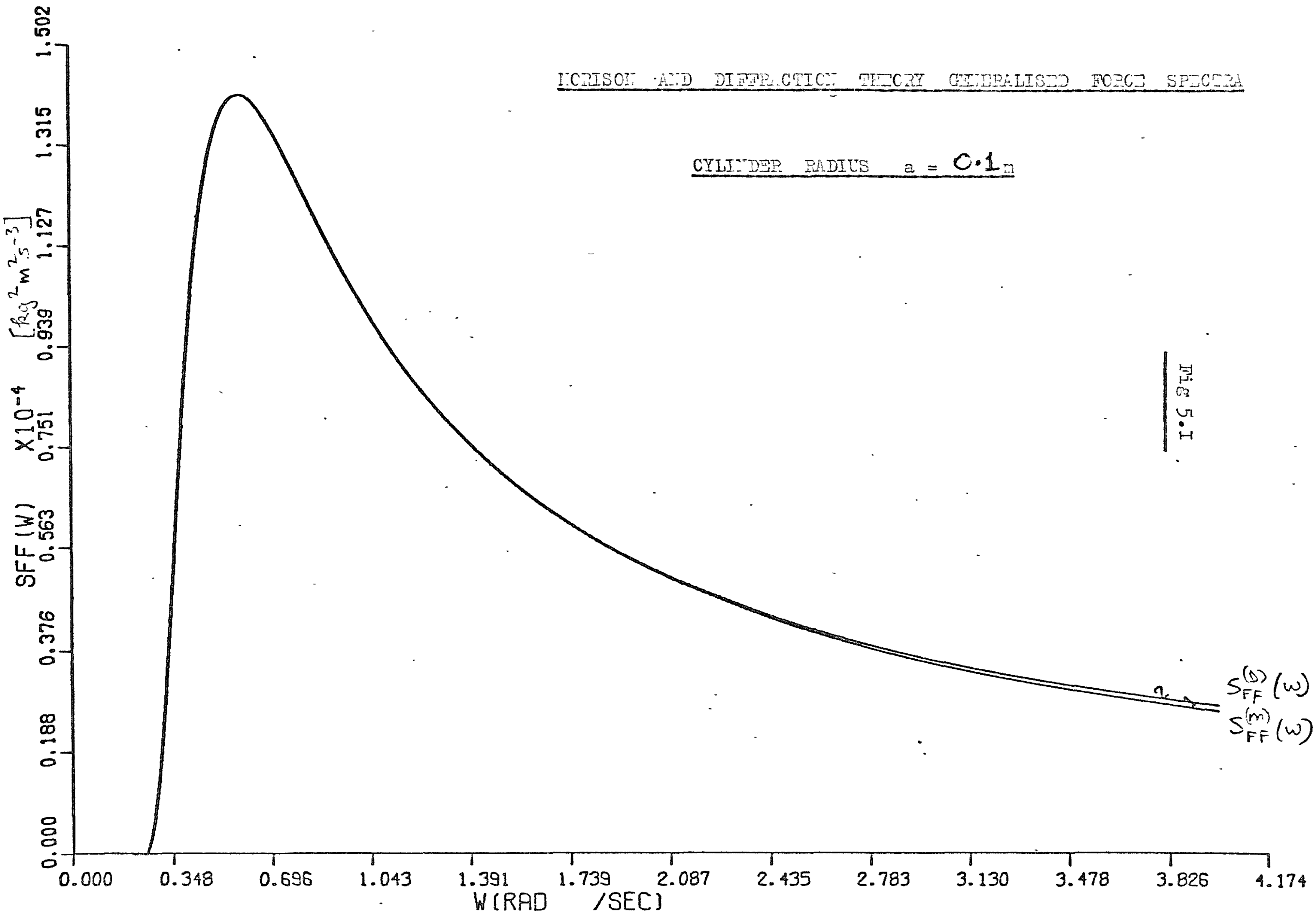
MORISON AND DIFFRACTION THEORY GENERALISED FORCE SPECTRA
CYLINDER RADIUS a = 0.1 m
SFF(W) X10^-4 [kg^2 m^2 s^-3]
0.000
0.188
0.376
0.563
0.751
0.939
1.127
1.315
1.502
0.000
0.348
0.696
1.043
1.391
1.739
2.087
2.435
2.783
3.130
3.478
3.826
4.174
W(RAD /SEC)
$S_{FF}^{(D)}(\omega)$
$S_{FF}^{(m)}(\omega)$

Fig 5.1

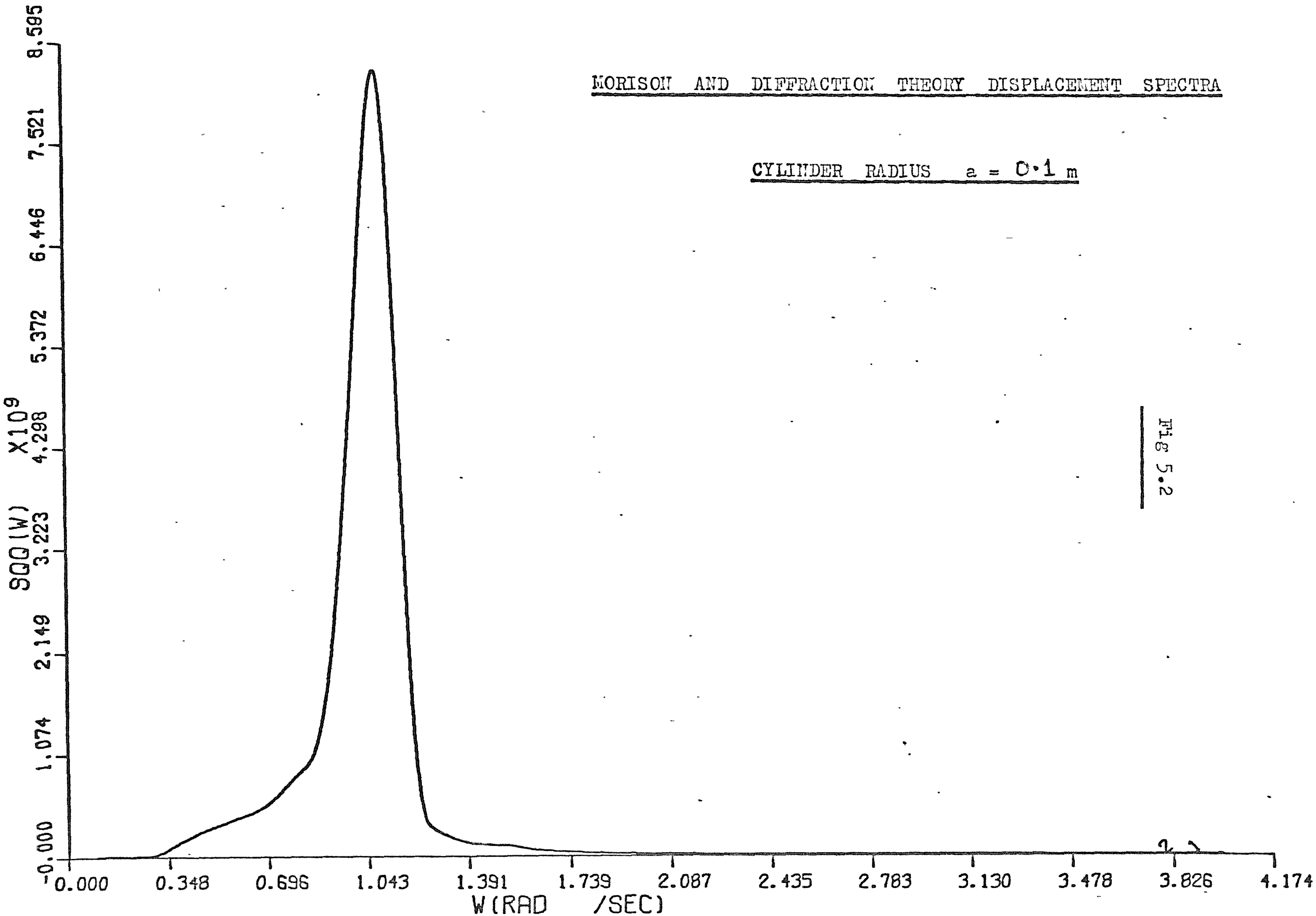
MORISON AND DIFFRACTION THEORY DISPLACEMENT SPECTRA
CYLINDER RADIUS a = 0·1 m
SQQ(W) X10[9]
8.595
7.521
6.446
5.372
4.298
3.223
2.149
1.074
0.000
-0.000
0.348
0.696
1.043
1.391
1.739
2.087
2.435
2.783
3.130
3.478
3.826
4.174
W(RAD /SEC)

Fig 5.2

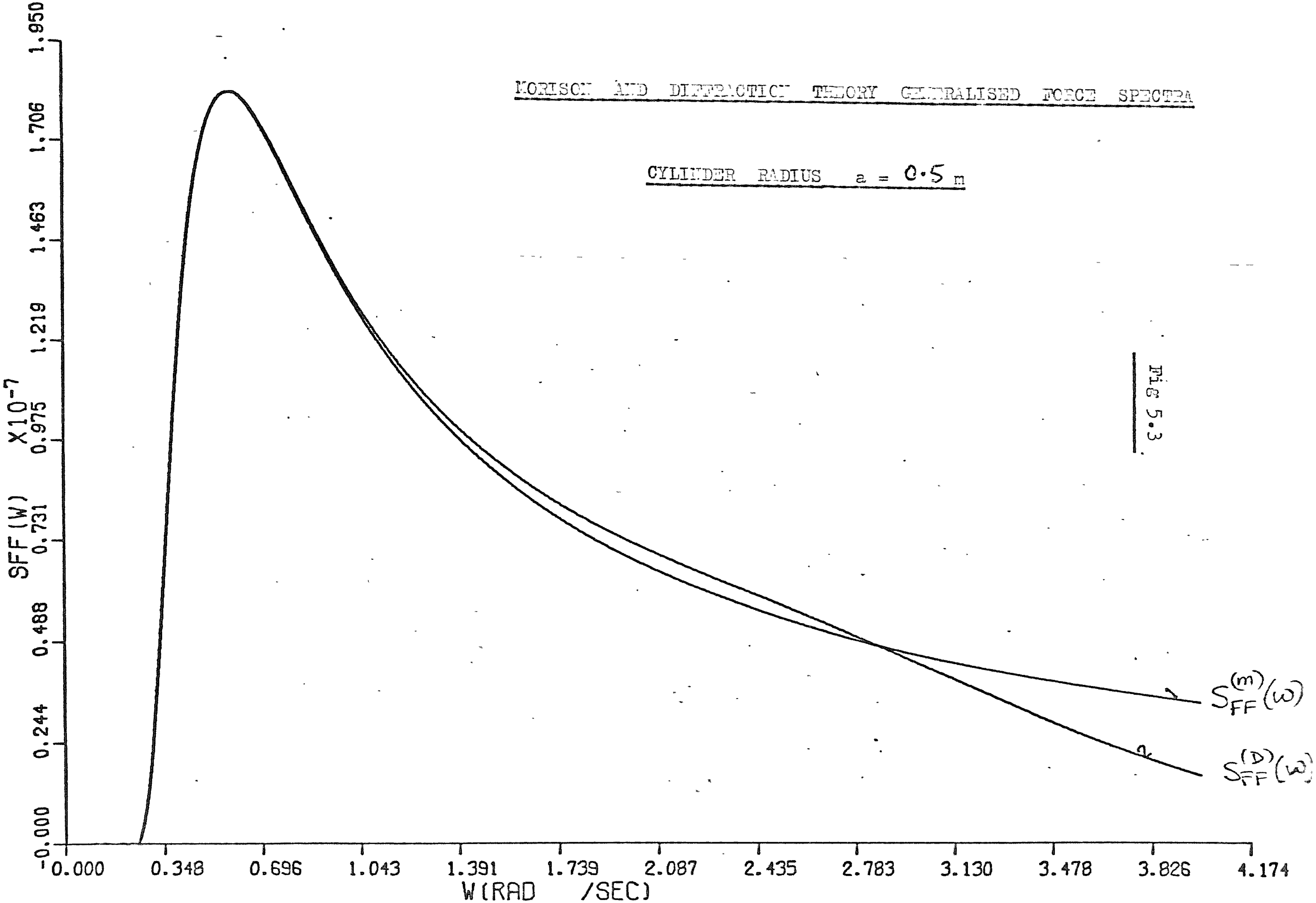

MORISON AND DIFFRACTION THEORY GENERALISED FORCE SPECTRA
CYLINDER RADIUS a = 0·5 m
SFF(W) X10^-7
1.950
1.706
1.463
1.219
0.975
0.731
0.488
0.244
-0.000
0.000
0.348
0.696
1.043
1.391
1.739
2.087
2.435
2.783
3.130
3.478
3.826
4.174
W(RAD /SEC)
$S_{FF}^{(m)}(\omega)$
$S_{FF}^{(D)}(\omega)$

Fig 5.3

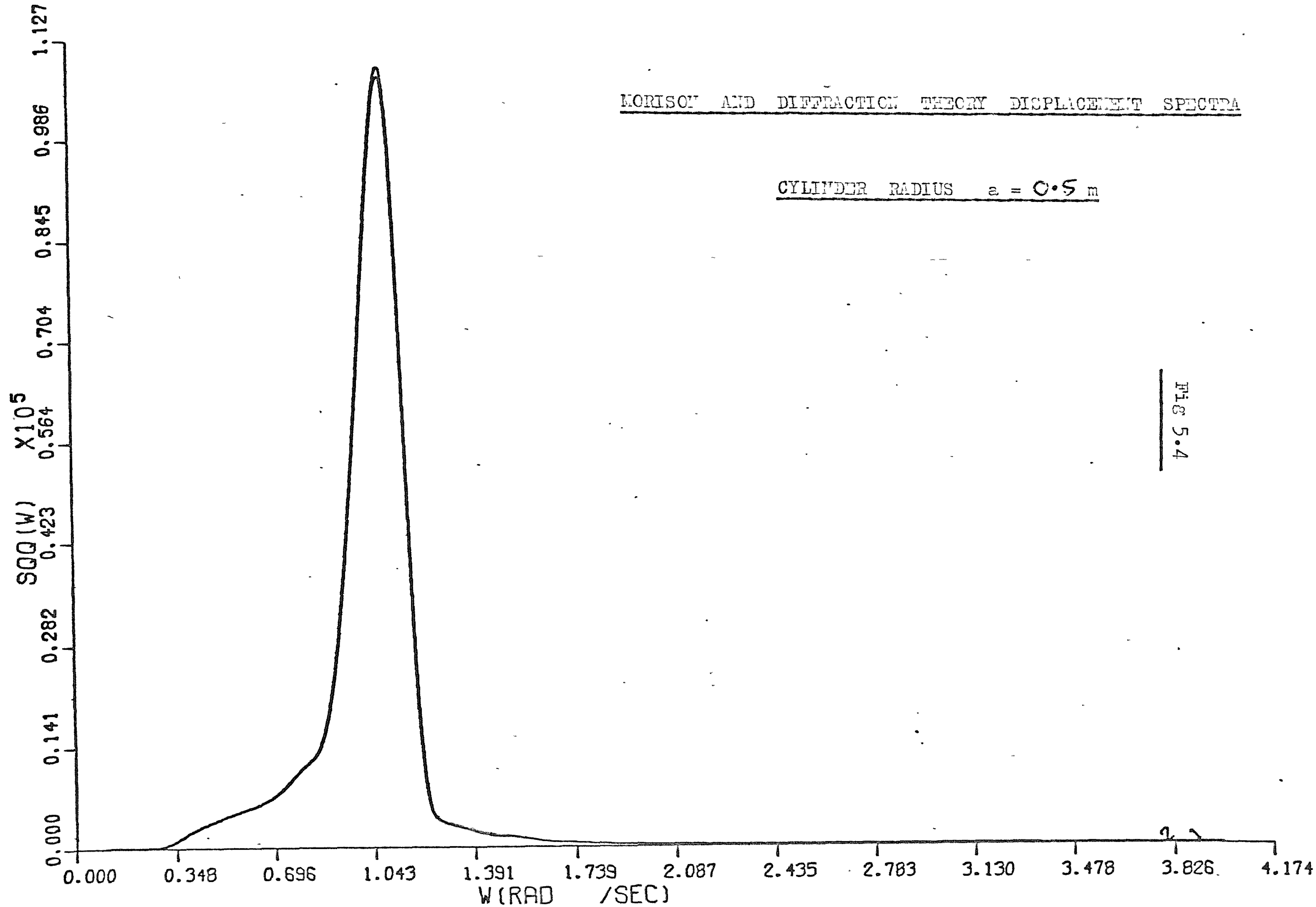

MORISON AND DIFFRACTION THEORY DISPLACEMENT SPECTRA

CYLINDER RADIUS $a = 0{\cdot}5$ m

Fig 5.4

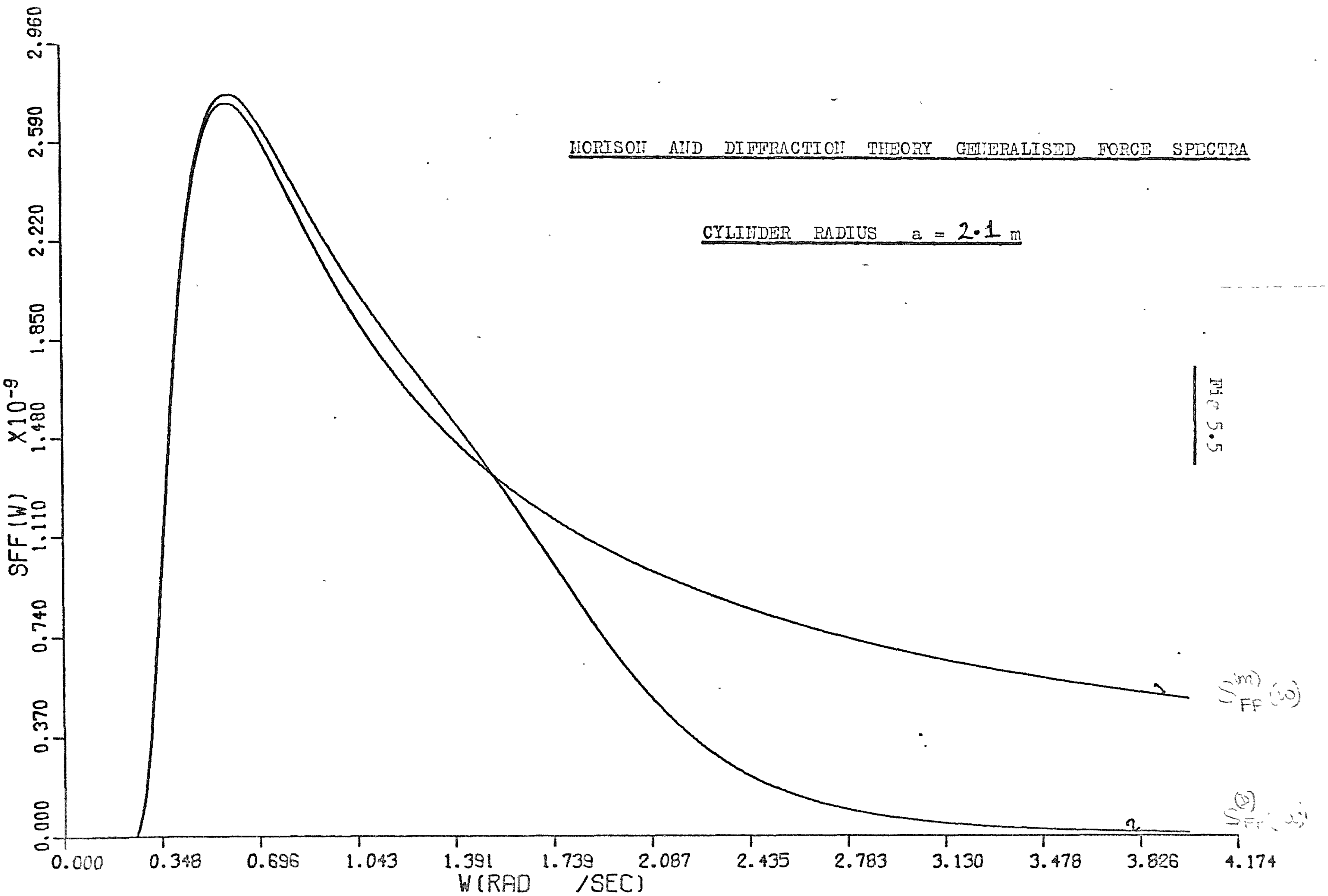

MORISON AND DIFFRACTION THEORY GENERALISED FORCE SPECTRA
CYLINDER RADIUS a = 2·1 m
SFF(W) X10^-9
0.000
0.370
0.740
1.110
1.480
1.850
2.220
2.590
2.960
0.000
0.348
0.696
1.043
1.391
1.739
2.087
2.435
2.783
3.130
3.478
3.826
4.174
W(RAD /SEC)
1
2

Fig 5.5

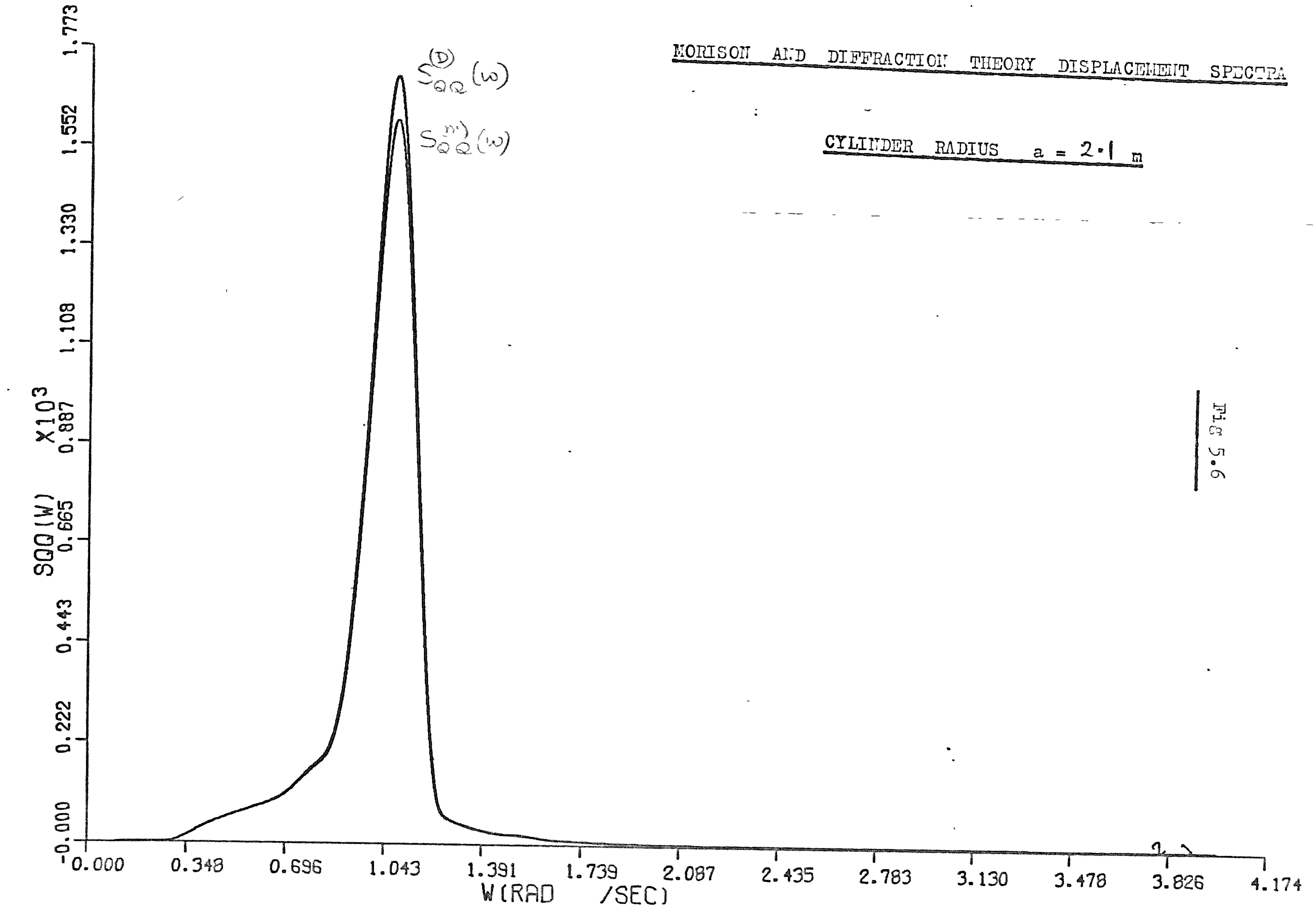
MORISON AND DIFFRACTION THEORY DISPLACEMENT SPECTRA
CYLINDER RADIUS a = 2·1 m
$S_{QQ}^{(D)}(\omega)$
$S_{QQ}^{(M)}(\omega)$
SQQ(W) X10^3
-0.000
0.222
0.443
0.665
0.887
1.108
1.330
1.552
1.773
0.000
0.348
0.696
1.043
1.391
1.739
2.087
2.435
2.783
3.130
3.478
3.826
4.174
W(RAD /SEC)

Fig 5.6

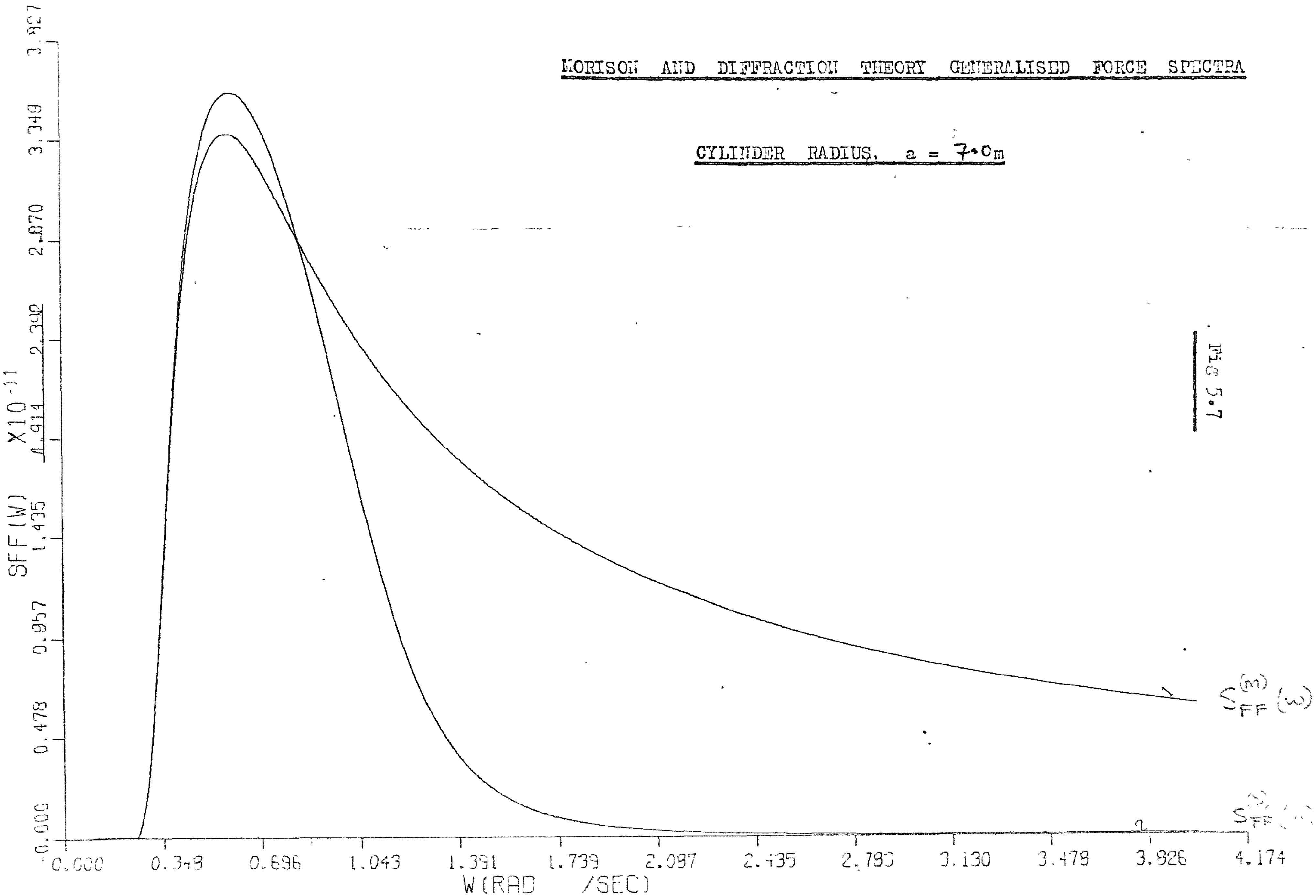
MORISON AND DIFFRACTION THEORY GENERALISED FORCE SPECTRA
CYLINDER RADIUS, a = 7·0m
SFF(W) X10⁻¹¹
0.000
0.478
0.957
1.435
1.914
2.392
2.870
3.349
3.827
0.000
0.348
0.696
1.043
1.391
1.739
2.087
2.435
2.783
3.130
3.478
3.826
4.174
W(RAD /SEC)
$S_{FF}^{(m)}(\omega)$

Fig 5.7

MORISON AND DIFFRACTION THEORY DISPLACEMENT SPECTRA

CYLINDER RADIUS a = 7.0 m

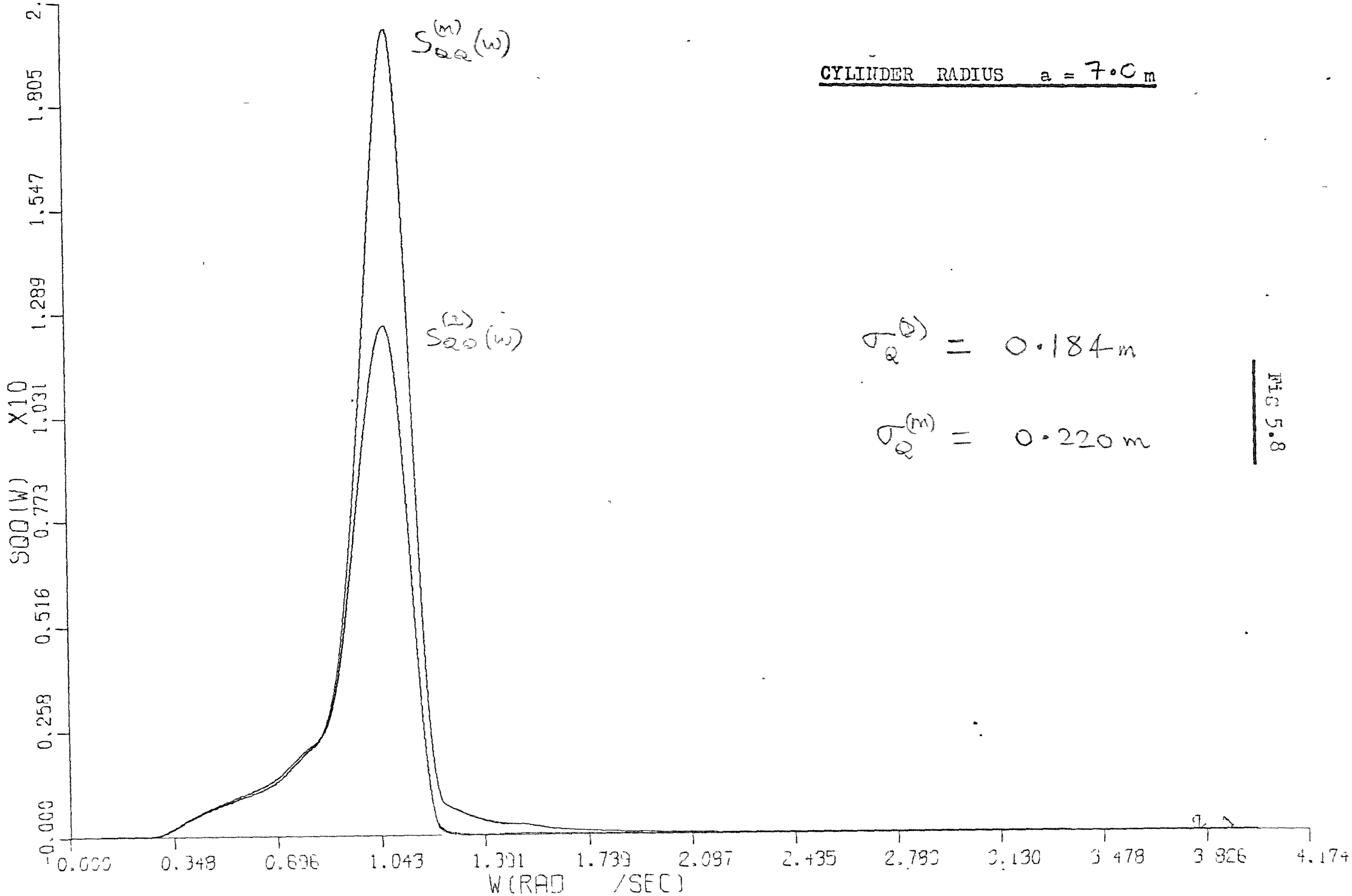

Fig 5.8

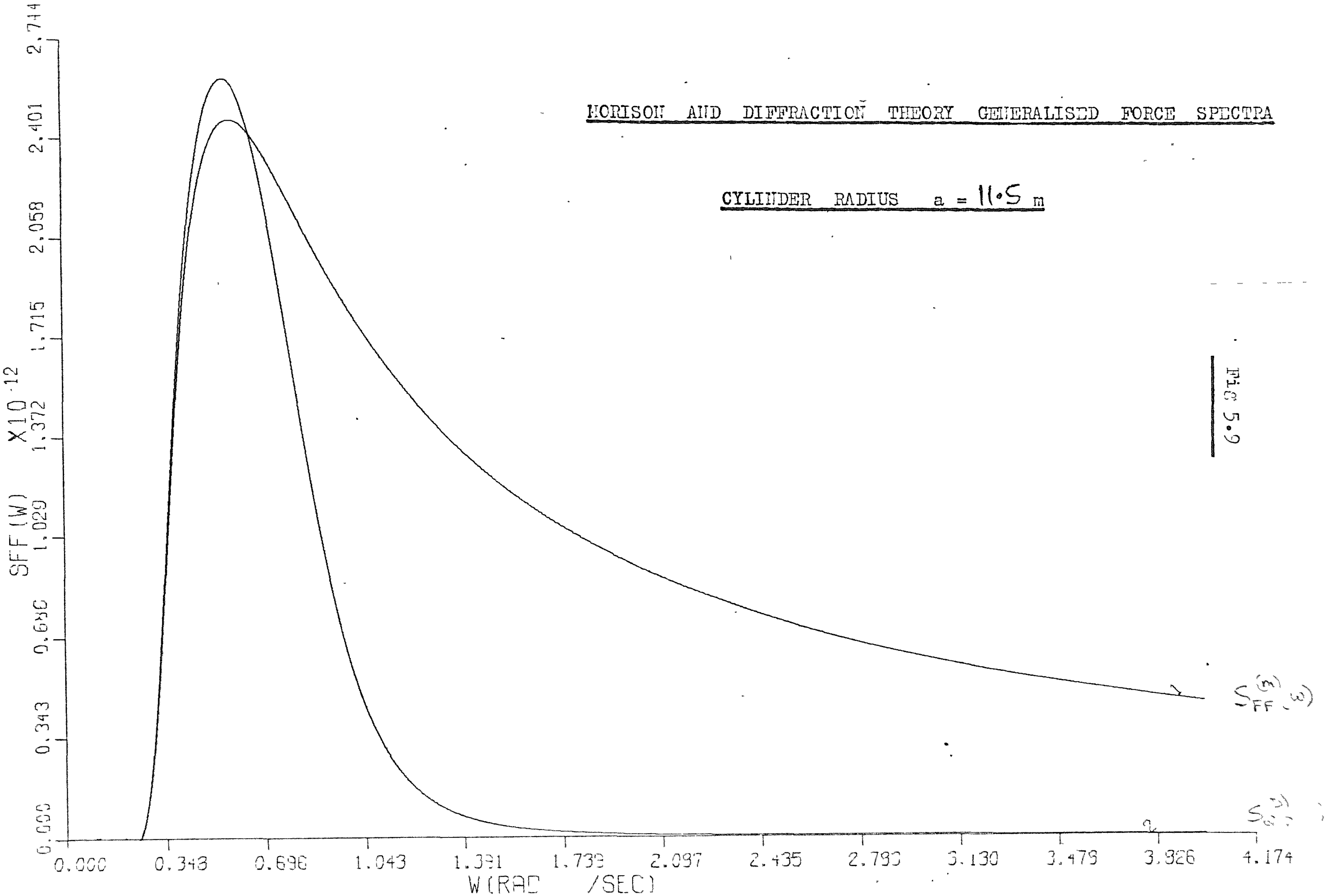

MORISON AND DIFFRACTION THEORY GENERALISED FORCE SPECTRA
CYLINDER RADIUS a = 11·5 m
SFF(W) X10^12
0.000
0.343
0.686
1.029
1.372
1.715
2.058
2.401
2.744
0.000
0.348
0.696
1.043
1.391
1.739
2.087
2.435
2.783
3.130
3.479
3.826
4.174
W(RAD /SEC)
$S_{FF}^{(3)}(\omega)$

Fig 5.9

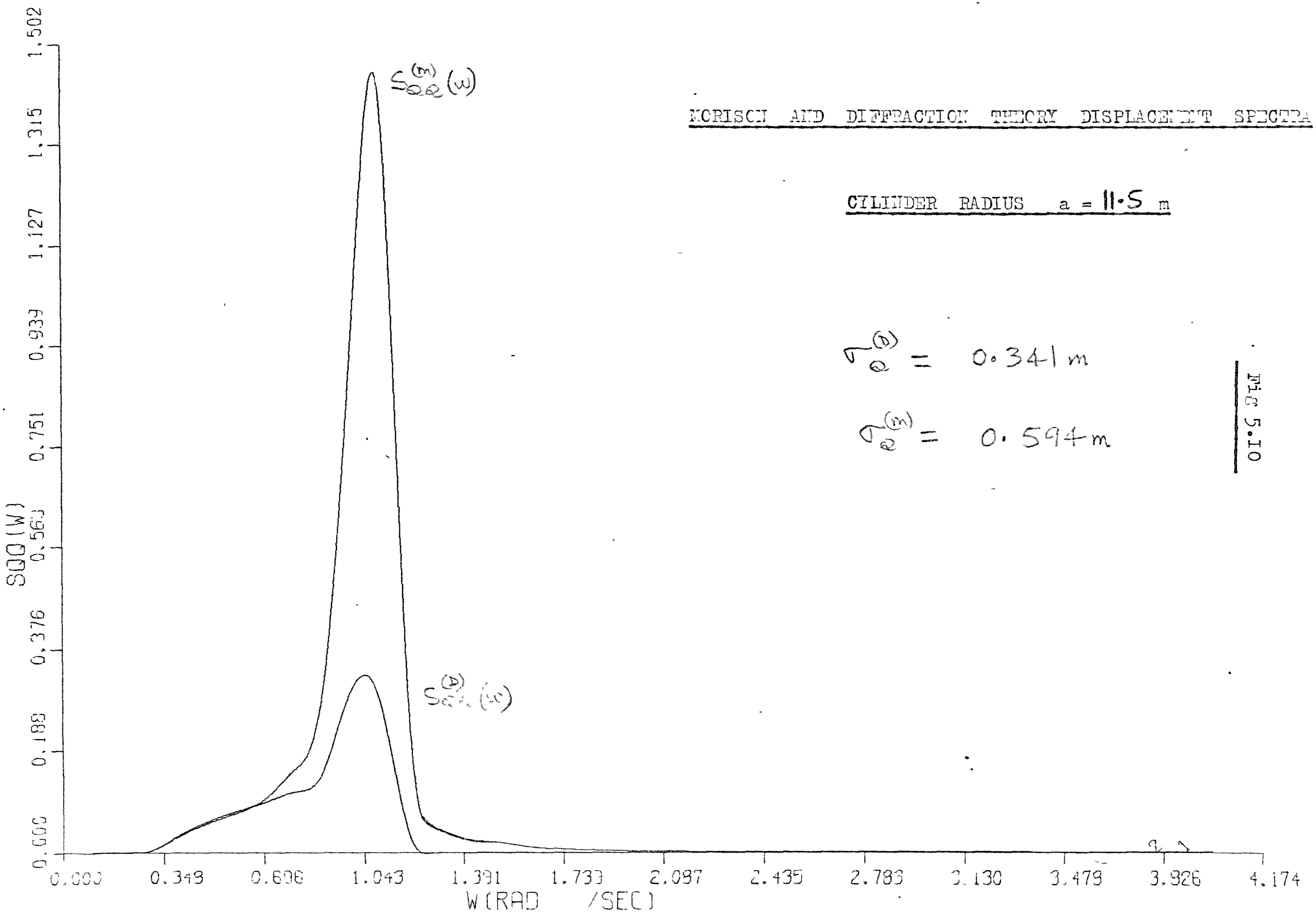
KORISCH AND DIFFRACTION THEORY DISPLACEMENT SPECTRA
CYLINDER RADIUS a = 11·5 m
$\sigma_Q^{(D)} = 0.341$ m
$\sigma_Q^{(m)} = 0.594$ m
$S_{QQ}^{(m)}(\omega)$
$S_{QQ}^{(D)}(\omega)$
SQQ(W)
W(RAD /SEC)
0.000
0.188
0.376
0.563
0.751
0.939
1.127
1.315
1.502
0.348
0.696
1.043
1.391
1.733
2.087
2.435
2.783
3.130
3.478
3.826
4.174

Fig 5.10

MORISON AND DIFFRACTION THEORY GENERALISED FORCE SPECTRA

CYLINDER RADIUS a = 16·0 m

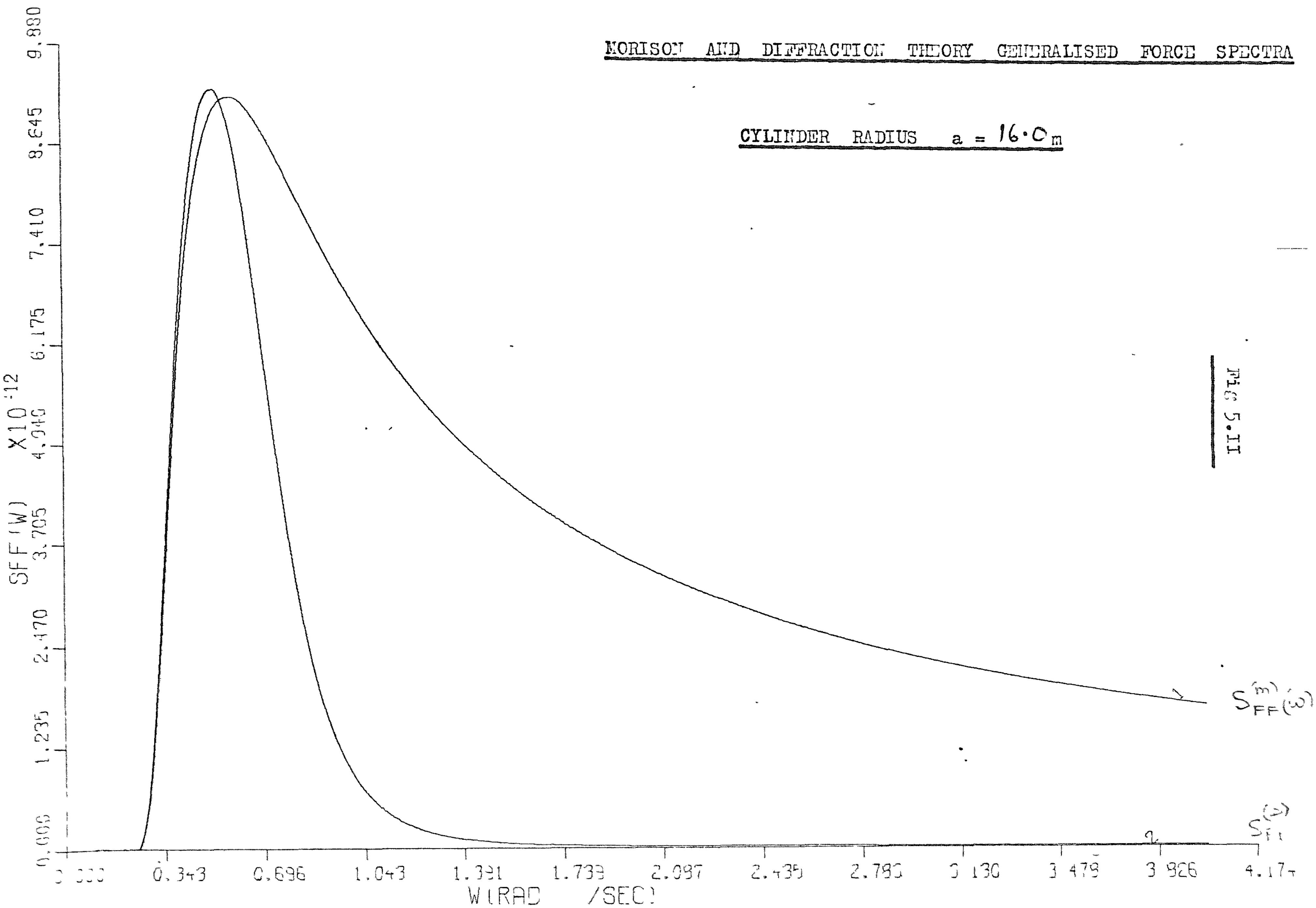

Fig. 5.11

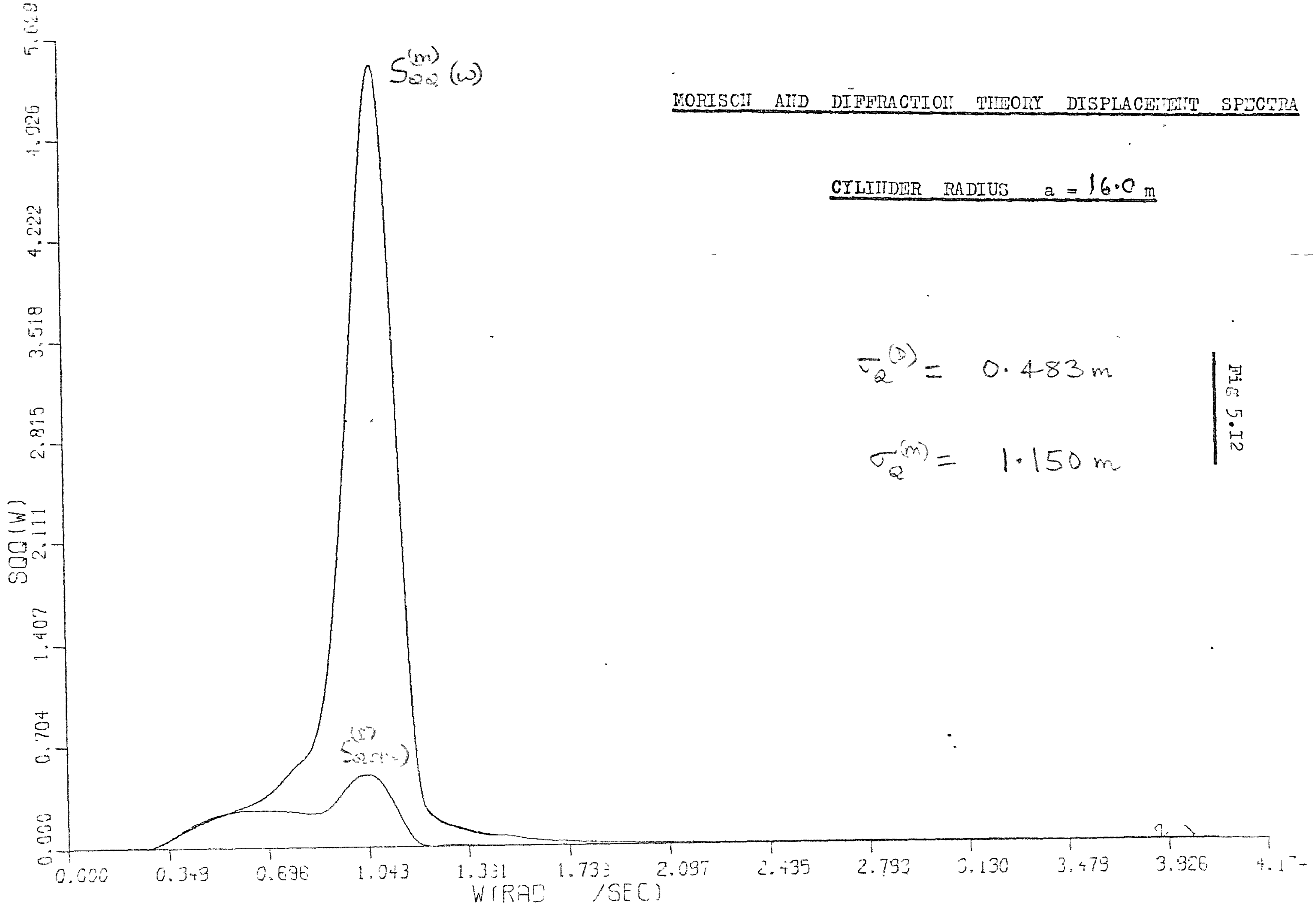

MORISCH AND DIFFRACTION THEORY DISPLACEMENT SPECTRA
CYLINDER RADIUS a = 16.0 m
$\sigma_Q^{(D)} = 0.483$ m
$\sigma_Q^{(m)} = 1.150$ m
$S_{QQ}^{(m)}(\omega)$
$S_{QQ}^{(D)}(\omega)$
SQQ(W)
W(RAD /SEC)
0.000
0.704
1.407
2.111
2.815
3.518
4.222
4.926
0.000
0.348
0.696
1.043
1.391
1.739
2.087
2.435
2.783
3.130
3.479
3.826

Fig 5.12

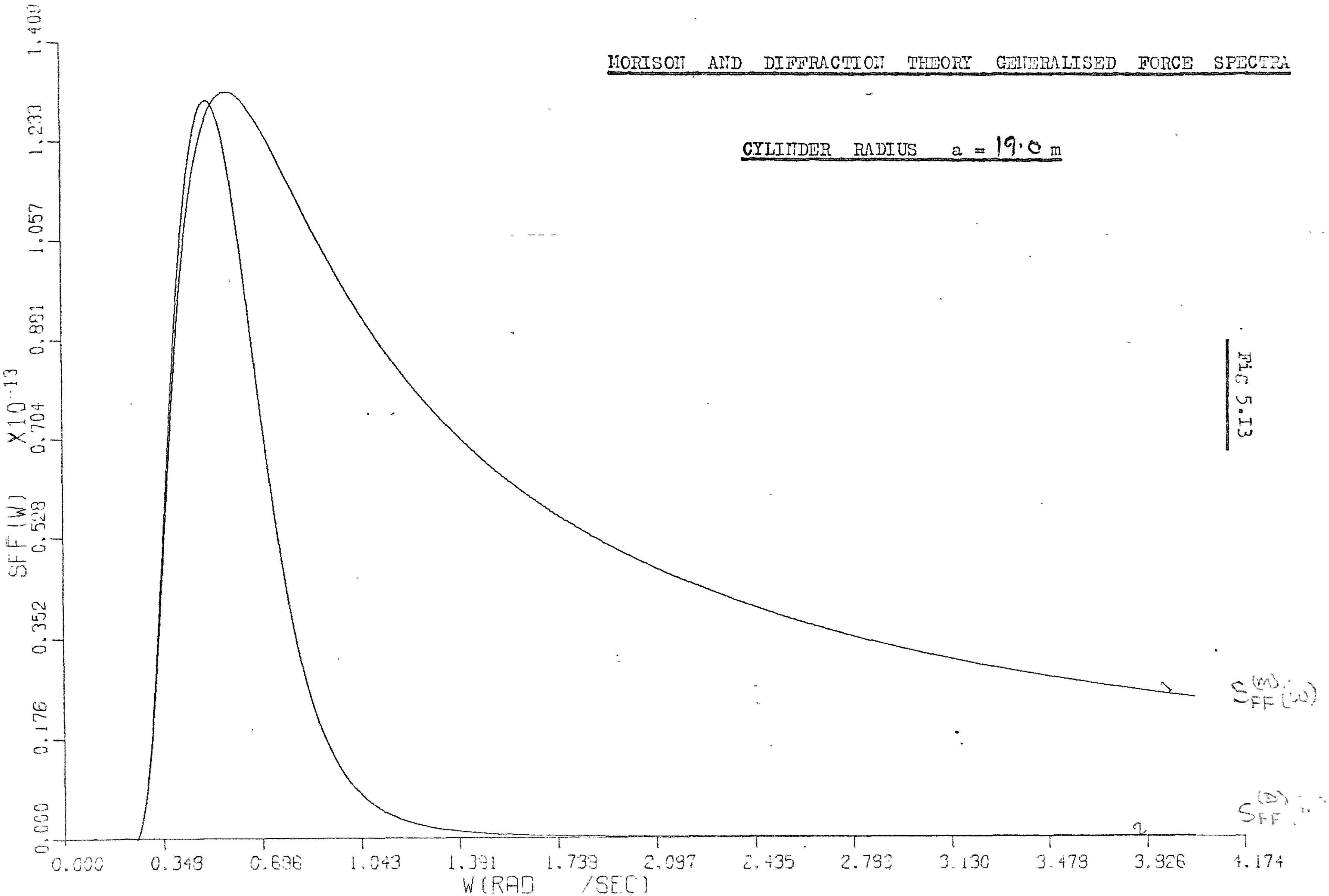
MORISON AND DIFFRACTION THEORY GENERALISED FORCE SPECTRA
CYLINDER RADIUS a = 19·0 m
SFF(W) X10⁻¹³
1.409
1.233
1.057
0.881
0.704
0.528
0.352
0.176
0.000
0.000
0.348
0.696
1.043
1.391
1.739
2.087
2.435
2.783
3.130
3.478
3.826
4.174
W(RAD /SEC)
$S_{FF}^{(m)}(\omega)$
$S_{FF}^{(D)}$

Fig 5.13

MORISON AND DIFFRACTION THEORY DISPLACEMENT SPECTRA

CYLINDER RADIUS a = 19.0 m

$\sigma_{e}^{(D)} = 0.532\,m$

$\sigma_{e}^{(M)} = 1.375\,m$

Fig 5.14

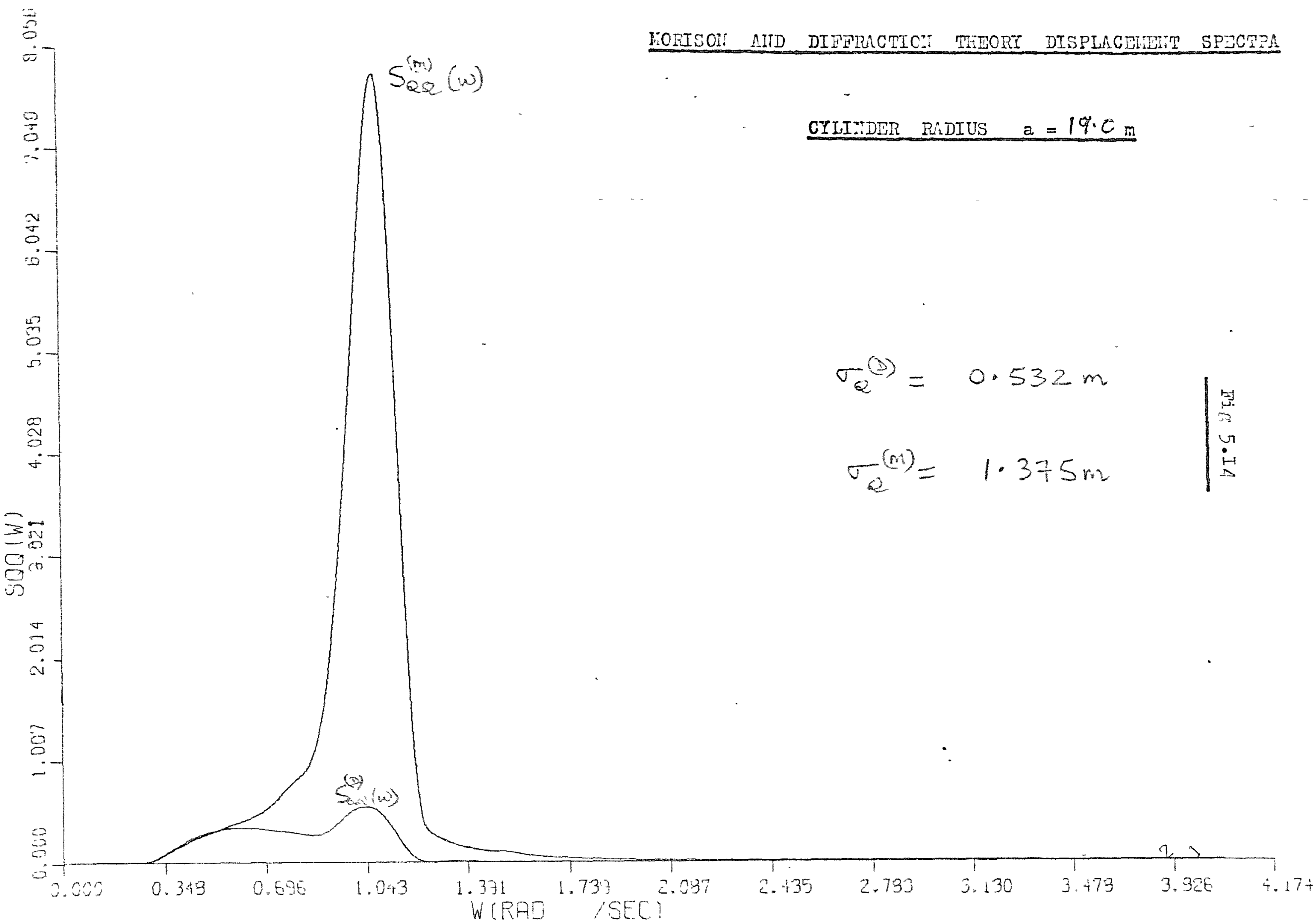

APPENDIX 6 : MASS, STIFFNESS AND DAMPING MATRICES FOR A BEAM ELEMENT

A6.I STRUCTURAL STIFFNESS AND MASS MATRICES, k_s and m_s

The beam element used throughout this thesis has six degrees of freedom, numbered I - 6 in the figure .

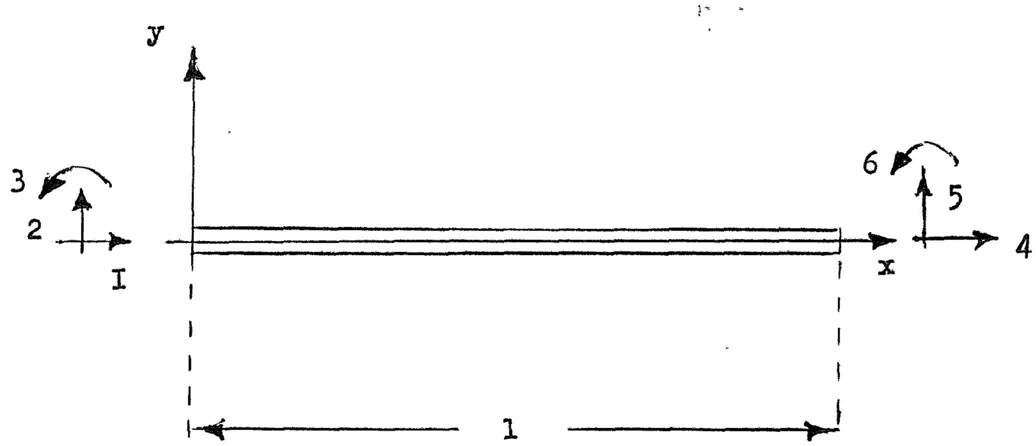

The displacements at any point are given in terms of the nodal point displacements by the equation :

$$\begin{bmatrix} u_x \\ u_y \\ u_\theta \end{bmatrix} = \begin{bmatrix} & \underline{\Phi} & \end{bmatrix} \begin{bmatrix} u_{x_I} \\ u_{y_I} \\ u_{\theta_I} \\ u_{x_2} \\ u_{y_2} \\ u_{\theta_2} \end{bmatrix} \qquad (A6.I)$$

where $\underline{\Phi}$ is an interpolation matrix , given overleaf .

$$
\underline{\phi}^T = \begin{bmatrix}
1-\frac{x}{l} & 0 & 0 \\
0 & \left[1-3\left(\frac{x}{l}\right)^2+2\left(\frac{x}{l}\right)^3\right] & \left[-6\frac{x}{l^2}+6\frac{x^2}{l^3}\right] \\
0 & \left[x-2\frac{x^2}{l}+\frac{x^3}{l^2}\right] & \left[1-4\frac{x}{l}+3\frac{x^2}{l^2}\right] \\
\frac{x}{l} & 0 & 0 \\
0 & \left[3\left(\frac{x}{l}\right)^2-2\left(\frac{x}{l}\right)^3\right] & \left[6\frac{x}{l^2}-6\frac{x^2}{l^3}\right] \\
0 & \left[-\frac{x^2}{l}+\frac{x^3}{l^2}\right] & \left[-2\frac{x}{l}+3\frac{x^2}{l^2}\right]
\end{bmatrix} \qquad \text{(A6.Ia)}
$$

The derivation of the structural stiffness and mass matrices is standard (see for example Przemieniecki, Ref I5). They are given by equations (4.2) , which when evaluated result in :

$$
\underline{k}_s = \iiint \underline{B}^T \, \underline{D} \, \underline{B} \; d(\mathrm{Vol})
$$

$$
\underline{k}_s = \begin{bmatrix}
\frac{EA}{l} & 0 & 0 & -\frac{EA}{l} & 0 & 0 \\
 & \frac{12\,EI}{l^3} & \frac{4\,EI}{l^2} & 0 & -\frac{12\,EI}{l^3} & \frac{6\,EI}{l^2} \\
 & & \frac{4\,EI}{l} & 0 & -\frac{6\,EI}{l^2} & \frac{2\,EI}{l} \\
 & & & \frac{EA}{l} & 0 & 0 \\
 & \text{SYMMETRIC} & & & \frac{12\,EI}{l^3} & -\frac{6\,EI}{l^2} \\
 & & & & & \frac{4\,EI}{l}
\end{bmatrix} \qquad \text{(A6.2)}
$$

$$m_s = \iiint \phi^T \rho \, \phi \ d(Vol)$$

$$m_s = \frac{\rho A l}{420}\begin{bmatrix} 140 & & & & & \\ 0 & 156 & & \text{SYMMETRIC} & & \\ 0 & 22\,l & 4\,l^2 & & & \\ 70 & 0 & 0 & 140 & & \\ 0 & 54 & 13\,l & 0 & 156 & \\ 0 & -13\,l & -3\,l^2 & 0 & -22\,l & 4\,l^2 \end{bmatrix} \qquad (A6.3)$$

$$+ \frac{\rho I}{30\,l}\begin{bmatrix} 0 & & & & & \\ 0 & 36 & & \text{SYMMETRIC} & & \\ 0 & 3\,l & 4\,l^2 & & & \\ 0 & 0 & 0 & 0 & & \\ 0 & -36 & -3\,l & 0 & 36 & \\ 0 & 3\,l & -l^2 & 0 & -3\,l & 4\,l^2 \end{bmatrix}$$

where ρA is the mass per unit length of the beam . The terms containing the moment of inertia I represent rotary inertia , while the first matrix represents translational mass inertia. Shear deformation effects are not included , although in principle there is no difficulty in doing this , (Ref 15) .

A6.2 THE HYDRODYNAMIC MASS MATRIX , $\underline{m}_H$

The hydrodynamic or 'added' mass matrix m_H is obtained by treating the hydrodynamic inertia force as a body force transverse to the element

$$\underline{b}_H = - \rho_H c_{AM} \begin{bmatrix} 0 \\ \ddot{u}_y \\ 0 \end{bmatrix} = - \rho_H c_{AM} \begin{bmatrix} 0 & 0 & 0 \\ 0 & 1 & 0 \\ 0 & 0 & 0 \end{bmatrix} \begin{bmatrix} \ddot{u}_x \\ \ddot{u}_y \\ \ddot{u}_\theta \end{bmatrix} \qquad (A6.4)$$

$$= - \rho_H c_{AM} \underline{S} \ \ddot{\underline{u}}$$

Hence

$$\underline{m}_H = \iiint \rho_H c_{AM} \underline{\phi}^T \underline{S} \ \underline{\phi} \ dV$$

or

$$\underline{m}_H = \frac{m_a l}{420} \begin{bmatrix} 0 & & & & & \\ 0 & 156 & & \text{SYMMETRIC} & & \\ 0 & 22 l & 4 l^2 & & & \\ 0 & 0 & 0 & 0 & & \\ 0 & 54 & 13 l & 0 & 156 & \\ 0 & -13 l & -3 l^2 & 0 & -22 l & 4 l^2 \end{bmatrix} \qquad (A6.5)$$

where ρ_H is the density of the water (1027 kg/ cu m)

m_a is the water displaced per metre of the cylinder .

A6.3 THE HYDRODYNAMIC DAMPING MATRIX , C_H

The hydrodynamic damping can be thought of as a force transverse to the element (see section (3.2.3)) , equal in magnitude to :

$$\bar{c} = \sqrt{\frac{8}{\pi}}\; C_D\, \sigma_v(x) \qquad (A6.6)$$

The hydrodynamic damping matrix C_H is then given by :

$$\underline{C}_H = \int_0^1 \underline{\phi}^T \begin{bmatrix} 0 & 0 & 0 \\ 0 & \bar{c} & 0 \\ 0 & 0 & 0 \end{bmatrix} \underline{\phi} \quad dx \qquad (A6.7)$$

The standard deviation of the fluid particle velocity , $\sigma_v(x)$, is here taken to be linearly varying , i.e.

$$\sigma_v(x) = \sigma_I + (\sigma_2 - \sigma_I) \frac{x}{l} \qquad (A6.8)$$

where $\sigma_I = \sigma_v(0)$ and $\sigma_2 = \sigma_v(l)$.

The resultant expression for $\underline{C}_H$ is given overleaf .

$$C_H = \sqrt{\frac{8}{\pi}}\, C_D \begin{bmatrix} 0 & 0 & 0 & 0 & 0 & 0 \\ & \frac{1}{35}(10\sigma_I + 3\sigma_2) & \frac{1^2}{420}(15\sigma_I + 7\sigma_2) & 0 & \frac{9\,1}{140}(\sigma_I + \sigma_2) & -\frac{1^2}{420}(7\sigma_I + 6\sigma_2) \\ & & \frac{1^3}{840}(5\sigma_I + 3\sigma_2) & 0 & \frac{1^2}{420}(6\sigma_I + 7\sigma_2) & -\frac{1^3}{280}(\sigma_I + \sigma_2) \\ & & 0 & 0 & 0 & 0 \\ & \text{SYMMETRIC} & & & \frac{1}{35}(3\sigma_I + 10\sigma_2) & -\frac{1^2}{420}(7\sigma_I + 15\sigma_2) \\ & & & & & \frac{1^3}{840}(3\sigma_I + 5\sigma_2) \end{bmatrix} \qquad (A6.9)$$

APPENDIX 7: THE SPECTRAL DENSITY OF CONSISTENT ELEMENT NODAL FORCES FOR AN INCLINED CYLINDER

A7.I

The objective is to solve equation (4.33) for $S_p(i,j,\omega)$, the cross-spectral density between consistent nodal forces P_i and P_j. This will be done for an inclined cylinder, from which the results for a vertical cylinder may be deduced by inserting $\sin\theta = I$, $\cos\theta = 0$, where θ is the inclination of the cylinder to the horizontal.

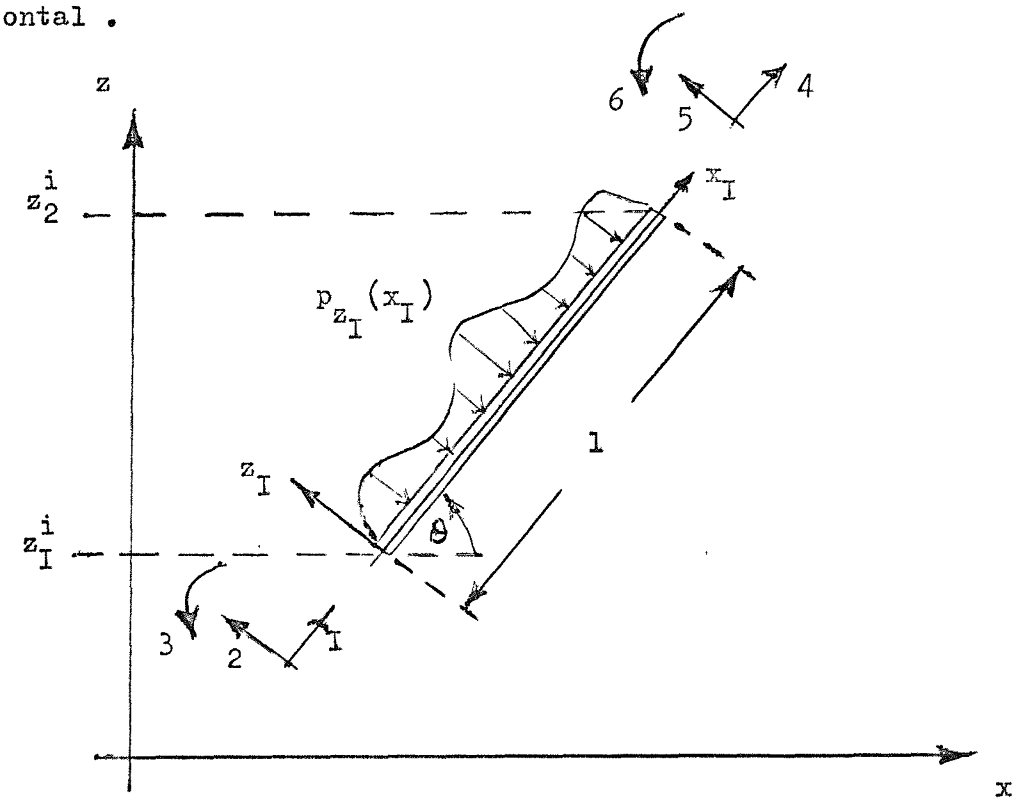

Fig (A7.I) : The i th Element

For a prismatic member, such as that shown in Fig (A7.I), consistent element nodal forces in local coordinates (x_I, z_I) are given by :

$$\underline{P}_e = \int_0^1 \underline{\phi}^T(x_I) \, \underline{p}(x_I) \, dx_I \tag{A7.I}$$

The 6 nodal forces are numbered I to 6 in the figure, and the interpolation matrix $\underline{\phi}$ is the same as that used for generating the element mass and stiffness matrices (equation (A6.Ia)) .

Making the assumption that the normal component of the wave force is the only relevant one (in other words, assuming that the tangential drag coefficient C_{D_t} is small compared with the normal coefficients), the only non-zero force term is $P_{z_I}(x_I)$, and equation (A7.I) becomes :

$$\underline{P}_e = \int_0^1 \underline{P}_{z_I}(x_I) \, \underline{\phi}_2^T \, dx_I \tag{A7.3}$$

where $\underline{\phi}_2$ is the second row of $\underline{\phi}$.

We must now consider how to insert this expression into equation (4.33) . Restating equation (4.33) for ease of reference , we have :

$$S_p(i,j,\omega) = \int_{z_I^i}^{z_2^i} \int_{z_I^j}^{z_2^j} g_i(z_i) \, g_j(z_j) \left[\frac{8}{\pi} C_i \, C_j \, \sigma_v(z_i) \, \sigma_v(z_j) \times S_{u_n u_n}(i,j,\omega) + K_i \, K_j \, S_{\dot{u}_n \dot{u}_n}(i,j,\omega) \right] dz_i dz_j \tag{A7.4}$$

in which

$$S_{u_n u_n}(\omega) = \Big[\cosh kz_i \cosh kz_j \sin\theta_i \sin\theta_j + \sinh kz_i \sinh kz_j \cos\theta_i \cos\theta_j$$

$$- (\sinh kz_i \cosh kz_j \sin\theta_j \cos\theta_i + \sinh kz_j \cosh kz_i \sin\theta_i \cos\theta_j) \Big]$$

$$\times \quad \frac{\omega^2 S_{\eta\eta}(\omega)}{\sinh^2 kd} \cos k(x_j - x_i) \qquad \text{(A7.5)}$$

and $S_{\dot{u}_n \dot{u}_n}(i,j,\omega)$ is the same with ω^2 replaced by ω^4. Inserting equation (A7.5) into (A7.4), (A7.4) can be re-written as :

$$S_p(i,j,\omega) = \Big[\frac{8}{\pi} \Big\{ \bar{\xi}^{\,i}_n(\omega)\, \bar{\xi}^{\,j}_m(\omega) \sin^2\theta + \bar{\mu}^{\,i}_n(\omega)\, \bar{\mu}^{\,j}_m(\omega) \cos^2\theta$$

$$- (\bar{\mu}^{\,i}_n(\omega)\, \bar{\xi}^{\,j}_m(\omega) + \bar{\mu}^{\,j}_m(\omega)\, \bar{\xi}^{\,i}_n(\omega)) \sin\theta \cos\theta \Big\}$$

$$+ \Big\{ \bar{\varsigma}^{\,i}_n(\omega)\, \bar{\varsigma}^{\,j}_m(\omega) \sin^2\theta + \bar{\rho}^{\,i}_n(\omega)\, \bar{\rho}^{\,j}_m(\omega) \cos^2\theta$$

$$- (\bar{\rho}^{\,i}_n(\omega)\, \bar{\varsigma}^{\,j}_m(\omega) + \bar{\rho}^{\,j}_n(\omega)\, \bar{\varsigma}^{\,i}_m(\omega)) \sin\theta \cos\theta \Big\} \Big]$$

$$\times \quad S_{\eta\eta}(\omega) \cos k(x_j - x_i) \qquad \text{(A7.6)}$$

where

$$\bar{\xi}^{\,i}_n(\omega) = \frac{C_i\, \omega}{\sinh kd} \int_{z^n_I}^{z^n_2} \bar{\phi}_{2i}(z_i)\, \sigma_v(z_i) \cosh kz_i \, dz_i$$

$$
\left.
\begin{aligned}
\bar{\zeta}_n^i(\omega) &= \frac{K_i\ \omega^2}{\sinh\ kd} \int_{z_I^n}^{z_2^n} \bar{\phi}_{2i}(z_i)\ \cosh\ kz_i\ \ dz_i \\
\bar{\mu}_n^i(\omega) &= \frac{C_i\ \omega}{\sinh\ kd} \int_{z_I^n}^{z_2^n} \bar{\phi}_{2i}(z_i)\ \sigma_v(z_i)\ \sinh\ kz_i\ \ dz_i \\
\bar{\rho}_n^i(\omega) &= \frac{K_i\,\omega^2}{\sinh\ kd} \int_{z_I^n}^{z_2^n} \bar{\phi}_{2i}(z_i)\ \sinh\ kz_i\ \ dz_i
\end{aligned}
\right| \quad (A7.7)
$$

for $i = I, 2, \ldots, 6$. Here the bar over ζ_n^i , ϕ , etc., indicates that the relevant quantities are in global coordinates (the $x - z$ coordinates) .

A7.2

The problem has been reduced to that of integrating the expressions in equations (A7.7) . One way of proceeding is to replace $\bar{\Phi}_2$ by the corresponding expression in the local coordinate system . Thus, the interpolation functions $\bar{\Phi}_2$ and ϕ_2 , in global and local coordinates, respectively , are related by :

$$\begin{bmatrix} \bar{\phi}_{21} \\ \bar{\phi}_{22} \\ \bar{\phi}_{23} \\ \bar{\phi}_{24} \\ \bar{\phi}_{25} \\ \bar{\phi}_{26} \end{bmatrix} = \begin{bmatrix} C & S & 0 & 0 & 0 & 0 \\ -S & C & 0 & 0 & 0 & 0 \\ 0 & 0 & 1 & 0 & 0 & 0 \\ 0 & 0 & 0 & C & S & 0 \\ 0 & 0 & 0 & -S & C & 0 \\ 0 & 0 & 0 & 0 & 0 & 1 \end{bmatrix} \begin{bmatrix} \phi_{21} \\ \phi_{22} \\ \phi_{23} \\ \phi_{24} \\ \phi_{25} \\ \phi_{26} \end{bmatrix} \qquad (A7.8)$$

where $C = \cos\theta$, $S = \sin\theta$.

Replacing the $\bar{\phi}_{2i}$ by their equivalent in terms of the ϕ_{2i} , expressions (A7.7) can then be evaluated directly using the standard integrals given in section A7.3 .

An alternative method of evaluating equations (A7.7) is to evaluate ξ^i_n , ζ^i_n , μ^i_n , and ρ^i_n in local coordinates, and then transform them to the global coordinate system .

Considering the first method , the coordinate transformation :

$$z^i = z^i_1 + x_1 \sin\theta \qquad (A7.9)$$

(see Fig (A7.1)) will be needed , in order to replace z^i in equation (A7.7) .

The form of $\sigma_v(z)$ will also have to be decided on . For the purposes of this thesis , a linear variation of

$\sigma_v(z)$ is assumed between the two ends of each element , i.e.

$$\sigma_v(z) = \sigma_I + (\sigma_2 - \sigma_I) \frac{z}{l} \qquad (A7.IO)$$

where σ_I and σ_2 are the values of $\sigma_v(z)$ at ends I and 2 of the element , respectively , and are known .

Inserting equations(A7.9) and (A7.IO) into equations (A7.7) , and using the integrals in section A7.3 , it is possible (after a considerable amount of laborious algebra !) to evaluate equations (A7.7) . Hence , the cross-spectral density of the nodal forces i and j can be found via equation (A7.6) .

A7.3 SOME BASIC INTEGRALS

$$I_1 = \int_a^b \cosh u \; du = \sinh b - \sinh a$$

$$I_2 = \int_a^b u \cosh u \; du = \Big[u \sinh u - \cosh u\Big]_a^b$$

$$I_3 = \int_a^b \sinh u \; du = \cosh b - \cosh a$$

$$I_4 = \int_a^b u \sinh u \; du = \Big[u \cosh u - \sinh u\Big]_a^b$$

$$I_5 = \int_a^b u^2 \cosh u \; du = \Big[u^2 \sinh u\Big]_a^b - 2\, I_4$$

$$I_6 = \int_a^b u^2 \sinh u \; du = \Big[u^2 \cosh u\Big]_a^b - 2\, I_2$$

$$I_7 = \int_a^b u^3 \cosh u \; du = \Big[u^3 \sinh u\Big]_a^b - 3\, I_6$$

$$I_8 = \int_a^b u^3 \sinh u \; du = \Big[u^3 \cosh u\Big]_a^b - 3\, I_5$$

$$I_9 = \int_a^b u^4 \cosh u \; du = \Big[u^4 \sinh u\Big]_a^b - 4\, I_8$$

$$I_{10} = \int_a^b u^4 \sinh u \; du = \Big[u^4 \cosh u\Big]_a^b - 4\, I_7$$

APPENDIX 8 : VARIOUS WATER PARTICLE VELOCITY SPECTRA

In Figs (A8.I) - (A8.6) , the graphs of $S_{uu}(\omega)$, $S_{ww}(\omega)$ and $S_{wu}(\omega)$, as given by equations (3.3I) , are shown , together with their appropriate transfer functions . In all cases, the wave height spectrum $S_{\eta\eta}(\omega)$ is the Pierson-Moskowitz spectrum (equation (3.26)) with $A = 2.56$ and $B = 0.0299$. It is seen that the transfer functions are almost identical in the three cases , except for low values of ω . This clearly confirms the belief that for large values of kz , cosh kz = sinh kz .

In Figs (A8.7) - (A8.I2) , the graph of $S_{u_n u_n}(\omega)$ (equation (3.33)) is given for various values of θ , the angle of inclination of the member to the horizontal .

In terms of its transfer function , $S_{u_n u_n}$ is given by :

$$S_{u_n u_n}(\omega) = T_{u_n u_n}(\omega) \ S_{\eta\eta}(\omega) \qquad (A8.I)$$

where

$$T_{u_n u_n}(\omega) = \Big[\cosh^2 kz \ \sin^2\theta + \sinh^2 kz \ \cos^2\theta - 2 \sinh kz \ \cosh kz \ \sin\theta \cos\theta\Big] \frac{\omega^2}{\sinh^2 kd} \qquad (A8.2)$$

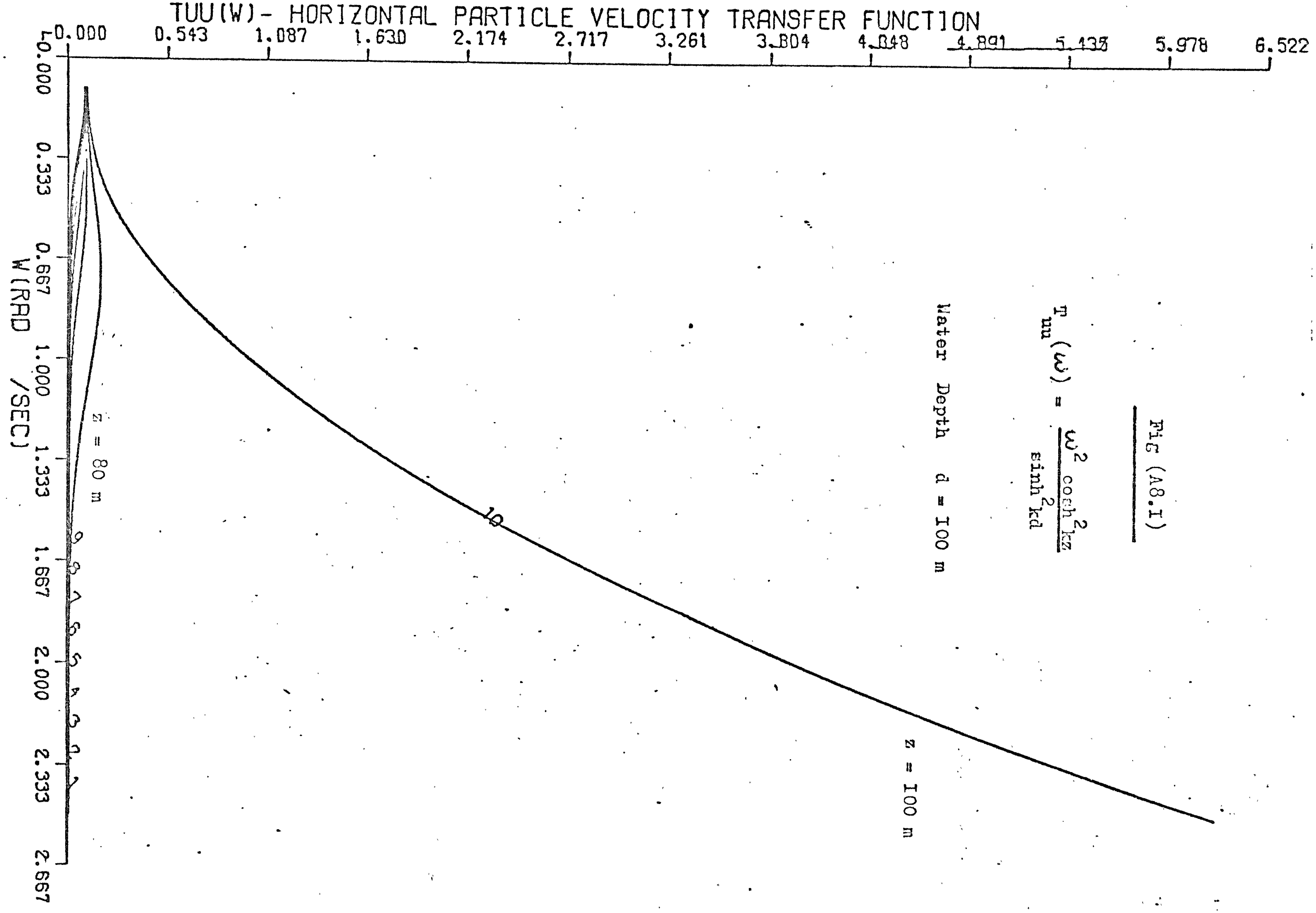

Fig (A8.1)

$$T_{uu}(\omega) = \omega^2 \frac{\cosh^2 kz}{\sinh^2 kd}$$

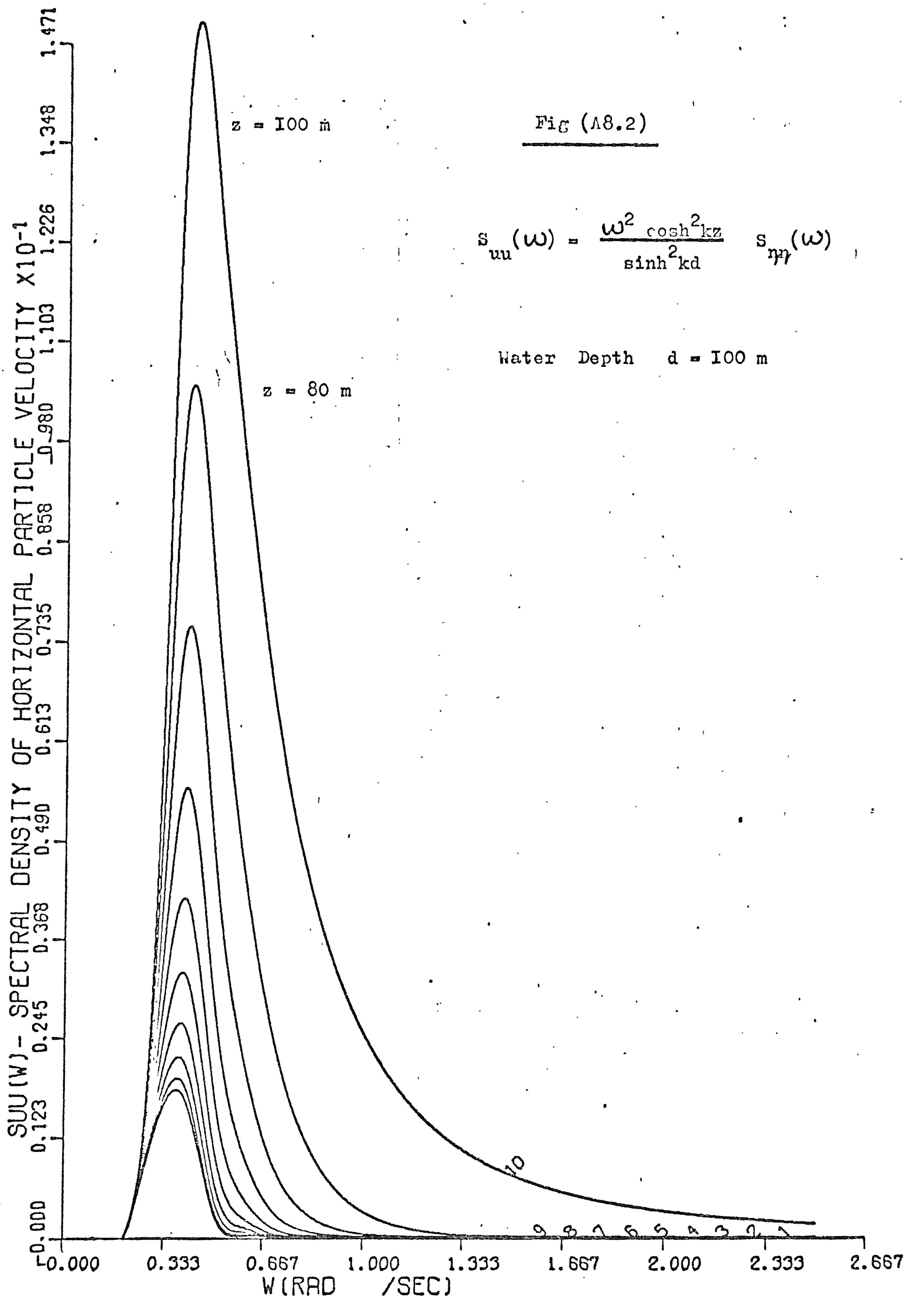

Fig (A8.2)
$S_{uu}(\omega) = \frac{\omega^2 \cosh^2 kz}{\sinh^2 kd} S_{\eta\eta}(\omega)$
Water Depth d = I00 m
z = I00 m
z = 80 m
SUU(W)- SPECTRAL DENSITY OF HORIZONTAL PARTICLE VELOCITY X10-1
0.000
0.123
0.245
0.368
0.490
0.613
0.735
0.858
0.980
1.103
1.226
1.348
1.471
0.000
0.333
0.667
1.000
1.333
1.667
2.000
2.333
2.667
W(RAD /SEC)
10
9
8
7
6
5
4
3
2
1

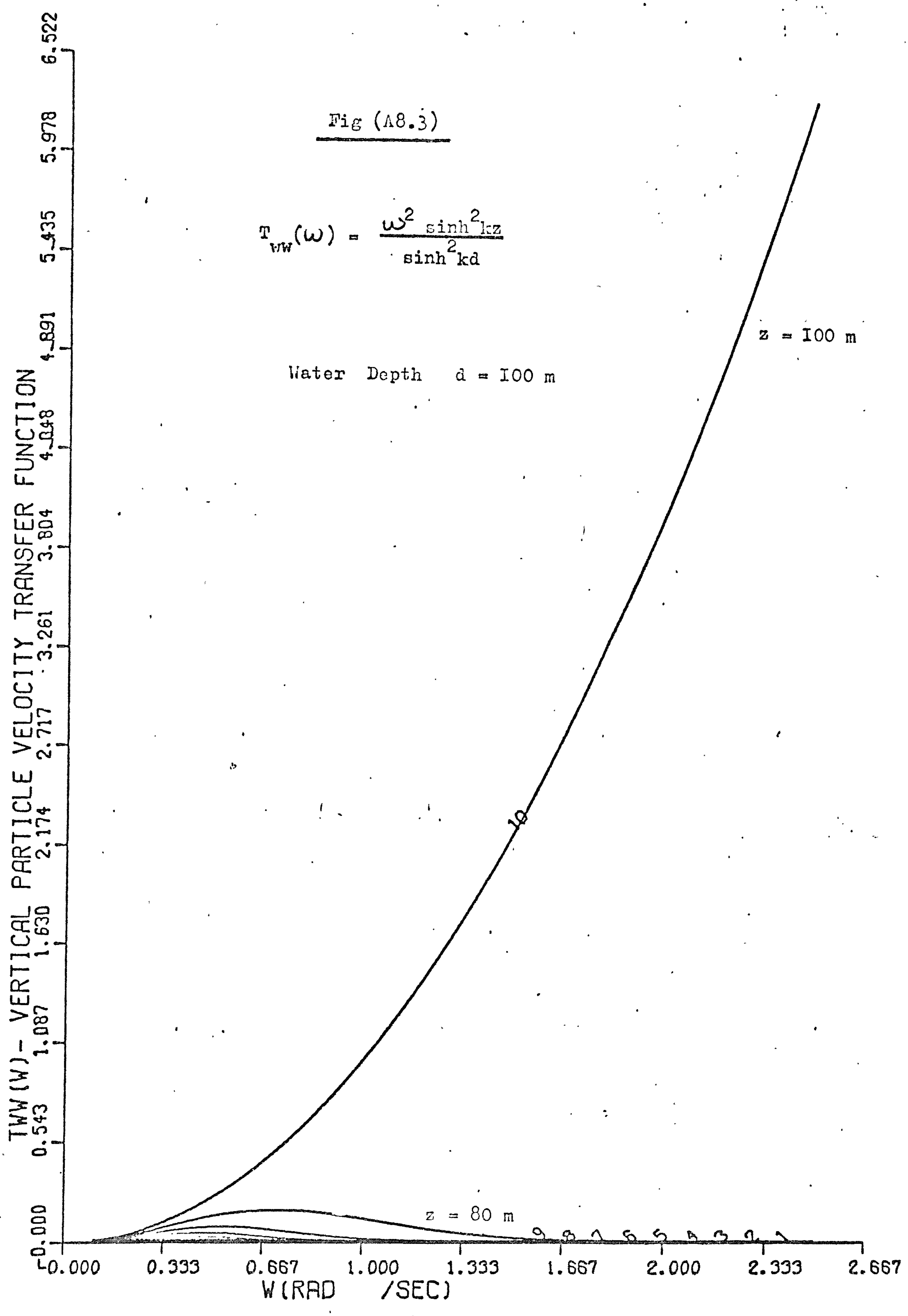

Fig (A8.3)
$T_{ww}(\omega) = \dfrac{\omega^2 \sinh^2 kz}{\sinh^2 kd}$
Water Depth d = 100 m
z = 100 m
z = 80 m
10
9 8 7 6 5 4 3 2 1
TWW(W)- VERTICAL PARTICLE VELOCITY TRANSFER FUNCTION
0.000
0.543
1.087
1.630
2.174
2.717
3.261
3.804
4.348
4.891
5.435
5.978
6.522
0.000
0.333
0.667
1.000
1.333
1.667
2.000
2.333
2.667
W(RAD /SEC)

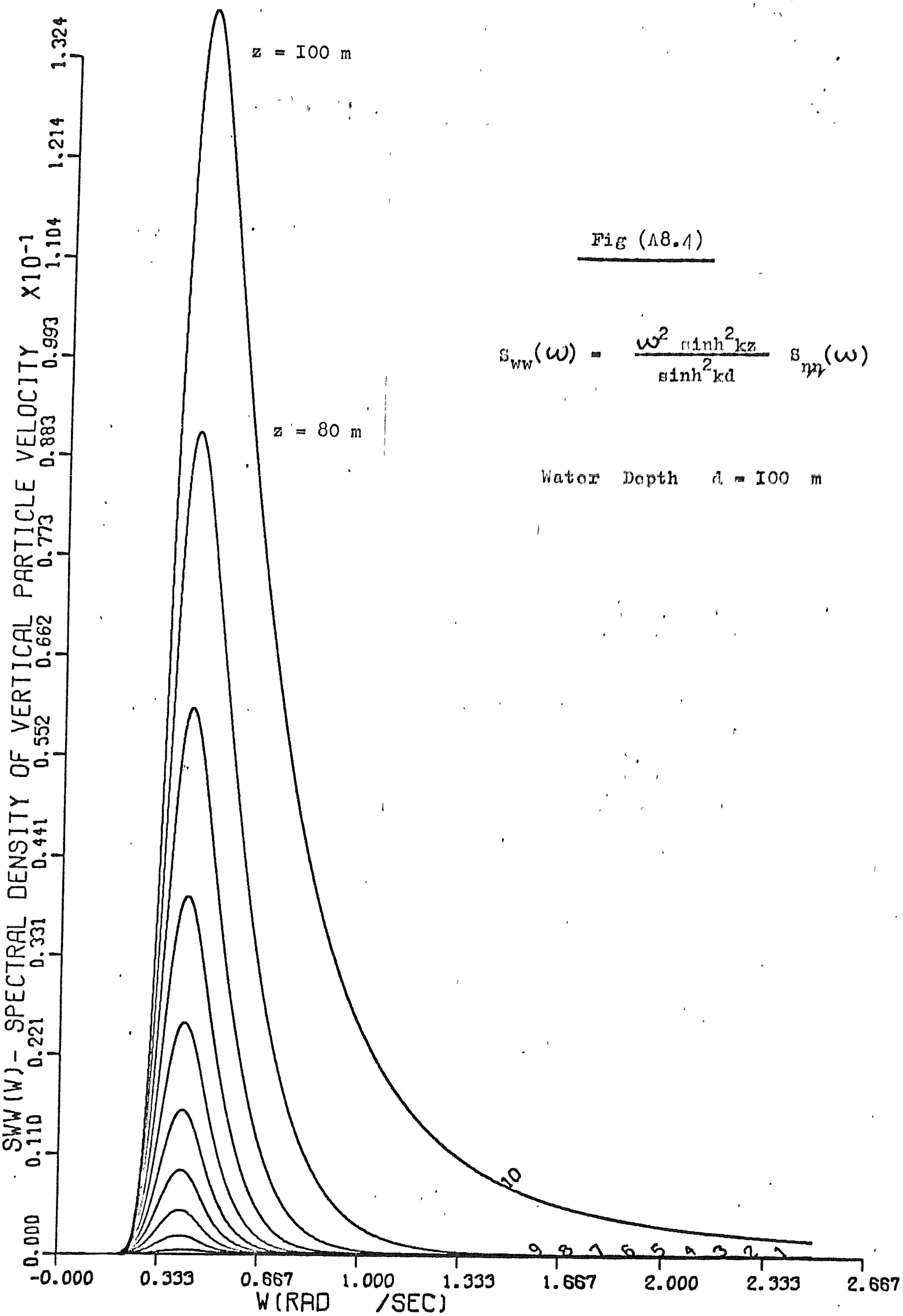

Fig (A8.4)

$$S_{ww}(\omega) = \frac{\omega^2 \sinh^2 kz}{\sinh^2 kd} S_{\eta\eta}(\omega)$$

Water Depth d = 100 m

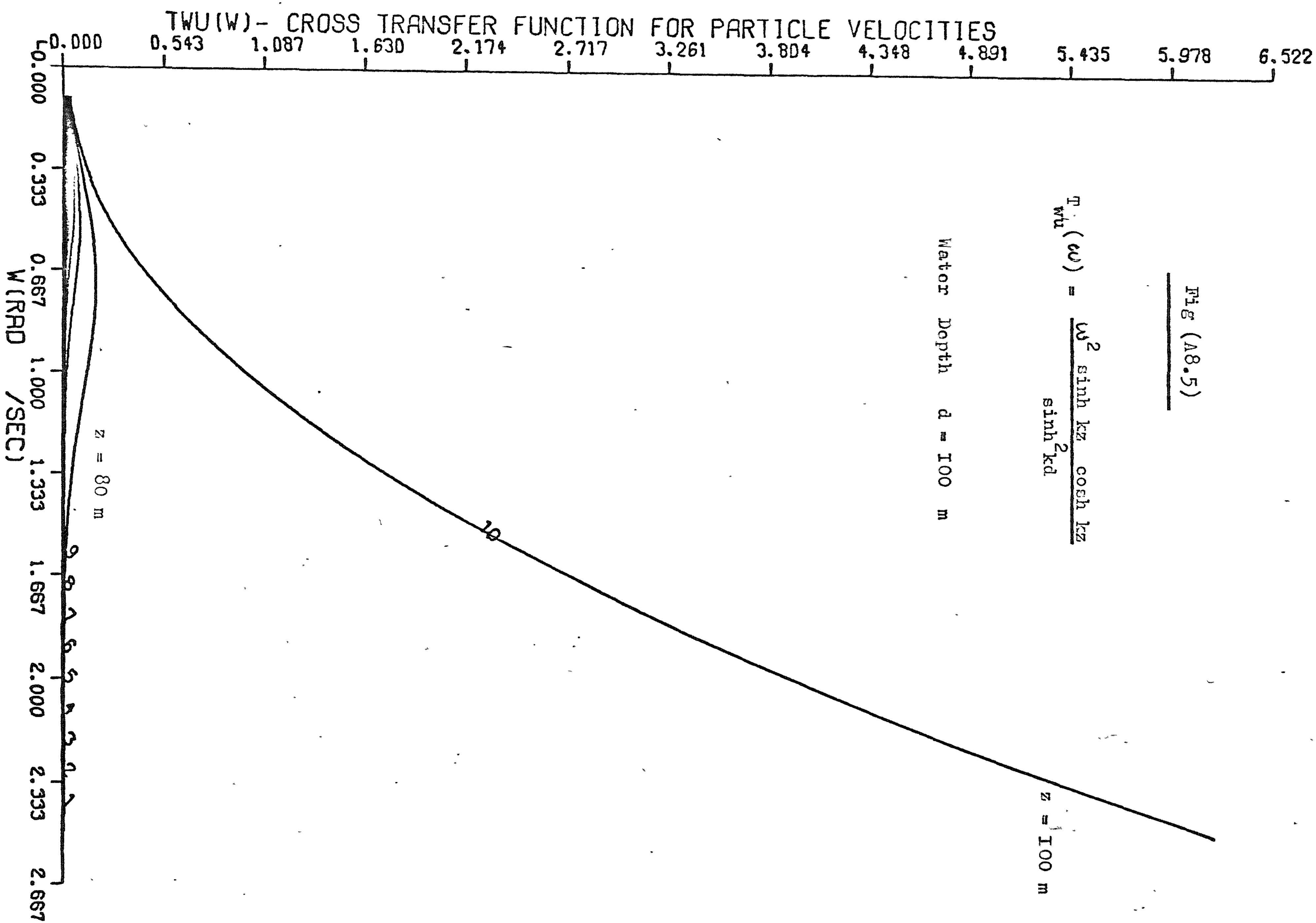
TWU(W)- CROSS TRANSFER FUNCTION FOR PARTICLE VELOCITIES
0.000
0.543
1.087
1.630
2.174
2.717
3.261
3.804
4.348
4.891
5.435
5.978
6.522
0.000
0.333
0.667
1.000
1.333
1.667
2.000
2.333
2.667
W(RAD /SEC)
z = 80 m
10
9
8
7
6
5
4
3
2
1
z = 100 m
Water Depth d = 100 m
$T_{wu}(\omega) = \frac{\omega^2 \sinh kz \cosh kz}{\sinh^2 kd}$
Fig (A8.5)

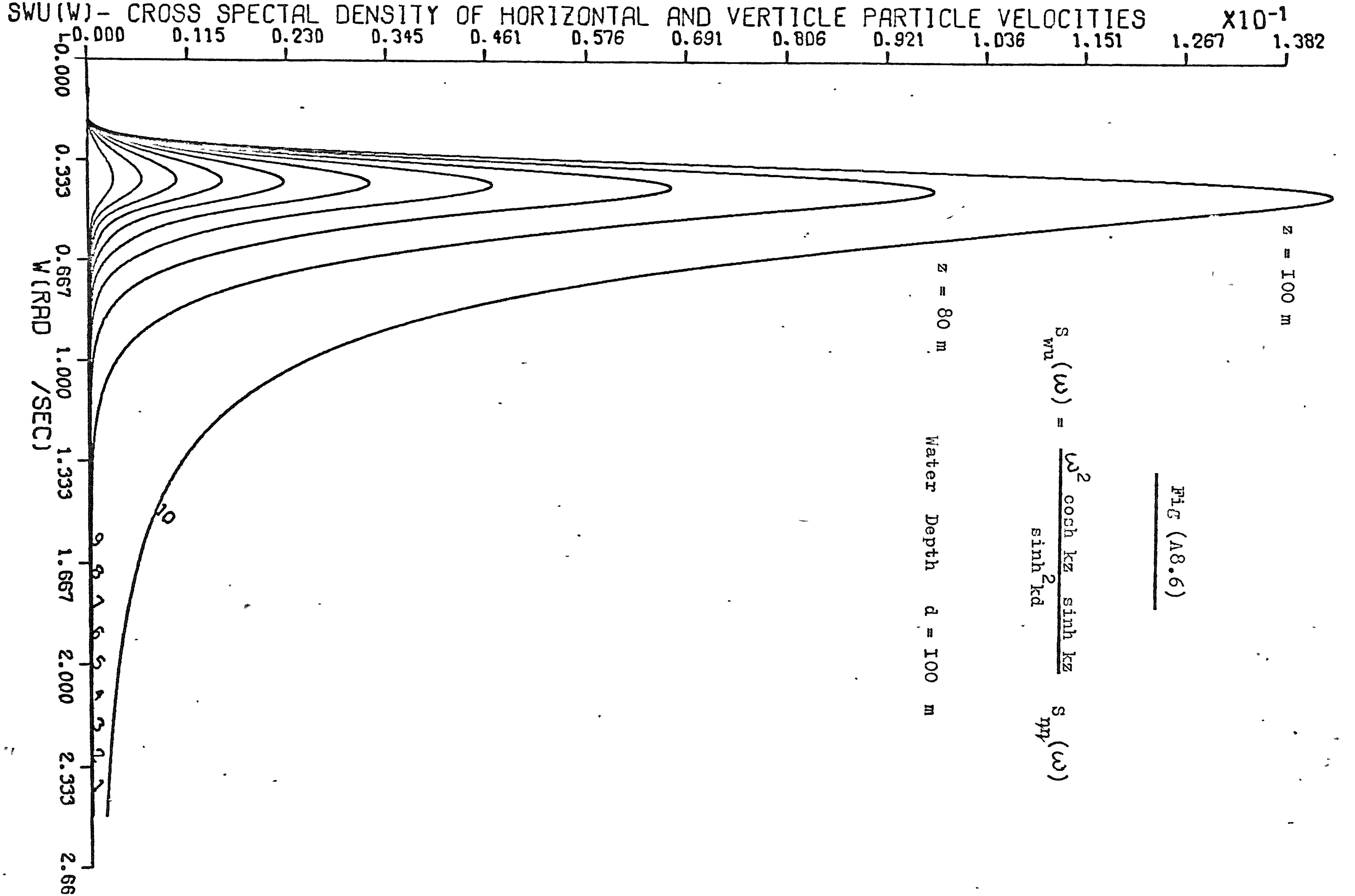
SWU(W)- CROSS SPECTAL DENSITY OF HORIZONTAL AND VERTICLE PARTICLE VELOCITIES X10^{-1}
0.000
0.115
0.230
0.345
0.461
0.576
0.691
0.806
0.921
1.036
1.151
1.267
1.382
0.000
0.333
0.667
1.000
1.333
1.667
2.000
2.333
2.66
W(RAD /SEC)
1
2
3
4
5
6
7
8
9
10
z = 80 m
z = 100 m
$S_{wu}(\omega) = \dfrac{\omega^2 \cosh kz \sinh kz}{\sinh^2 kd} S_{\eta\eta}(\omega)$
Water Depth d = 100 m

Fig (A8.6)

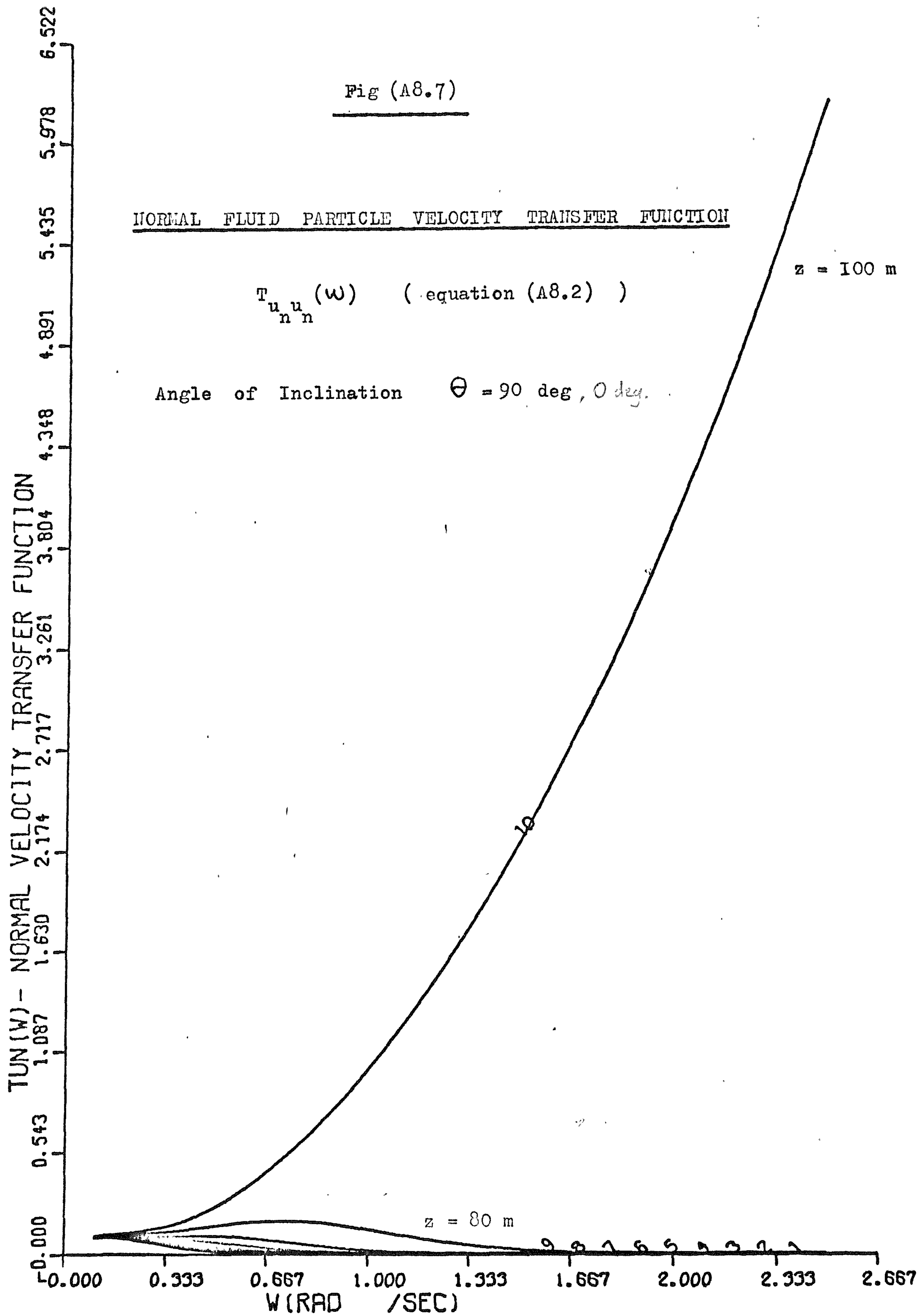
Fig (A8.7)
NORMAL FLUID PARTICLE VELOCITY TRANSFER FUNCTION
$T_{u_n u_n}(\omega)$ (equation (A8.2))
Angle of Inclination Θ = 90 deg , 0 deg.
z = 100 m
z = 80 m
10
9 8 7 6 5 4 3 2 1
TUN(W)- NORMAL VELOCITY TRANSFER FUNCTION
W(RAD /SEC)
-0.000
0.543
1.087
1.630
2.174
2.717
3.261
3.804
4.348
4.891
5.435
5.978
6.522
0.000
0.333
0.667
1.000
1.333
1.667
2.000
2.333
2.667

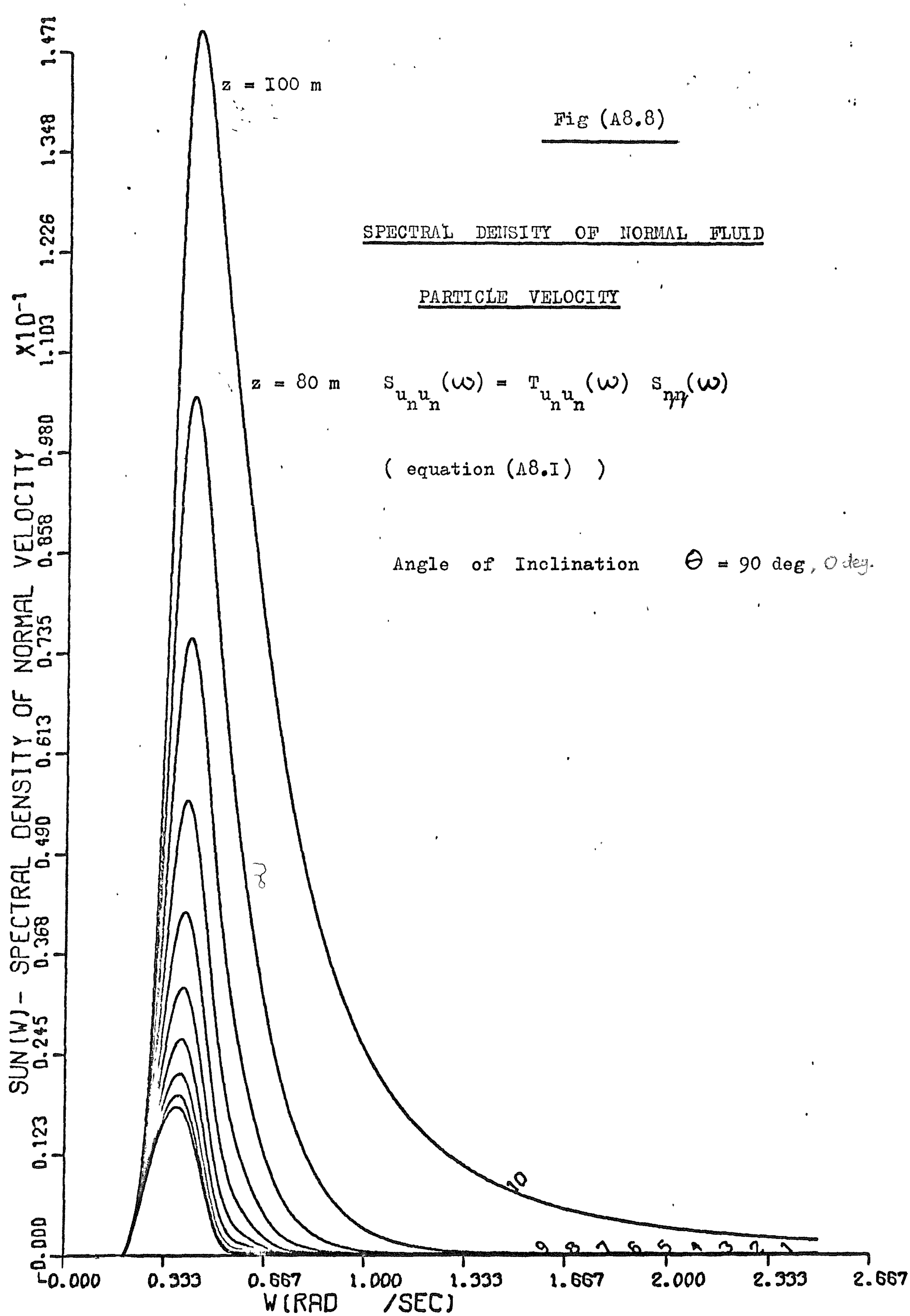
z = 100 m
Fig (A8.8)
SPECTRAL DENSITY OF NORMAL FLUID
PARTICLE VELOCITY
z = 80 m
$S_{u_n u_n}(\omega) = T_{u_n u_n}(\omega)\ S_{\eta\eta}(\omega)$
(equation (A8.1))
Angle of Inclination θ = 90 deg, 0 deg.
SUN(W) - SPECTRAL DENSITY OF NORMAL VELOCITY X10-1
W(RAD /SEC)
0.000
0.123
0.245
0.368
0.490
0.613
0.735
0.858
0.980
1.103
1.226
1.348
1.471
0.000
0.333
0.667
1.000
1.333
1.667
2.000
2.333
2.667
10
9 8 7 6 5 4 3 2 1

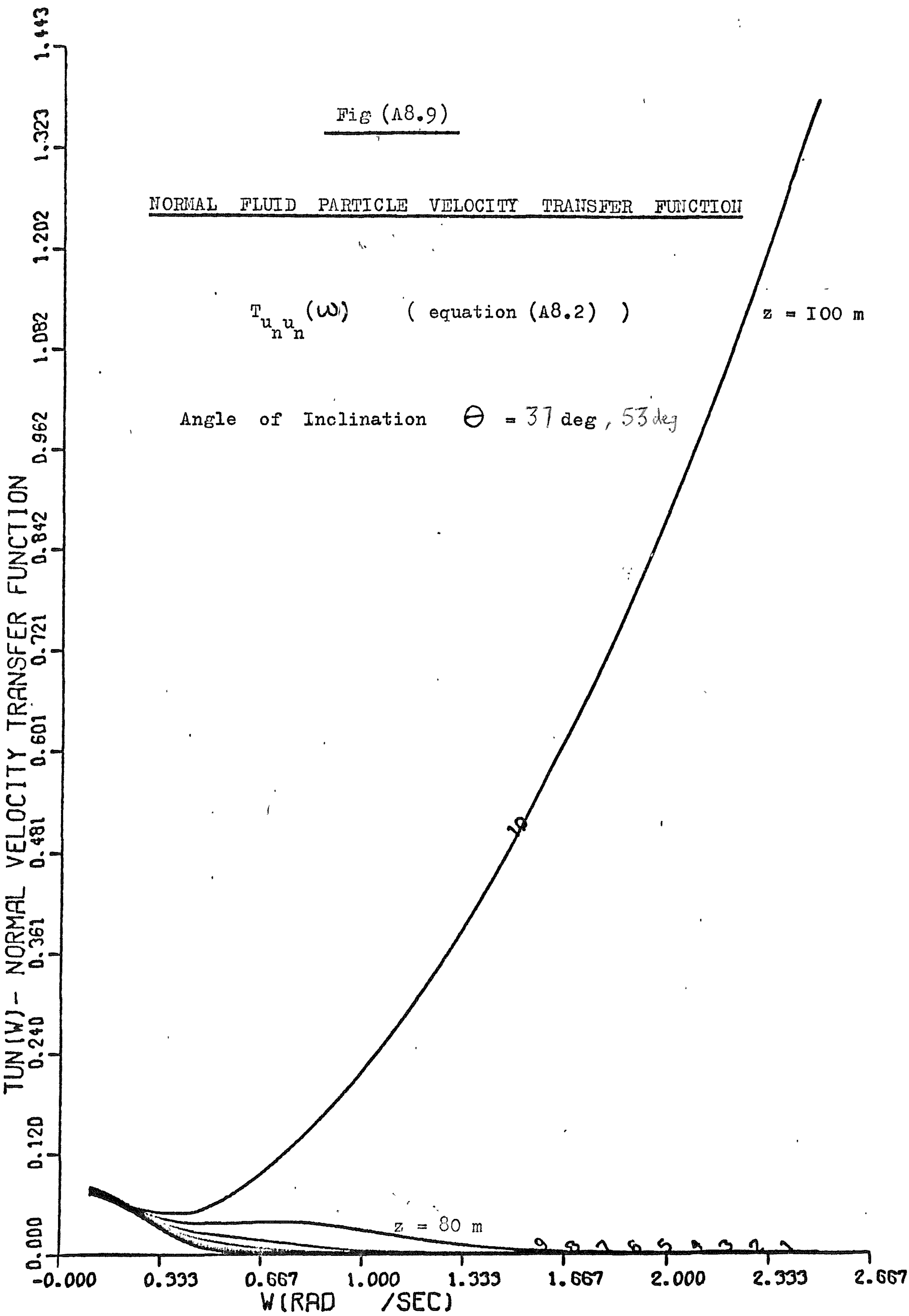

Fig (A8.9)
NORMAL FLUID PARTICLE VELOCITY TRANSFER FUNCTION
$T_{u_n u_n}(\omega)$ (equation (A8.2))
Angle of Inclination Θ = 37 deg , 53 deg
z = 100 m
z = 80 m
10
9 8 7 6 5 4 3 2 1
TUN(W) - NORMAL VELOCITY TRANSFER FUNCTION
0.000
0.120
0.240
0.361
0.481
0.601
0.721
0.842
0.962
1.082
1.202
1.323
1.443
-0.000
0.333
0.667
1.000
1.333
1.667
2.000
2.333
2.667
W(RAD /SEC)

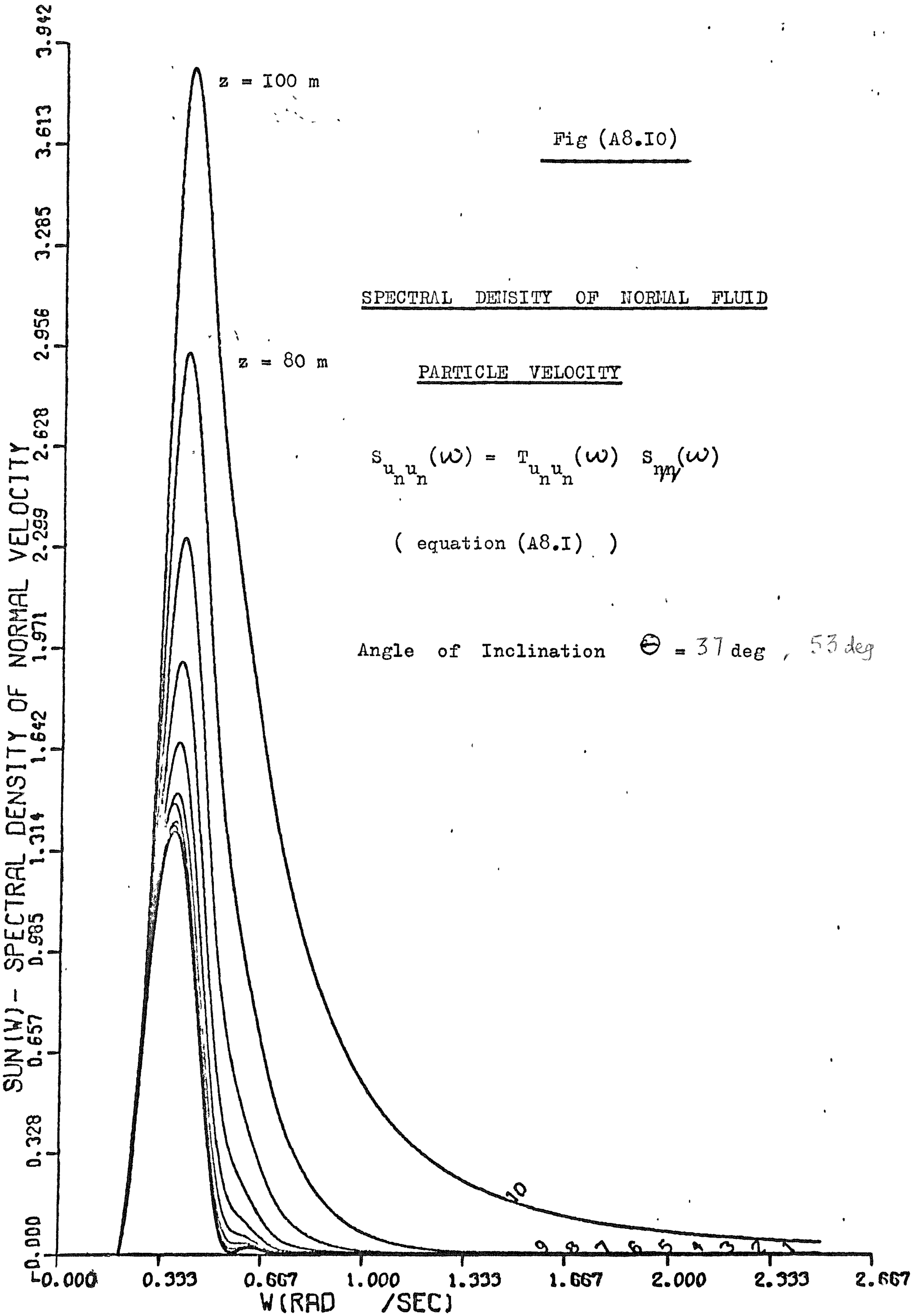

z = I00 m
z = 80 m
Fig (A8.IO)
SPECTRAL DENSITY OF NORMAL FLUID
PARTICLE VELOCITY
$S_{u_n u_n}(\omega) = T_{u_n u_n}(\omega)\ S_{\eta\eta}(\omega)$
(equation (A8.I))
Angle of Inclination Θ = 37 deg , 53 deg
SUN(W) - SPECTRAL DENSITY OF NORMAL VELOCITY
0.000
0.328
0.657
0.985
1.314
1.642
1.971
2.299
2.628
2.956
3.285
3.613
3.942
0.000
0.333
0.667
1.000
1.333
1.667
2.000
2.333
2.667
W(RAD /SEC)
10
9 8 7 6 5 4 3 2 1

Fig (A8.11)

NORMAL FLUID PARTICLE VELOCITY TRANSFER FUNCTION

$T_{u_n u_n}(\omega)$ (equation (A8.2))

Angle of Inclination Θ = 23 deg, 67 deg

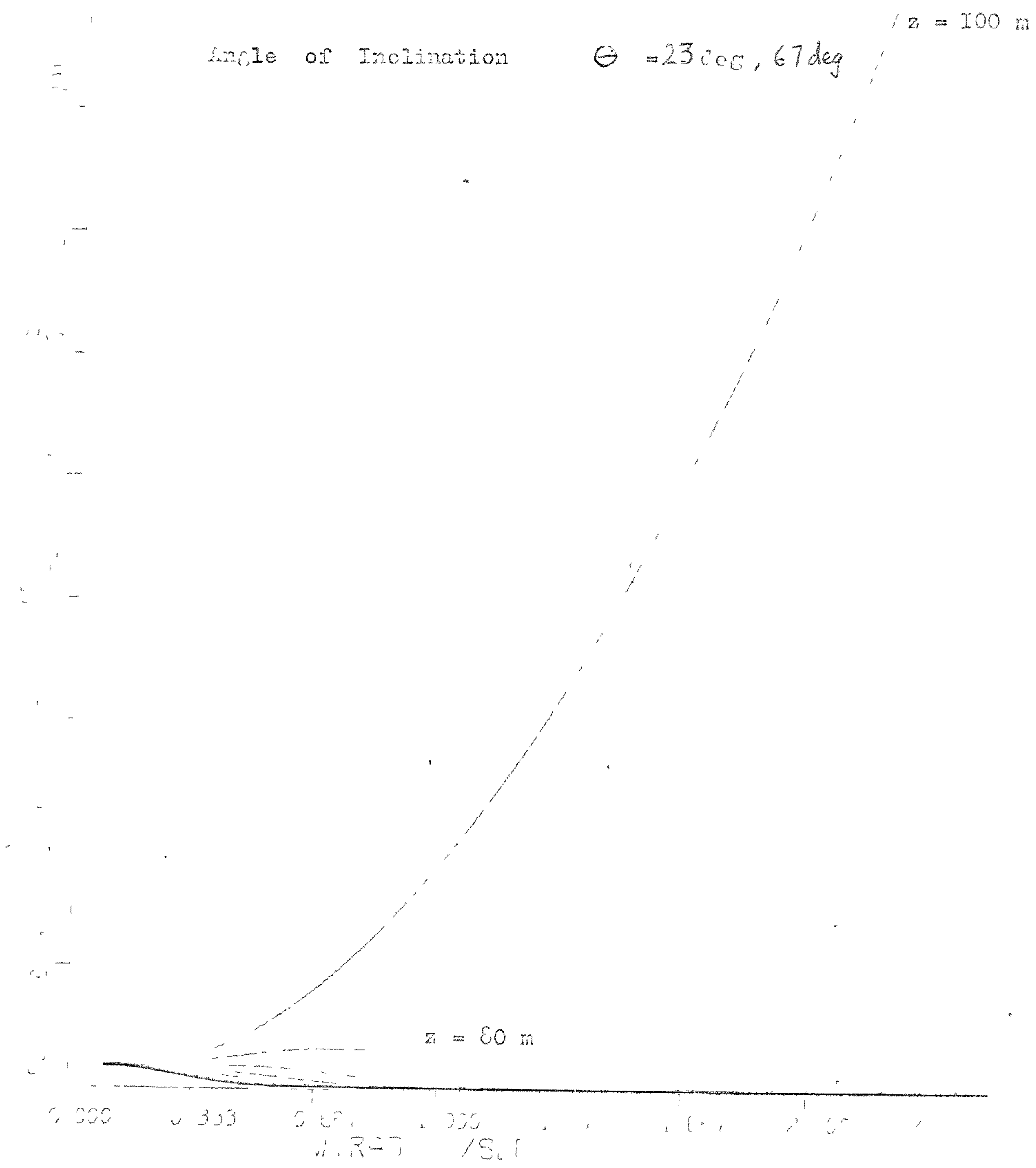

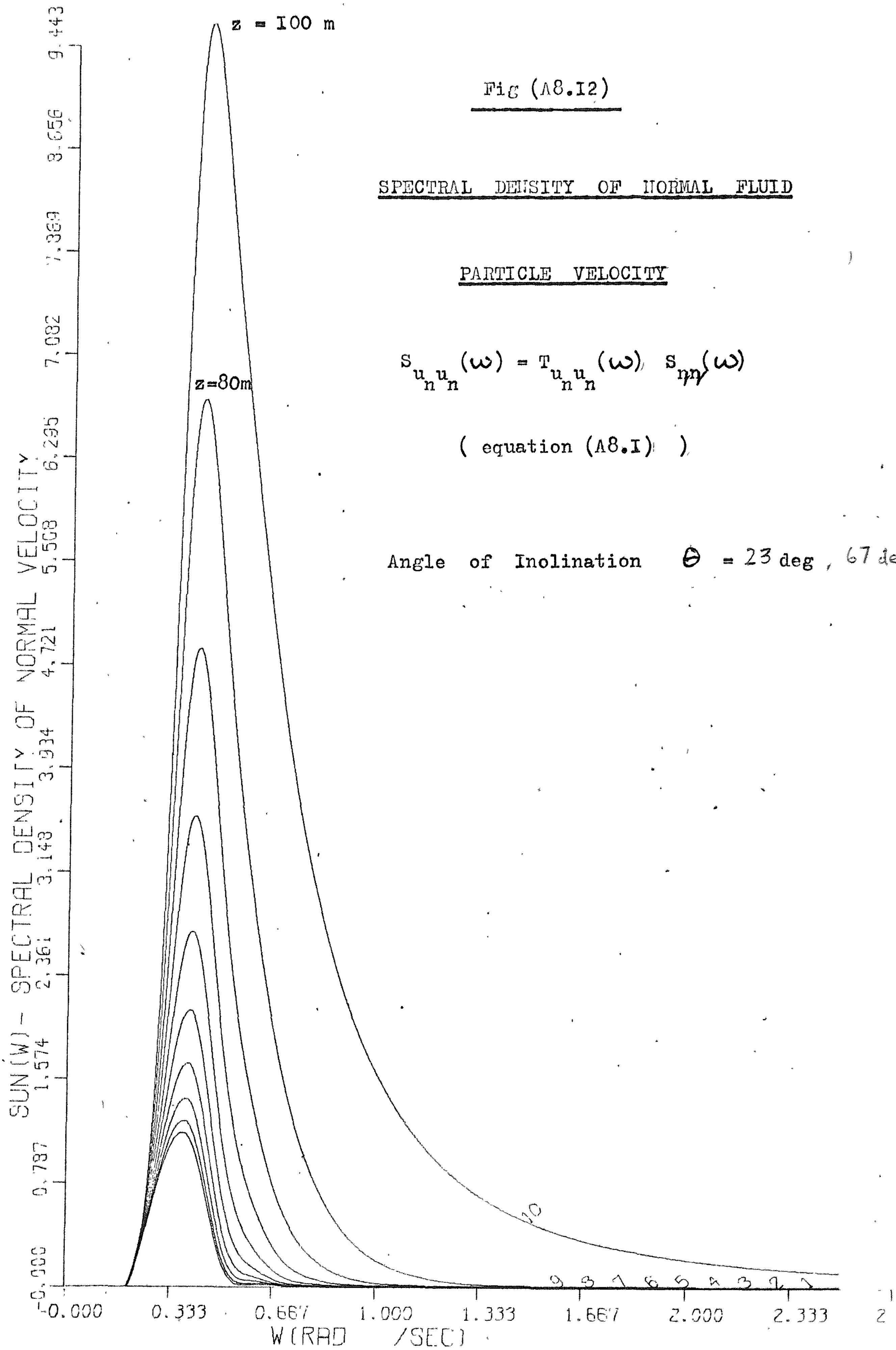

Fig (A8.12)

SPECTRAL DENSITY OF NORMAL FLUID

PARTICLE VELOCITY

$$S_{u_n u_n}(\omega) = T_{u_n u_n}(\omega) \; S_{\eta\eta}(\omega)$$

(equation (A8.1))

Angle of Inclination θ = 23 deg , 67 deg.

APPENDIX 9 : COMPUTER LISTING (PROGRAMME SPECTA3) AND RESULTS

(i) Listing , programme SPECTA3 (section 4.5.5)

(ii) Results from SPECTA3 for I2 m diameter single-leg platform (section 5.4.I)

(iii) Results from SPECTAI (section 4.5.3) for I2 m diameter single-leg platform (section 5.4.I)

(iv) Results from SPECTA3 for the 4-leg ANDOC concrete platform (section 5.4.3)

(a) including the drag force

(b) excluding the drag force

(v) Results from SPECTA3 for the Halcrow-Ewbank steel-framed jacket (section 5.4.3)

(a) including drag

(b) excluding drag

```
   LIST(LP)
  PROGRAM(SPECTA3)
  INPUT 5=CR
  OUTPUT 6=LP
  END



  MASTER SPECTRA

C      RANDOM RESPONSE ANALYSIS OF PLANE FRAMES TO WAVE LOADING, SPECTA3

C      REAL                    KG(NEQ,IBAND),MG(IEQ,IBAND),KE(6,6),ME(6,6)
C      DIMENSION        CG(NEQ,IBAND),CE(6,6),D(NEQ),ES(NEQ),G(NEQ),E2(NEQ),
C     *X(NNP),Y(NNP),CON(NEL,2),E(NEL),ELI(NEL),A(NEL),ELM(NEL),
C     *AM(NEL),R(NEQ),V(NEQ,NEQ),SV(NNP),CD(NEL),CI(NEL),
C     *  INOD(NNP,NEL),IREAC(IREAC,2),QTM(NEQ)
C     *  ,SXL(NEQ,3),TT(NEQ),UU(NEQ),VV(NEQ),WW(NEQ),SN(NEL),CN(NEL),
C     *   ,RL(NEL),H(6),DL(NEL),DIS(NEQP)

       REAL   KE(6,6),ME(6,6)
       REAL   ST(84,15),MG(84,15)
       DIMENSION   CG(84,15),CE(6,6),D(84),ES(84),G(84),E2(84),X(28),
      *    Y(28),CON(66, 2),E(66),ELI(66),A(66),ELM(66),IREAC(12,2),
      *   AM(66),R(84),R(84),V(84,84),SV(28),CD(66),CI(66),INOD(28,66),
      *    QTM(84),SPEC(84,84),SXL(84,3),TT(84),UU(84),VV(84),WW(84),
      *    SN(66),CN(66),RL(66),H(6),DL(66)
      *   ,STR(6),SS(6),SIGMA1(3),SIGMA2(3),DIS(84)
       DATA NNPP,NELP,IREACP,IBANDP  / 28,66,12,15   /

    FORMAT (I10,I10,10X,F14.4,13X,E14.4  )
  102 FORMAT (I10 )
  124 FORMAT (/////25,10H MEMBER NO  ,10X,14H INERTIA COEFF  ,10X,17H TO
     *TAL DRAG COEFF        /    )
  126 FORMAT (///// ,X,41H HIGHEST VALUE OF FREQUENCY CONSIDERED =  ,
```

```
   *    F8.3,10H(SQ/SEC),F3.3,5HCPS  //  )
161 FORMAT (///// 5X,35H NUMBER OF SIGNIFICANT FREQUENCIES= ,I3// )
153 FORMAT (//5X,41H MODAL STIFFNESS AND DAMPING COEFFICIENTS   //
   *    5H MODE,20X,1HK,20X,1HC  /  )
156 FORMAT (5X,I3,3(7X,E14.4 ))
175 FORMAT (/5X, 33H TOTAL DAMPING COEFFICIENT IN MODE ,I3,1H=,E14.4/)
184 FORMAT (/5X,4HMODE,I3,5X,5HGAMMA,F9.4 )
207 FORMAT ( /// 5X, 7H E2(J)=  ,E10.3,7H FOR J= ,I4  /  )
220 FORMAT ( //// 5X,90(1H*) / 1H0,5X,14(1H*),7X,50H STANDARD DEVIATIO
   *NS OF DISPLACEMENT RESPONSES (M)    ,6X,13(1H*) / 1H0,5X,90(1H*) )
226 FORMAT ( /// 24X,7HNODE NO ,24X,9HDIRECTION / 44X,1HX,13X,1HY,12X,
   *    3HROT   /   )
227 FORMAT ( 30X,I3,5X,3E14.4 )
251 FORMAT (  ////5X,11H ELEMENT NO)                   ,25X,5HEND 1,34X,
   *   5HEND 2  / 24X,5HHORIZ,9X,5HVERT ,8X,6HMOMENT,11X,5HHORIZ,9X,
   *   5HVERT ,8X,6HMOMENT  / 27X,3H(N),11X,3H(N),10X,4H(NM),13X,3H(N),
   *    11X,3H(N),10X,4H(NM) // )
234 FORMAT (5X, I7,2X,3E14.4,2X,3E14.4  )
245 FORMAT ( /// 5X,42H MAXIMUM DISPLACEMENT STANDARD DEVIATION =    ,
   *     E14.4,2H M   //
   *5X,42H PROB. IS 66.3 PC THAT DISPL. IS LESS THAN    ,E14.4,2H M //
   *5X,42H PROB. IS 95.4 PC THAT DISPL. IS LESS THAN    ,E14.4,2H M //
   *5X,42H PROB. IS 99.7 PC THAT DISPL. IS LESS THAN    ,E14.4,2H M //)
252 FORMAT ( //// 5X,90(1H*) /  1H0,5X,16(1H*),7X,42H STANDARD DEVIATI
   *ONS OF ELEMENT FORCES         , 3X,17(1H*) /  1H0,5X,90(1H*) /// )
250 FORMAT (4(1X),2X,I4  )
256 FORMAT ( //// 5X,90(1H*) / 1H0,5X,22(1H*),7X, 31H EXPECTED EXTREME
   * ELEMENT LOADS    ,3X,22(1H*)  /  1H0,5X,90(1H*) /// )
300 FORMAT (1H1///10X,46H ANALYSIS WITH WAVE SPECTRUM DEFINED BY    A=
   *   ,F8.3,3H B=,F8.4  )
797 FORMAT (///10X,54H ***SUBMERGED PART OF STRUCTURE INCORRECTLY SPE
   *CIFIED  /  )
10  FORMAT ( /// 10X, 25H NUMBER OF NODAL POINTS =    ,I4,
   *    17H = GREATER THAN  ,I4 // )

    READ (5,102 ) ICANAR ,NREAD
    IF (NR?.GT.NE) ) GO TO 999
```

```
      NEQ=NJP*3
      NEQP=NJPP*3
      CALL DATA(   (TOAID,     NJP,X,Y,NEL,NREAC,ICON,E,ELI,A,ELM,AM,
     * IREAC,DEPTH,  ,PH,CAM,CIM,CDRAG,PDAMP,NSP,NNPP,NELP,NREACP,DL )
      DO 2 I=1,NEQ
      DO 2 J=1,NEQ
      KG(I,J)=0.
      MG(I,J)=0.
    2 CG(I,J)=0.
C     CALCULATION OF ADDED MASS/UNIT LENGTH(AM) AND TOTAL DRAG AND
C     INERTIA COEFFICIENTS FOR EACH MEMBER (CD,CI )
      WRITE (6,124 )
      DO 5 I=1,NEL
      CI(I)=CIM*A(I)*1025.
      CD(I)=CDRAG*SQRT(4*AM(I)/3.141593)*512.5
      WRITE (6,  ) (  CI(I),CD(I)
    5 AM(I)=CAM*A(I)*1025.
C     CALCULATION OF STANDARD DEVIATIONS OF HORIZONTAL PARTICLE VELOCITY
C     AT EACH NODE
      CALL SIGVEL(NJP ,Y,SV,DA,PH,DEPTH,NNPP )
C     ASSEMBLY OF MASS,STIFFNESS AND DAMPING MATRICES
C     KE,ME=ELEMENT MASS AND STIFFNESS MATRICES
C     KG,MG =GLOBAL MASS AND STIFFNESS MATRICES
C     CG,CE =HYDRODYNAMIC DAMPING MATRICES
      DO 10  I=1,NEL
      X1=X(ICON(I,1))
      X2=X(ICON(I,2))
      Y1=Y(ICON(I,1))
      Y2=Y(ICON(I,2))
      CALL ELEMNT (X1,X2,Y1,Y2,SV(ICON(I,1)),SV(ICON(I,2)),E(I),A(I),
```

```
     *  ELI(I),EL(I),AM(I),CD(I),KE,ME,CE,I,RL,NELP,CN,SN  )
      CALL ROTATE (KE,X1,X2,Y1,Y2 )
      CALL ROTATE (ME,X1,X2,Y1,Y2 )
      CALL ROTATE (CE,X1,X2,Y1,Y2 )
      DO 10 IM=1,2
      IR1=(ICON(I,IM)-1)*3
      DO 10 IN=1,2
      IC1=(ICON(I,IN)-1)*3
      DO 10 K=1,3
      IR=IR1+K
      DO 10 J=1,3
      IC=IC1+J
      ID=IC-(IR-1)
      IF (ID.LT.1 )  GO TO 10
      IMK=(IM-1)*3+K
      INJ=(IN-1)*3+J
      KG(IR,ID)=KG(IR,ID)+KE(IMK,INJ  )
      MG(IR,ID)=MG(IR,ID)+ME(IMK,INJ  )
      CG(IR,ID)=CG(IR,ID)+CE(IMK,INJ  )
   10 CONTINUE
C   IMPOSITION OF BOUNDARY CONDITIONS AND RENUMBERING OF MATRICES
C   NUM (J)=INTEGRAL NUMBER OF DEGREE OF FREEDOM J

      N=NEQ
      DO 105 I=1,NEQ
  105 NU1 (I)=I
      DO 120 I=1,NREAC
      IR=(IREAC(I,1)-1)*3+IREAC(I,2)
      IRA=IR
      IR1=IR+1
      DO 115 J=IR1,NEQ
      NU1 (J)=NU1 (J)-1
  115 IF(NU1 (J).LT.1 ) NU1 (J)=0
      IR=NU1 (IR)
      NU1 (IRA)=0
      IF(IR.EQ.0 )GO TO 112
```

```
      IR1=IR+1
      DO 110 J=IR1,I
      DO 110 K=1,IBAND
      MG((J-1),K)=MG(J,K)
      CG((J-1),K)=CG(J,K)
  110 KG((J-1),K)=KG(J,K)
  112 N=N-1
      IR1=IR-1
      DO 116 K=1,IR1
      IF (K.GT.(IBAND-1)) GO TO 116
      KP1=K+1
      DO 116 J=KP1,IBAND
      IF (J.EQ.IBAND ) GO TO 115
      KG((IR-K),J)=KG((IR-K),(J+1))
      MG((IR-K),J)=MG((IR-K),(J+1))
      CG((IR-K),J)=CG((IR-K),(J+1))
      GO TO 116
  115 KG((IR-K),J)=0.
      MG((IR-K),J)=0.
      CG((IR-K),J)=0.
  116 CONTINUE
  120 CONTINUE

C     FIND ELEMENTS MEETING AT EACH NODE

      DO 400 IY=1,NND
      DO 400 IW=1,NEL
      INOD(IY,IW)=0
      IF ((ICON(IW,1).EQ.IY).OR.(ICON(IW,2).EQ.IY)) INOD(IY,IW)=1
  400 CONTINUE

C   SOLUTION OF EIGENVALUE PROBLEM
C   EIGENVALUES STORED IN R, EIGENVECTORS IN V

      U0=20*(0.3*D0)**0.25
      U01=U0/3.281
      WRITE (6,125) U0,U01
```

```
      CALL INVERT (S3,SPEC,N,IBAND,NEQP,IBANDP,NEQP )
      CALL EIGEN (SPEC,Q,N,IBAND,N,100,0.00001,D,ES,G,R,V,UB1,NEQP,M1,
     *    NEQP,IBANDP  )
      WRITE (6,151 ) N
      DO 602 J=1,N
      DIS(J)=V(J,1)
  602 CONTINUE
      INDEF=1
  72  CONTINUE

C    CALCULATION OF MODAL STIFFNESS AND DAMPING COEFFICIENTS
C    STIFFNESS COEFFICIENT FOR MODE J STORED IN ES(J)
C    MASS COEFFICIENT FOR MODE J STORED IN G(J)
C    DAMPING COEFFICIENT FOR MODE J STORED IN D(J)


C    NORMALISE MODAL MODES W.R.T. MASS MATRIX,   QT*M*Q=1

      CALL MATPRD (V,WT1,G,M,M1,N,IBAND,NEQP,IBANDP   )
      DO 162 J=1,N
      QG=SQRT(G(J))
      ES(J)=D(J)*G(J)
      DO 162 II=1,N
  162 V(II,J)=V(II,J)/QG
      CALL MATPRD (V,WT1,D,C,M1,N,IBAND,NEQP,IBANDP   )
      WRITE (6,155 )
      DO 161 J=1,N
      WRITE (6,156 )J, ES(J),D(J)
  161 CONTINUE

C    ADD STRUCTURAL DAMPING TO DAMPING COEFFICIENTS

      PDAMP=2*PDAMP/D(1)
      DO 170 J=1,N
      D(J)=D(J)+PDAMP*ES(J)
      WRITE (6,173) J,D(J)
```

```
C     CHANGE D(J) TO PROPORTION OF CRITICAL DAMPING

      D(J)=D(J)*T(J)/(2*ES(J))
  170 WRITE (6,132) J,D(J)

C     CALCULATION OF RESPONSE

      DO 200 J=1,J
      SXL(J,K)=0.
  200 E2(J)=0.
      CALL INPUT(J,P,R(1),N    )
      DO 185 I=1,4
      IF ( R(I).EQ.0. ) GO TO 185
      DO 201 J=1,J
  201 SXL(J,1)=SXL(J,3)
      DO 184 K=1,2
      U=U+ H(I)
      K1=K+1
      CALL [illegible](J,SXL,Y,[illegible],INP,INPP,NUI,TT,UU,VV,WW,ICON,NELP,NEL,
     *    CI,[illegible],CI,RL,[illegible],V,ES,R,DEPTH,PA,PB,K1,SV,I,K,DL )
  184 CONTINUE
      DO 204 J=1,J
  204 E2(J)=E2(J)+H(I)*(SXL(J,1)+4.*SXL(J,2)+SXL(J,3))/3.
  185 CONTINUE
      DO 205 J=1,J
      IF (E2(J)) 206,205,205
  206 WRITE (6,210 ) E2(J),J
  205 D(J)=SQRT(E2(J))

C     WRITE STANDARD DEVIATIONS OF DISPLACEMENT RESPONSES

      WRITE (6,220)
      WRITE (6,230)
      F=0.
      DO 230 J=1,J
      DO 225 K=1,
```

```
      ID=N (( -1)*2+IR)
      KE(IR,1)=0.
      IF (ID.EQ.0 ) GO TO 225
      KE(IR,1)=D(ID)
 225  CONTINUE
      WRITE (6,247) I,(KE(I,1),I=1,3)
      IF (KE(1,1)-F ) 230,230,211
 211  F=KE(1,1)
 230  CONTINUE
      S2=2.*F
      S3=3.*F
      WRITE (6,245 ) F,   F,S2,S3

C     CALCULATE AND PRINT STANDARD DEVIATIONS OF STRESS RESULTANTS

      WRITE (6,232)
      WRITE (6,235 )
      DO 600 J=1,N
 600  DIS(J)=DIS(J)*F
      DO 300 I=1,NEL
      N1=ICON(I,1)
      N2=ICON(I,2)
      X1=X(N1)
      X2=X(N2)
      Y1=Y(N1)
      Y2=Y(N2)
      DO 241 J=1,3
      SD(J)=0.
      SD(J+3)=0.
      M1=NUM((N1-1)*3+J)
      M2=NUM((N2-1)*3+J)
      IF (M1.EQ.0 ) GO TO 241
      SD(J)=DIS(M1)
 241  IF (M2.EQ.0 ) GO TO 240
      SD(J+3)=DIS(M2)
 240  CONTINUE
      CALL KL  (X1,X2,Y1,Y2,E(I),A(I),ELI(I),KE  )
```

```
      CALL ROTATE (SC,X1,X2,Y1,Y2 )
      CALL MULT ( KE,SD,STR,6,6,1 )
      DO 351 J=1,6
      KG(I,J)=STR(J)*1.414
 351  STR(J)=ABS(STR(J))
      WRITE (6,234 )  I, (STR(J),J=1,6 )
 350  CONTINUE
      WRITE (6,232)
      WRITE (6,233)
      DO 353 I=1,NEL
 353  WRITE (6,234 )   I,(KG(I,J),J=1,6   )
      IF (NSP.EQ.1 ) GO TO 37
      READ (5,300) PA,PB,TWIFE
      WRITE (6,35 ) PA,PB
      NSP=NSP-1
      PDAMP=PA+R(1)/2.
      GO TO 320
 15   WRITE (6,222 )
      STOP
 12   WRITE (6,22 ) NNP,NNPP
 37   CONTINUE
      STOP
      END



      SUBROUTINE DATAIN   (IBAND,     NNP,X,Y,NEL,NREAC,ICON,E,ELI,A,ELM,
     *  NREAC,IREAC,KP,PA,PB,CAM,CIN,CDRAG,PDAMP,NSP,NNPP,NELP,NREACP,DL )

      DIMENSION DASH (120),NAME(20)
      DIMENSION X(NNPP),Y(NNPP),ICON(NELP,2),E(NELP),ELI(NELP),A(NELP),
     *   ELM(NELP),AM(NELP),IREAC(NREACP,2),DL(NELP)
      DATA DASH / 120*1H- /

 100  FORMAT (20A4 )
```

```
101 FORMAT (////5X,      20A4 //// )
102 FORMAT ( 9X,50H NUMBER OF ELEMENTS - - - - -     ,I4 //
   *           9X,50H NUMBER OF NODAL POINTS - - -    ,I4  //
   *           9X,50H NUMBER OF REACTIONS - - - - -   ,I4  /// )
103 FORMAT (/9X,93(1H*)  )
104 FORMAT ( / 6X,72(1H*),10X,66HRANDOM RESPONSE ANALYSIS OF PLANE FRAM
   *ES TO WAVE LOADING, SPECTA3  ,9X,6(1H*)  )
```

```
100 FORMAT (/////5X,24H NODAL POINT COORDINATES     )
101 FORMAT (///15X,5X/10HNODE POINT ,4X,10HX-COORD(M),5X,
   *   10HY-COORD(M)  /  )
113 FORMAT (I10,2F10.3  )
117 FORMAT (5X,I5,5X,F8.4,7X,F8.4   )
120 FORMAT (/////5X,38H STRUCTURE CONNECTIVITY AND PROPERTIES     )
121 FORMAT (/// 5X,9HMEMBER NO ,1X,13HEND 1    END 2  ,4X,7HE(N/M2),7X,
   *    5HI(M4),8X,7HAREA(M),7X,8HMASS(KG),2X,17HVOL DISPL(CU.M/M),
   *    1X,5HSTELT,  /  102X,5H FACT  )
122 FORMAT (3I10,F12.5,F8.2,3F10.5  )
125 FORMAT ( 5X,I5,I8 ,I8,5E14.4,E11.3  )
135 FORMAT(/////5X,24H DETAILS OF FIXED POINTS    )
136 FORMAT (///,7X,23HNODE NO  DIRECTION OF FIXITY  /  )
137 FORMAT (3F10.5 )
138 FORMAT (2I10 )
139 FORMAT (4I5,2I12 )
145 FORMAT (////21X,34HMAXIMUM JOINT NUMBERING DIFFERENCE ,4A1,I4 )
147 FORMAT (/21X,16HMEAN WATER DEPTH(M),19A1,F6.1   )
148 FORMAT (/21X,23HPARAMETER A OF WAVE SPECTRUM ,10A1,F8.3   )
149 FORMAT (/21X,23HPARAMETER B OF WAVE SPECTRUM ,10A1,F9.4   )
150 FORMAT (/21X,23HCOEFFICIENT OF ADDED MASS ,13A1,F7.2 )
151 FORMAT (/21X,22HCOEFFICIENT OF INERTIA  ,16A1,F7.2   )
152 FORMAT (/21X,19HCOEFFICIENT OF DRAG ,19A1,F7.2 )
155 FORMAT (/21X,33HSTRUCTURAL CRITICAL DAMPING RATIO ,5A1,F8.3   )
159 FORMAT (I10 )
161 FORMAT (/21X,33HSEMI-BANDWIDTH OF STIFFNESS MATRIX,ETC    ,I4    )

      WRITE (5,113 )
      WRITE (5,114 )
      WRITE (5,113 )
      READ(1,101 ) NAME
      WRITE (5,111 ) NAME
      WRITE (5,112 ) NEL,NNP,NREAC
      WRITE (5,115 )
      WRITE (5,116 )
      DO 120 I=1,NNP
      READ (1,110 ) II,X(II),Y(II)
```

```
120 WRITE (6,112 ) N,X(N),Y(N)
    WRITE (6,125 )
    WRITE (6,126 )
    MAXD=0
    DO 130 I=1,NEL
    READ (5,121 ) N,ICON(N,1),ICON(N,2),E(N),ELI(N),A(N),ELM(N),AM(N)
    READ (5,137 ) DL(N)
    MD=IABS(ICON(N,2)-ICON(N,1))
    IF (MD.GT.MAXD) MAXD=MD
130 WRITE (6,139 ) N,ICON(N,1),ICON(N,2),E(N),ELI(N),A(N),ELM(N),AM(N)
   *    ,DL(N)
    IBAND=2*(MAXD+1 )
    WRITE (6,135 )
    WRITE (6,136 )
    DO 140 I=1,IREAC
    READ(5,133 ) IREAC(I,1),IREAC(I,2)
140 WRITE (6,139 ) IREAC(I,1),IREAC(I,2)
    READ (5,132 )D,PA,PB
    READ (5,137 ) CAM,CII,CDRAG
    READ (5,132 ) PDAMP
    WRITE (6,145 ) (DASH(I),I=1,4 ),MAXD
    WRITE (6,141) IBAND
    WRITE (6,147 ) (DASH(I),I=1,19 ),D
    WRITE (6,148 ) (DASH(I),I=1,10 ),PA
    WRITE (6,149 ) (DASH(I),I=1,10),PB
    WRITE (6,150 ) (DASH(I),I=1,13 ),CAM
    WRITE (6,151 ) (DASH(I),I=1,16),CII
    WRITE (6,152 ) (DASH(I),I=1,19),CDRAG
    WRITE (6,153 ) (DASH(I),I=1,5 ),PDAMP
    READ (5,155 ) ISP
    RETURN
    END
```

```
      SUBROUTINE ELEMNT (X1,X2,Y1,Y2,S1,S2,E,A,I,M,AM,C,KE,ME,CE,LZ,RL,
     *   NELP,CN,SN )

C     COMPUTATION OF ELEMENT MATRICES

      DIMENSION CE(6,6),RL(NELP),CN(NELP),SN(NELP)
      REAL KE(6,6),ME(6,6),I,M,L
      DO 10 J=1,6
      DO 10 K=1,6
      CE(J,K)=0.
   10 ME(J,K)=0.
      L=SQRT((X2-X1)*(X2-X1)+(Y2-Y1)*(Y2-Y1))
      RL(LZ)=L
      CN(LZ)=(X2-X1)/L
      SN(LZ)=(Y2-Y1)/L
      L3=L*L*L
      ME(1,1)=M*L/3.
      ME(1,4)=M*L/6.
      ME(2,2)=13.*(M+AM)*L/35.+6.*M*I/(5.*A*L)
      ME(3,2)=11.*(M+AM)*L*L/210.+M*I/(10.*A)
      ME(5,2)=9.*(M+AM)*L/70.-6.*M*I/(5.*A*L )
      ME(6,2)=-13.*(M+AM)*L*L/420.+M*I/(10.*A)
      ME(3,3)=(M+AM)*L3   /105.+2.*M*I*L/(15.*A)
      ME(5,3)=-ME(6,2)
      ME(6,3)=-(M+AM)*L3   /140.-M*I*L/(30.*A)
      ME(4,4)=ME(1,1)
      ME(5,5)=ME(2,2)
      ME(6,5)=-ME(3,2)
      ME(6,6)=ME(3,3)
      C=1.5/1.707*C
      CL=C*L
      CLL=CL*L
      CLLL=CLL*L
      CE(2,2)= CL*(10*S1+3*S2)/35
      CE(3,2)=    CLL*(15*S1+7*S2)/420.
      CE(5,2)=9.*CL*(S1+S2)/140.
      CE(6,2)=-   CLL*(7*S1+6*S2)/420.
```

```
      CE([illegible])=  CLLL*(3*S1+3*S2)/840.
      CE(3,[illegible])=  CLL*([illegible]*S1+7*S2)/420.
      CE([illegible])=-  CL*L*(S1+S2)/43).
      CE([illegible])= CL*([illegible]*S1+1[illegible]*S2)/33.
      CE([illegible])=-  CLL*(7*S1+15*S2)/42).
      CE(6,[illegible])=  CLLL*(3*S1+5*S2)/840.
      C=[illegible]/1,[illegible]
      DO 20 I=2,[illegible]
      J 1=J-1
      DO 20 [illegible]=1,J 1
      CE(J,[illegible])=CE([illegible],I)
[illegible] ME(J,[illegible])=[illegible]([illegible],J)
      ENTRY CLK ([illegible],[illegible]2,Y1,Y2,E,A,I,KE   )
      DO 3[illegible] J=1,[illegible]
      DO 3[illegible] [illegible]=1,[illegible]
3[illegible] KE(J,[illegible])=[illegible].
      L=SQRT((X[illegible]-[illegible])*(X2-X1)+(Y2-Y1)*(Y2-Y1))
      KE(1,1)=E*[illegible]/L
      KE(1,[illegible])=-K[illegible](1,1)
      KE(2,[illegible])=1[illegible].*E*I/(L*L*L)
      KE(2,[illegible])=[illegible].*E*I/(L*L)
      KE(2,[illegible])=-KE(2,2)
      KE(2,[illegible])=KE(2,3)
      KE(3,[illegible])=4.*E*I/L
      KE([illegible])=-KE(2,3)
      KE(3,[illegible])=KE([illegible],3)/2.
      KE(4,[illegible])=KE(1,1)
      KE([illegible])=KE([illegible],2)
      KE([illegible])=KE([illegible])
      KE(6,[illegible])=KE([illegible],3)
      DO [illegible] I=2,[illegible]
      J 1=J-1
      DO [illegible] [illegible]=1,I1
[illegible] KE(J,[illegible])=KE(K,J)
      RETURN
      END
```

```
      SUBROUTINE SPECT (O,SXL,Y,NEQP,D,NNP,NNPP,NUM,TT,UU,VV,WW,ICON,
     *   NELP,NEL,CI,CD,INOD,SN,CN,RL,N,NS,A,ES,R,DD,PA,B,K,SV,IY,KY,DL)
C     FORMS SPECTRAL DENSITY   SXL   FOR EACH DEGREE OF FREEDOM   L   AT
C     FREQUENCY   O
      DIMENSION SXL(NEQP,3),Y(NNPP),NUM(NEQP),TT(NEQP),UU(NEQP),VV(NEQP)
     *   ,WW(NEQP),ICON(NELP,2),SV(NNPP),CI(NELP),CD(NELP),
     *   INOD(NNPP,NELP),SN(NELP),CN(NELP),RL(NELP),A(NEQP,NEQP),
     *   ES(NEQP),R(NEQP),D(NEQP),DL(NELP)
     * , Q(10),SQ(10,10),SA(10,60)
      SP(A,B,O)=A*EXP(-B/O**4)/(O**5)
C     FORM   TJ,UJ,VJ,WJ
      DO 50 J=1,N
      TT(J)=0.
      UU(J)=0.
      VV(J)=0.
   50 WW(J)=0.
      W=WAVN(O,DD)
      DO 60 J=1,NNP
      IF (Y(J).GT.D) ) GO TO 60
      DO 60 IJ=1,2
      IR=NUM((J-1)*3+IJ)
      IF (IR.EQ.0 ) GO TO 60
      CALL TUVW (TT(IR),UU(IR),VV(IR),WW(IR),Y,ICON,NNPP,NELP,SV,W,NEL,
     *   CI,CD,INOD,J,IJ,SN,CN,RL,DD,DL )
   60 CONTINUE
      SPABW=SP(PA,B,O)
      DO 404 L=1,N
  404 SXL(L,K)=0.
      DO 401 I=1,NS
      PI=0.
      QI=0.
      RI=0.
```

```
      SI=0.
      DO 402 J=1,N
      PI=PI*A(J,I)*TT(J)
      QI=QI*A(J,I)*UU(J)
      RI=RI*A(J,I)*JJ(J)
  402 SI=SI*A(J,I)*VV(J)
      RI=-RI*1.5958
      SI=SI*1.5958
      AKK=ES(I)*(1.-((Q/R(I))**2))
      SQQ=SI+Q*QI
      RP=RI+Q*PI
      CW=D(I)*Q
      AI=SQQ*AKK+CW*RP
      BI=RP*AKK-CW*SQQ
      W(I)=(AI*AI+BI*BI)*((Q/(CW*CW+AKK))**2)
  401 CONTINUE
      NSS=MIN0(NS,10)
      DO 405 J=1,NSS
      DO 405 L=1,NSS
  405 SW(J,L)=W(J)*W(L)*SPABW
      DO 100 I=1,NSS
      DO 100 J=1,N
      SA(I,J)=0.
      DO 100 L=1,NSS
  100 SA(I,J)=SA(I,J)+SW(I,L)*A(J,L)
      DO 403 L=1,N
      DO 403 I=1,NSS
  403 SXL(L,K)=SXL(L,K)+A(L,I)*SA(I,L)
      RETURN
      END


      SUBROUTINE TUVW (TI,UI,VI,WI,Y,ICON,NNPP,NELP,SV,W,NEL,CI,CD,
     *   INOD,I,L,SW,CW,RL,D,DL )

C     EVALUATES  TI, UI,VI, AND WI ,  THE CONTRIBUTIONS TO FORCE L(1 OR 2),NODE I
```

```
C      DUE TO ALL THE ELEMENTS MEETING THERE

       DIMENSION Y(NNPP),ICON(NELP,2),SV(NNPP),INOD(NNPP,NELP)
      *    ,CI(NELP),CO(NELP),SN(NELP),CN(NELP),RL(NELP),DL(NELP)
       TI=0.
       UI=0.
       VI=0.
       WI=0.
       DO 58 IY=1,NEL
       IF (INOD(I,IY).EQ.0 ) GO TO 58
       AR=SN(IY)
       IF (L.EQ.2 ) AR=-CN(IY)
       IF (AR ) 60,58,60
    60 CONTINUE
       Z2=Y(ICON(IY,2))
       Z1=Y(ICON(IY,1))
       IF (Z1.GT.D.OR.Z2.GT.D ) GO TO 58
       SIG1=SV(ICON(IY,1))
       SIG2=SV(ICON(IY,2))
       WZ1=W*Z1
       WZ2=W*Z2
       WD=W*D

C      EVALUATE SHELTERING FACTOR  FS

       FS=1.
       XX=1.3*W*DL(IY)-1.45
       IF (XX.LT.1.5 )  GO TO 100
       FS=1.+0.33333333*S17ACF(XX,1 )
       IF ( FS.LT.1. )  FS=1.
   100 CONTINUE
       DS2=DS(WZ2,WD)
       DS1=DS(WZ1,WD)
       DC2=DC(WZ2,WD)
       DC1=DC(WZ1,WD)
       KI1=(DS2-DS1)/
       KI2=(DC2-DC1)/
```

```
      RI3=WZ2*DS2-DC2-WZ1*DS1+DC1
      RI4=WZ2*DC2-DS2-WZ1*DC1+DS1
      TI=TI+AR*SN(IY)*RI1*CI(IY)*FS
      UI=UI+AR*CN(IY)*RI2*CI(IY)*FS
      VI=VI+AR*SN(IY)*(SIG1*RI1+(SIG2-SIG1)*RI3/(W*W*RL(IY)))*CD(IY)
      WI=WI+AR*CN(IY)*(SIG1*RI2+(SIG2-SIG1)*RI4/(W*W*RL(IY)))*CD(IY)
   38 CONTINUE
      RETURN
      END


      FUNCTION DS(WZ,WD)

      IF (WD.GT.150. ) GO TO 100
      DS=SINH(WZ)/(2.*SINH(WD))
      GO TO 101
  100 DS=((EXP((WZ-WD)*0.1))**10)*0.5
  101 CONTINUE
      RETURN
      END


      FUNCTION DC(WZ,WD)

      IF (WD.GT.150. ) GO TO 100
      DC=COSH (WZ)/(2.*SINH(WD))
      GO TO 101
  100 DC=((EXP((WZ-WD)*0.1))**10)*0.5
  101 CONTINUE
      RETURN
      END
```

```
      SUBROUTINE ROTATE (K,X1,X2,Y1,Y2 )
C     TRANSFORMATION OF ELEMENT MATRICES FROM LOCAL COORDINATES TO
C     GLOBAL COORDINATES    K=AT*K*A
      DIMENSION A(6,6),B(6,6)
      REAL K(6,6),L
      L=SQRT((X2-X1)*(X2-X1)+(Y2-Y1)*(Y2-Y1))
      C=((X2-X1)/L)
      S=(Y2-Y1)/L
      DO 10 I=1,6
      DO 10 J=1,6
   10 A(I,J)=0.
      A(1,1)=C
      A(1,2)=S
      A(2,1)=-S
      A(2,2)=C
      A(3,3)=1.
      A(4,4)=C
      A(4,5)=S
      A(5,4)=-S
      A(5,5)=C
      A(6,6)=1.
      CALL MATMULT (K,A,B,6,6,6 )
      CALL TRANSPOSE (A,K,6,6 )
      CALL MATEQUAL (A,K,6,6 )
      CALL MATMULT (A,B,K,6,6,6  )
      RETURN
      END


      SUBROUTINE MATEQUAL (A,B,M,N  )
      DIMENSION A(M,N),B(M,N)
```

```
      DO 10 I=1,N
      DO 10 J=1,M
   10 A(I,J)=B(I,J)
      RETURN
      END


      SUBROUTINE MATMULT (A,B,C,L,M,N )

      DIMENSION A(L,M),B(M,N),C(L,N)
      DO 10 I=1,L
      DO 10 J=1,N
      C(I,J)=0.
      DO 10 K=1,M
   10 C(I,J)=C(I,J)+A(I,K)*B(K,J)
      RETURN
      END


      SUBROUTINE TRANSPOSE (A,B,M,N )

      DIMENSION A(M,N),B(N,M)
      DO 10 I=1,N
      DO 10 J=1,M
   10 B(I,J)=A(J,I)
      RETURN
      END
```

```
      SUBROUTINE INVERT (A,B,LR,IR,LS,IS,NEQ  )
C  INVERTS A SYMMETRIC BANDED MATRIX USING GAUSS ELIMINATION
      DIMENSION A(NEQ,IB),B(LS,LS)
      DO 1001 IR=1,LS
      DO 1001 IS=1,LS
 1002 B(IR,IS)=0.
 1001 B(IR,IR)=1.
      IA=LR-I +1
      IN=LR-1
      DO 1 I=1,LR
      A(I,1)=1./A(I,1)
      DO 101 IS=1,LS
  101 B(I,IS)=B(I,IS)*A(I,1)
      IF(IA-I) 13,13,15
   15 IB=LR-I
      IF(IB) 1,1,13
   13 J1=1
      DO 2 J=1,IB
      J1=J+1
      A(I,J1)=A(I,J1)*A(I,1)
    2 CONTINUE
      DO 4 J=1,IB
      IJ=I+J
      JJ= L+1-J
      J1=J+1
      DO 104 IS=1,LS
  104 B(IJ,IS)=B(IJ,IS)-B(I,IS)*A(I,J1)/A(I,1)
      DO 5 K=1,JJ
      KJ=K+J
      A(IJ,K)=A(IJ,K)-A(I,J1)*A(I,KJ)/A(I,1)
    5 CONTINUE
    4 CONTINUE
    1 CONTINUE
```

```
      J=LR
      N1=LR-1
      DO 3 K=1,N1
      MA=NR-1
      J=J-1
      IF (MA-J) 25,35,25
   25 IB=LR-J
   35 DO 3 I=1,IB
      IJ=J+I
      JJ=I+1
      DO 100 IS=1,LR
  100 B(J,IS)=B(J,IS)-B(IJ,IS)*A(J,JJ)
    3 CONTINUE
      DO 501 IR=1,LR
      DO 501 IS=IR,LR
  501 B(IS,IR)=B(IR,IS)
      RETURN
      END




      SUBROUTINE EIGEN(D,M,NL,ND,NEV,NIT,ERT,Y,XV,XN,P,V,UB1,NM ,M1,NEQ,
     *     I  )
C     SOLVES BY ITERATION THE EIGENVALUE PROBLEM D*M*X=LAMBDA*X, WHERE D
C     IS THE INVERSE OF THE STIFFNESS MATRIX

      REAL M
      DIMENSION D(NL,ND),M(NEQ,I1),XV(NEQ),XN(NEQ),Y(NEQ),P(NEQ),
     *    V(NEQ,NEV )

   99 FORMAT (/////5X,30H NATURAL FREQUENCIES AND MODE SHAPES /
     *    5X,30(1H-) /// )
  100 FORMAT (1H ,24HITERATION COUNT EXCEEDED  )
  101 FORMAT (5X,I10,E20.5,I10 / )
  104 FORMAT (//5X,14HEIGENVALUE NO. ,3X,9HFREQUENCY ,3X,21HNO.OF ITERATI
```

```
     *0H; ) ) IE    )
  1)) FO; AT (/// )X,5H MODE NO  ,10X,7(11X,I3)      )
  1)) F)R AT (/5X, 15H FREQUENCY(CPS)   ,3X,7E14.5  //   )
  1)7 F)R AT (   13X,7E14.5   )
  1)9 F)R AT ( /  5)X,19H NORMAL MODE SHAPES/ )
33)55 F)R AT ( //5X,40H OPERATION FINISHED WITH CONTROL ON EIGENVALUE   ,
     *   I5   )

      WRITE (6,99 ).
      D) 20 IEV=1,NEV
      P)LD=).
      PIE J=).
      IT)=-IT
      D) 1 IL=1,IL
    1 XV(IL)=1,
    2 C)NTI)UE
      P)LD=P,EV
      D) 5 IL=1,IL
      Y(IL)=).
      NV=))=1
      IF (IL.LT.I) )   NV=IL-1
      N) ),)
      IF (IL.,I(.IL-1)+1) NU=NL-IL+1
      D) 3 IL2=1,)
    ) Y(IL)=Y(IL)+ (IL,IL2)*XV(IL+IL2-1)
      IF(NV.E),0 ) G) T) 5
      D) 4 IL2=1,NV
    4 Y(IL)=Y(IL)+A(IL-IL2,IL2+1)*XV(IL-IL2)
    5 C)NTI)UE
      D) 6 IL=1,IL
      X (IL)=0.
      D) 6 IL1=1,IL
    ) X (IL)=X (IL)+ (IL,IL1)*Y(IL1)
      EI)=X (1)
      D) 25 I2=2,NL
      IF (X (IZ),GT,EIG ) EIG=X (IZ)
   2) C)NTI)UE
```

```
      DO 2 IL=1,JL
    2 XI(IL)=XI(IL)/EIG
      PIEJ=0.
      DO 10 IL=1,JL
      CONST=XI(IL)
      IF (CONST.EQ.0. ) CONST=XV(IL)
      IF (CONST) 20,10,20
   20 ER=(XI(IL)-(V(IL))) /CONST
      IF (ABS(ER)-ERT) 10,10,11
   10 CONTINUE
      GO TO 13
   11 ITS=ITS+1
      ERA=(PIEJ-XI(IL))/PIEJ
      IF(ABS(ERA).LE.ERT) WRITE (6,33665) IEV
      IF(ABS(ERA).LE.ERT) GO TO 15
      IF (ITS) 12,12,13
   12 WRITE (6,1)
      GO TO 15
   13 DO 14 IL=1,JL
   14 XV(IL)=XN(IL)
      GO TO 2
   15 P(IEV)=1./EIG
      AA=P(IEV)
      IF (AA.GE.1. ) P(IEV)=SQRT(AA)/6.2?184
      WRITE (6,1)
      NITS=ITI-ITS
      WRITE (6,111) IEV,P(IEV),NITS
      DO 200 IL=1,JL
  200 V(IL,IEV)=XN(IL )
      IF (P(IEV)-.001 ) 205,206,204
  204 M=IEV
      GO TO 1?
  205 CONTINUE
      IF (IEV.-1.IEV ) GO TO 20
      ALPHA=1.
      DO 16 IL=1,JL
   16 ALPHA=ALPHA+XI(IL)*Y(IL)
```

```
      ALPHA=EI/ALPI
      DO 10 IL=1,NL
      DO 10 IS=1,NL
   10 D(IL,IS)=D(IL,IS)-ALPHA*XN(IL)*XN(IS)
   20 CONTINUE
  407 CONTINUE
      N2=MIN0 (N1,7 )
      WRITE (6,105 ) (J,J=1,N2  )
      WRITE (6,106 ) (P(J),J=1,N2  )
      WRITE (6,109 )
      DO 105 I=1,NL
      WRITE (6,107 ) (V(I,J),J=1,N2  )
  105 CONTINUE
      N1=N1-1
      DO 110 I=1,N1
  110 P(I)=P(I)*0.29134
      RETURN
      END


      SUBROUTINE MATMUL (V,DT1,G,H,N1,N,IBAND,NEQ,IBANDP  )
C     FORMS TRIPLE PRODUCT DT*T*D WHERE T IS BANDED
      REAL T(NEQ,IBANDP  )
      DIMENSION V(NEQ,NEQ),DT1(NEQ),G(NEQ)
      DO 105 K=1,N1
      G(K)=0.
      DO 101 I=1,N
      DT1(I)=0.
      KK1=MAX0 (1,I-IBAND+1 )
      KK2=MIN0 (N,I+IBAND-1 )
      DO 101 J=KK1,KK2
      RIJ=0.
```

```
      IF (I.GE.J ) RIJI=1(J,I=J+1 )
      IF (I.LT.J ) RIJI=1(I,J=I+1 )
      WTI(I)=WTI(I)*V(J,IR)*RMJI
111   CONTINUE
11    CONTINUE
      DO 102 I=1,N
1D    G(IR)=G(IR)+WTI(I)*V(I,IR )
102   CONTINUE
      RETURN
      END


      SUBROUTINE SIDVEL (N,Z,S,A,B,D,NOD )

      DIMENSION Z(NOD),S(NOD)
      SP(A,B,D)=A*EXP(-B/D**4)/(D**5)
      D=(D,D*D)**0.25
5     FORMAT (/////1X,20H S.D. OF PARTICLE VELOCITY  ,10X,8HLEVEL(M) / )
6     FORMAT (1X,F5.4,15X,F8.4  )
      WRITE (6,5 )
      D=0.5*D
      DO 10 I=1,N
10    S(I)=0.
      S0=SP(A,B,D )
      W0=WA(D )
      DO 30 J=1,N
      H=0.25*D
      IF (J.LT.3 ) H=0.105*D
      IF (J.GT.3 ) H=D
      S1=S0
      S2=SP(A,B,D+H)
      S3=SP(A,B,D+2.*H)
      W1=W0
      W2=WA(D+H)
```

```
      43= ,\/ ((S )*2* 1),0)
      0) 4) I=1, ,
      IF (Z(I).IF. ) ) G) TO 40
      ST1=ST +(V(), 11,Z(I),0 )
      ST2=S *TV(()+1),U2,Z(I),) )
      ST3=3 *TV(()+2*1)/ 13,Z(I),) )
      S(I)= (I)+(ST1+4*ST2+ST3 )*H/3.
 4)   C) TI UF
 3)   )= +2* 
      ) ) 5) I=1, 
      S(I)=S )RT(S(I))
      WRITE ( , ) ) S(I),Z(I)
 5)   C) TI UF
      RET JR 
      E )

      F  TI ), F (  ),U,Z,D  )

      ) )= J*)
      )Z= )*Z
      IF (J).GT.150. ) G) T) 100
      SK)=S I H(J))
      CK =C ( (IZ)
      CC=CK/'SK)
      G) TO 1( 
 1))  CC=(E( (IZ/1 ),-U0/10.))**1)
 1)1  C) TI UE
      TV=( )* ( )**2
      RETUR 
      E )
```

```
      FUNCTION WAVN (W,D  )
C     FINDS WAVE NUMBER K, FROM W**2=G*K*TANH(K*D), W,G,D, KNOWN
      REAL K1,K2,K3
      G=9.81
      W2G=W*W/G
      K1=W2G
   12 K2=1.1*K1
      K3=K2*TANH(K2*D  )
      IF (K3-W2G) 10,11,11
   10 K1=K2
      GO TO 12
   11 K3=K2
      K1=W2G
   13 K2=(K3+K1)*0.5
      WAVN=K2*TANH(K2*D )
      IF (ABS(WAVN-W2G).LT.0.02*W2G ) GO TO 15
      IF (WAVN-W2G ) 16,14,14
   16 K1=K2
      GO TO 13
   14 K3=K2
      GO TO 13
   15 WAVN=K2
      RETURN
      END



      SUBROUTINE INPUT (N,PH,RPH  )
C     GIVES INTEGRATION POINTS BASED ON VALUE OF NATURAL FREQUENCY
```

```
      DIMENSION H(5)
      DO 20 I=1,5
   20 H(I)=0.
      R=(D.3*DB)**0.25
      IF (R.LT.0.3*D ) GO TO 30
      IF (R.GT.1.3*D ) GO TO 40
      IF (R.LT.D ) GO TO 10
      H(1)=0.2*D
      H(2)=(D-D)/2
      H(3)=(1.5*D-R)/2
      GO TO 20
   10 H(1)=(D-0.5*D)/2
      H(2)=(D-R)/2
      H(3)=0.5*D
   20 H(4)=0.4*D
      H(5)=0.5*D
      D=0.6*D
      RETURN
   30 H(1)=0.05*D
      H(2)=0.2*D
      H(3)=0.3*D
      H(4)=0.7*D
      H(5)=0.
      D=0.5*D
      GO TO 20
   40 H(1)=0.2*D
      H(2)=0.5*D
      H(3)=1.0*D
      H(4)=1.2*D
      H(5)=0.
      D=0.6*D
   50 DO 60 I=1,4
      IF (R.GT.D.AND.R.LT.(D+2*H(I))) GO TO 70
   60 D=D+2*H(I)
      GO TO 80
   70 I0=5-I
      DO 75 J=1,I0
```

```
7  H(J-K)=H(J-[illegible])
   H(I)=([illegible]-J)/2
   H(I+1)=H(I+1)-H(I)
10 D=1.6*W
   IF (R.LT.1.3*W) D=1.5*W
   RETURN
   END



   SUBROUTINE ROTATE (B,N,X1,X2,Y1,Y2  )

   DIMENSION B(6,N),A(6)
   REAL L
   L=SQRT((X2-X1)**2+(Y2-Y1)**2 )
   C=(X2-X1)/L
   S=(Y2-Y1)/L
   DO 10 I=1,N
   A(1)=B(1,I)*C+B(2,I)*S
   A(2)=-B(1,I)*S+B(2,I)*C
   A(3)=B(3,I)
   A(4)=B(4,I)*C+B(5,I)*S
   A(5)=-B(4,I)*S+B(5,I)*C
   A(6)=B(6,I)
   DO 5 J=1,6
 5 B(J,I)=A(J)
10 CONTINUE
   RETURN
   END



   FINISH
```

******* RANDOM RESPONSE ANALYSIS OF PLANE FRAMES TO WAVE LOADING, SPECTA3 ******

VERTICAL CANTILEVER, 12 M DIAMETER, 100 M WATER DEPTH

NUMBER OF ELEMENTS = = = = = 6

NUMBER OF NODAL POINTS = = = 7

NUMBER OF REACTIONS = = = = = 3

NODAL POINT COORDINATES

NODE POINT	X=COORD(M)	Y=COORD(M)
1	0.0000	0.0000
2	0.0000	25.0000
3	0.0000	50.0000
4	0.0000	75.0000
5	0.0000	100.0000
6	0.0000	125.0000
7	0.0000	150.0000

STRUCTURE CONNECTIVITY AND PROPERTIES

MEMBER NO	END 1	END 2	E(N/M2)	I(M4)	A(SQ,M)	MASS(KG)	VOL DISPL(CU,M/M)	SHELT, FACT
1	1	2	0,1600E 11	0,3800E 03	0,1810E 02	0,4530E 05	0,1130E 03	0,000E 00
2	2	3	0,1600E 11	0,3800E 03	0,1810E 02	0,4530E 05	0,1130E 03	0,000E 00
3	3	4	0,1600E 11	0,3800E 03	0,1810E 02	0,4530E 05	0,1130E 03	0,000E 00
4	4	5	0,1600E 11	0,3800E 03	0,1810E 02	0,4530E 05	0,1130E 03	0,000E 00
5	5	6	0,1600E 11	0,3800E 03	0,1810E 02	0,4530E 05	0,0000E 00	0,000E 00
6	6	7	0,1600E 11	0,3800E 03	0,1810E 02	0,1000E 07	0,0000E 00	0,000E 00

DETAILS OF FIXED POINTS

NODE NO	DIRECTION OF FIXITY
1	1
1	2
1	3

MAXIMUM JOINT NUMBERING DIFFERENCE---- 1

SEMI-BANDWIDTH OF STIFFNESS MATRIX,ETC 6

MEAN WATER DEPTH(M)------------------ 100,0

PARAMETER A OF WAVE SPECTRUM---------- 2,560

PARAMETER B OF WAVE SPECTRUM---------- 0,0299

COEFFICIENT OF ADDED MASS------------- 1,00

COEFFICIENT OF INERTIA---------------- 2,00

COEFFICIENT OF DRAG------------------- 1,00

STRUCTURAL CRITICAL DAMPING RATIO----- 0,050

MEMBER NO	INERTIA COEFF	TOTAL DRAG COEFF
1	0,2317E 06	0,6147E 04
2	0,2317E 06	0,6147E 04
3	0,2317E 06	0,6147E 04
4	0,2317E 06	0,6147E 04
5	0,0000E 00	0,0000E 00
6	0,0000E 00	0,0000E 00

S.D. OF PARTICLE VELOCITY	LEVEL(M)
0,3579	0,00
0,6064	25,00
0,7866	50,00
1,2087	75,00
2,5809	100,00
0,0000	125,00
0,0000	150,00

HIGHEST VALUE OF FREQUENCY CONSIDERED = 7,865RAD/SEC, 1,252CPS

NATURAL FREQUENCIES AND MODE SHAPES

OPERATION FINISHED WITH CONTROL ON EIGENVALUE 1

```
EIGENVALUE NO,   FREQUENCY    NO,OF ITERATIONS DONE
      1          0,17169E 00          5


OPERATION FINISHED WITH CONTROL ON EIGENVALUE    2

EIGENVALUE NO,   FREQUENCY    NO,OF ITERATIONS DONE
      2          0,10793E 01          7


OPERATION FINISHED WITH CONTROL ON EIGENVALUE    3

EIGENVALUE NO,   FREQUENCY    NO,OF ITERATIONS DONE
      3          0,28858E 01          6



MODE NO                      1              2              3

FREQUENCY(CPS)        0,17169E 00    0,10793E 01    0,28858E 01

                          NORMAL MODE SHAPES

                   0,50341E-01    0,35337E 00    0,72365E-01
                   0,91348E-13    0,37534E-06    0,22507E 00
                  -0,43117E-02   -0,22859E-01   -0,33451E-02
                   0,22339E 00    0,89196E 00    0,83280E-01
                   0,17977E-12    0,73863E-06    0,44292E 00
                  -0,74916E-02   -0,15943E-01    0,29656E-02
                   0,44024E 00    0,10000E 01   -0,37066E-01
                   0,20443E-12    0,10783E-05    0,64658E 00
                  -0,95125E-02    0,88154E-02    0,50117E-02
                   0,67339E 00    0,45531E 00   -0,91794E-01
                   0,33637E-12    0,13833E-05    0,82950E 00
                  -0,10016E-01    0,33219E-01   -0,13401E-02
                   0,94312E 00   -0,54079E 00    0,12375E-01
                   0,40012E-12    0,16441E-05    0,98584E 00
                  -0,10992E-01    0,43770E-01   -0,60821E-02
                   0,10000E 01   -0,76035E 00    0,43349E-01
                   0,40337E-12    0,16677E-05    0,10000E 01
                  -0,10997E-01    0,43969E-01   -0,62455E-02
```

NUMBER OF SIGNIFICANT FREQUENCIES= 2

MODAL STIFFNESS AND DAMPING COEFFICIENTS

MODE	K	C
1	0,1197E 01	0,2459E-01
2	0,4512E 02	0,5465E-01

TOTAL DAMPING COEFFICIENT IN MODE 1= 0,1326E 00

MODE 1 GAMMA 0,0614

TOTAL DAMPING COEFFICIENT IN MODE 2= 0,4324E 01

MODE 2 GAMMA 0,5183

****

************* STANDARD DEVIATIONS OF DISPLACEMENT RESPONSES (M) *************

****

NODE ID	DIRECTION X	Y	ROT
1	0,000000E 00	0,000000E 00	0,000000E 00
2	0,249376E 00	0,252295E-06	0,164172E-01
3	0,660059E 00	0,496502E-06	0,146606E-01
4	0,877111E 00	0,724793E-06	0,140641E-01
5	0,953624E 00	0,929848E-06	0,264801E-01
6	0,131825E 01	0,110509E-05	0,329064E-01
7	0,143496E 01	0,112097E-05	0,330287E-01

MAXIMUM DISPLACEMENT STANDARD DEVIATION = 0.1435E 01 M

PROB. OF 68.5 PC THAT DISPL. IS LESS THAN 0.1435E 01 M

PROB. OF 95.4 PC THAT DISPL. IS LESS THAN 0.2870E 01 M

PROB. OF 99.7 PC THAT DISPL. IS LESS THAN 0.4305E 01 M

****

****************   STANDARD DEVIATIONS OF ELEMENT FORCES   ****************

****

ELEMENT NO	END 1 HORIZ (N)	END 1 VERT (N)	END 1 MOMENT (NM)	END 2 HORIZ (N)	END 2 VERT (N)	END 2 MOMENT (NM)
1	0.1638E 08	0.1518E-02	0.1709E 10	0.1638E 08	0.1518E-02	0.1300E 10
2	0.1596E 08	0.1470E-02	0.1299E 10	0.1596E 08	0.1470E-02	0.8997E 09
3	0.1455E 08	0.1374E-02	0.8976E 09	0.1455E 08	0.1374E-02	0.5339E 09
4	0.1170E 08	0.1234E-02	0.5312E 09	0.1170E 08	0.1234E-02	0.2387E 09
5	0.8978E 07	0.1055E-02	0.2436E 09	0.8978E 07	0.1055E-02	0.1918E 08
6	0.4504E 07	0.4777E-03	0.1911E 08	0.4504E 07	0.4777E-03	0.3412E 07

****

*********************   EXPECTED EXTREME ELEMENT LOADS   *********************

****

ELEMENT NO	END 1 HORIZ (N)	END 1 VERT (N)	END 1 MOMENT (NM)	END 2 HORIZ (N)	END 2 VERT (N)	END 2 MOMENT (NM)
1	-0.2316E 03	-0.2147E-02	0.2417E 10	0.2316E 08	0.2147E-02	-0.1838E 10
2	-0.2257E 03	-0.2078E-02	0.1836E 10	0.2257E 08	0.2078E-02	-0.1272E 10
3	-0.2057E 08	-0.1943E-02	0.1269E 10	0.2057E 08	0.1943E-02	-0.7549E 09
4	-0.1654E 03	-0.1745E-02	0.7511E 09	0.1654E 08	0.1745E-02	-0.3375E 09
5	-0.1269E 03	-0.1491E-02	0.3445E 09	0.1269E 08	0.1491E-02	-0.2712E 08
6	-0.6368E 07	-0.6755E-03	0.2702E 08	0.6368E 07	0.6755E-03	0.4824E 07

```
**********************************************************************************************
*******          RANDOM RESPONSE ANALYSIS OF PLANE FRAMES TO WAVE LOADING, SPECTA1        ******
**********************************************************************************************


VERTICAL CANTILEVER, 14 M DIAMETER, 100  M  WATER DEPTH


NUMBER OF ELEMENTS = = = = =     6
NUMBER OF NODAL POINTS = = =     7
NUMBER OF REACTIONS = = = = =    3


NODAL POINT COORDINATES

                    NODE POINT    X=COORD(M)     Y=COORD(M)

                        1           0.0000          0.0000
                        2           0.0000         25.0000
                        3           0.0000         50.0000
                        4           0.0000         75.0000
                        5           0.0000        100.0000
                        6           0.0000        125.0000
                        7           0.0000        150.0000
```

STRUCTURE CONNECTIVITY AND PROPERTIES

MEMBER NO	END 1	END 2	E(N/M2)	I(M4)	A(SQ.M)	MASS(KG)	VOL DISPL(CU.M/M)	SHELT. FACT
1	1	2	0.1600E 11	0.3800E 03	0.1810E 02	0.4550E 05	0.1130E 05	0.000E 00
2	2	3	0.1600E 11	0.3800E 03	0.1810E 02	0.4550E 05	0.1130E 05	0.000E 00
3	3	4	0.1600E 11	0.3800E 03	0.1810E 02	0.4550E 05	0.1130E 05	0.000E 00
4	4	5	0.1600E 11	0.3800E 03	0.1810E 02	0.4550E 05	0.1130E 05	0.000E 00
5	5	6	0.1600E 11	0.3800E 03	0.1810E 02	0.4550E 05	0.0000E 00	0.000E 00
6	6	7	0.1600E 11	0.3800E 03	0.1810E 02	0.1000E 07	0.0000E 00	0.000E 00

DETAILS OF FIXED POINTS

NODE NO	DIRECTION OF FIXITY
1	1
1	2
1	3

MAXIMUM JOINT NUMBERING DIFFERENCE---- 1

SEMI-BANDWIDTH OF STIFFNESS MATRIX,ETC 6

MEAN WATER DEPTH(M)------------------- 100.0

PARAMETER A OF WAVE SPECTRUM---------- 2.560

PARAMETER B OF WAVE SPECTRUM---------- 0.0299

COEFFICIENT OF ADDED MASS------------- 1.00

COEFFICIENT OF INERTIA---------------- 2.00

COEFFICIENT OF DRAG------------------- 1.00

MEMBER NO	INERTIA COEFF	TOTAL DRAG COEFF
1	0.2317E 06	0.6147E 04
2	0.2317E 06	0.6147E 04
3	0.2317E 06	0.6147E 04
4	0.2317E 05	0.6147E 04
5	0.0000E 00	0.0000E 00
6	0.0000E 00	0.0000E 00

S.D. OF PARTICLE VELOCITY	LEVEL(M)
0.5579	0.00
0.6064	25.00
0.7806	50.00
1.2087	75.00
2.5809	100.00
0.0000	125.00
0.0000	150.00

HIGHEST VALUE OF FREQUENCY CONSIDERED = 7.865RAD/SEC, 1.252CPS

NATURAL FREQUENCIES AND MODE SHAPES

```
OPERATION FINISHED WITH CONTROL ON EIGENVALUE     1

  EIGENVALUE NO.    FREQUENCY    NO.OF ITERATIONS DONE
        1          0.17169E 00          5


OPERATION FINISHED WITH CONTROL ON EIGENVALUE     2

  EIGENVALUE NO.    FREQUENCY    NO.OF ITERATIONS DONE
        2          0.10793E 01          7


OPERATION FINISHED WITH CONTROL ON EIGENVALUE     3

  EIGENVALUE NO.    FREQUENCY    NO.OF ITERATIONS DONE
        3          0.28858E 01          6


MODE NO                        1             2             3

FREQUENCY(CPS)         0.17169E 00   0.10793E 01   0.28858E 01

                           NORMAL MODE SHAPES

                  0.50341E-01   0.55357E 00   0.72365E-01
                  0.91168E-13   0.37534E-06   0.22507E 00
                 -0.43117E-02  -0.22659E-01  -0.33451E-02
                  0.20039E 00   0.39196E 00   0.83280E-01
                  0.17977E-12   0.73663E-06   0.44292E 00
                 -0.74016E-12  -0.13943E-01   0.29656E-02
                  0.44024E 00   0.10000E 01  -0.37066E-01
                  0.20643E-12   0.10783E-05   0.64658E 00
                 -0.95115E-02   0.33154E-02   0.50117E-02
                  0.67339E 00   0.45531E 00  -0.91794E-01
                  0.35057E-12   0.13833E-05   0.82950E 00
                 -0.10016E-01   0.33219E-01  -0.15401E-02
                  0.94202E 00  -0.54079E 00   0.12375E-01
                  0.40012E-12   0.16441E-05   0.98534E 00
                 -0.11902E-01   0.43770E-01  -0.60821E-02
                  0.10000E 01  -0.76035E 00   0.43349E-01
                  0.40237E-12   0.16677E-05   0.10000E 01
                 -0.10997E-01   0.43969E-01  -0.62455E-02
```

NUMBER OF SIGNIFICANT FREQUENCIES=   2

MODAL STIFFNESS AND DAMPING COEFFICIENTS

MODE	K	C
1	0.1107E 01	0.2459E-01
2	0.4012E 02	0.3465E-01

NORMALISED MODES

0.21916E-04	0.10703E-03
0.34075E-16	0.11364E-09
-0.10934E-05	-0.69198E-05
0.75411E-04	0.27001E-03
0.67037E-16	0.22360E-09
-0.27433E-05	-0.43260E-05
0.15576E-03	0.30271E-03
0.97300E-16	0.32641E-09
-0.33434E-05	0.26683E-05
0.23136E-03	0.13783E-03
0.12358E-15	0.41873E-09
-0.39578E-05	0.11050E-04
0.33431E-03	-0.15370E-03
0.14935E-15	0.49764E-09
-0.41913E-05	0.13250E-04
0.37312E-03	-0.43017E-03
0.15140E-15	0.57464E-09
-0.41320E-05	0.13310E-04

TOTAL DAMPING COEFFICIENT IN MODE   1=   0.1326E 00

MODE 1   GAMMA   0.0014

TOTAL DAMPING COEFFICIENT IN MODE   2=   0.4324E 01

```
****************************************************************************************
**************          STANDARD DEVIATIONS OF DISPLACEMENT RESPONSES(M)      **************
****************************************************************************************

        NODE  ID                          DIRECTION
                            X                 Y               ROT

           1          0.000000E 00   0.000000E 00   0.000000E 00
           2          0.331911E-01   0.559293E-08   0.406495E-02
           3          0.193379E 00   0.110066E-07   0.701379E-02
           4          0.395073E 00   0.160674E-07   0.893750E-02
           5          0.632336E 00   0.206131E-07   0.998512E-02
           6          0.887337E 00   0.244980E-07   0.103472E-01
           7          0.939518E 00   0.248499E-07   0.103516E-01

MAXIMUM DISPLACEMENT STANDARD DEVIATION =        0.9395E 00 M

PROB. OF 68.3 PC THAT DISPL. IS LESS THAN        0.9395E 00 M

PROB. OF 95.4 PC THAT DISPL. IS LESS THAN        0.1879E 01 M

PROB. OF 99.7 PC THAT DISPL. IS LESS THAN        0.2819E 01 M
```

****

******   RANDOM RESPONSE ANALYSIS OF PLANE FRAMES TO WAVE LOADING, SPECTAS   ******

****

FOUR LEG PLATFORM , NHOC

NUMBER OF ELEMENTS = = = = =   9

NUMBER OF NODAL POINTS = = =   10

NUMBER OF REACTIONS = = = = =   6

NODAL POINT COORDINATES

NODE POINT	X=COORD(M)	Y=COORD(M)
1	0.0000	0.0000
2	40.0000	0.0000
3	0.0000	30.0000
4	40.0000	30.0000
5	0.0000	130.0000
6	40.0000	130.0000
7	0.0000	150.0000
8	40.0000	150.0000
9	0.0000	180.0000
10	40.0000	180.0000

STRUCTURE CONNECTIVITY AND PROPERTIES

MEMBER NO	END 1	END 2	E(N/M2)	I(M4)	A(SQ.M)	MASS(KG)	VOL DISPL(CU.M/M)	SHELT. FACT
1	1	3	0.2000E 11	0.6140E 06	0.6240E 03	0.1560E 07	0.6240E 03	0.400E 02
2	2	4	0.2000E 11	0.6140E 06	0.6240E 03	0.1560E 07	0.6240E 03	0.000E 00
3	3	5	0.2000E 11	0.5500E 03	0.2300E 02	0.5750E 05	0.8660E 02	0.400E 02
4	4	6	0.2000E 11	0.5500E 03	0.2300E 02	0.5750E 05	0.8660E 02	0.000E 00
5	5	7	0.2000E 11	0.6140E 02	0.8693E 01	0.2160E 05	0.2827E 02	0.400E 02
6	6	8	0.2000E 11	0.6140E 02	0.8693E 01	0.2160E 05	0.2827E 02	0.000E 00
7	7	9	0.2000E 11	0.6140E 02	0.8693E 01	0.2160E 05	0.0000E 00	0.000E 00
8	8	10	0.2000E 11	0.6140E 02	0.8693E 01	0.2160E 05	0.0000E 00	0.000E 00
9	9	11	0.2000E 11	0.3000E 06	0.9000E 02	0.2250E 06	0.0000E 00	0.000E 00

DETAILS OF FIXED JOINTS

NODE NO	DIRECTION OF FIXITY
1	1
1	2
1	3
2	1
2	2
2	3

MAXIMUM JOINT NUMBERING DIFFERENCE---- 2

SEMI-BANDWIDTH OF STIFFNESS MATRIX,ETC 9

MEAN WATER DEPTH(M)------------------- 130.0

PARAMETER A OF WAVE SPECTRUM---------- 2.030

COEFFICIENT OF ADDED MASS-------------- 1.00

COEFFICIENT OF INERTIA---------------- 2.00

COEFFICIENT OF DRAG------------------- 1.00

STRUCTURAL CRITICAL DAMPING RATIO----- 0.050

MEMBER (I)	INERTIA COEFF	TOTAL DRAG COEFF
1	0.1279E 07	0.1445E 05
2	0.1279E 07	0.1445E 05
3	0.1775E 06	0.3382E 04
4	0.1775E 06	0.3382E 04
5	0.5793E 05	0.3075E 04
6	0.5793E 05	0.3075E 04
7	0.0000E 00	0.0000E 00
8	0.0000E 00	0.0000E 00
9	0.0000E 00	0.0000E 00

S.D. OF PARTICLE VELOCITY	LEVEL(M)
0.0804	0.00
0.0804	0.00
0.0993	50.00
0.0993	50.00
0.7302	130.00
0.7302	130.00
1.3293	130.00
1.3293	130.00
0.0000	180.00
0.0000	180.00

NATURAL FREQUENCIES AND MODE SHAPES

```
EIGENVALUE NO.   FREQUENCY    NO.OF ITERATIONS DONE
      1         0.21312E 00         5

EIGENVALUE NO.   FREQUENCY    NO.OF ITERATIONS DONE
      2         0.90904E 00        100

OPERATION FINISHED WITH CONTROL ON EIGENVALUE     5

EIGENVALUE NO.   FREQUENCY    NO.OF ITERATIONS DONE
      3         0.98209E 00         21

OPERATION FINISHED WITH CONTROL ON EIGENVALUE     4

EIGENVALUE NO.   FREQUENCY    NO.OF ITERATIONS DONE
      4         0.12478E 01         7

OPERATION FINISHED WITH CONTROL ON EIGENVALUE     5

EIGENVALUE NO.   FREQUENCY    NO.OF ITERATIONS DONE
      5         0.30029E 01         12

MODE NO                  1          2          3          4          5
```

NORMAL MODE SHAPES

0.69544E-04	0.35535E-03	0.41710E-03	0.75646E-03	0.11865E-05
0.55312E-04	-0.14120E-04	-0.16556E-02	0.42417E-02	0.58636E-02
-0.44205E-05	-0.21669E-04	-0.25346E-04	-0.45613E-04	-0.69517E-07
0.69544E-04	-0.34809E-03	0.43247E-03	0.75646E-03	0.23605E-05
-0.55312E-04	0.14171E-04	0.16556E-02	-0.42416E-02	0.58639E-02
-0.44205E-05	0.21223E-04	-0.26283E-04	-0.45612E-04	-0.13880E-06
0.66369E 00	0.10000E 01	0.95668E 00	0.10000E 01	-0.47565E-03
0.50735E-02	-0.12783E-02	-0.14995E 00	0.38193E 00	0.49161E 00
-0.97741E-02	0.22509E-02	0.73467E-02	0.25499E-01	0.35232E-04
0.66369E 00	-0.93328E 00	0.10000E 01	0.10000E 01	-0.91792E-03
-0.50735E-02	0.12835E-02	0.14995E 00	-0.38193E 00	0.49163E 00
-0.97741E-02	-0.21246E-02	0.74423E-02	0.25499E-01	0.85570E-04
0.85023E 00	0.63844E 00	0.39339E 00	-0.68080E-01	-0.46118E-03
0.77205E-02	-0.19358E-02	-0.22698E 00	0.57589E 00	0.70473E 00
-0.83411E-02	0.23508E-01	0.42536E-01	0.66331E-01	-0.32652E-04
0.85023E 00	-0.63148E 00	0.42113E 00	-0.68083E-01	-0.15961E-02
-0.77265E-02	0.19423E-02	0.22698E 00	-0.57589E 00	0.70476E 00
-0.83411E-02	-0.27770E-01	0.43765E-01	0.66331E-01	-0.24945E-04
0.10000E 01	-0.50322E-02	-0.74062E 00	-0.91770E 00	0.16634E-03
0.11705E-01	-0.29140E-02	-0.34168E 00	0.86334E 00	0.99996E 00
-0.58573E-03	0.15563E-03	0.17087E-01	-0.43157E-01	0.36941E-04
0.10000E 01	-0.76219E-02	-0.74056E 00	-0.91770E 00	0.16463E-03
-0.11705E-01	0.29246E-02	0.34168E 00	-0.86333E 00	0.10000E 01
-0.58573E-03	0.13635E-03	0.17088E-01	-0.43157E-01	-0.34894E-04

NUMBER OF SIGNIFICANT FREQUENCIES= 4

MODAL STIFFNESS AND DAMPING COEFFICIENTS

MODE	K	C
1	0.1798E 01	0.1809E-01
2	0.3271E 02	0.4326E-01
3	0.3813E 02	0.1930E-01
4	0.6164E 02	0.8342E-02

4 0,5510E 02 0,1331E-01

TOTAL DAMPING COEFFICIENT IN MODE 1= 0,1106E 00

MODE 1 GAMMA 0,0556

TOTAL DAMPING COEFFICIENT IN MODE 2= 0,1655E 01

MODE 2 GAMMA 0,1462

TOTAL DAMPING COEFFICIENT IN MODE 3= 0,1561E 01

MODE 3 GAMMA 0,1445

TOTAL DAMPING COEFFICIENT IN MODE 4= 0,2590E 01

MODE 4 GAMMA 0,1384

****

************* STANDARD DEVIATIONS OF DISPLACEMENT RESPONSES (M) *************

****

NODE NO	DIRECTION X	Y	ROT
1	0,000000E 00	0,000000E 00	0,000000E 00
2	0,000000E 00	0,000000E 00	0,000000E 00
3	0,325327E-04	0,314768E-03	0,505078E-05
4	0,325195E-04	0,314766E-03	0,504998E-05
5	0,235912E 00	0,284149E-01	0,305939E-02
6	0,235893E 00	0,284146E-01	0,305940E-02
7	0,259468E 00	0,429184E-01	0,694606E-02
8	0,259453E 00	0,429180E-01	0,694518E-02
9	0,318244E 00	0,644573E-01	0,322272E-02
11	0,318244E 00	0,644568E-01	0,322272E-02

MAXIMUM DISPLACEMENT STANDARD DEVIATION = 0,3182E 00 M

PROB, OF 68,3 PC THAT DISPL, IS LESS THAN 0,3182E 00 M

PROB, OF 95,4 PC THAT DISPL, IS LESS THAN 0,6365E 00 M

PROB, OF 99,7 PC THAT DISPL, IS LESS THAN 0,9547E 00 M

****

**************** STANDARD DEVIATIONS OF ELEMENT FORCES *****************

****

ELEMENT NO	END 1 HORIZ (N)	END 1 VERT (N)	END 1 MOMENT (NM)	END 2 HORIZ (N)	END 2 VERT (N)	END 2 MOMENT (NM)
1	0,7291E 07	0,8610E 07	0,8970E 09	0,7291E 07	0,8610E 07	0,6783E 09
2	0,7291E 07	0,8610E 07	0,8970E 09	0,7291E 07	0,8610E 07	0,6783E 09
3	0,6610E 07	0,8605E 07	0,6633E 09	0,6610E 07	0,8605E 07	0,2349E 07
4	0,6610E 07	0,8605E 07	0,6633E 09	0,6610E 07	0,8605E 07	0,2349E 07
5	0,4199E 07	0,8596E 07	0,2932E 08	0,4199E 07	0,8596E 07	0,5466E 08
6	0,4199E 07	0,8596E 07	0,2932E 08	0,4199E 07	0,8596E 07	0,5466E 08
7	0,3674E 07	0,8592E 07	0,5483E 08	0,3674E 07	0,8592E 07	0,1650E 09
8	0,3674E 07	0,8592E 07	0,5483E 08	0,3674E 07	0,8592E 07	0,1650E 09
9	0,0000E 00	0,8189E 07	0,1638E 09	0,0000E 00	0,8189E 07	0,1638E 09

****

********************** EXPECTED EXTREME ELEMENT LOADS **********************

ELEMENT NO	END 1 HORIZ (N)	END 1 VERT (N)	END 1 MOMENT (NM)	END 2 HORIZ (N)	END 2 VERT (N)	END 2 MOMENT (NM)
1	-0,1031E 03	-0,1218E 08	0,1268E 10	0,1031E 08	0,1218E 08	-0,9591E 09
2	-0,1031E 03	0,1218E 08	0,1268E 10	0,1031E 08	-0,1218E 08	-0,9591E 09
3	-0,9346E 07	-0,1217E 08	0,9380E 09	0,9346E 07	0,1217E 08	-0,3322E 07
4	-0,7346E 07	0,1217E 08	0,9380E 09	0,9346E 07	-0,1217E 08	-0,3322E 07
5	-0,5937E 07	-0,1215E 08	0,4146E 08	0,5937E 07	0,1215E 08	0,7729E 08
6	-0,5937E 07	0,1215E 08	0,4146E 08	0,5937E 07	-0,1215E 08	0,7729E 08
7	-0,5194E 07	-0,1215E 08	-0,7752E 08	0,5194E 07	0,1215E 08	0,2334E 09
8	-0,5194E 07	0,1215E 08	-0,7752E 08	0,5194E 07	-0,1215E 08	0,2334E 09
9	0,0000E 00	-0,1158E 08	-0,2316E 09	0,0000E 00	0,1158E 08	-0,2316E 09

******* RANDOM RESPONSE ANALYSIS OF PLANE FRAMES TO WAVE LOADING, SPECTAS ******

****

FOUR LEG PLATFORM , ANDUC

NUMBER OF ELEMENTS = = = = = 9

NUMBER OF NODAL POINTS = = = 10

NUMBER OF REACTIONS = = = = = 6

NODAL POINT COORDINATES

NODE POINT	X=COORD(M)	Y=COORD(M)
1	0,0000	0,0000
2	40,0000	0,0000
3	0,0000	30,0000
4	40,0000	30,0000
5	0,0000	130,0000
6	40,0000	130,0000
7	0,0000	150,0000
8	40,0000	150,0000
9	0,0000	180,0000
10	40,0000	180,0000

STRUCTURE CONNECTIVITY AND PROPERTIES

MEMBER NO	END 1	END 2	E(N/M2)	I(M4)	A(SQ,M)	MASS(KG)	VOL DISPL(CU,M/M)	SHELT, FACT
1	1	3	0,2000E 11	0,6140E 06	0,9240E 03	0,1360E 07	0,6240E 03	0,400E 02
2	2	4	0,2000E 11	0,6140E 06	0,9240E 03	0,1360E 07	0,6240E 03	0,000E 00
3	3	5	0,2000E 11	0,5500E 03	0,2300E 02	0,5750E 05	0,8660E 02	0,400E 02
4	4	6	0,2000E 11	0,5500E 03	0,2300E 02	0,5750E 05	0,8660E 02	0,000E 00
5	5	7	0,2000E 11	0,6140E 02	0,8693E 01	0,2160E 05	0,2827E 02	0,400E 02
6	6	8	0,2000E 11	0,6140E 02	0,9693E 01	0,2160E 05	0,2827E 02	0,000E 00
7	7	9	0,2000E 11	0,6140E 02	0,9693E 01	0,2160E 05	0,0000E 00	0,000E 00
8	8	10	0,2000E 11	0,6140E 02	0,8693E 01	0,2160E 05	0,0000E 00	0,000E 00
9	9	10	0,2000E 11	0,3000E 06	0,9000E 02	0,2250E 06	0,0000E 00	0,000E 00

DETAILS OF FIXED POINTS

NODE NO	DIRECTION OF FIXITY
1	1
1	2
1	3
2	1
2	2
2	3

MAXIMUM JOINT NUMBERING DIFFERENCE---- 2

SEMI-BANDWIDTH OF STIFFNESS MATRIX,ETC 9

MEAN WATER DEPTH(M)------------------- 130,0

PARAMETER A OF WAVE SPECTRUM---------- 2,030

PARAMETER B OF WAVE SPECTRUM---------- 0,0080

COEFFICIENT OF ADDED MASS--------------- 1.00

COEFFICIENT OF INERTIA--------------- 2.00

COEFFICIENT OF DRAG------------------ 0.05

STRUCTURAL CRITICAL DAMPING RATIO----- 0.030

MEMBER NO	INERTIA COEFF	TOTAL DRAG COEFF
1	0.1279E 07	0.7223E 03
2	0.1279E 07	0.7223E 03
3	0.1775E 06	0.2691E 03
4	0.1775E 06	0.2691E 03
5	0.5793E 05	0.1537E 03
6	0.5793E 05	0.1537E 03
7	0.0000E 00	0.0000E 00
8	0.0000E 00	0.0000E 00
9	0.0000E 00	0.0000E 00

S.D. OF PARTICLE VELOCITY	LEVEL(M)
0.0864	0.00
0.0864	0.00
0.0973	30.00
0.0973	30.00
0.7302	130.00
0.7302	130.00
1.8293	150.00
1.8293	150.00
0.0000	180.00
0.0000	180.00

HIGHEST VALUE OF FREQUENCY CONSIDERED = 9.659RAD/SEC, 1.537CPS

NATURAL FREQUENCIES AND MODE SHAPES

EIGENVALUE NO. FREQUENCY NO.OF ITERATIONS DONE
1 0.21112E 00 5

EIGENVALUE NO. FREQUENCY NO.OF ITERATIONS DONE
2 0.90994E 00 100

OPERATION FINISHED WITH CONTROL ON EIGENVALUE 3

EIGENVALUE NO. FREQUENCY NO.OF ITERATIONS DONE
3 0.98209E 00 21

OPERATION FINISHED WITH CONTROL ON EIGENVALUE 4

EIGENVALUE NO. FREQUENCY NO.OF ITERATIONS DONE
4 0.12478E 01 7

OPERATION FINISHED WITH CONTROL ON EIGENVALUE 5

EIGENVALUE NO. FREQUENCY NO.OF ITERATIONS DONE
5 0.30029E 01 12

MODE NO 1 2 3 4 5

FREQUENCY(CPS) 0.41312E 00 0.90904E 00 0.98209E 00 0.12478E 01 0.30029E 01

NORMAL MODE SHAPES

0.69544E-04	0.35535E-03	0.41710E-03	0.75646E-03	0.11865E-05
0.55312E-04	-0.14120E-04	-0.16556E-02	0.42417E-02	0.58636E-02
-0.44265E-05	-0.21569E-04	-0.25346E-04	-0.45613E-04	-0.69517E-07
0.69544E-04	-0.34809E-03	0.43247E-03	0.75646E-03	0.23605E-05
-0.55312E-04	0.14171E-04	0.16556E-02	-0.42416E-02	0.58639E-02
-0.44265E-05	0.21223E-04	-0.26283E-04	-0.45612E-04	-0.13880E-06
0.66359E 00	0.10000E 01	0.95668E 00	0.10000E 01	-0.47565E-03
0.50735E-02	-0.12783E-02	-0.14995E 00	0.38193E 00	0.49161E 00
-0.97741E-02	0.22509E-02	0.73467E-02	0.25499E-01	0.35232E-04
0.66359E 00	-0.93328E 00	0.10000E 01	0.10000E 01	-0.91792E-03
-0.50735E-02	0.12835E-02	0.14995E 00	-0.38193E 00	0.49163E 00
-0.97741E-02	-0.21246E-02	0.74423E-02	0.25499E-01	0.85570E-04
0.85023E 00	0.63844E 00	0.39339E 00	-0.68080E-01	-0.46118E-03
0.77265E-02	-0.19358E-02	-0.22698E 00	0.57589E 00	0.70473E 00
-0.83411E-02	0.23508E-01	0.42516E-01	0.66331E-01	-0.52652E-04
0.85023E 00	-0.63148E 00	0.42113E 00	-0.68083E-01	-0.15961E-02
-0.77265E-02	0.19423E-02	0.22698E 00	-0.57589E 00	0.70476E 00
-0.83411E-02	-0.27770E-01	0.43765E-01	0.66331E-01	-0.24945E-04
0.10000E 01	-0.50322E-02	-0.74062E 00	-0.91770E 00	0.16634E-03
0.11705E-01	-0.29140E-02	-0.34168E 00	0.86334E 00	0.99996E 00
-0.58573E-03	0.15563E-03	0.17087E-01	-0.43157E-01	0.36941E-04
0.10000E 01	-0.76219E-02	-0.74056E 00	-0.91770E 00	0.16463E-03
-0.11705E-01	0.29246E-02	0.34168E 00	-0.86333E 00	0.10000E 01
-0.58573E-03	0.13635E-03	0.17088E-01	-0.43157E-01	-0.34894E-04

NUMBER OF SIGNIFICANT FREQUENCIES= 4

MODAL STIFFNESS AND DAMPING COEFFICIENTS

MODE	K	C
1	0.1793E 01	0.1809E-01
2	0.3271E 02	0.4326E-01
3	0.3813E 02	0.1930E-01
4	0.6164E 02	0.8342E-02

```
TOTAL DAMPING COEFFICIENT IN MODE   1=    0,9422E-01

    MODE  1     GAMMA   0,0303

TOTAL DAMPING COEFFICIENT IN MODE   2=    0,1620E 01

    MODE  2     GAMMA   0,1450

TOTAL DAMPING COEFFICIENT IN MODE   3=    0,1518E 01

    MODE  3     GAMMA   0,1411

TOTAL DAMPING COEFFICIENT IN MODE   4=    0,2377E 01

    MODE  4     GAMMA   0,1576


****************************************************************************************************
**************        STANDARD DEVIATIONS OF DISPLACEMENT RESPONSES (M)        **************
****************************************************************************************************
```

NODE NO	DIRECTION X	DIRECTION Y	DIRECTION ROT
1	0,000000E 00	0,000000E 00	0,000000E 00
2	0,000000E 00	0,000000E 00	0,000000E 00
3	0,767012E-04	0,289269E-03	0,469659E-05
4	0,766493E-04	0,289267E-03	0,469586E-05
5	0,226329E 00	0,261114E-01	0,296385E-02
6	0,226312E 00	0,261112E-01	0,296386E-02
7	0,255094E 00	0,394375E-01	0,646587E-02
8	0,255090E 00	0,394372E-01	0,646508E-02
9	0,309415E 00	0,592270E-01	0,296120E-02
10	0,309415E 00	0,592266E-01	0,296120E-02

MAXIMUM DISPLACEMENT STANDARD DEVIATION = 0,3098E 00 M

PROB, OF 68,3 PC THAT DISPL, IS LESS THAN 0,3098E 00 M

PROB, OF 95,4 PC THAT DISPL, IS LESS THAN 0,6196E 00 M

PROB, OF 99,7 PC THAT DISPL, IS LESS THAN 0,9294E 00 M

****

****************   STANDARD DEVIATIONS OF ELEMENT FORCES   ****************

****

ELEMENT NO	END 1 HORIZ (N)	END 1 VERT (N)	END 1 MOMENT (NM)	END 2 HORIZ (N)	END 2 VERT (N)	END 2 MOMENT (NM)
1	0,7263E 07	0,8392E 07	0,9128E 09	0,7263E 07	0,8392E 07	0,6949E 09
2	0,7263E 07	0,8392E 07	0,9128E 09	0,7263E 07	0,8392E 07	0,6949E 09
3	0,6676E 07	0,8387E 07	0,6805E 09	0,6676E 07	0,8387E 07	0,1268E 08
4	0,6676E 07	0,8387E 07	0,6805E 09	0,6676E 07	0,8387E 07	0,1268E 08
5	0,4294E 07	0,8376E 07	0,3920E 08	0,4294E 07	0,8376E 07	0,4669E 08
6	0,4294E 07	0,8376E 07	0,3920E 08	0,4294E 07	0,8376E 07	0,4669E 08
7	0,3763E 07	0,8372E 07	0,4687E 08	0,3763E 07	0,8372E 07	0,1598E 09
8	0,3763E 07	0,8372E 07	0,4687E 08	0,3763E 07	0,8372E 07	0,1598E 09
9	0,3750E 00	0,7924E 07	0,1585E 09	0,3750E 00	0,7924E 07	0,1585E 09

****

*********************   EXPECTED EXTREME MEMBER LOADS   *********************

****

ELEMENT NO	END 1 HORIZ (N)	END 1 VERT (N)	END 1 MOMENT (NM)	END 2 HORIZ (N)	END 2 VERT (N)	END 2 MOMENT (NM)
1	-0.1027E 08	-0.1187E 08	0.1291E 10	0.1027E 08	0.1187E 08	-0.9826E 09
2	-0.1027E 08	0.1187E 08	0.1291E 10	0.1027E 08	-0.1187E 08	-0.9826E 09
3	-0.9440E 07	-0.1186E 08	0.9622E 09	0.9440E 07	0.1186E 08	-0.1821E 08
4	-0.9440E 07	0.1186E 08	0.9622E 09	0.9440E 07	-0.1186E 08	-0.1821E 08
5	-0.6072E 07	-0.1184E 08	0.5543E 08	0.6072E 07	0.1184E 08	0.6602E 08
6	-0.6072E 07	0.1184E 08	0.5543E 08	0.6072E 07	-0.1184E 08	0.6602E 08
7	-0.5321E 07	-0.1184E 08	-0.6628E 08	0.5321E 07	0.1184E 08	0.2259E 09
8	-0.5321E 07	0.1184E 08	-0.6628E 08	0.5321E 07	-0.1184E 08	0.2259E 09
9	-0.5503E 00	-0.1120E 08	-0.2241E 09	0.5503E 00	0.1120E 08	-0.2241E 09

****

*******   R1D01 RESPONSE ANALYSIS OF PLANE FRAMES TO WAVE LOADING, SPECTA3   ******

****

HALCROW-EIBANK STEEL JACKET , ELEVATION THROUGH LINES 1 AND 4

NUMBER OF ELEMENTS - - - - - 36

NUMBER OF NODAL POINTS - - - 20

NUMBER OF REACTIONS - - - - - 6

NODAL POINT COORDINATES

NODE POINT	X-COORD(M)	Y-COORD(M)
1	0.0000	0.0000
2	80.0000	0.0000
3	3.3450	37.0000
4	40.0000	37.0000
5	76.6550	37.0000
6	6.5990	73.0000
7	40.0000	73.0000
8	73.4010	73.0000
9	9.4920	105.0000
10	40.0000	105.0000
11	70.5080	105.0000
12	12.2030	135.0000
13	40.0000	135.0000

14	67,7970	155,0000
15	14,0110	155,0000
16	40,0000	155,0000
17	65,9890	155,0000
18	16,0000	177,0000
19	40,0000	177,0000
20	64,0000	177,0000

STRUCTURE CONNECTIVITY AND PROPERTIES

MEMBER NO	END 1	END 2	E(N/M2)	I(M4)	A(SQ,M)	MASS(KG)	VOL DISPL(CU,M/M)	SHELT, FACT
1	1	3	0,2000E 12	0,3067E 02	0,1467E 01	0,1152E 05	0,6567E 02	0,000E 00
2	1	4	0,2000E 12	0,2958E 00	0,2599E 00	0,2040E 04	0,3575E 01	0,000E 00
3	2	4	0,2000E 12	0,2958E 00	0,2599E 00	0,2040E 04	0,3575E 01	0,000E 00
4	2	5	0,2000E 12	0,3067E 02	0,1467E 01	0,1152E 05	0,6567E 02	0,000E 00
5	3	4	0,2000E 12	0,1551E 00	0,1855E 00	0,1456E 04	0,2627E 01	0,000E 00
6	4	5	0,2000E 12	0,1551E 00	0,1855E 00	0,1456E 04	0,2627E 01	0,000E 00
7	3	6	0,2000E 12	0,1820E 01	0,5756E 00	0,4518E 04	0,9931E 01	0,000E 00
8	3	7	0,2000E 12	0,2184E 00	0,2612E 00	0,2051E 04	0,2627E 01	0,000E 00
9	5	7	0,2000E 12	0,2184E 00	0,2612E 00	0,2051E 04	0,2627E 01	0,000E 00
10	5	8	0,2000E 12	0,1820E 01	0,5756E 00	0,4518E 04	0,9931E 01	0,000E 00
11	6	7	0,2000E 12	0,8043E-01	0,1267E 00	0,9943E 03	0,1267E 01	0,000E 00
12	7	8	0,2000E 12	0,8043E-01	0,1267E 00	0,9943E 03	0,1267E 01	0,000E 00
13	6	9	0,2000E 12	0,1148E 01	0,4945E 00	0,3882E 04	0,7296E 01	0,000E 00
14	6	10	0,2000E 12	0,1868E 00	0,2234E 00	0,1754E 04	0,2627E 01	0,000E 00
15	8	10	0,2000E 12	0,1868E 00	0,2234E 00	0,1754E 04	0,2627E 01	0,000E 00
16	8	11	0,2000E 12	0,1148E 01	0,4945E 00	0,3882E 04	0,7296E 01	0,000E 00
17	9	10	0,2000E 12	0,6433E-01	0,1368E 00	0,1073E 04	0,1477E 01	0,000E 00
18	10	11	0,2000E 12	0,6433E-01	0,1368E 00	0,1073E 04	0,1477E 01	0,000E 00
19	9	12	0,2000E 12	0,6669E 00	0,4135E 00	0,3246E 04	0,5067E 01	0,000E 00
20	9	13	0,2000E 12	0,1868E 00	0,2234E 00	0,1754E 04	0,2627E 01	0,000E 00
21	11	13	0,2000E 12	0,1868E 00	0,2234E 00	0,1754E 04	0,2627E 01	0,000E 00
22	11	14	0,2000E 12	0,6669E 00	0,4135E 00	0,3246E 04	0,5067E 01	0,000E 00
23	12	13	0,2000E 12	0,3540E-01	0,9525E-01	0,7477E 03	0,1167E 01	0,000E 00
24	13	14	0,2000E 12	0,3540E-01	0,9525E-01	0,7477E 03	0,1167E 01	0,000E 00
25	12	15	0,2000E 12	0,1322E 00	0,1488E 00	0,1168E 04	0,2483E 01	0,000E 00
26	12	16	0,2000E 12	0,1868E 00	0,2234E 00	0,1754E 04	0,2627E 01	0,000E 00
27	14	16	0,2000E 12	0,1868E 00	0,2234E 00	0,1754E 04	0,2627E 01	0,000E 00
28	14	17	0,2000E 12	0,1322E 00	0,1488E 00	0,1168E 04	0,2483E 01	0,000E 00
29	15	16	0,2000E 12	0,3540E-01	0,9525E-01	0,7477E 03	0,1167E 01	0,000E 00

30	16	17	0.2000E 12	0.3540E-01	0.9525E-01	0.7477E 03	0.1167E 01	0.000E 00
31	15	18	0.2000E 12	0.1322E 00	0.1488E 00	0.1168E 04	0.2483E 01	0.000E 00
32	15	19	0.2000E 12	0.1868E 00	0.2234E 00	0.1754E 04	0.2627E 01	0.000E 00
33	17	19	0.2000E 12	0.1868E 00	0.2234E 00	0.1754E 04	0.2627E 01	0.000E 00
34	17	20	0.2000E 12	0.1322E 00	0.1488E 00	0.1168E 04	0.2483E 01	0.000E 00
35	18	19	0.2000E 12	0.1000E 04	0.1000E 02	0.1596E 06	0.0000E 00	0.000E 00
36	19	20	0.2000E 12	0.1000E 04	0.1000E 02	0.1596E 06	0.0000E 00	0.000E 00

DETAILS OF FIXED POINTS

NODE NO	DIRECTION OF FIXITY
1	1
1	2
1	3
2	1
2	2
2	3

MAXIMUM JOINT NUMBERING DIFFERENCE---- 4

SEMI-BANDWIDTH OF STIFFNESS MATRIX,ETC 15

MEAN WATER DEPTH(M)------------------- 135.0

PARAMETER A OF WAVE SPECTRUM---------- 2.560

PARAMETER B OF WAVE SPECTRUM---------- 0.0499

COEFFICIENT OF ADDED MASS------------- 1.00

COEFFICIENT OF INERTIA---------------- 2.00

COEFFICIENT OF DRAG------------------- 1.00

STRUCTURAL CRITICAL DAMPING RATIO----- 0.050

MEMBER NO	INERTIA COEFF	TOTAL DRAG COEFF
1	0.1540E 06	0.4686E 04
2	0.7329E 04	0.1093E 04
3	0.7329E 04	0.1093E 04
4	0.1540E 06	0.4686E 04
5	0.5385E 04	0.9374E 03
6	0.5385E 04	0.9374E 03
7	0.2056E 05	0.1824E 04
8	0.5385E 04	0.9374E 03
9	0.5385E 04	0.9374E 03
10	0.2056E 05	0.1824E 04
11	0.2597E 04	0.6509E 03
12	0.2597E 04	0.6509E 03
13	0.1496E 05	0.1564E 04
14	0.5385E 04	0.9374E 03
15	0.5385E 04	0.9374E 03
16	0.1496E 05	0.1564E 04
17	0.5029E 04	0.7029E 03
18	0.5029E 04	0.7029E 03
19	0.1039E 05	0.1304E 04
20	0.5385E 04	0.9374E 03
21	0.5385E 04	0.9374E 03
22	0.1039E 05	0.1304E 04
23	0.2392E 04	0.6247E 03
24	0.2392E 04	0.6247E 03
25	0.5090E 04	0.9114E 03
26	0.5385E 04	0.9374E 03
27	0.5385E 04	0.9374E 03
28	0.5090E 04	0.9114E 03
29	0.2392E 04	0.6247E 03
30	0.2392E 04	0.6247E 03
31	0.5090E 04	0.9114E 03
32	0.5385E 04	0.9374E 03
33	0.5385E 04	0.9374E 03
34	0.5090E 04	0.9114E 03
35	0.0000E 00	0.0000E 00
36	0.1000E 00	0.0000E 00

S.D. OF PARTICLE VELOCITY LEVEL(M)

0.2746	0.00
0.2746	0.00
0.3109	57.00
0.3109	57.00
0.3109	57.00
0.4384	73.00
0.4384	73.00
0.4384	73.00
0.7022	105.00
0.7022	105.00
0.7022	105.00
1.2946	135.00
1.2946	135.00
1.2946	135.00
2.5348	155.00
2.5348	155.00
2.5348	155.00
0.0000	177.00
0.0000	177.00
0.0000	177.00

HIGHEST VALUE OF FREQUENCY CONSIDERED = 7.865RAD/SEC, 1.252CPS

NATURAL FREQUENCIES AND MODE SHAPES

OPERATION FINISHED WITH CONTROL ON EIGENVALUE 1

EIGENVALUE NO.	FREQUENCY	NO.OF ITERATIONS DONE
1	0.50506E 00	6

ITERATIVE PROCESS WITH CONTROL ON EIGENVALUE 2

EIGENVALUE NO.	FREQUENCY	NO. OF ITERATIONS DONE
2	0.17053E 01	14

MODE NO	1	2
FREQUENCY(CPS)	0.30566E 00	0.17053E 01

NORMAL MODE SHAPES

0.50126E-01	0.23224E-02
0.21345E-01	0.53749E-01
-0.22475E-02	0.94029E-04
0.41653E-01	0.69829E-03
0.44370E-08	0.13119E-02
-0.22953E-03	0.20567E-04
0.63126E-01	-0.74012E-03
-0.21345E-01	0.59984E-01
-0.22475E-02	-0.17856E-03
0.22550E 00	0.54550E-02
0.50033E-01	0.19298E 00
-0.53731E-02	0.30434E-03
0.10724E 00	0.13777E-02
0.20739E-06	0.61181E-01
-0.59752E-03	0.84301E-04
0.22550E 00	-0.49284E-05
-0.60092E-01	0.10389E 00
-0.53721E-02	-0.46448E-03
0.42452E 00	0.41986E-02
0.33435E-01	0.53254E 00
-0.63341E-02	0.69479E-03
0.37555E 00	0.25531E-02
0.69520E-06	0.21420E 00
-0.11024E-02	0.10803E-03
0.42452E 00	0.13990E-02
-0.63432E-01	0.53407E 00
-0.50341E-02	-0.63894E-03
0.60435E 00	0.16303E-01
0.90631E-01	0.43342E 00
-0.73902E-02	-0.72924E-03
0.59202E 00	0.20534E-02
0.11052E-05	0.34320E 00

[illegible]E-02	0.[illegible]E-04
0.66255E 00	-0.12842E-01
-0.90848E-01	0.43539E 00
-0.78992E-02	0.81062E-03
0.84694E 00	0.98411E-01
0.10438E 00	0.74845E 00
-0.81929E-02	0.59921E-02
0.78316E 00	0.11501E-02
0.17640E-05	0.51914E 00
-0.18003E-02	0.59514E-04
0.84694E 00	-0.96506E-01
-0.10437E 00	0.75111E 00
-0.81929E-02	-0.58909E-02
0.10000E 01	-0.75170E-03
0.92455E-01	0.99445E 00
-0.38523E-02	0.33836E-03
0.99971E 00	-0.42188E-03
0.33979E-05	0.10000E 01
-0.38521E-02	0.65084E-04
0.10000E 01	-0.93809E-04
-0.92449E-01	0.99757E 00
-0.38524E-02	-0.20841E-03

NUMBER OF SIGNIFICANT FREQUENCIES= 1

MODAL STIFFNESS AND DAMPING COEFFICIENTS

MODE	K	C
1	0.1452E 02	0.1768E-02

TOTAL DAMPING COEFFICIENT IN MODE 1= 0.2304E 00

MODE 1 GAMMA 0.0302

****

************** STANDARD DEVIATIONS OF DISPLACEMENT RESPONSES (M) **************

****

NODE NO	DIRECTION X	DIRECTION Y	DIRECTION ROT
1	0,000000E 00	0,000000E 00	0,000000E 00
2	0,000000E 00	0,000000E 00	0,000000E 00
3	0,107008E-01	0,365213E-02	0,428453E-03
4	0,709034E-02	0,755533E-09	0,389264E-04
5	0,107007E-01	0,365212E-02	0,428453E-03
6	0,379036E-01	0,102884E-01	0,910643E-03
7	0,283201E-01	0,352410E-07	0,101305E-03
8	0,379036E-01	0,102882E-01	0,910643E-03
9	0,719790E-01	0,141434E-01	0,116696E-02
10	0,633217E-01	0,117626E-06	0,186880E-03
11	0,719790E-01	0,141430E-01	0,116696E-02
12	0,112512E 00	0,154006E-01	0,133903E-02
13	0,100864E 00	0,197688E-06	0,273246E-03
14	0,112512E 00	0,154001E-01	0,133903E-02
15	0,143368E 00	0,176938E-01	0,138881E-02
16	0,132758E 00	0,299031E-06	0,305169E-03
17	0,143368E 00	0,176930E-01	0,138882E-02
18	0,169515E 00	0,156725E-01	0,653029E-03
19	0,169466E 00	0,575997E-06	0,652980E-03
20	0,169515E 00	0,156714E-01	0,653030E-03

MAXIMUM DISPLACEMENT STANDARD DEVIATION = 0,1695E 00 M

PROB, OF 68,3 PC THAT DISPL, IS LESS THAN 0,1695E 00 M

PROB, OF 95,4 PC THAT DISPL, IS LESS THAN 0,3390E 00 M

PROB, OF 99,7 PC THAT DISPL, IS LESS THAN 0,5085E 00 M

****

**************** STANDARD DEVIATIONS OF ELEMENT FORCES ****************

ELEMENT NO	END 1 HORIZ (N)	END 1 VERT (N)	END 1 MOMENT (NM)	END 2 HORIZ (N)	END 2 VERT (N)	END 2 MOMENT (NM)
1	0.6661E 07	0.3589E 08	0.1339E 09	0.6661E 07	0.3589E 08	0.7552E 07
2	0.3659E 07	0.3362E 07	0.4916E 06	0.3659E 07	0.3362E 07	0.4071E 06
3	0.3659E 07	0.3362E 07	0.4916E 06	0.3659E 07	0.3362E 07	0.4071E 06
4	0.6661E 07	0.3589E 08	0.1339E 09	0.6661E 07	0.3589E 08	0.7552E 07
5	0.3649E 07	0.3715E 05	0.1011E 07	0.3649E 07	0.3715E 05	0.3511E 06
6	0.3649E 07	0.3715E 05	0.3511E 06	0.3649E 07	0.3715E 05	0.1011E 07
7	0.2808E 07	0.2871E 08	0.8687E 07	0.2808E 07	0.2871E 08	0.1023E 07
8	0.7283E 07	0.7146E 07	0.1427E 06	0.7283E 07	0.7146E 07	0.4136E 06
9	0.7283E 07	0.7146E 07	0.1427E 06	0.7283E 07	0.7146E 07	0.4136E 06
10	0.2808E 07	0.2871E 08	0.8687E 07	0.2808E 07	0.2871E 08	0.1023E 07
11	0.7246E 07	0.3425E 05	0.9618E 06	0.7246E 07	0.3425E 05	0.1822E 06
12	0.7246E 07	0.3425E 05	0.1822E 06	0.7246E 07	0.3425E 05	0.9618E 06
13	0.1932E 07	0.2117E 08	0.2116E 07	0.1932E 07	0.2117E 08	0.1548E 07
14	0.7837E 07	0.7511E 07	0.6234E 06	0.7837E 07	0.7511E 07	0.5458E 06
15	0.7837E 07	0.7511E 07	0.6234E 06	0.7837E 07	0.7511E 07	0.5458E 06
16	0.1932E 07	0.2117E 08	0.2116E 07	0.1932E 07	0.2117E 08	0.1548E 07
17	0.7763E 07	0.3539E 05	0.9531E 06	0.7763E 07	0.3539E 05	0.1265E 06
18	0.7763E 07	0.3539E 05	0.1265E 06	0.7763E 07	0.3539E 05	0.9531E 06
19	0.1341E 07	0.1334E 08	0.2802E 07	0.1341E 07	0.1334E 08	0.1278E 07
20	0.7950E 07	0.7322E 07	0.8384E 06	0.7950E 07	0.7822E 07	0.7223E 06
21	0.7950E 07	0.7322E 07	0.8384E 06	0.7950E 07	0.7822E 07	0.7223E 06
22	0.1341E 07	0.1334E 08	0.2802E 07	0.1341E 07	0.1334E 08	0.1278E 07
23	0.7845E 07	0.2772E 05	0.6567E 06	0.7845E 07	0.2772E 05	0.1138E 06
24	0.7845E 07	0.2772E 05	0.1138E 06	0.7845E 07	0.2772E 05	0.6567E 06
25	0.8179E 06	0.7509E 07	0.1456E 07	0.8179E 06	0.7509E 07	0.1325E 07
26	0.8028E 07	0.5827E 07	0.1837E 07	0.8028E 07	0.5827E 07	0.4187E 06
27	0.8028E 07	0.5827E 07	0.1837E 07	0.8028E 07	0.5827E 07	0.4187E 06
28	0.8178E 06	0.7509E 07	0.1456E 07	0.8178E 06	0.7509E 07	0.1325E 07
29	0.7924E 07	0.2090E 05	0.5668E 06	0.7924E 07	0.2090E 05	0.2358E 05
30	0.7924E 07	0.2091E 05	0.2356E 05	0.7924E 07	0.2091E 05	0.5669E 06
31	0.1410E 06	0.4242E 06	0.2478E 06	0.1410E 06	0.4242E 06	0.2010E 07
32	0.8315E 07	0.7106E 07	0.1682E 07	0.8315E 07	0.7106E 07	0.6754E 05
33	0.8315E 07	0.7106E 07	0.1682E 07	0.8315E 07	0.7106E 07	0.6750E 05
34	0.1409E 06	0.4239E 06	0.2478E 06	0.1409E 06	0.4239E 06	0.2010E 07
35	0.4078E 07	0.2785E 05	0.7464E 06	0.4078E 07	0.2785E 05	0.7793E 05

[illegible] 0,4078E 07 0,2771E 05 0,7473E 06

****

********************** EXPECTED EXTREME ELEMENT LOADS **********************

****

ELEMENT NO	END 1 HORIZ (N)	END 1 VERT (N)	END 1 MOMENT (NM)	END 2 HORIZ (N)	END 2 VERT (N)	END 2 MOMENT (NM)
1	-0,9418E 07	-0,5075E 08	0,1894E 09	0,9418E 07	0,5075E 08	-0,1068E 08
2	-0,5174E 07	-0,4755E 07	0,6951E 06	0,5174E 07	0,4755E 07	0,5756E 06
3	-0,5174E 07	0,4755E 07	0,6951E 06	0,5174E 07	-0,4755E 07	0,5756E 06
4	-0,9418E 07	0,5075E 08	0,1894E 09	0,9418E 07	-0,5075E 08	-0,1068E 08
5	0,5160E 07	-0,5253E 05	-0,1429E 07	-0,5160E 07	0,5253E 05	-0,4964E 06
6	-0,5160E 07	-0,5253E 05	-0,4965E 06	0,5160E 07	0,5253E 05	-0,1429E 07
7	-0,3971E 07	-0,4060E 08	0,1228E 08	0,3971E 07	0,4060E 08	-0,1446E 07
8	-0,1030E 08	-0,1010E 08	-0,2018E 06	0,1030E 08	0,1010E 08	0,5848E 06
9	-0,1030E 08	0,1010E 08	-0,2018E 06	0,1030E 08	-0,1010E 08	0,5848E 06
10	-0,3971E 07	0,4060E 08	0,1228E 08	0,3971E 07	-0,4060E 08	-0,1446E 07
11	0,1025E 08	-0,4343E 05	-0,1360E 07	-0,1025E 08	0,4843E 05	-0,2577E 06
12	-0,1025E 08	-0,4343E 05	-0,2577E 06	0,1025E 08	0,4843E 05	-0,1360E 07
13	-0,2732E 07	-0,2994E 08	0,2993E 07	0,2732E 07	0,2994E 08	-0,2190E 07
14	-0,1108E 08	-0,1062E 08	-0,8814E 06	0,1108E 08	0,1062E 08	0,7717E 06
15	-0,1108E 08	0,1062E 08	-0,8814E 06	0,1108E 08	-0,1062E 08	0,7717E 06
16	-0,2732E 07	0,2994E 08	0,2993E 07	0,2732E 07	-0,2994E 08	-0,2190E 07
17	0,1098E 08	-0,5004E 05	-0,1348E 07	-0,1098E 08	0,5004E 05	-0,1788E 06
18	-0,1098E 08	-0,5004E 05	-0,1788E 06	0,1098E 08	0,5004E 05	-0,1348E 07
19	-0,1896E 07	-0,1886E 08	0,3962E 07	0,1896E 07	0,1886E 08	0,1807E 07
20	-0,1124E 08	-0,1106E 08	-0,1185E 07	0,1124E 08	0,1106E 08	0,1021E 07
21	-0,1124E 08	0,1106E 08	-0,1185E 07	0,1124E 08	-0,1106E 08	0,1021E 07
22	-0,1896E 07	0,1886E 08	0,3962E 07	0,1896E 07	-0,1886E 08	0,1807E 07
23	0,1109E 08	-0,3920E 05	-0,9286E 06	-0,1109E 08	0,3920E 05	-0,1609E 06
24	-0,1109E 08	-0,3920E 05	-0,1609E 06	0,1109E 08	0,3920E 05	-0,9286E 06
25	-0,1156E 07	-0,1062E 08	0,2059E 07	0,1156E 07	0,1062E 08	0,1873E 07
26	-0,1135E 08	-0,8239E 07	-0,2598E 07	0,1135E 08	0,8239E 07	0,5921E 06

27	-0.1135E 08	0.8239E 07	-0.2598E 07	0.1135E 08	-0.8239E 07	0.5921E 06
28	-0.1156E 07	0.1062E 08	0.2059E 07	0.1156E 07	-0.1062E 08	0.1873E 07
29	0.1120E 08	-0.2956E 05	-0.8015E 06	-0.1120E 08	0.2956E 05	0.3334E 05
30	-0.1120E 08	-0.2956E 05	0.3331E 05	0.1120E 08	0.2956E 05	-0.8016E 06
31	-0.1993E 06	-0.5999E 06	0.3504E 06	0.1993E 06	0.5999E 06	0.2842E 07
32	-0.1176E 08	-0.1005E 08	-0.2379E 07	0.1176E 08	0.1005E 08	-0.9551E 05
33	-0.1176E 08	0.1005E 08	-0.2379E 07	0.1176E 08	-0.1005E 08	-0.9545E 05
34	-0.1993E 06	0.5994E 06	0.3504E 06	0.1993E 06	-0.5994E 06	0.2842E 07
35	0.5766E 07	-0.3938E 05	-0.1055E 07	-0.5766E 07	0.3938E 05	0.1102E 06
36	-0.5766E 07	-0.3918E 05	0.1163E 06	0.5766E 07	0.3918E 05	-0.1057E 07

****

*******   RA1001 RESPONSE ANALYSIS OF PLANE FRAMES TO WAVE LOADING, SPECTA3   ******

****

HALCROW-EJBAIK STEEL JACKET , ELEVATION THROUGH LINES 1 AND 4

NUMBER OF ELEMENTS = = = = = 35

NUMBER OF NODAL POINTS = = = 21

NUMBER OF REACTIONS = = = = = 6

NODAL POINT COORDINATES

NODE POINT	X-COORD(M)	Y-COORD(M)
1	0.0000	0.0000
2	30.0000	0.0000
3	3.3450	37.0000
4	40.0000	37.0000
5	76.6550	37.0000
6	6.5990	73.0000
7	40.0000	73.0000
8	73.4010	73.0000
9	9.4920	105.0000
10	40.0000	105.0000
11	70.5080	105.0000
12	12.2030	135.0000
13	40.0000	135.0000

14	67.7970	155.0000
15	14.0110	155.0000
16	40.0000	155.0000
17	65.9890	155.0000
18	16.0000	177.0000
19	40.0000	177.0000
20	64.0000	177.0000

STRUCTURE CONNECTIVITY AND PROPERTIES

MEMBER NO	END 1	END 2	E(N/M2)	I(M4)	A(SQ.M)	MASS(KG)	VOL DISPL(CU.M/M)	SHELT. FACT
1	1	3	0.2000E 12	0.3067E 02	0.1467E 01	0.1152E 05	0.6567E 02	0.000E 00
2	1	4	0.2000E 12	0.2958E 00	0.2599E 00	0.2040E 04	0.3575E 01	0.000E 00
3	2	4	0.2000E 12	0.2958E 00	0.2599E 00	0.2040E 04	0.3575E 01	0.000E 00
4	2	5	0.2000E 12	0.3067E 02	0.1467E 01	0.1152E 05	0.6567E 02	0.000E 00
5	3	4	0.2000E 12	0.1551E 00	0.1855E 00	0.1456E 04	0.2627E 01	0.000E 00
6	4	5	0.2000E 12	0.1551E 00	0.1855E 00	0.1456E 04	0.2627E 01	0.000E 00
7	3	6	0.2000E 12	0.1820E 01	0.5756E 00	0.4518E 04	0.9931E 01	0.000E 00
8	3	7	0.2000E 12	0.2184E 00	0.2612E 00	0.2051E 04	0.2627E 01	0.000E 00
9	5	7	0.2000E 12	0.2184E 00	0.2612E 00	0.2051E 04	0.2627E 01	0.000E 00
10	5	8	0.2000E 12	0.1820E 01	0.5756E 00	0.4518E 04	0.9931E 01	0.000E 00
11	6	7	0.2000E 12	0.8043E-01	0.1267E 00	0.9943E 03	0.1267E 01	0.000E 00
12	7	8	0.2000E 12	0.8043E-01	0.1267E 00	0.9943E 03	0.1267E 01	0.000E 00
13	6	9	0.2000E 12	0.1148E 01	0.4945E 00	0.3882E 04	0.7296E 01	0.000E 00
14	6	10	0.2000E 12	0.1868E 00	0.2234E 00	0.1754E 04	0.2627E 01	0.000E 00
15	8	10	0.2000E 12	0.1868E 00	0.2234E 00	0.1754E 04	0.2627E 01	0.000E 00
16	8	11	0.2000E 12	0.1148E 01	0.4945E 00	0.3882E 04	0.7296E 01	0.000E 00
17	9	10	0.2000E 12	0.6433E-01	0.1368E 00	0.1073E 04	0.1477E 01	0.000E 00
18	10	11	0.2000E 12	0.6433E-01	0.1368E 00	0.1073E 04	0.1477E 01	0.000E 00
19	9	12	0.2000E 12	0.6609E 00	0.4135E 00	0.3246E 04	0.5067E 01	0.000E 00
20	9	13	0.2000E 12	0.1868E 00	0.2234E 00	0.1754E 04	0.2627E 01	0.000E 00
21	11	13	0.2000E 12	0.1868E 00	0.2234E 00	0.1754E 04	0.2627E 01	0.000E 00
22	11	14	0.2000E 12	0.6609E 00	0.4135E 00	0.3246E 04	0.5067E 01	0.000E 00
23	12	13	0.2000E 12	0.3540E-01	0.9525E-01	0.7477E 03	0.1167E 01	0.000E 00
24	13	14	0.2000E 12	0.3540E-01	0.9525E-01	0.7477E 03	0.1167E 01	0.000E 00
25	12	15	0.2000E 12	0.1322E 00	0.1488E 00	0.1168E 04	0.2483E 01	0.000E 00
26	12	16	0.2000E 12	0.1868E 00	0.2234E 00	0.1754E 04	0.2627E 01	0.000E 00
27	14	16	0.2000E 12	0.1868E 00	0.2234E 00	0.1754E 04	0.2627E 01	0.000E 00
28	14	17	0.2000E 12	0.1322E 00	0.1488E 00	0.1168E 04	0.2483E 01	0.000E 00
29	15	16	0.2000E 12	0.3540E-01	0.9525E-01	0.7477E 03	0.1167E 01	0.000E 00

30	16	17	0.2000E 12	0.3540E-01	0.9525E-01	0.7477E 03	0.1167E 01	0.000E 00
31	15	18	0.2000E 12	0.1322E 00	0.1488E 00	0.1168E 04	0.2483E 01	0.000E 00
32	15	19	0.2000E 12	0.1868E 00	0.2234E 00	0.1754E 04	0.2627E 01	0.000E 00
33	17	19	0.2000E 12	0.1868E 00	0.2234E 00	0.1754E 04	0.2627E 01	0.000E 00
34	17	20	0.2000E 12	0.1322E 00	0.1488E 00	0.1168E 04	0.2483E 01	0.000E 00
35	18	19	0.2000E 12	0.1000E 04	0.1000E 02	0.1396E 06	0.0000E 00	0.000E 00
36	19	20	0.2000E 12	0.1000E 04	0.1000E 02	0.1396E 06	0.0000E 00	0.000E 00

DETAILS OF FIXED POINTS

NODE NO	DIRECTION OF FIXITY
1	1
1	2
1	3
2	1
2	2
2	3

MAXIMUM JOINT NUMBERING DIFFERENCE---- 4

SEMI-BANDWIDTH OF STIFFNESS MATRIX,ETC 15

MEAN WATER DEPTH(D)------------------- 135.0

PARAMETER A OF WAVE SPECTRUM---------- 2.560

PARAMETER B OF WAVE SPECTRUM---------- 0.0299

COEFFICIENT OF ADDED MASS------------- 1.00

COEFFICIENT OF INERTIA---------------- 2.00

COEFFICIENT OF DRAG------------------- 1.00

STRUCTURAL CRITICAL DAMPING RATIO----- 0.050

MEMBER NO	INERTIA COEFF	TOTAL DRAG COEFF
1	0,1346E 06	0,2345E 03
2	0,7329E 04	0,5467E 02
3	0,7329E 04	0,5467E 02
4	0,1346E 06	0,2345E 03
5	0,5385E 04	0,4686E 02
6	0,5385E 04	0,4686E 02
7	0,2056E 05	0,9112E 02
8	0,5385E 04	0,4686E 02
9	0,5385E 04	0,4686E 02
10	0,2056E 05	0,9112E 02
11	0,2597E 04	0,3254E 02
12	0,2597E 04	0,3254E 02
13	0,1496E 05	0,7810E 02
14	0,5385E 04	0,4686E 02
15	0,5385E 04	0,4686E 02
16	0,1496E 05	0,7810E 02
17	0,3029E 04	0,3515E 02
18	0,3029E 04	0,3515E 02
19	0,1059E 05	0,6509E 02
20	0,5385E 04	0,4686E 02
21	0,5385E 04	0,4686E 02
22	0,1059E 05	0,6509E 02
23	0,2392E 04	0,3125E 02
24	0,2392E 04	0,3125E 02
25	0,5090E 04	0,4556E 02
26	0,5385E 04	0,4686E 02
27	0,5385E 04	0,4686E 02
28	0,5090E 04	0,4556E 02
29	0,2392E 04	0,3125E 02
30	0,2392E 04	0,3125E 02
31	0,5090E 04	0,4556E 02
32	0,5385E 04	0,4686E 02
33	0,5385E 04	0,4686E 02
34	0,5090E 04	0,4556E 02
35	0,0000E 00	0,0000E 00
36	0,0000E 00	0,0000E 00

5,7, OF PARTICLE VELOCITY LEVEL(M)

0,2746	0.00
0,2746	0.00
0,3109	37.00
0,3109	37.00
0,3109	37.00
0,4364	73.00
0,4364	73.00
0,4364	73.00
0,7022	105.00
0,7022	105.00
0,7022	105.00
1,2946	135.00
1,2946	135.00
1,2946	135.00
2,5348	155.00
2,5348	155.00
2,5348	155.00
0,0000	177.00
0,0000	177.00
0,0000	177.00

HIGHEST VALUE OF FREQUENCY CONSIDERED = 7,865RAD/SEC, 1,252CPS

NATURAL FREQUENCIES AND MODE SHAPES

OPERATION FINISHED WITH CONTROL ON EIGENVALUE 1

EIGENVALUE NO.	FREQUENCY	NO.OF ITERATIONS DONE
1	0,30906E 00	6

. . . . ROUTINE IN EIGENVALUE 2

EIGENVALUE NO. FREQUENCY NO. OF ITERATIONS DONE
2 0.17053E 01 14

MODE NO 1 2

FREQUENCY(CPS) 0.59566E 00 0.17053E 01

NORMAL MODE SHAPES

0.69126E-01	0.23224E-02
0.21045E-01	0.55749E-01
-0.22275E-02	0.94020E-04
0.41353E-01	0.60326E-03
0.44390E-03	0.13110E-02
-0.22753E-03	0.20567E-04
0.63126E-01	-0.74012E-03
-0.21045E-01	0.53984E-01
-0.25275E-02	-0.17858E-03
0.22530E 00	0.54550E-02
0.60093E-01	0.10293E 00
-0.53721E-02	0.59434E-03
0.15724E 00	0.13777E-02
0.20739E-06	0.91181E-01
-0.59752E-03	0.34801E-04
0.22530E 00	-0.42234E-03
-0.60902E-01	0.19389E 00
-0.53721E-02	-0.46448E-03
0.42452E 00	0.41986E-02
0.83435E-01	0.53254E 00
-0.63341E-02	0.69479E-03
0.37535E 00	0.25581E-02
0.69300E-06	0.21420E 00
-0.11124E-02	0.11303E-03
0.42452E 00	0.13990E-02
-0.85432E-01	0.53407E 00
-0.60341E-02	-0.63894E-03
0.60435E 00	0.16863E-01
0.90331E-01	0.43342E 00
-0.73902E-02	-0.72924E-03
0.57502E 00	0.21534E-02
0.11532E-05	0.34320E 00

0.66255E 00	-0.12842E-01
-0.90848E-01	0.43539E 00
-0.78992E-02	0.81062E-03
0.84694E 00	0.98411E-01
0.10438E 00	0.74845E 00
-0.81929E-02	0.59921E-02
0.78316E 00	0.11501E-02
0.17640E-05	0.51914E 00
-0.18003E-02	0.59514E-04
0.84694E 00	-0.96506E-01
-0.10437E 00	0.75111E 00
-0.81929E-02	-0.58909E-02
0.10000E 01	-0.75170E-03
0.92455E-01	0.99445E 00
-0.38523E-02	0.33836E-03
0.99971E 00	-0.42138E-03
0.33979E-05	0.10000E 01
-0.38521E-02	0.65084E-04
0.10000E 01	-0.93809E-04
-0.92449E-01	0.99757E 00
-0.38524E-02	-0.20841E-03

NUMBER OF SIGNIFICANT FREQUENCIES= 1

MODAL STIFFNESS AND DAMPING COEFFICIENTS

MODE	K	C
1	0.1452E 02	0.1768E-02

TOTAL DAMPING COEFFICIENT IN MODE 1= 0.2304E 00

MODE 1 GAMMA 0.0302

****

STANDARD DEVIATIONS OF DISPLACEMENT RESPONSES (M) *************

NODE NO	DIRECTION X	Y	ROT
1	0.000000E 00	0.000000E 00	0.000000E 00
2	0.000000E 00	0.000000E 00	0.000000E 00
3	0.394824E-02	0.134754E-02	0.158086E-03
4	0.261833E-02	0.278768E-09	0.143626E-04
5	0.394824E-02	0.134752E-02	0.158086E-03
6	0.139852E-01	0.379610E-02	0.335998E-03
7	0.104603E-01	0.130028E-07	0.373785E-04
8	0.139852E-01	0.379601E-02	0.335999E-03
9	0.265580E-01	0.521847E-02	0.430571E-03
10	0.233637E-01	0.434002E-07	0.689528E-04
11	0.265580E-01	0.521833E-02	0.430572E-03
12	0.414395E-01	0.568235E-02	0.494059E-03
13	0.372158E-01	0.729405E-07	0.100819E-03
14	0.414395E-01	0.568214E-02	0.494058E-03
15	0.529722E-01	0.652847E-02	0.512429E-03
16	0.489834E-01	0.110333E-06	0.112598E-03
17	0.529722E-01	0.652815E-02	0.512431E-03
18	0.625455E-01	0.578267E-02	0.240947E-03
19	0.625275E-01	0.212525E-06	0.240929E-03
20	0.625455E-01	0.578224E-02	0.240947E-03

MAXIMUM DISPLACEMENT STANDARD DEVIATION = 0.6255E-01 M

PROB. OF 68.3 PC THAT DISPL. IS LESS THAN 0.6255E-01 M

PROB. OF 95.4 PC THAT DISPL. IS LESS THAN 0.1251E 00 M

PROB. OF 99.7 PC THAT DISPL. IS LESS THAN 0.1876E 00 M

**************** STANDARD DEVIATIONS OF ELEMENT FORCES ****************

ELEMENT NO	END 1 HORIZ (N)	END 1 VERT (N)	END 1 MOMENT (NM)	END 2 HORIZ (N)	END 2 VERT (N)	END 2 MOMENT (NM)
1	0.2458E 07	0.1324E 08	0.4942E 08	0.2458E 07	0.1324E 08	0.2786E 07
2	0.1350E 07	0.1241E 07	0.1814E 06	0.1350E 07	0.1241E 07	0.1502E 06
3	0.1350E 07	0.1241E 07	0.1814E 06	0.1350E 07	0.1241E 07	0.1502E 06
4	0.2458E 07	0.1324E 08	0.4942E 08	0.2458E 07	0.1324E 08	0.2786E 07
5	0.1346E 07	0.1371E 05	0.3728E 06	0.1346E 07	0.1371E 05	0.1295E 06
6	0.1346E 07	0.1371E 05	0.1295E 06	0.1346E 07	0.1371E 05	0.3728E 06
7	0.1036E 07	0.1059E 08	0.3205E 07	0.1036E 07	0.1059E 08	0.3773E 06
8	0.2687E 07	0.2637E 07	0.5267E 05	0.2687E 07	0.2637E 07	0.1526E 06
9	0.2687E 07	0.2637E 07	0.5267E 05	0.2687E 07	0.2637E 07	0.1526E 06
10	0.1036E 07	0.1059E 08	0.3205E 07	0.1036E 07	0.1059E 08	0.3773E 06
11	0.2673E 07	0.1264E 05	0.3549E 06	0.2673E 07	0.1264E 05	0.6723E 05
12	0.2673E 07	0.1264E 05	0.6724E 05	0.2673E 07	0.1264E 05	0.3549E 06
13	0.7129E 06	0.7813E 07	0.7809E 06	0.7129E 06	0.7813E 07	0.5713E 06
14	0.2892E 07	0.2771E 07	0.2300E 06	0.2892E 07	0.2771E 07	0.2014E 06
15	0.2892E 07	0.2771E 07	0.2300E 06	0.2892E 07	0.2771E 07	0.2014E 06
16	0.7123E 06	0.7812E 07	0.7809E 06	0.7128E 06	0.7812E 07	0.5713E 06
17	0.2864E 07	0.1306E 05	0.3517E 06	0.2864E 07	0.1306E 05	0.4666E 05
18	0.2864E 07	0.1306E 05	0.4667E 05	0.2864E 07	0.1306E 05	0.3517E 06
19	0.4948E 06	0.4920E 07	0.1034E 07	0.4948E 06	0.4920E 07	0.4716E 06
20	0.2933E 07	0.2886E 07	0.3093E 06	0.2933E 07	0.2886E 07	0.2665E 06
21	0.2933E 07	0.2886E 07	0.3093E 06	0.2933E 07	0.2886E 07	0.2665E 06
22	0.4948E 06	0.4920E 07	0.1034E 07	0.4948E 06	0.4920E 07	0.4716E 06
23	0.2895E 07	0.1023E 05	0.2423E 06	0.2895E 07	0.1023E 05	0.4199E 05
24	0.2895E 07	0.1023E 05	0.4200E 05	0.2895E 07	0.1023E 05	0.2423E 06
25	0.3018E 06	0.2771E 07	0.5372E 06	0.3018E 06	0.2771E 07	0.4888E 06
26	0.2962E 07	0.2150E 07	0.6778E 06	0.2962E 07	0.2150E 07	0.1545E 06
27	0.2962E 07	0.2150E 07	0.6778E 06	0.2962E 07	0.2150E 07	0.1545E 06
28	0.3018E 06	0.2771E 07	0.5372E 06	0.3018E 06	0.2771E 07	0.4888E 06
29	0.2924E 07	0.7713E 04	0.2091E 06	0.2924E 07	0.7713E 04	0.8699E 04
30	0.2924E 07	0.7713E 04	0.8692E 04	0.2924E 07	0.7713E 04	0.2092E 06
31	0.5201E 05	0.1565E 06	0.9143E 05	0.5201E 05	0.1565E 06	0.7415E 06
32	0.3068E 07	0.2622E 07	0.6207E 06	0.3068E 07	0.2622E 07	0.2492E 05
33	0.3068E 07	0.2622E 07	0.6207E 06	0.3068E 07	0.2622E 07	0.2491E 05
34	0.5200E 05	0.1564E 06	0.9144E 05	0.5200E 05	0.1564E 06	0.7415E 06
35	0.1505E 07	0.1028E 05	0.2754E 06	0.1505E 07	0.1028E 05	0.2876E 05

[illegible] [illegible] 0.3036E 05 0.1505E 07 0.1022E 05 0.2757E 06

****

********************   EXPECTED EXTREME ELEMENT LOADS   ********************

****

ELEMENT NO	END 1 HORIZ (N)	END 1 VERT (N)	END 1 MOMENT (NM)	END 2 HORIZ (N)	END 2 VERT (N)	END 2 MOMENT (NM)
1	-0.3475E 07	-0.1873E 08	0.6988E 08	0.3475E 07	0.1873E 08	-0.3940E 07
2	-0.1909E 07	-0.1754E 07	0.2565E 06	0.1909E 07	0.1754E 07	0.2124E 06
3	-0.1909E 07	0.1754E 07	0.2565E 06	0.1909E 07	-0.1754E 07	0.2124E 06
4	-0.3475E 07	0.1872E 08	0.6988E 08	0.3475E 07	-0.1872E 08	-0.3940E 07
5	0.1904E 07	-0.1938E 05	-0.5272E 06	-0.1904E 07	0.1938E 05	-0.1832E 06
6	-0.1904E 07	-0.1938E 05	-0.1832E 06	0.1904E 07	0.1938E 05	-0.5272E 06
7	-0.1465E 07	-0.1498E 08	0.4532E 07	0.1465E 07	0.1498E 08	-0.5335E 06
8	-0.3800E 07	-0.3728E 07	-0.7447E 05	0.3800E 07	0.3728E 07	0.2158E 06
9	-0.3800E 07	0.3728E 07	-0.7447E 05	0.3800E 07	-0.3728E 07	0.2158E 06
10	-0.1465E 07	0.1498E 08	0.4532E 07	0.1465E 07	-0.1498E 08	-0.5335E 06
11	0.3780E 07	-0.1787E 05	-0.5018E 06	-0.3780E 07	0.1787E 05	-0.9507E 05
12	-0.3780E 07	-0.1787E 05	-0.9507E 05	0.3780E 07	0.1787E 05	-0.5018E 06
13	-0.1008E 07	-0.1105E 08	0.1104E 07	0.1008E 07	0.1105E 08	-0.8079E 06
14	-0.4089E 07	-0.3918E 07	-0.3252E 06	0.4089E 07	0.3918E 07	0.2847E 06
15	-0.4089E 07	0.3918E 07	-0.3252E 06	0.4089E 07	-0.3918E 07	0.2847E 06
16	-0.1008E 07	0.1105E 08	0.1104E 07	0.1008E 07	-0.1105E 08	-0.8079E 06
17	0.4050E 07	-0.1846E 05	-0.4973E 06	-0.4050E 07	0.1846E 05	-0.6598E 05
18	-0.4050E 07	-0.1846E 05	-0.6599E 05	0.4050E 07	0.1846E 05	-0.4973E 06
19	-0.6997E 06	-0.6958E 07	0.1462E 07	0.6997E 06	0.6958E 07	0.6668E 06
20	-0.4148E 07	-0.4081E 07	-0.4374E 06	0.4148E 07	0.4081E 07	0.3769E 06
21	-0.4148E 07	0.4081E 07	-0.4374E 06	0.4148E 07	-0.4081E 07	0.3769E 06
22	-0.6997E 06	0.6957E 07	0.1462E 07	0.6997E 06	-0.6957E 07	0.6668E 06
23	0.4093E 07	-0.1446E 05	-0.3426E 06	-0.4093E 07	0.1446E 05	-0.5938E 05
24	-0.4093E 07	-0.1446E 05	-0.5938E 05	0.4093E 07	0.1446E 05	-0.3426E 06
25	-0.4267E 06	-0.3918E 07	0.7596E 06	0.4267E 06	0.3918E 07	0.6912E 06
26	-0.4188E 07	-0.3040E 07	-0.9585E 06	0.4188E 07	0.3040E 07	0.2185E 06

27	-0.4188E 07	0.3040E 07	-0.9585E 06	0.4188E 07	-0.3040E 07	0.2185E 06
28	-0.4267E 06	0.3918E 07	0.7596E 06	0.4267E 06	-0.3918E 07	0.6911E 06
29	0.4134E 07	-0.1091E 05	-0.2957E 06	-0.4134E 07	0.1091E 05	0.1230E 05
30	-0.4134E 07	-0.1091E 05	0.1229E 05	0.4134E 07	0.1091E 05	-0.2957E 06
31	-0.7354E 05	-0.2213E 06	0.1293E 06	0.7354E 05	0.2213E 06	0.1048E 07
32	-0.4338E 07	-0.3707E 07	-0.8777E 06	0.4338E 07	0.3707E 07	-0.3524E 05
33	-0.4338E 07	0.3707E 07	-0.8777E 06	0.4338E 07	-0.3707E 07	-0.3522E 05
34	-0.7353E 05	0.2211E 06	0.1293E 06	0.7353E 05	-0.2211E 06	0.1048E 07
35	0.2127E 07	-0.1453E 05	-0.3894E 06	-0.2127E 07	0.1453E 05	0.4066E 05
36	-0.2127E 07	-0.1446E 05	0.4292E 05	0.2127E 07	0.1446E 05	-0.3899E 06